DTU

Graduate School Yearbook 2018

Graduate School Yearbook **2018**

Editors:

Professor, Head of Department, Kim Dam-Johansen
Associate Professor, Peter Szabo
PhD student, Sara Krpović

PREFACE

Welcome to this year's Graduate School Yearbook.

In Denmark, the PhD study is a three-year fulltime programme after graduation with a MSc degree. At DTU Chemical Engineering we host about 100 PhD students from all over the world. In this book, you can read about most of our current PhD projects. Some students have just initiated their work whereas others are close to writing their thesis.

The work of our PhD students is of utmost importance to fulfil the mission and vision of our department:

Mission
Being responsible for research, education and innovation, DTU Chemical Engineering will develop and utilize knowledge, methods, technologies and sustainable solutions within:

- Chemical and biochemical process engineering and production.
- Design of chemical and biochemical products and processes.
- Energy and environment.

Vision
DTU Chemical Engineering:
- Is acknowledged as a world leading chemical engineering department.
- Is an attractive partner for university departments and research-based industry.
- Helps to retain, develop and attract knowledge-based national working places.
- Supports development of sustainable solutions in the fields of chemistry, biotechnology, food, pharma and energy through research and research based consultancy.
- Is attractive as a place to work for ambitious and technology-passionate staff members.

We hope you will find the book interesting, and we invite all readers to contact us for further details.

Yours sincerely
Kim Dam-Johansen
Professor, Head of Department

Peter Szabo & Sara Krpović
Editors

Contents

Resul Al

Phone: +45 4525 55 10
E-mail: resal@kt.dtu.dk

Supervisors: Gürkan Sin
                   Krist V. Gernaey
                   Alexandr Zubov

PhD Study
  Started: May 2017
  To be completed: April 2020

Sustainable process synthesis and design

Abstract
Available treatment technologies for wastewater are diversifying as the industry is undergoing a paradigm shift from considering wastewater as a waste to treat to an increasingly valuable source for energy production and resources recovery. Utilities in the developed countries are aiming for energy neutrality or even surplus energy production in their modern wastewater treatment plants (WWTP). The technological advancements in the industry are also driven by the increasingly stringent effluent quality limits, especially on discharged nitrogen and ammonia levels. Given steadily growing number of competing treatment technologies and ever-ambitious performance goals, the need for the use of simulation, optimization, and systematic process synthesis methodologies for engineering design of WWTPs is becoming more pronounced among design professionals. This project aims at the development of a new computational framework which will enable design professionals to easily integrate various process design tools; such as stochastic simulation-based optimization framework, life cycle analysis, global sensitivity analysis, and uncertainty analysis, into the early-stage conceptual design of WWTPs.

Introduction

Process systems engineering promotes the application of systematic computer-based methods to process design and synthesis, which encompasses a vast range of industries and requires integration of significant amount of knowledge from diverse scientific disciplines, practical industrial experience, and a number of tools and methods to carry out sustainable process design. One of the critical pain points for process design engineers is the lack of available tool regarding the comparative analysis and synthesis of alternative processing networks, which makes it not-so-easy for them to implement innovative processing configurations with newly arising process technologies. Given the lack of data regarding these new processes and the uncertainty in the available process data, there exists a need for new supporting methods and tools for both generating alternative processing flowsheets and the selection of the optimum flowsheet under uncertainty with sustainability aspects also incorporated into the early stage process design.

The design of domestic wastewater treatment plants (WWTPs) have been witnessing an unprecedented shift since the inception of most widely used activated sludge process. The priority for a design engineer was mainly to ensure effective removal of chemical oxygen demand (COD), representing carbon pollutant in wastewater. However, with ever growing complexity such as population growth, stringent environmental laws, energy neutrality and contributing to circular economy, the layout of WWTP looks gigantic than ever before. The WWTP design intricacy has been further exacerbated by the remarkable innovation and availability of treatment technology (both matured and emerging) in the market.

Methodology

Simulation is an established tool for evaluating and predicting the performance of complex engineering systems. Optimization is usually performed to make the best decisions, usually of controllable design and operational variables, under the given circumstances desired level of system performance subject to technical and economic constraints. Stochastic simulation optimization, also referred to as simulation optimization, uses simulation to find values of decision variables that will optimize the system's key performance indicators of interest, which are obtained by performing stochastic simulations like Monte Carlo simulations. Promoted by recent advancements in computing power, simulation optimization allows one to work with arbitrarily complex simulation models, eliminating the need to keep model complexity to mathematically tractable forms as required by deterministic optimization frameworks (Pasupathy et al., 2011). As the design of WWTPs is subject to
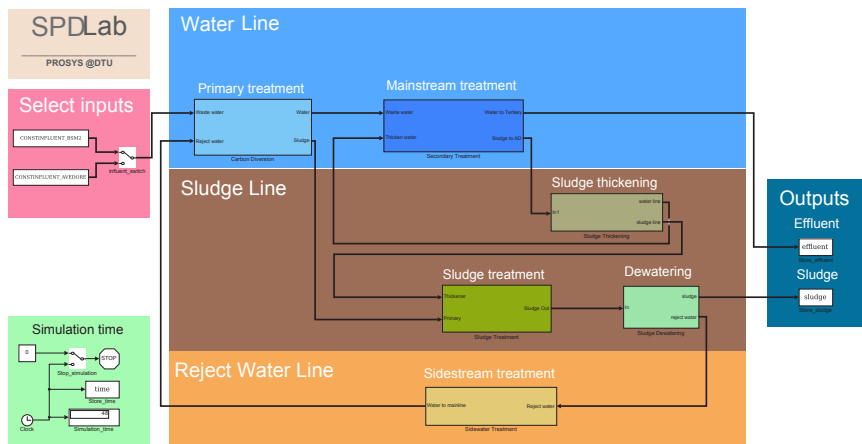
Figure 1: The main user interface of the new decision support tool, SPDLab.

significant stochasticities such as varying levels of pollutant loadings, deterministic design optimization formulations provide non-robust results.

SPDLab: A new decision support tool

To help address aforementioned design challenge, a new stochastic simulation-based optimization under uncertainty tool for sustainable process synthesis and design, SPDLab, has been developed to assist design professionals in early-stage engineering design of advanced wastewater treatment plants. SPDLab provides computational tools for interfacing with complex bio-process models implemented in Simulink environment and searches for an optimal plant layout configuration for the given design objective. Using a model library of high fidelity process models for advanced wastewater treatment technologies, SPDLab employs a superstructure-based approach to process synthesis to create and investigate alternative plant configurations. Simulation-based optimization is used to find optimal plant configuration with optimized set of design related parameters. Further investigations of system uncertainties is also conducted by a stochastic kriging-based optimization under uncertainty framework. Figure 1 shows the main user interface of SPDLab.

Results

The tool investigates configurations with optimal design variables to find WWTP designs satisfying technical, economic, and environmental constraints. Figure 2 shows populations of designs after effluent quality filters are being imposed.

Conclusions

A new decision support tool for sustainable process design has been developed. The final framework is expected to provide novel methods and approaches for both the design of next generation WWTPs and the retrofitting of existing plant designs.

Acknowledgements
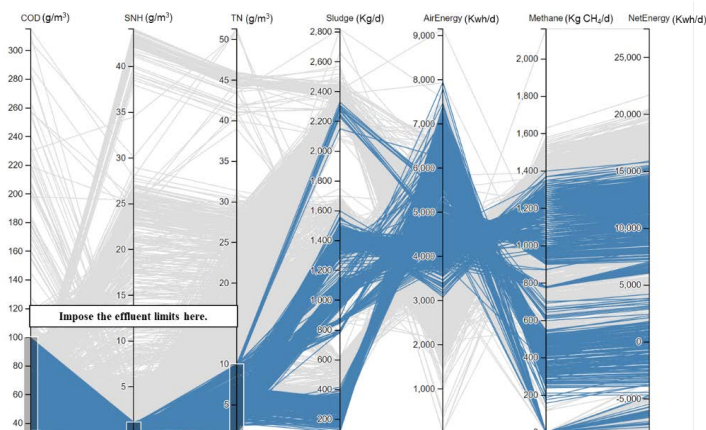
References

Pasupathy, R., Henderson, S.G., 2011. SimOpt: A library of simulation optimization problems, in: Proceedings of the 2011 Winter Simulation Conference (WSC). IEEE, pp. 4075–4085.

Figure 2: The tool provides interactive visualizations of all feasible designs after imposing effluent quality constraints.

Antonio Grimalt Alemany

Phone: +45 50 34 44 26

E-mail: angral@kt.dtu.dk

Supervisors: Hariklia N. Gavala

Ioannis V. Skiadas

PhD Study

Started: March 2016

To be completed: July 2019

Mixed microbial consortia-based syngas fermentation to ethanol

Abstract

This work evaluated the potential of mixed microbial consortia for the production of ethanol through syngas fermentation. The results showed that the enrichment cultures were significantly affected by the fermentation conditions, where lower initial pH was found to favor solvent production. The results obtained experimentally were consistent with the thermodynamic analysis on the metabolic network and demonstrated that thermodynamics could be used for directing microbial activity towards specific products.

Introduction

The ever increasing energy demands along with the climate crisis and the rising waste generation rates worldwide have motivated a paradigm shift towards the development of more sustainable processes for the production of chemicals and fuels. One of the alternative approaches with a high potential to contribute to this transition is based on mixed microbial consortia (MMC) biotechnology field, which holds a dual role of waste treatment and production of valuable chemicals and fuels. This field of study is currently expanding beyond the conventional anaerobic digestion process towards the development of new technological platforms for the production of a variety of chemicals and fuels [1]. Syngas fermentation is one of such innovative platforms that has recently emerged as an alternative to conventional catalytic syngas conversion and carbohydrate-based bioconversion processes. This technology consists of a combination of thermochemical and biochemical conversion methods, where the biomass is first gasified into a mixture of H_2, CO and CO_2, and further converted biologically into a range of valuable chemicals and fuels. The adoption of a mixed culture approach in syngas fermentation processes has recently gained attention as it presents a series of potential advantages over pure cultures derived from the non-sterile operation and the higher resiliency and adaptive capacity of microbial communities [2], which ultimately result in lower operating costs. However, the use of mixed cultures is currently limited by their high complexity and the poor understanding of the microbial interactions within the microbial community. Therefore, prediction tools for

shaping and engineering microbial communities are still needed [3].

Specific Objectives

The aim of this study is to evaluate the potential of mixed microbial consortia for the production of ethanol through syngas fermentation in batch experiments. The specific objectives are:

- Designing of suitable enrichment strategies for the production of ethanol as the main product.
- Study the role of thermodynamics on the regulation of the metabolic network of mixed microbial consortia in syngas fermentation processes.

Results and Discussion

A number of batch microbial enrichments were performed based on pH and nutrients availability (yeast extract) as the main drivers of the microbial selection to evaluate the effect of the pH and nutrients on the ethanol yield [4]. The results showed that both yeast extract and pH had a strong effect on the product distribution of the fermentation. Decreasing the initial pH generally favored the production of solvents and had a negative effect on the production of acids (fig. 1). On the other hand, the addition of yeast extract to the fermentation broth allowed decreasing further the initial pH to 5 and triggered the production of longer carbon chain products, including butyrate, butanol and caproate (fig. 1). The maximum ethanol yield was obtained in the enrichment at the lowest initial pH tested (HT-pH5 YE), which corresponded to a maximum of $59.2 \pm 0.2\%$ of the stoichiometric yield.
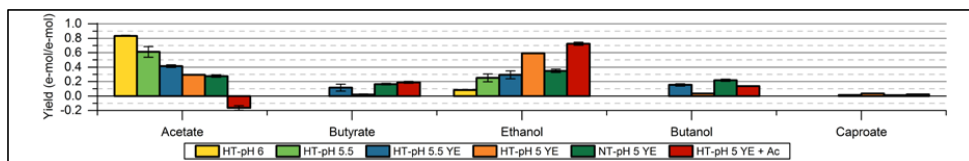
Figure 1. Product yield for all enriched microbial consortia at the end of the enrichment process. HT stands for heat-shock treated inoculum, NT for non-treated inoculum and YE for yeast extract. The pH given in the legend corresponds to the initial pH of the fermentation.
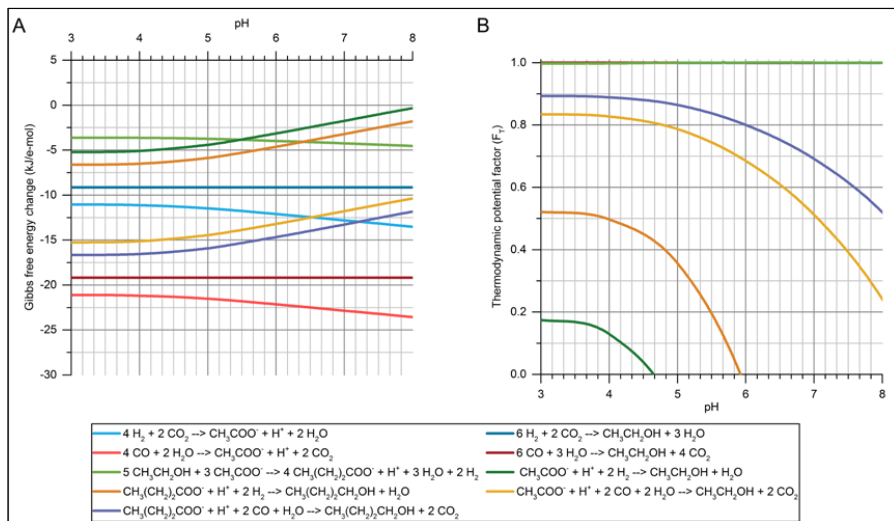
Figure 2. A Calculated $\Delta_r G'_{310\,K}$ for the metabolic network of microbial consortia as a function of pH, normalized for e-mol transferred per reaction. Process conditions considered were: temperature of 310K, ionic strength of 0.08 M, P_{H2} of 1.05 atm, P_{CO2} of 0.6 atm, P_{CO} of 0.45 atm and concentration of metabolites of 0.001 M. **B** Thermodynamic potential factor calculated for all reactions as a function of pH using a ΔGp of 57.5 kJ/mol ATP. Extracted from Grimalt-Alemany et al. [4].

A thermodynamic analysis on the network of net reactions taking place during the fermentations was carried out based on the Gibbs free energy change and the thermodynamic potential factor. The results of the analysis of the effect of the initial pH on the metabolic network showed that direct acetate- and ethanol-producing reactions were strictly subject to kinetic control (F_T value of 1), which favored the production of acetate initially. In turn, acetate-reducing reactions were subject to thermodynamic control from the beginning of the fermentation and became significantly favored by the decrease in pH (fig. 2). Overall, the results suggested that acetate-reducing reactions were responsible for the higher ethanol yields obtained experimentally.

Based on thermodynamic analysis on the effect of acetate concentration, an additional enrichment was performed using an initial acetate concentration of 20 mM (HT-pH5-YE-Ac) in order to boost further the reduction of acetate to ethanol at pH 5. Through this approach it was possible to increase the ethanologenic potential of the enriched culture, achieving a maximum ethanol yield of $72.4 \pm 2.1\%$ of the stoichiometric yield (fig. 1).

Conclusions
This study demonstrated that applying thermodynamic control over sensitive reactions composing the metabolic network can contribute to enhancing the product selectivity in mixed microbial consortia-based fermentations.

References
1. D.J. Batstone and B. Virdis, Curr Opin Biotechnol, 27 (2014) 142–149.
2. R. Kleerebezem and M.C. van Loosdrecht, Curr Opin Biotechnol, 18 (2007) 207–212.
3. C. Zerfa, J. Chen and O.S. Soyer, Curr Opin Biotechnol, 50 (2018) 121–127.
4. A. Grimalt-Alemany, M. Łężyk, L. Lange, I.V. Skiadas and H.N. Gavala, Biotechnol Biofuels, 11 (2018) 1–22.

Wael Fadi Al-Masri

Phone:	+45 25 68 64 11
E-mail:	wafa@kt.dtu.dk

Supervisors: Alexander Shapiro
     Wei Yan

PhD Study
 Started: January 2018
 To be completed: December 2020

Gas Liberation in Tight Porous Medium

Abstract

During oil production, solution gas is liberated and forms a free-gas phase due to the decline in reservoir pressure. The nature of the liberated gas phase is crucial to the reservoir drive mechanism. Within this work, experimental studies of the gas liberation in a porous medium of a low permeability reservoir under decreasing pressure will be conducted. The mobility of the formed gas bubbles and their effect on the effective oil permeability will be determined. Along with the experimental work, modelling part of the study will be developed to correlate the amount of liberated gas to the reduction of oil permeability.

Introduction

The liberated free-gas phase, generated due to reservoir pressure decline, can either be a handicap or a benefit during oil production. The bad scenario is that disconnected immobile gas bubbles can block individual pore throats, lowering thus, the effective permeability of the reservoir. Unfavourable pore geometry along with capillary forces/wettability balance are the main contributors to that possibility. On the other hand, a favourable case is that the liberated gas bubbles coalesce easily forming a mobile gas phase, which can provide energy to the reservoir by a competent gas-oil gravity drainage mechanism. For such an effective upwards gas migration though, crucial parameters are permeability and dip of the reservoir, layering/stratigraphy, as well as the relative permeabilities of the fluid phases[1,2,3].
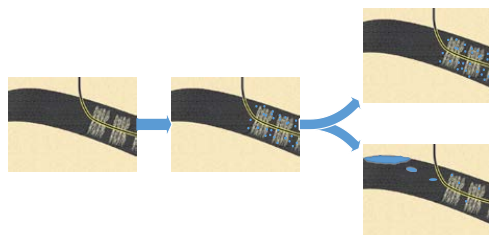
Figure 1: Illustration of the expected fate of the liberated gas bubbles.

Objectives

The experimental study of this work aims to determine the mobility of the formed gas bubbles and their effect on the effective permeability of the oil. The experiments involve gas liberation in a low permeability reservoir sample, induced by pressure decrease. The pressure will range from above to below the saturation pressure, while X-ray computer tomography will be applied to detect the in-situ gas liberation. Effective oil permeability versus pressure drop will be monitored. The onset of gas phase production, if occurred, will be monitored as well.
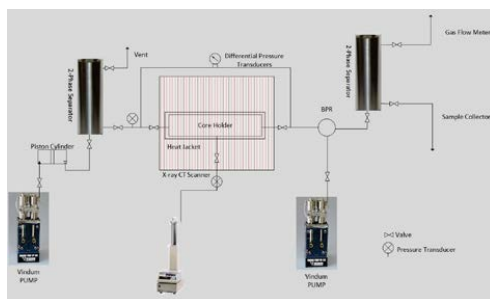
Figure 2: Schematic of the experimental setup.

Along with the experimental work, the modelling part of the study will be developed. For calculating the amount of the produced gas, a previously developed thermodynamic model (DTU) will be adjusted and applied[4]. The model involves oil and gas equilibrium under the action of capillary forces. If the released gas stays in the pores in the form of bubbles, a correlation

between the amount of liberated gas and the reduction of oil permeability will be provided. In the case of gas phase production, a more advanced dynamic model has to be developed, for the determination of the gas-oil relative permeabilities.

References
1. Zhelezny P.V., Shapiro A.A., Vu D.T., and Stenby E.H., On the Process of Gas Liberation in Porous Media, Journal of Porous Media, vol. 9 (6), 503-521 (2006).
2. Shapiro A.A., Potsch K., Kristensen, J.G., Stenby, E.H.: Effect of Low Permeable Porous Media on Behavior of Gas Condensates, paper SPE 65182 prepared for presentation at the SPE European Petroleum Conference EUROPEC\ 2000 held in Paris, France, 24-25 October 2000.
3. Shapiro A.A., Stenby E.H.: Effects of Capillary Forces and Adsorption on Reserves Distribution, paper SPE 36922 prepared for presentation at the 1996 SPE European Petroleum Conference held in Milan, Italy, 22-24 October 1996.
4. Shapiro A.A., Stenby E.H.: Thermodynamics of Two-Phase Capillary Equilibrium in Multicomponent Mixtures, Fluid Phase Equilibria 178, 17-32 (2001).

Christian Andersen

| Phone: | +45 30 69 51 90 |
| E-mail: | chrand@kt.dtu.dk |

| Supervisors: | Anders E. Daugaard |
| | Niels J. Madsen, Coloplast A/S |

PhD Study
| Started: | January 2017 |
| To be completed: | January 2020 |

Screening Platform for Easy Surface Modification of Polymers

Abstract
Many polymer materials undergo surface modifications in order to change their physical or chemical nature. This then allows them to be used for special applications as for instance in chemical resistant tubings and pipelines, biocompatible materials for cell scaffolds or anti-foiling materials for medical devices. However, finding new suitable materials that can be used in complex environments can be difficult and time consuming. Being able to modify and screen large libraries of different surface chemistries is therefore a key step in order to identify novel adaptable materials. In this project, a high throughput screening platform was developed in order to allow grafting of polymers via UV initiated free radical polymerization (FRP) of different monomer systems onto polymer substrates in a simple and easy manner.

Introduction
An important aspect for a materials potential application is its physical and chemical surface properties. Polymers offer an inexpensive bulk material with good mechanical properties, but do not often possess the desired surface properties. Complex environments, especially biological, puts high demands on the interaction between the surroundings and the surface of the respective material. Many biomedical devices such as e.g. stents or implants are rejected by the body, due to activation of platelets leading to blood clotting [1] or unfavorable immune responses [2]. Surface modification techniques such as plasma, radiation or photochemical grafting have paved the way for alteration of the chemistry, topology, wettability etc. of polymers, widely expanding their range of application [3],[4]. However, predicting the outcome for a given surface modification can be difficult and time-consuming, even through a rational design approach. A way to overcome this is by using high throughput screening platforms to fast and reliably explore large libraries of different surface chemistries for suitable candidates. Much research have focused on automated picoliter scale synthesis of polymer libraries conducted on standard microscope glass slides [5]. Through this approach, only little material is needed to make hundreds of formulations that all can be run simultaneously on a single slide. The disadvantage of this method is that such small volumes exclusively run in bulk. This only permits investigations of different ratios of monomers and not the effect of solvent or concentration. Furthermore, the base substrate is glass,

which is a non-ideal representation of the final application.

Specific Objectives
The objectives of this project is to establish a method that allows for:
- Direct grafting of polymers or monomers onto a polymer substrate.
- The study of reaction parameters such as monomer concentration on grafting outcome.
- A fast and easy screening of multiple formulations
- Validation by parallelized analysis such as e.g. WCA measurements.

Results and Discussion
The design and dimensions of the screening platform illustrated in Figure 1 (I) is based on a standard 96 well microtiter plate. The setup is divided into three separate parts: a) a Teflon coated aluminum top plate, b) the polymer substrate, which in this case is a PU film and c) a stainless steel support. The top plate a) has been applied a Teflon coating for easy cleaning and detachment and can accommodate a total of 96 individual formulations. On the bottom side (see Figure 1 (I)), metal rings beneath each well have been milled. This serves to ensure a tight seal between the polymer and top plate, avoiding leakage and mixing of contents. By having the polymer as a separate part, permits for easy exchange of the base substrate. This feature makes for a versatile setup enabling the study of different relevant surfaces on a single system. The only requirement for the polymer is

that it can be formed into a sheet or film. The steel support keeps the polymer substrate in place and ensures a smooth and even film. This is required to be able to perform e.g. reliable WCA measurements.

contact angle of 40° obtained at 1.31 M, reflecting a conversion from a hydrophobic to a hydrophilic surface. Copolymers of di(ethylene glycol) methyl ether methacrylate-co-poly(ethylene glycol) methyl ether
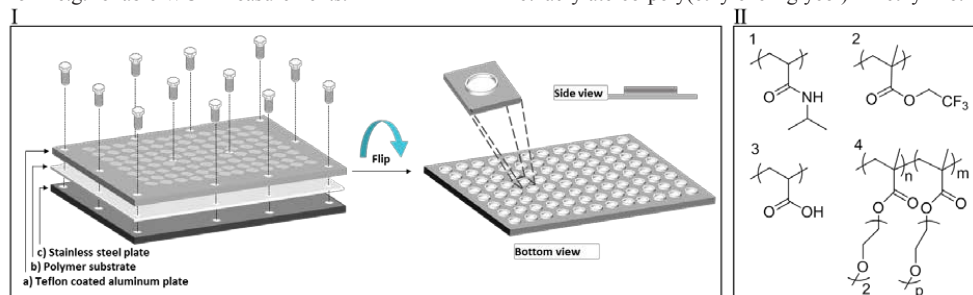
Figure 1: I)Schematic illustration of screening platform. II) Polymer systems grafted to the Polyurethane substrate. 1) N-isopropylacrylamide 2) 2,2,2-trifluoroethyl methacrylate 3) acrylic acid and 4) di(ethylene glycol) methyl ether methacrylate-co-poly(ethylene glycol) methyl ether methacrylate

Grafting of monomers were done through activation of the surface by addition of a photo initiator into each well. Monomer solutions were then added and subsequently exposed to UV-light to facilitate polymerization. Both hydrophilic, hydrophobic or thermoresponsive surfaces were obtained using the monomers acrylic acid (AA), di(ethylene glycol) methyl ether methacrylate and poly(ethylene glycol) methyl ether methacrylate (MDEGMA and MPEGMA), 2,2,2-trifluoroethyl methacrylate (TrFEMA) and N-isopropylacrylamide (NIPAAm) as shown in Figure 1 (II).

At first, homopolymerization of acrylic acid (AA) was conducted to obtain carboxylic acid functionalities. The polar groups was intended to create a more hydrophilic surface. The monomer was added in a series of molar concentrations and their respective WCA can be seen in Figure 2.

methacrylate (MDEGMA-co-MPEGMA) was also studied. These polymers are interesting, not only for their low friction surfaces, but also the ethylene glycol side chain is biocompatible and FDA approved. This makes them especially popular choices for coatings in biomedical device [6]. Grafting was conducted at various ratios of the two monomers and their resulting WCA can be viewed in Figure 3
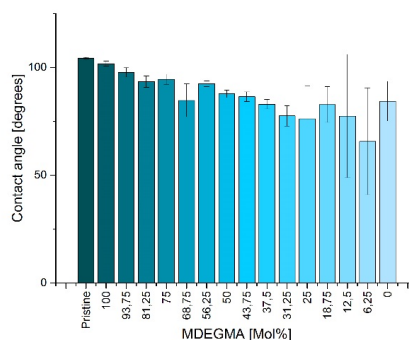
Figure 3: WCA of MDEGMA-co-MPEGMA grafted to a PU substrate at various ratios

At 100 mol% MDEGMA, only a slight decrease in contact angle is observed to 101°. For these very hydrophilic monomers, a lower contact angle would normally be expected. This could indicate that only a very thin layer of polymer is present at the surface. As the content of MDEGMA is slowly replaced with MPEGMA throughout the series, the lower the contact angle becomes. The longer ethylene glycol side chain of MPEGMA makes for a more hydrophilic monomer and, thereby, a more hydrophilic surface is seen.

Fluor containing polymers are generally known to possess low energy surfaces. Similarly, grafting of 2,2,2-trifluoroethyl methacrylate was done in an attempt to create a highly hydrophobic surface. The monomer

Figure 2: WCA of AA grafted to a PU substrate at various monomers concentrations.

A clear difference can be seen in WCA from the pristine surface (104°) to that of the modified surfaces (89-40°). There is a clear trend of decreasing contact angle with increasing molar concentration of AA, with the lowest

concentration and their respective WCA can be seen in Figure 4. The contact angle at the highest molar concentration increased from 104° to 116°. The effect on the WCA is less dominant than that of AA since the PU itself is hydrophobic by nature.
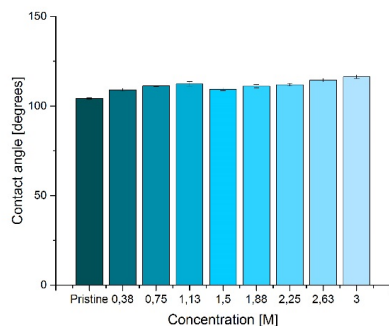
Figure 4: WCA of TrFEMA grafted to PU substrate at various monomer concentration.

Likewise, a trend between increasing monomer feed concentration and increase in contact angle can also be observed.

Polymers of N-isopropylacryl amide (NIPAAm) have been shown to be able to change its hydrophilicity upon thermal stimuli and have shown great potential for controlled drug delivery system [7]. It has a lower critical solution temperature (LCST) around 31-33 °C, by which below this point is very hydrophilic and when above changes to hydrophobic. The low temperature favors a linear conformation making amide groups available for hydrogen bonding with water. When heated, the chains obtain a curled conformation instead, making intra and inter molecular hydrogen bonds, exposing only the hydrophobic carbon backbone of the polymer. The contact angles of the NIPAAm modified PU surface at different temperatures are presented in Figure 5.
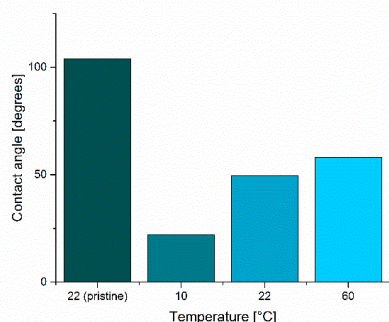
Figure 5: WCA of NIPAAm grafted to a PU substrate at various temperatures.

To show that the surface possessed thermoresponsive properties, WCA of both above and below LCST were measured (see Figure 5). A sample at 0.56 M had a WCA of 50° at room temperature. When raising the temperature to 60 °C the contact angle increased to 59° and when lowered to 10 °C the angle dropped to 22°. This proved that the thermoresponsive properties of NIPAAm had been successfully implemented onto a PU surface. In addition, an important limitation regarding the monomer concentration was observed for NIPAAM, where concentrations above 1 M resulted in cross-linking, creating large gels on the surface. The large gels were not mechanically stable and did not bind well to the substrate. This is a good example as to why not only ratios of monomers but also concentration is important for the outcome of the grafting.

Conclusion

A novel screening platform was developed as a high throughput method to establish suitable candidates for surface modifications of polymers. The grafting was conducted via UV initiated FRP onto a PU substrate with a series of monomer and comonomer systems. The systems was successfully applied giving both hydrophilic (AA and MDEGMA with MPEGMA), hydrophobic (TrFEMA) and thermoresponsive (NIPAAm) surface properties as proved by WCA analysis. The extent of grafting was also shown to be dependent on the monomer feed concentration.

References

[1]   V. L. Serebruany, C. C. Cummings, A. I. Malinin, S. R. Steinhubl, P. A. Gurbel, and S. Antonio, *Am. Heart J.*, 142 (4) (2001) 611–616.

[2]   S. Franz, S. Rammelt, D. Scharnweber, and J. C. Simon, *Biomaterials*, 32 (28) 6692–6709.

[3]   G. Geuskens, A. Etoc, and P. Di Michele, *Eur. Polym. J.*, 36 (2) (2000) 265–271.

[4]   C.-M. Chan, T.-M. Ko, and H. Hiraoka, *Surf. Sci. Rep.*, 24 (1–2) (1996) 1–54.

[5]   A. J. Urquhart, D. G. Anderson, M. Taylor, M. R. Alexander, R. Langer, and M. C. Davies, *Adv. Mater.* 19 (18) (2007) 2486–2491.

[6]   D. Hutanu, M. D. Frishberg, L. Guo, and C. C. Darie, *Mod. Chem. Appl.*, 2 (2) (2014) 2–7.

[7]   Z. M. O. Rzaev, S. Dinçer, and E. Pişkin, *Prog. Polym. Sci.*, 32 (5) (2007) 534–595.

Konstantinos Asimakopoulos

Phone: +45 50389784
E-mail: kona@kt.dtu.dk

Supervisors: Ioannis V. Skiadas
                Hariklia N. Gavala

PhD Study
    Started: February 2016
    To be completed: January 2019

Biomethanation of Syngas by Mixed Microbial Consortia in a Trickle Bed Bioreactor

Abstract

Gasification of biomass results in the production of syngas, a gas mixture with a high energy and carbon content which can be further anaerobically fermented to methane. Existing syngas fermentation technologies face important challenges such as a) the need of maintaining sterile conditions and b) the mass transfer of sparingly soluble syngas compounds (CO, H_2) to the water-based microbial cultures. Using mixed microbial consortia under mesophilic conditions in a trickle bed reactor proved to be an effective solution and resulted in high volumetric productivity of methane.

Introduction

The Paris Agreement, which was adopted by 196 state parties of the United Nations Framework Convention on Climate Change, has set a long term goal to withhold the increase of the global average temperature below 2 °C. Recycling of both organic and inorganic carbon is a necessity in order to achieve this goal.

Synthesis gas or syngas, mainly consisting of CO, H_2 and CO_2, is a product of biomass gasification and other industrial processes. Its high energy and carbon content can be exploited by converting it to CH_4 and supplying it to the already developed natural gas grids. This process can be performed both biologically and chemically with the former presenting great merits over the latter such as mild conditions, low infrastructure costs, cheap catalysts (microbes) and no demand for fixed H_2/CO ratio [1].

The main bottlenecks of syngas fermentation are the mass transfer of the sparingly soluble syngas compounds (CO and H_2) to water-based media and the relatively low growth rate of the microbes that leads to relatively low productivity rates [2]. It has been demonstrated that trickle bed reactors provide higher mass transfer rates than CSTRs and bubble columns and additionally enhance cell retention through biofilm formation. As a result, in this study lab scale experiments with a trickle bed reactor for the biomethanation of syngas were designed and performed under various operational conditions.

Specific Objectives

The goal of this study was to assess the use of a trickle bed reactor for the biological conversion of syngas to methane and determine the impact of specific operational parameters on the performance of the reactor.

Bioreactor Design and Operating Conditions
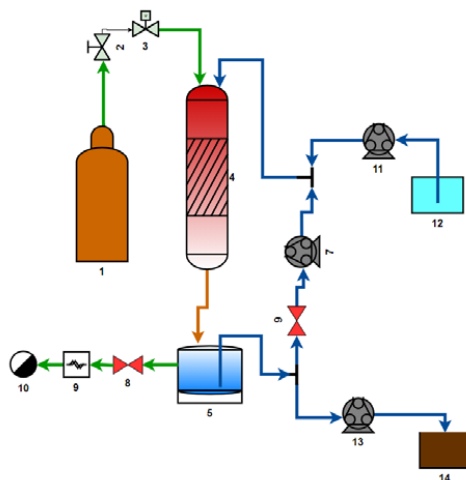
Figure 1: Process Flow Diagram of the setup

A detailed process flow diagram is presented in Fig. 1. Syngas with a composition of 45% H_2, 25% CO_2, 20%

CO and 10% CH_4 was flowing into an anaerobically sealed trickle bed column (4) filled with packing material. After flowing through the trickle bed column, the gas entered the headspace of a liquid reservoir (5) and then it was flowing through a gas sampling port (8) and a gas flowmeter (9) before it exited the setup (10). Liquid medium containing minerals, salts and vitamins was continuously recirculated by a peristaltic pump (7) from the liquid reservoir to the top of the trickle bed column.

The trickle bed column volume was 180 mL. The liquid recirculation rate was kept constant at 200 mL/min and the pH was buffered at 7. The examined operational parameters are presented in Table 1.

Table 1: Examined Operational Parameters

Temperature (°C)	Syngas inflow rate (mL/min)			
37	1	1.3	1.6	2.05

Results and Discussion

The trickle bed was operated in mesophilic (37 °C) conditions for the conversion of syngas to biomethane. The bioreactor was inoculated with enriched mixed microbial consortia and experimental data regarding the conversion efficiency of the substrate and the volumetric methane productivity were collected under steady state conditions.
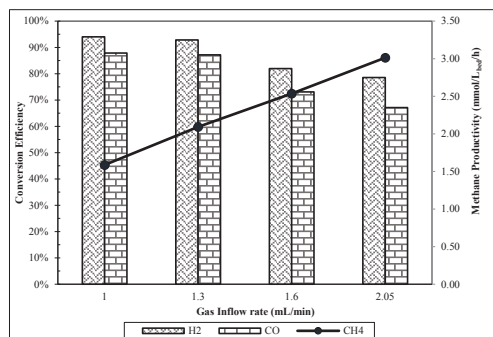
Figure 2: Conversion efficiency of H_2 and CO and volumetric productivity of methane

The uptake rate of the substrate presented a decrease when the gas inflow rate increased to values higher than 1.3 mL/min (Fig. 2). Increase of the gas inflow rate may result in higher CH_4 productivity but at a cost of the conversion efficiency of the substrate and, as a result, the content of CH_4 in the outflow. Therefore, this trade off should be optimized depending on the desired outcome.
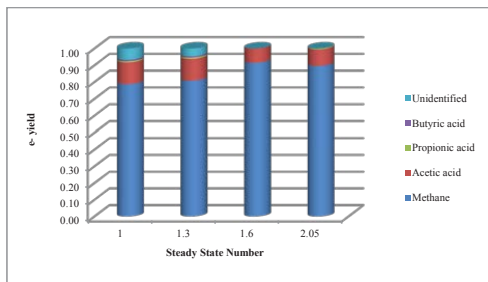
Figure 3: Electron yield to products

Apart from the conversion efficiency of the substrate it is important to identify the compounds the released energy is fixed to and up to what levels. More than 80% of the electrons were fixed to the desired product (methane) in all cases. The dominant byproduct of the process was acetic acid with propionic acid and butyric acid traced in much lower amounts (Fig. 3). Preliminary experiments at thermophilic conditions (60 °C) have shown that significantly higher efficiencies and volumetric productivities of methane can be achieved.

Conclusions

Syngas biomethanation was performed in a trickle bed reactor under mesophilic conditions at varying gas inflow rates. The results showed that the selected bioreactor configuration was effective and that a high conversion efficiency of the substrate can be achieved up to gas inflow rates of 1.3 mL/min. The main byproduct was acetic acid assimilating 10% of the released energy from the conversion of substrate. The outcome of this research sheds also more light on the use of mixed microbial consortia performing syngas biomethanation and paves the way for the design of a scaled-up process.

Acknowledgments

References

1. K. Asimakopoulos, H.N. Gavala, I. V. Skiadas, Chem. Eng. J. 348 (2018) 732–744
2. A. Grimalt-Alemany, I. V. Skiadas, H. N. Gavala, , Biofuels, Bioproducts & Biorefining 12 (2018) 139–158.

Hadise Baghooee

Phone: +45 5035 9199
E-mail: hadise@kt.dtu.dk

Supervisors: Alexander Shapiro
                     Charlotte Lassen
                     Wei Yan

PhD Study
   Started: June 2018
   To be completed: June 2021

Characterization of the non-uniform fluid distribution in tight petroleum reservoirs

Abstract
Due to the spontaneous heat flux from the Earth and the action of the gravitational field, no petroleum reservoir is in thermodynamic equilibrium especially in the case of tight reservoirs. Valdemar field is an example of a tight petroleum reservoir over which the fluid compositions are varying and there remains an uncertainty in the fluid properties. The observed lateral variation is puzzling and could be formed by non-equilibrium effects which behavior is unknown. A pressure-volume-temperature (PVT) model is required to capture the variations seen in the composition of reservoir fluid samples and in the produced Gas Oil Ratio (GOR). The purpose of this project is to reduce uncertainties in the reservoir fluid characterization and the lateral and vertical compositional grading observed in the tight reservoirs of the Danish sector of North Sea.

Introduction
It has been observed many times that distribution of hydrocarbons in petroleum reservoirs may be non-uniform. This variation may be especially high in tight reservoirs, where equilibrium between the different parts of a reservoir may be slow and difficult. Gravity and temperature differences could contribute to this variance. The different parts of a reservoir may contain an oil or a gas of a different composition; the content of methane, ethane, intermediate and heavy hydrocarbons may vary from one to another point. Gravity and temperature variances could contribute to differences in petroleum composition. Another complication comes from inaccurate determination of the composition of the reservoir fluids caused by recombination problems or contamination of the fluid samples.

The problem of fluid distribution is relevant to a number of tight petroleum reservoirs in the North Sea, especially Valdemar and neighboring Adda. Indefiniteness in the lateral variation of the hydrocarbon composition is an important factor affecting prospective development of these tight Lower Cretaceous reservoirs.

It is very difficult to obtain representative fluid samples in Lower Cretaceous due to low permeability of the reservoir rock and the fluids being near saturation. Earlier PVT syntheses performed with PVT data from the Valdemar, Tyra, Adda and Boje reservoirs have been

challenging and resulted in remaining uncertainties of the fluid compositions. Two fluid communication studies have been carried out between the wells in Valdemar and between Tyra and Adda. In neither of the studies, the depth gradient analysis could verify that the fluids were in communication, indicating that a lateral component could be missing.

Past studies of variation in reservoir fluid composition have focused on the effects of gravity and the geothermal gradient [1]–[3]. Some experience exists in description of the slow convective and diffusive fluxes in the reservoir. However, the lateral variation remains puzzling. It may be formed by non-equilibrium effects. The connectivity of the reservoirs may also be questioned. The oil or gas may come from different sources, and the time of reservoir formation may simply not be large enough for complete mixing. Other factors such as geochemistry of the reservoir may also influence the fluid distribution.

Depending on temperature, pressure, and composition conditions, some components tend to diffuse to the hotter or colder regions of the reservoir, a phenomenon known as "Soret effect", that is, a mass flux due to a temperature gradient. Consider a multicomponent system, the gravity force makes the heavy components' molecules stay at the bottom while the lighter stay at the top, Soret effect could accelerate or weaken the gravitational effect and distribute the components by thermal effect. [4]

Presence of the thermal gradient leads to redistribution of the components in the reservoir in accordance with the Soret effect as well. It has been noted that non-isothermal effects may be of the same order of magnitude as gravitational effects. They should be taken into account in order to explain deviations from the segregated state predicted by thermodynamic equilibrium models. Additionally, the thermal field may sometimes cause instability of an equilibrium state and formation of the convective fluxes.

Objectives

The present PhD project is a research collaboration between the Centre for Energy Resources Engineering (CERE) and Danish Hydrocarbon Research and Technology Center (DHRTC) at DTU. The goal of the project is to study the fluid distribution in petroleum reservoirs. The model objects will be the tight reservoirs of the Danish sector of the North Sea, especially, Valdemar and the adjacent reservoirs. Advanced methods for fluid characterization and the principles of nonequilibrium thermodynamics will be applied for the study [5], [6]. An important practical outcome of the study will be reduction of indefiniteness in the fluid characterization of various tight petroleum reservoirs in the North Sea, improving the prospects of their development.

Progress

As the PVT experiments are not free of systematic errors, we check the fluid properties determined by the laboratory from sampling reports before application in the thermodynamics model. In the first phase, we have studied the quality control of PVT measurements on collected samples from Lower Cretaceous chalk fields to select the representative reservoir fluid. Different methods such as material balance, cross plots and the K-values equilibrium trend analysis, for verifying the consistency of PVT data have been studied. [7] Material balance assess consistency of compositional and flash data and an example of the results from material balance study is illustrated in Figure 1. In addition, theoretical predictions with an equation of state provide a clearer picture of the consistency of PVT data from the experiments. The oil formation volume factor is an important reservoir fluid property modelled using an equation of state (EOS) and compared with experimental measurements from the sampling reports as shown in Figure 2.

Conclusion

In the first phase of the project, the consistency check is under development, which will help in finding high quality PVT data to be used in construction of thermodynamic model for representative reservoir fluid and compositional grading study. The PhD project will fill a technical gap and can potentially assist in de-risking the PVT uncertainties on undeveloped Lower Cretaceous reservoirs. Previous studies have been zooming in on single field fluid PVT studies. A regional study of the fluids in Lower Cretaceous combined with other types of data might give new insight.
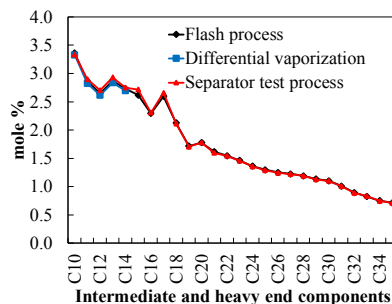
Figure 1: Consistency check of the reservoir fluid composition from various PVT tests
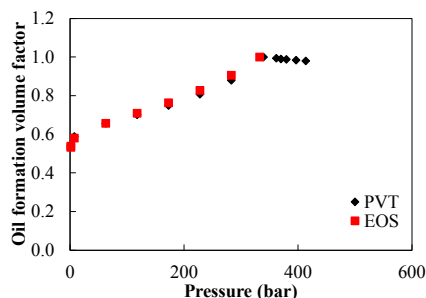
Figure 2: Oil formation volume factor obtained from PVT tests and theoretical EOS

References

[1]   C. H. Whitson and P. Belery, "Compositional Gradients in Petroleum Reservoirs," *Univ. Tulsa Centen. Pet. Eng. Symp.*, pp. 443–459, 1994.

[2]   F. Montel and P. L. Gouel, "Prediction of Compositional Grading in a Reservoir Fluid Column," *SPE Annu. Tech. Conf. Exhib.*, 1995.

[3]   B. Faissat, K. Knudsen, E. H. Stenby, and F. Montel, "Fundamental statements about thermal diffusion for a multicomponent mixture in a porous medium," *Fluid Phase Equilib.*, vol. 100, no. C, pp. 209–222, Sep. 1994.

[4]   R. O. Espósito, P. H. R. Alijó, J. A. Scilipoti, and F. W. Tavares, *Compositional Grading in Oil and Gas Reservoirs*. 2017.

[5]   S. R. de Groot, "Non-equilibrium Thermodynamics," *Am. J. Phys.*, vol. 31, no. 7, p. 558, 1963.

[6]   I. Prigogine, *Introduction to Thermodynamics of Irreversible Processes*, vol. 84, no. 24. 1962.

[7]   K. Potsch, P. Toplack, and T. Gumpenberger, "A Review and Extension of Existing Consistency Tests for PVT Data From a Laboratory," *SPE Reserv. Eval. Eng.*, vol. 20, no. 02, pp. 269–284, 2017.

Franz David Bähner

Phone: +45 2132 4964
E-mail: fdav@kt.dtu.dk

Supervisors: Jakob K. Huusom
Jens Abildskov

PhD Study
Started: February 2016
To be completed: October 2019

Plant wide Monitoring and Control of Bio-Based Processes

Abstract
Bio-based processes already constitute an important part of the global, and overproportionally so, of the Danish economy. As bio-based chemicals breach into competitive bulk markets, developing countries call for increased amounts of diverse processed foods, and new drug development is sped up, the importance of bio-based processes is expected to grow. Due to input- and process uncertainties, entirely unknown states or dynamics, and business cases complicated by small scale, control of bioprocesses is known to be a tough discipline. Plantwide control of bioprocesses has, overall, not received significant academic attention, and this thesis is an attempt at building a better understanding of the chances and challenges. To this end, academic plantwide control literature has been reviewed and is held in contrast to experiences made in actual bio-based production sites in Denmark.

Introduction

Plantwide control (PWC) describes a variety of heuristics, methods, and whole frameworks for the optimization of process operation and control in large-scale continuous chemical plants. The bio-based industry that has traditionally relied on operators and feed-forward- as well as statistical process control to obtain on-spec product, is calling for more efficient processes and broader use of feedback control principles. Advanced process analytical technology, federal regulation with wider design spaces for process optimization purposes, and not lastly increased competition through e.g. rapid development of bioequivalents call for change. This project aims at identifying to which extent PWC principles can be of use in this paradigm shift, and furthermore detect whether there are attributes that characterize PWC of bioprocesses in contrast to PWC of chemical processes.

Bio-based Processes

This class of processes incorporates a wide array of applications that differ in nature and scale, however, share some characteristics. Besides common unit operations, a disjoint topology of up- and downstream processes is frequently shared among them. This is often represented in the according organizational structures (operations and R&D departments), and may stem from the fact that personnel working with one or the other require different expertise [1], but might also be attributed to some extent to enterprise history and development. It bears the disadvantage that up- and downstream lines do not work properly aligned, and there is, often, a lack of experts with extensive knowledge of and experiences with both.

Plantwide Control

There is a vast amount of academic literature concerned with 'control of bioprocesses' – it is important to point out that the discipline 'plantwide control of bio-based processes' is a fundamentally different one. Where state-of-the-art control of bioprocesses usually deals with monitoring and multivariable optimizing control of upstream processes (bioreactors), see for instance the book by [2], plantwide control - also of bioprocesses - deals with the structural decisions regarding control topology (decentralized vs. centralized) and controller type (PID, cascade control, linear MPC, non-linear MPC, further types of constrained control). The plantwide control task touches many aspects such as operability / operator acceptance, adaptability and maintainability, all of which need to be taken into account to assure that a solution is sustainable and thus long-term optimal.

Academic plantwide control is generally divided into three research streams, namely optimization-based or algorithmic frameworks such as e.g. [3], heuristics [4], or hybrid frameworks incorporating aspects of the two [5], [6].
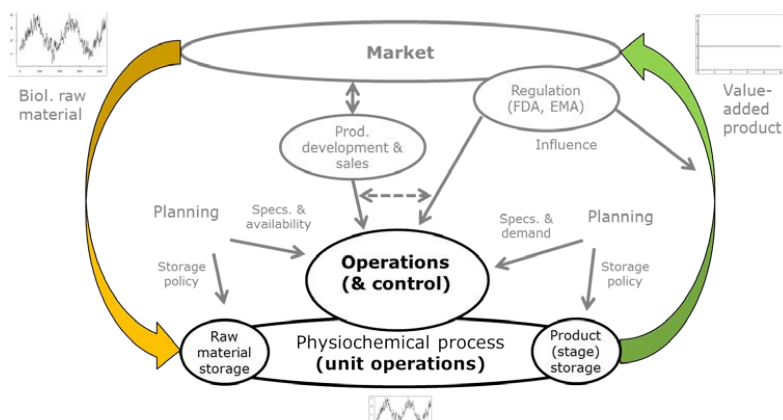
Figure 1: Factors that may directly influence the operational optimality achievable in the process: raw material / process variability, also regulation and planning.

Experiences from Assessing Plantwide Control Structures of two Bio-Based Production Sites

In the course of the PhD project, two Danish plants (a pectin production- and a pharmaceutical plant) have been visited and observed in great detail with the ambition of assessing the viability of the above-mentioned plantwide control structure synthesis frameworks. In the case of the pectin plant, where the overall operational paradigm is continuous, heuristic plantwide control aspects were found to be applicable and insightful. Through parallelization of batch units (upstream as well as downstream) and the presence of large surge tanks, and not lastly a process that is robust against contamination, continuous operation becomes feasible. However, the absence of a high-fidelity plantwide model is a limiting factor in control structure optimization, the complexity of the task is fortunately reduced by a sequential arrangement of unit operations [7]. At this point, due to unquantified input disturbances, a lack of measurements, and furthermore a disparity between required effort and prospective gains, plantwide modelling of most production sites is unrealistic. This is also true for the assessed pharmaceutical plant, where a further complication arises from the fact that the plant's operational paradigm is batch.

Conclusion

The absence of models of a quality that most researches in PWC would be used to, calls for heuristic approaches. As classical plantwide control does not account for batch plants, PWC of bio-based processes should be extended by methods and best practices connected to bio-based batch processes. Industrial norms, e.g. [8] for chemical processes, make for a good example. However, overall a number of further factors need to be taken into account, as it seems that countless influencers may limit the degree of optimality achievable in a bio-based process. Manual operation and a lack of measurements utilizable in feedback control loops are clearly limiting factors, but also the actors depicted in figure 1 can directly influence a plants operational regime. This is in contrast to many

chemical plants, where, at least for large-scale utility-intensive bulk processes, performance is benchmarked against the thermodynamic optimum. In bio-based and i.e. pharmaceutical plants, delays in a qualification or audit process are, on the other hand, much more costly than a moderate 'waste' of utilities or product. This drastically changes the process design and plantwide control scenario to be considered; future work will aim at collecting and formalizing these differences.

References

1. P. M. Doran, "Bioprocess Development," *Bioprocess Eng. Princ.*, pp. 3–11, 2013.
2. C. Mandenius and N. J. Titchener-Hooker, *Measurement, Monitoring, Modelling and Control of Bioprocesses*, vol. 132. 2013.
3. A. Zheng, R. V Mahajanam, and J. M. Douglas, "Hierchical procedure for plantwide control system synthesis," *AIChe J.*, vol. 45, no. 6, pp. 1255–1265, 1999.
4. W. L. Luyben, "Heuristics for Plantwide Control," in *Plantwide Control: Recent Developments and Applications*, 2012.
5. S. Skogestad, "Economic Plantwide Control," in *Plantwide Control: Recent Developments and Applications*, 2012.
6. N. V. S. N. Murthy Konda, G. P. Rangaiah, and P. R. Krishnaswamy, "Plantwide Control of Industrial Processes: An Integrated Framework of Simulation and Heuristics," *Ind. Eng. Chem. Res.*, vol. 44, no. 22, pp. 8300–8313, 2005.
7. G. Stephanopoulos, "Synthesis of Control Systems for Chemical Plants - A Challenge for Creativity," *Comput. Chem. Eng.*, vol. 7, no. 4, pp. 331–365, 1983.
8. ANSI/ISA-88.01-1995, "Batch control - Part 1: Models and terminology," 1995.

Chitta Ranjan Behera

Phone: +45 71435647

E-mail: cbeh@kt.dtu.dk

Supervisors: Gürkan Sin

                Krist V. Gernaey

PhD Study

  Started: August 2016

  To be completed: August 2019

A multi-scale biofilm model development and validation for a pilot scale Anammox based mainstream process

Abstract

The mainstream Anammox process is pivotal to achieve energy neutrality in the wastewater treatment plant (WWTP). Unlike sidestream processes, mainstream Anammox operation poses several challenges, such as the low influent nitrogen concentration, higher sCOD/NH4+ ratio, low temperature etc. These challenges are motivating researchers to explore various configurations (based on reactor type and biofilm media) to achieve a stable mainstream Anammox operation (especially surpassing NOB activity) with higher nitrogen removal efficiency. In this study, a one dimensional biofilm model for pilot scale integrated fixed film activated sludge (IFAS) reactor is developed assuming carriers as flat sheet. To this end the developed model is validated on a pilot scale mainstream Anammox process experimental data.

Introduction

The Anammox based nitrogen removal process has been widely used for sidestream nitrogen removal in wastewater treatment plants (WWTPs), and helps to bring down the aeration energy demand in the activated sludge (AS) reactor and the external carbon demand for the denitrification process. The success stories of the sidestream Anammox process along with a growing energy neutrality demand has motivated researchers to explore the mainstream Anammox application for sewage wastewater treatment. There are several Anammox based process configurations [1, 2] used for mainstream nitrogen removal with various reactor designs (CSTR, SBR, PFR etc.) and biofilm types (granular, fixed film etc.). A recent studies [1] based on a pilot scale integrated fixed film activated sludge (IFAS) reactor has demonstrated a stable mainstream Anammox process operation at low influent nitrogen concentration and higher sCOD/NH4-N ratio.

In order to carry out model based analysis for sidestream Anammox processes several biofilm models [4, 5] have been developed and validated. However, for the mainstream Anammox process, especially for the IFAS process, a calibrated biofilm model needs to be developed for facilitating model based analysis. Calibration of such a biofilm model is strongly dependent on the final objective of the modelling project, where the model could be used for applications such as design of experiments, prediction of process performance during plant-wide simulation and optimization. Several schools of thought are used when performing model calibration such as a systems analysis approach by using parameter estimation theory and a comprehensive sensitivity/identifiability analysis, and an expert approach which mainly depends on plant/process experiences.

In this study, a multiscale biofilm model for the IFAS system is developed by extending a granular biofilm based model [4]. The main difference here is that the carriers are model as 1-D flat sheet to simplify the computational intricacy. To this end, the developed biofilm model is validated using the experimental data reported in [1].

Results and discussions

The developed one dimensional multiscale model (as shown in Figure 1) is simulated using the influent waste water concentration reported in the literature [1]. The biofilm is divided in to 49 different layers and in each layer the concentration profile of both soluble and particulates are plotted in the Figure 1. The effluent nitrate concentration is quite high because the activity of NOB bacteria are not fully suppressed (see Figure 1). It is also quite clear that the Anammox bacterial are residing inner side of the biofilm whereas the AOB and NOB and HB are on the outer layers. The developed

model is able to predict the total nitrogen removal efficiency as well as other effluent concentration (see Table 1). In this period the removal rate was quite low as there was not enough biomass present in the reactor [1].

Table 1: Validation of model prediction with experimental data.

Parameters	Experimental [1]	Simulation
Effluent NH_4^+ (mg/l)	13.8	12.5
Effluent NO_3^- (mg/l)	11.8	11.41
Effluent DO (mg/l)	0.44	0.44
Nitrogen removal efficiency (Kg N/m3.d)	0.018	0.025
TN removal efficiency (%)	35.34	32.45

Conclusion

A carrier based biofilm model is developed assuming 1 dimension flat sheet to explain the dynamics of a pilot scale IFAS reactor used for the mainstream Anammox process. The developed model is able to predict the effluent concentration and nitrogen removal performance with higher accuracy. It is believed that the developed biofilm model will further facilitate carrying out plant-wide impact assessment, and will furthermore allow exploring the potential combination of IFAS with other technologies to achieve energy neutrality.

References
1. Malovanyy, A., Trela, J. and Plaza, E.,(2015). Bioresource technology, 198, pp.478-487.
2. Lotti, T., Kleerebezem, R., Hu, Z., Kartal, B., De Kreuk, M.K., van Erp Taalman Kip, C., Kruit, J., Hendrickx, T.L.G. and Van Loosdrecht, M.C.M.,(2015).Environmental technology, 36(9), pp.1167-1177.
3. Henze, M., (2000). IWA Scientific and Tech. Rep.
4. Hao, X., Heijnen, J.J. and Van Loosdrecht, M.C., (2002). Water research, 36(19), pp.4839-4849.
5. Vangsgaard, A.K., Mutlu, A.G., Gernaey, K.V., Smets, B.F. and Sin, G., Journal of Chemical Technology & Biotechnology, 88(11), pp.2007-2015.
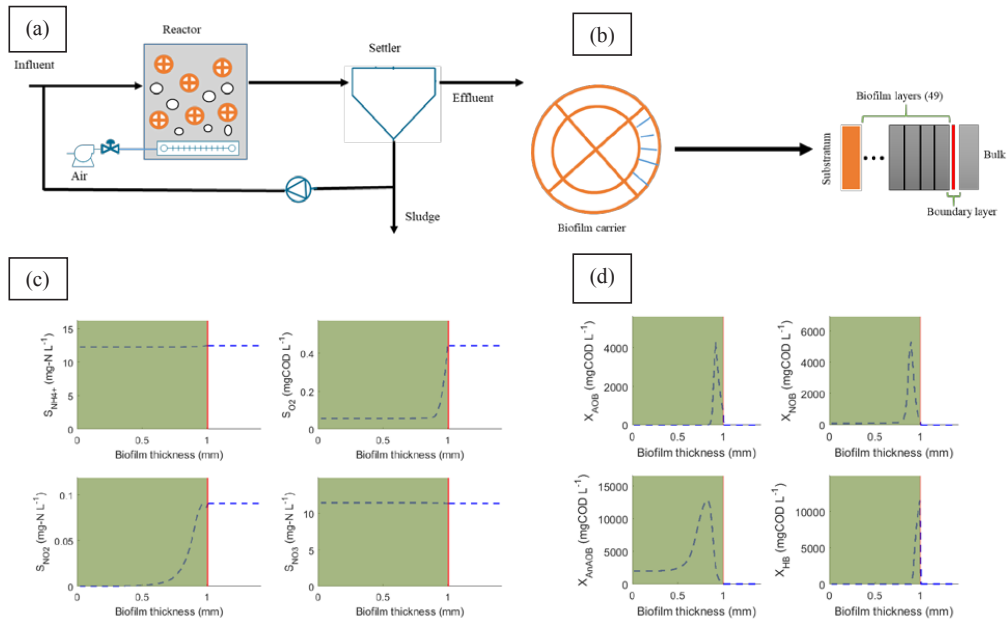
Figure 1: (a) Schematic diagram of the pilot scale reactor, (b) multi scale modelling approach illustration, (c) concentration profile of soluble components inside a carrier, d) concentration profile of particulate components inside a carrier.

Jonas Bisgaard

Phone: +45 20837204
E-mail: jonbis@kt.dtu.dk

Supervisors: Krist V. Gernaey
Jakob K. Huusom
Ole Skyggebjerg, Freesense ApS

PhD Study
Started: September 2017
To be completed: August 2020

Closing the knowledge gap in large-scale fermentations
– Free floating sensor particles

Abstract

Mixing phenomena are regarded as a major factor in unsuccessful scale-up of bioprocesses. Practical constraints related to acquisition of detailed process data leaves behind an extensive knowledge gap in the rough environments of large-scale reactors. With the use of novel free-floating sensor particles developed by Freesense ApS, it is now possible to obtain measurements from everywhere inside the reactors, thereby enabling data driven exploration and optimization. In this initial study, the sensor particles have been tested in a pilot-scale stirred tank reactor ($V_L = 0.7$ m³) at different impeller speeds. Circulation times and spatial distributions were determined based on measurements of hydrostatic pressure by the sensor particles. In addition, axial velocities were determined by the sensor particles and compared to CFD simulations of the tank. The determined circulation times were found to be proportional to mixing times determined by tracer experiments. The results have proven the sensor particles as a powerful tool for characterization of mixing during fermentation processes.

Introduction

When scaling up bioprocesses from pilot scale to industrial scale, practical limitations concerning design and monitoring emerges. Even though CFD is considered a potentially useful tool to better understand the effects of scale on bioreactor performance, its practical usefulness is hampered by the lack of full-scale bioreactor data, providing a detailed picture of the real conditions in a tank, and not just at a single point. With technological advances it is now possible to fit multiple sensors into free-floating particles with a reasonable size of Ø45 mm that can gather data on both gradients (pH, temperature) in process parameters and information about the flow characteristics throughout the bioreactors. Two useful features about the flow can be determined by the sensor particles: Axial distributions and circulation times. Circulation time is proportional to the mixing time and is a useful measure of the degree of mixing in the bioreactor. The mixing time in a stirred reactor can be approximated by $t_m \approx 4 t_c$ [1] or by $t_m \approx 5 t_c$ [2].

Specific Objectives

Development of a simple method for determination of axial distributions of the sensor particle and determination of circulation times inside stirred bioreactors, and to show that the calculated circulation times are correlated with the corresponding mixing times, determined by tracer responses at the same conditions.
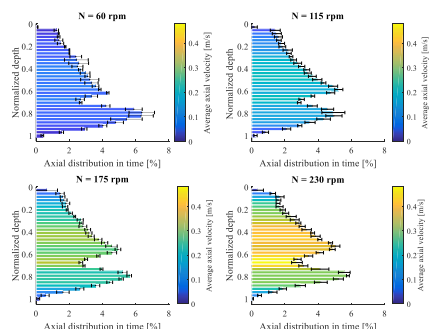
Figure 1: The axial distributions of the sensor particles in different compartments of equal size and at different speeds of impeller rotation. The y-axis is normalized to the liquid height (i.e. 0 = top and 1 = bottom) and the x-axis shows the percentage of the total time that the particles spent in each compartment. The average axial velocity can read from the color bar.

Results

Figure 1 shows the axial distributions of the sensor particles at impeller speeds: N = 60 rpm, N = 115 rpm, N = 175 rpm and N = 230 rpm. The y-axis is normalized to the liquid height (i.e. 0 = top and 1 = bottom) and the x-axis shows the percentage of the total time that the particles spent in each compartment. The average axial velocity can be read from the colorbar.

A comparison between the mean circulation times determined by the sensor particles and experimentally determined mixing times are shown in Figure 2. The circulation and mixing time were determined at the four different agitation levels.
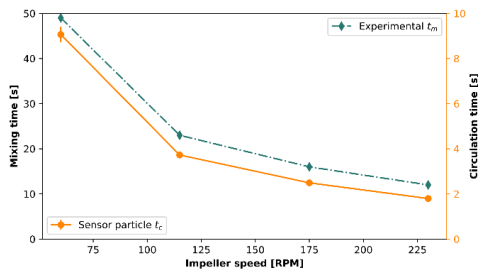
Figure 2: Mean circulation times determined by sensor particles ($\circ$) and mixing times determined by traditional tracer experiments ($\diamond$). It is evident that the circulation times and mixing times are correlated.

In Figure 3, the axial velocities determined by the sensor particles are compared to CFD simulations. The figure layout is similar to Figure 1, but here the axial velocities are presented on the x-axis instead of the color bar.
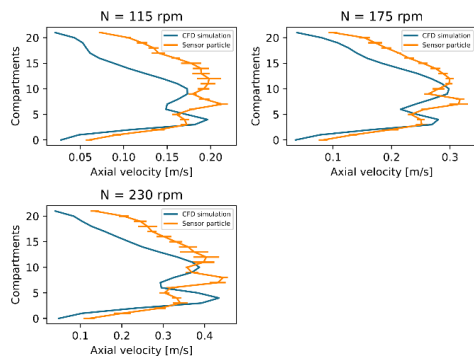
Figure 3: Comparison of axial velocities determined by the sensor particles and by CFD simulations. The compartments on the y-axis represent the liquid height of 0.94 m.

Discussion

It is evident that the axial distributions of the particles are independent of the impeller speed, except at low degrees of agitation. It is likely that this is due to fact that the drag force and small density deviation between the particle and the liquid has higher impact at low impeller speeds. It appears that the particles move in the same pattern, but with higher velocities (compartments are visited more often but at shorter time intervals). This information can be used to detect areas with deficient mixing inside large-scale bioreactors.

The circulation time seems to correlate very well with the mixing time determined by tracer experiments. The low standard deviation in the mean circulation times, together with the correlation with the experimental mixing times, suggests that the particles can be used as a reliable method to determine circulation times in stirred reactors. When comparing to axial velocities determined by CFD simulations, it is evident that the profiles have similar shape, but the particles seem to generally have lower velocity below the impeller and higher velocity above the impeller than the simulation predictions. Whether this is an effect of the size of the sensor particle or the simulation setup must be further investigated.

An additional velocity peak is also present in the axial velocity of the sensor particle. This is definitely a result of the size of the particles, as they occasionally are pushed up or down on impeller impact, instead of following the radial flow of the Rushton into the wall of the tank.

Conclusions

* The axial distributions and velocities of the sensor particles can be used to examine the flow inside bioreactors.

* The circulation times determined by the sensor particles correlates with mixing times determined by tracer response $t_c \approx (1/6) \, t_m$.

* Overall the axial velocities obtained by the sensor particles are comparable to CFD predictions. However, deviations occur which must be further investigated.

References

1. Voncken, R. M. (1966). Circulatierstroming en menging in geroerde vaten. PhD thesis, University of Rotterdam.
2. Khang SJ and Levenspiel O (1976), New scale-up and design criteria for stirrer agitated batch mixing vessels, Chem Eng Sci 31,569-577.
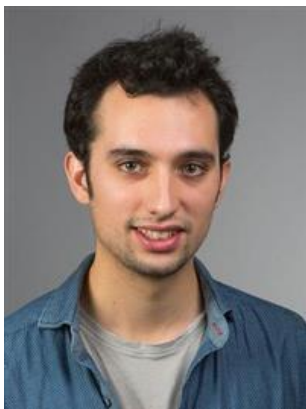
Pau Cabañeros-Lopez

E-mail: pacalo@kt.dtu.dk

Supervisors: Gernaey, Krist V.
                     Junicke, Helena

PhD Study
  Started: January 2017
  To be completed: December 2019

Using Spectroscopy for On-Line Monitoring of Lignocellulose to Ethanol Fermentations

Abstract
For many years, cellulosic-ethanol has been considered as an alternative to fossil and non-cellulosic fuels. However, the operational challenges, the lack of understanding of this process and the feed variability often result in processes operated far from its optimal point. In this project, on-line spectroscopy is used to obtain continuous and real-time information about key state variables of the fermentation, that can help to optimize the operation of cellulose to ethanol fermentation and to increase their competitively.

Introduction
Lignocellulosic ethanol production uses different types of agricultural waste (e.g., straw or woodchips) as a substrate for the fermentation. Since agricultural waste is a natural not-refined substrate, its composition change depending on the cultivar and meteorology. Also, the harsh conditions used to pretreat the raw material and to release the sugars, promote the generation of several inhibitors that affect the posterior fermentation. Altogether, result in a poorly understood process that is operated far from its optimal conditions and results in lower productivities.

Real-time monitoring allows the continuous assessment of various state variables of the fermentation, and to take control actions when deviations are found. Several options for on-line monitoring can be found depending on the monitoring target (the off-gas, the compounds dissolved in the liquid phase or the biomass). This project focusses on the monitoring of the compounds dissolved in the liquid phase and uses multi-wavelength spectroscopy in different ranges (mainly near-infrared and mid-infrared). Spectroscopy is a light-based analytical tool that allows the simultaneous quantification of different chemicals compounds from complex samples. Different on-line and at-line implementations of spectroscopic probes are used with the objective of monitoring the concentration of substrates (glucose and xylose) and products (ethanol).

Specific objectives of the study
The objective of this study is to successfully detect the concentration of substrates and products in real time so that the lack of understanding of the process can be compensated with knowledge of the actual state of the fermentation. This will allow taking control actions that optimize the operation of the fermentation.

Results and discussion
On-line near-infrared spectroscopy (NIR) was implemented in a closed loop through a flow cell as shown in Figure 1. The sample was withdrawn from the fermenter, analyzed in the flow cell and returned to the fermenter. The flow cell contained a transmission probe that records 64 spectra every minute. The fermentations were done with *Saccharomyces cerevisiae* in 250 mL reactors at pH of 6 and 30 degrees. Initially, the fermentations were done using clear YPD media. The recorded spectra are shown in Figure 2 (a). The concentrations of glucose, xylose, and ethanol were calculated from the recorded spectra using multivariate modeling. However, as shown in Figure 2, the baseline of the spectra increments with the course of the fermentation. This is because the concentration of cells increases (due to cell growth) and reflects the lights, appearing as an increased baseline. This was corrected using different data pretreatments (Figure 2 (b)). Partial least squares models were used to correlate the pretreated spectra with off-line samples measured with HPLC.
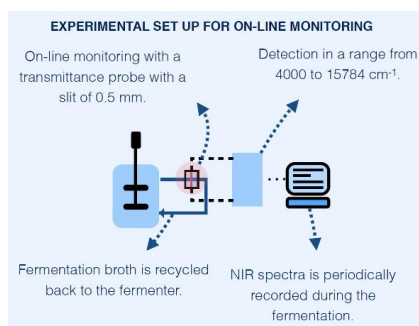
Figure 1: Experimental set-up used in to implement on-line NIR.

a)

b)
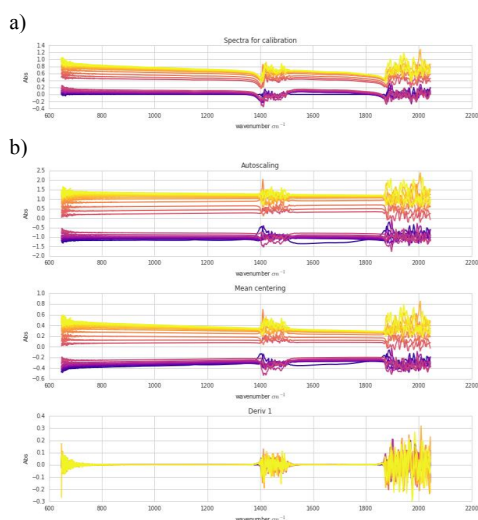
Figure 2: a) Collection of raw spectras recorded during the fermentation. b) Effect of different pretreatments on the spectra.
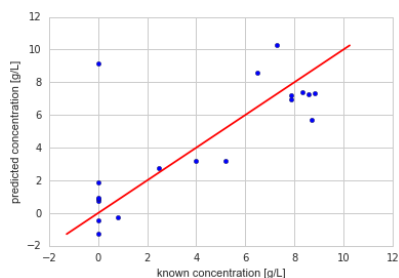
Figure 3: Predicted results against known results.

Figure 3 shows the predicted results against the reference data. Although the predicted results have a similar trend as the reference data, the predictions of the concentration of glucose are not satisfactory, and can not be used to monitor fermentation. This because the fermentation

matrix is very complex and contains many compounds that absorb in this range. In consequence, a more thorough calibration has to be done to break correlation within the data and get more accurate predictions. Another factor to take into account is the interference of the cells and other suspended solid particles with the light. In fermentations with clear media, it is not a big problem, as the reached cell density is not high enough to block the light. However, when using lignocellulosic media, the high content of suspended solid particles block the light and limit the applicability of transmittance spectroscopy. In these cases, spectroscopies based on reflected light (diffuse reflectance or attenuated total reflectance) might be more suited to monitor cellulose to ethanol fermentations as they are not so affected by the suspended solid particles.

Conclusions.

In order to compensate for the lack of understanding in the fermentation of lignocellulosic ethanol, to account for substrate variability and to operate closer to the optimal conditions, it is necessary to be able to assess the state of the fermentation in real time. The application of spectroscopic tools as a monitoring tool is an attractive because it is easy, inexpensive to implement, and can measure the concentrations of several compounds simultaneously. However, the high complexity of the media and the high content of suspended solid particles make the implementation of spectroscopy-based methods very challenging. The high complexity of the medium results on very overlapped spectra that require extensive calibration and mathematical modeling to extract the right information. On the other hand, the high content in suspended solid particles blocks the light and limits the application of spectroscopy to different types of reflectance spectroscopy.

References

1. K. Waldron (Ed.), Bioalcohol Prod. Biochem. Convers. Lignocellul. Biomass., Woodhead Publishing LTD., Oxford, 2010: pp. 315–39.
2. J.A. Iversen, B.K. Ahring Bioresour. Technol. 172 (2014) 112–120.
3. H. Juhl, O.W. Hansen, Method and device for monitoring of bioalcohol liquor prduction., WO 2009/121423 A1, 2009.
4. A.E. Cervera, N. Petersen, A.E. Lantz, A. Larsen, K. V. Gernaey, Biotechnol. Prog. 25 (2009) 1561–1581

Giovanni Cafaggi

Phone: +45 4525 2837
E-mail: gioc@kt.dtu.dk

Supervisors: Peter Arendt Jensen
                Peter Glarborg
                Kim Dam-Johansen

PhD Study
  Started: January 2017
  To be completed: December 2019

Alternative liquid fuels in burners optimized for low NO_X emissions and high burn out

Abstract
The marine industry is changing with new demands concerning high energy efficiency, fuel flexibility and lower emissions of NO_X and SO_X. A collaboration between the company Alfa Laval and Technical University of Denmark has been established to support the development of the next generation of marine burners. In this framework, the purpose of the present study is to support the development of a new generation of burners. To this end Computational Fluid Dynamic simulations and experimental methods will be used. During the project, also a spray characterization setup has been built and used to observe the changes in atomization quality at different operating conditions and liquid viscosity.

Introduction
On ships of large size, auxiliary boilers are used to meet the steam demand when the heat recovery system of the main engine is not sufficient. Currently, the marine sector is confronting new demands regarding these boilers. It is foreseen that in the next years legislators will demand decreased NO_X, SO_X and particulate emissions in coastal areas. Moreover, ship owners are increasingly interested in fuel flexibility: this would enable them to use the cheaper fuel on the local market instead of running solely on heavy oil fuels. The possibility to use renewable fuels on ships would also help in decreasing their net CO_2 emissions and fuel switching could be done according to the local legislation. An attractive application would be to use a relatively cheap renewable fuel, such as pyrolysis oil produced from wood. This fuel has some limitations as high water content, viscosity and acidity. Pyrolysis oil can be combusted in swirl stabilized burners, however only very limited work have been done to optimize burners using pyrolysis oil. The specific boiler object of this study uses a swirl stabilized liquid fuel burner, with a pressure swirl spill-return atomizer.

Specific Objectives
The goals of the project is to support the development of new marine burners that can cope with the above-mentioned demands, providing the partner companies with a technology that will help their future global competitiveness, while adding to the current knowledge in the use of renewable energy and providing improved

and verified CFD calculations on swirl stabilized flames. The first priority is to evaluate and test the combustion of multiple types of fuels in the boiler and possibly improve its performances with a new burner geometry; the second is to minimize emissions of NO_X, particulates and unburnt hydrocarbons.

At this stage of the project, the current goal is to improve the accuracy of the CFD simulations of the boiler.

CFD Simulations
Experimental and computational methods have been used in the past for simulating both liquid fuel flames and the atomization processes [1] [2] [3]. Results obtained via Computational Fluid Dynamics (CFD) provide detailed information about the local temperatures, compositions and flow fields within the furnace chamber [4]. However, due to its stochastic nature [5] and to the very small length- and time-scales at which it takes place, to simulate the droplet formation process with reasonable accuracy, huge computational resources would be required. To overcome this issue, the spray has not been directly simulated, and the fuel is instead injected into the computational domain as already formed droplets.

The commercial software ANSYS CFX has been used to do 3D CFD simulations of the boiler. During the simulation campaign, several models have been tested for turbulence, radiation and reaction chemistry. Being the CO emissions of interest for the project, the combustion was simulated with a two-step global reaction [6] [7],

while the NO_X formation can be calculated by post-processing of the results. Thanks to a sensitivity analysis, the size of the particles used to simulate the fuel spray was singled out as a crucial factor for flame stability and simulation accuracy. No documentation is given from the manufacturers regarding droplet size and velocity distribution, and the range of estimates obtained using correlations found in literature [8] proved to be too broad.

Therefore, a spray characterization setup has been built to observe the atomization quality of the nozzle and gain a better understanding of the atomization process at different operating conditions and for different fluids.

Spray Setup
The spray characterization setup was built to work at the same operating condition of the actual burner.

A measuring campaign has been conducted by using water and water-glycerol mixtures, thus reproducing some of the physical characteristics of different fuels [9] [10] for different operating conditions. The spray generated with the setup is then captured with an optical system and the pictures analyzed with a tailor made software to obtain information about droplet size and velocity distributions [11].

Full scale experimental campaign
An experimental campaign on the full-scale boiler was recently conducted to obtain further insight into the boiler operation and data to validate the CFD simulations.

The campaign included exhaust measurements for gas composition and particulate, and flame mapping for temperature and gas composition. Measurements have been taken for Heavy Fuel Oil and marine diesel, at three different loads, and by varying the excess combustion air between 1% and 6%. The data thus obtained will be used to validate the CFD simulations and to formulate suggested operation conditions for the boiler.

Current Results and Conclusions
To prepare the CFD simulations a number of different models, parameters and algorithms has been tested. While not universal and limited to the software used, the obtained combination can be considered as a starting point for future modelling. During the CFD study insights in the boiler operation has been obtained: fuel conversion, vortex shedding frequencies and positions of the recirculation zones have been determined. In addition, a sensitivity analysis showed that under the same conditions, a change from 10 to 25 μm of droplet mean diameter, leads to flame lift off.

Using the spray setup, it was possible to measure droplet size and velocities in different regions of the spray for different operating conditions and fluid viscosity. The data thus obtained has now been used to improve the accuracy of the CFD, bringing us one step closer to predict burner performances through computational methods.

Lastly, the measurements gathered during the experimental campaign on the boiler, besides being essential for validating CFD simulations, they also give a comprehensive picture of the emission variations of the boiler within its operating range.
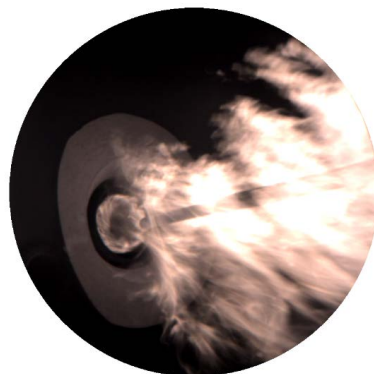
Figure 1: Auxiliary marine boiler flame with suction pyrometer. Frame of video taken during the full-scale experimental campaign.

References
1. P. Jenny, D. Roekaerts, N. Beishuizen, Prog Energ Combust 38 (2012) 846-887.
2. M. Linne, Prog Energ Combust 39 (2013) 403-440
3. Z. Ling, X. Zeng, T. Ren, H. Xu, Appl Therm Eng 79 (2015) 117-123.
4. I. Bonefačić, W. Igor, P. Blecich, Appl Therm Eng 110 (2017) 795-804
5. C. K. Westbrook, F. L. Dryer, Combust Sci Technol 27 (1981) 31-43.
6. B. Franzelli, E. Riber, M. Sanjosé, T. Poinsot, Combust Flame 157 (7) (2010) 1364-1373.
7. A. H. Lefebvre, Atomization and Sprays, Hemisphere Publishing co., 1989, p. 214.
8. A. Sänger, T. Jakobs, N. Djordjevic, T. Kolb, ILASS Europe 2014, Bremen, Germany.
9. A. Davanlou, J. D. Lee, S. Basu, R. Kumar, Chem Eng Sci 131 (2015) 243-255.
10. F. Cernuschi, C.Rothleitner, S.Clausen, U. Neuschaefer-Rube, J. Illemann, L. Lorenzoni, C. Guardamagna, H. Engelbrecht Larsen, Powder Technol 318 (2017) 95–109.
11. J. K. Park, S. Park, M. Kim, C. Ryu, S. H. Baek, Y. J.Kim, H.H.Kim and H.Y.Park, Fuel(2015) 324-333.
List of Publications
1. G. Cafaggi, P.A. Jensen, P. Glarborg, S. Clausen, K. Dam-Johansen, Proceedings of Nordic Flame Days 2017, Stockholm, Sweden.
2. G. Cafaggi, P.A. Jensen, P. Glarborg, S. Clausen, K. Dam-Johansen, Proceedings of the IFRF 2018 Conference, Sheffield, United Kingdom.

Yingjun Cai

Phone: +45 4525 2863
E-mail: ycai@kt.dtu.dk

Supervisors: Kaj Thomsen
Nicolas von Solms
Suojiang Zhang, IPE, CAS

PhD Study
Started: February 2017
To be completed: February 2020

Multifunctional ionic liquid as new electrolyte additives for Li-ion batteries

Abstract
A new type of ionic liquid based on imidazolium cations with vinyl and propanamide group and TFSI- anion was synthesized, as electrolyte additive for Li-ion batteries to stabilize carbonate-based electrolytes and improve the electrochemical properties of lithium batteries.

Introduction
Li-ion batteries (LIBs) are attractive power sources for portable electric devices, electric vehicles and energy storage systems [1-4] due to their high energy density and efficiency. Electrolytes used as a medium for charge transfer in lithium batteries greatly influence the performance with respect to cycle life, special capacity, charging/discharging rate, and safety. Current state-of-art electrolytes are highly flammable，volatile and have low conventional voltage limitation (~4.2V) based on organic carbonate. This feature prohibits the development of batteries with safe and wide operating temperature range. Ionic liquids were intensively studied as one component of the electrolyte in LIB, owing to their perfect characteristics of having low melting-temperature, being non-volatile, having high specific conductivity and having a wide ranging electrochemical window [5]. Development of ionic liquids as solvents of the LIB electrolyte was limited by: ⅰ) the high viscosity reduces the specific conductivity, ⅱ) incompatibility of ionic liquids and electrodes decrease the cyclic lifetime [6]. Fortunately, many experts are committed to develop new types of functionalized ionic liquids to enhance the performances of new LIB. Borgel et al. reported the use of quaternary ammonium-based ILs as electrolyte systems for high-voltage Li-ion batteries [7]. However, the rate performance was not satisfactory due to their high viscosity.

The introduction of cathode film forming additives to the conventional electrolytes may be an economic and effective method at the current stage [8]. Yang [9] and Hu [10] used inorganic lithium salt LiBOB and LiDFOB as electrolyte additives for the high-voltage cathode surface film. Cathode film forming additives based on organic molecules which can undergo cationic polymerization including 2, 5-dihydrofuran and γ-butyrolactone were also reported [11, 12]. Li [13] and Long et al. [14] confirmed that imidazolium based ionic liquids could be electrochemically polymerized to form a stable polymeric film on various substrates.

In this research, a new type of multifunctional ionic liquid 1-vinyl- 3-propanamide imidazole bis(trifluoro-methylsulfonyl) imide ([VPIM][TFSI]) was synthesized and used as multifunctional additive for lithium batteries. The charging and discharging properties were measured in several lithium batteries. And the effect on the water and hydrogen fluoride was also investigated, which can stabilize the LiPF6 based electrolyte.

Objective
The objective of this study is to evaluate the application of ionic liquid [VPIM][TFSI] as multifunctional additive for lithium batteries.

Results and discussion
Several electrolytes were prepared with different content of ionic liquid [VPIM][TFSI] into two standard electrolytes. The charging and discharging performances of electrolytes were investigated in different lithium batteries, containing different cathode and anode.

Figure 1: Electrode   **Figure 2:** Battery assembly

The mixture of active material, acetylene black, binder, and solvent N-methyl-2-pyrrolidone (NMP) was mixed by the method of ball-milling for 4h. Then the slurry was

coated on the current collector (aluminum foil or copper foil), after drying for 12h in the oven, we cut it into circular electrodes.

The coin cells were assembled in the glove box full of argon. Then the charging and discharging properties were measured by battery test system.

Table 1: Efficiency of electrolyte with and without IL

Cycle number	Efficiency of electrolyte without ionic liquid /%	Efficiency of electrolyte with 0.5% VPIMTFSI 0.5% VPIMTFSI ionic liquid /%
1	83.4	88
2	88.9	92.1
3	86.5	94.4

The efficiency of electrolyte without and with ionic liquid VPIMTFSI was measured in NCM622 (Lithium Nickel Manganese Cobalt Oxide) half cells. From table 1, it is shown that the efficiency of electrolyte with 0.5% VPIMTFSI is higher than that without VPIMTFSI. Figure 3 shows the discharging special capacity of LiFePO4 (lithium iron phosphate) half cells without and with ionic liquid VPIMTFSI. The discharging special capacity of electrolyte with 0.5% VPIMTFSI is higher than that without VPIMTFSI. We can get the similar results in the SiC/Li and LiTiO$_2$/Li half cells.
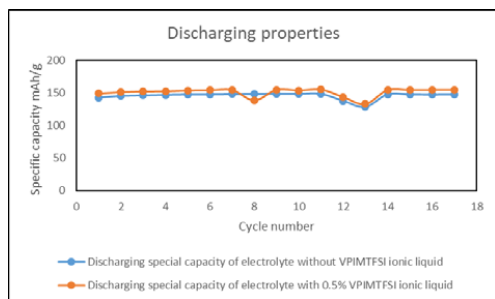
Figure 3: Discharging properties of electrolyte in LiFePO$_4$ (lithium iron phosphate) half cells.

Meanwhile, the effect of ionic liquid on the hydrogen fluoride and water of electrolyte was studied. From table 2, it can be seen that the hydrogen fluoride of electrolyte without ionic liquid increases with the time. However, the electrolyte with 1% ionic liquid is stable during one month. The similar result was obtained about the effect on the water in the table 3.

Table 2: The effect on the hydrogen fluoride

	0% ionic liquid	1% ionic liquid
Begining	35 ppm	29 ppm
7day	41 ppm	30 ppm
1 month later	58 ppm	30 ppm

Table 3: The effect on the water

	0% ionic liquid	1% ionic liquid
Begining	15.17 ppm	13.89 ppm
7day	18.61 ppm	14.21 ppm
1 month later	28.54 ppm	17.40 ppm

Conclusions

A new type of ionic liquid [VPIM][TFSI] was designed as multifunctional additive for lithium batteries. The multifunctional additive can not only keep the water and hydrogen fluoride of electrolyte in a lower level, but also improve the electrochemical performances of lithium batteries. Higher efficiency of electrolyte with 0.5% VPIMTFSI was obtained in the NCM622/Li half cells. The discharging specific capacity of electrolyte with 0.5%VPIMTFSI is higher than electrolyte without VPIMTFSI in the LiFePO$_4$/Li, SiC/Li and LiTiO$_2$/Li half cells.

References
1. J.M. Tarascon, M. Armand, Nature 414 (2001) 359.
2. P. G. Bruce, S. A. Freunberger, L. J. Hardwick, J. -M. Tarascon, Nature Materials 11 (2012) 19−29.
3. M. Armand, J.-M. Tarascon, Nature 451 (2008) 652−657.
4. J. B. Goodenough, Y. Kim, Chemistry of Materials 22 (2010) 587−603.
5. S. Fang, L. Yang, J. Wang, M. Li, K. Tachibana, K. Kamijima, Electrochim. Acta 54 (2009) 4269.
6. M. Egashira, H. Todo, N. Yoshimoto, M. Morita, J. I. Yamaki, Journal of Power Sources 174 (2) 2007 560-564.
7. V. Borgel, E. Markevich, D. Aurbach, G. Semrau, M. Schmidt, J. Power Sources 189 (2009) 331.
8. C. Korepp, W. Kern, E. A. Lanzer, P. R. Raimann, J. O. Besenhard, M. Yang, K. C. Möller, D. T. Shieh, M. Winter, J. Power Sources 174 (2007) 637.
9. L. Yang, T. Markmaitree, B. L. Lucht, J. Power Sources 196 (2011) 2251.
10. M. Hu, J. Wei, L. Xing, and Z. Zhou, J. Appl. Electrochem. 42 (2012) 291.
11. L. Yang, B.L. Lucht, Electrochem. Solid-State Lett. 12 (2009) A229.
12. L. Yang, B. Ravdel, B. L. Lucht, Electrochem. Solid-State Lett. 13 (2010) A95.
13. W. Zhang, Y. Li, C. Lin, Q. An, C. Tao, Y. Gao, G. Li, J. Polym. Sci., Part A: Polym. Chem. 46 (2008) 4151.
14. M. D. Green, D. Salas-de la Cruz, Y. Ye, J. M. Layman, Y. A. Elabd, K. I. Winey, T. E. Long, Macromol. Chem. Phys. 212 (2011) 2522.

Simoneta Caño de Las Heras

E-mail: simoca@kt.dtu.dk

Supervisors: Seyed Soheil Mansouri
                   Ulrich Krünhe

PhD Study
  Started: September 2018
  To be completed: August 2021

Development of a Virtual Educational Bioprocess Plant

Abstract

Bioprocesses are experiencing a fast growth with the involvement of complex technologies and therefore, creating an educational need for trainees and new graduates. However, providing an understandable hand-on experience for an increasing number of students and trainees is almost impossible due to time and resources limitations as well as safety reasons. On the other hand, simulators are able to support a learning based on action as the users are in control of the decision-making. Even so, the simulators commonly used in engineering education are not prepare to explain the choices made by the user and consequently, failing in providing a complete educational experience to the unexperienced students. Therefore, in this project, it is created a software that integrates the simulation of complex models with a thoughtful learning design and involving motivational elements.

Introduction

The use of simulators as learning tools in higher education started in the 1970s and many areas such as wastewater treatment [1], [2] robotic [3], electronic circuit [4], control [5], etc. have so far benefited from its use. One of the disciplines that benefits from virtual laboratories is biochemical engineering. Biochemical engineering is based on full-scale industrial processes, and providing a hands-on experience for the student can be a challenge considering safety and costs. However, the most common computational tools for teaching bioprocess development, design and implementation lack of a learning design and require previous knowledge of the systems. This is due to the design of commercial simulators commonly aims to solve a specific question and/or develop a process. On the other hand, students require for an instructional computational laboratory to learn something practicing engineers are assumed to already know [12]. That something needs to be defined by carefully designed learning objectives. In addition, the acquisition of knowledge and skills can be facilitated through an enjoyable experience and considering the new habits and interests of the students [6]. Therefore, it is integrated game elements inside the software platform.

Specific Objectives

The novelty in this project will be the creation of a software tool with the help of a thoughtful learning, real industrial conditions and the consideration of the fast growth in bioprocess. Consequently, this computational-aided tool is designed supported on three milestones:

1) A careful learning design.
2) The use of templates models that can be displayed, reuse and modified [7].
3) A motivational approach based on the use of gamification.

The main challenges are:

– To provide an organized and free-flowing learning experience. To solve this problem, clear directions are supplied in the platform. Also, the software content should be trusted by the user and reference are provided.

– It must allow and encourage the modification of the model. Also, template models creates the model with a combination of a set equations. This equations can be combined by the user to generate a new model that can be stored and reuse.

– The learning process should be enjoyable and promoting reflection, decision-making and critical thinking.

Current state of development

The computational tool is the result of the implementation of a previously developed computer-aided modeling framework [8]. In this first stage, the software has been developed as a desktop application, although it is expected to have part of the content and activities in internet. Furthermore, the software is written

in python programming language as it is *interpreted, interactive, object-oriented*, and it allows the creation of GUI with the PyQt toolkit. As a free object-oriented open-source language, python is suited to create the template model library.

The current platform is preliminary called FermProc (Fig. 1) and so far, it is focused in the content related to fermentation. Further than a simulator for different bioconversion, FermProc has implemented different mini-games using fermentation concepts (with an example in Fig. 2), the possibility to modified the different parameters of the chosen models with information related to the parameter theory and range (Fig. 3), the creation of a problem-solution database, and multimedia resource.
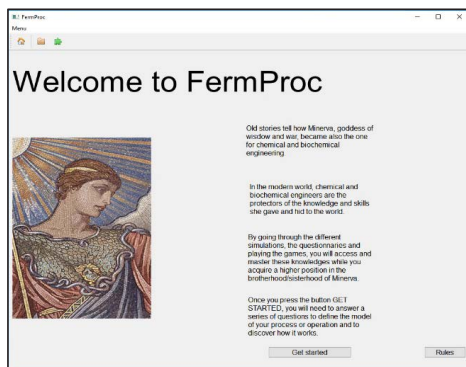
Figure 1. The initial screen of FermProc, in which it is introduced the space of action. In this screen, the users get introduce to how Minerva, goddess of Chemical and Biochemical Engineering, has hidden and protected her knowledge in chemical and biochemical processes and the user has the possibility to discover it by going through the software.
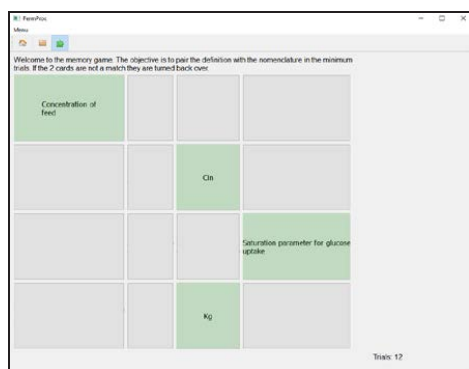
Figure 2. A memory game to associate the parameters and its nomenclature. In the advances levels, it is introduces the association of the parameters and its SI units.
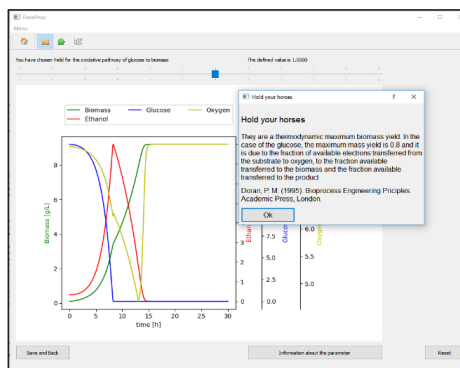
Figure 3. Screen for the modification of parameters inside the model. When the users choose an out-of-range value, the software display a warming window with the information and reference of the limits of the parameter.

Conclusions

A bioprocess simulator designed for and by students with a prime pedagogical aim can provide the students and trainees with a tailored tool for the understanding of the complex theoretical knowledge as well as train critical-thinking and decision making abilities inside bioprocess operations.

References
[1]   D. Group, "WEST," 2017. [Online]. Available: https://www.mikepoweredbydhi.com/products/west. [Accessed: 15-Jan-2018].
[2]   Ifak e.V, "SIMBA." [Online]. Available: http://www.inctrl.ca/software/simba/. [Accessed: 15-Jan-2018].
[3]   E. Guimarães *et al.*, "REAL: A Virtual Laboratory for Mobile Robot Experiments.," *IEEE Trans. Educ.*, vol. 46, no. 1, p. 37, 2003.
[4]   G. J. Kerala, "KTechLab," *2007*. [Online]. Available: http://www-mdp.eng.cam.ac.uk/web/CD/engapps/ktechlab/ktechlab.pdf. [Accessed: 15-Jan-2018].
[5]   J. Sanchez, F. Morilla, S. Dormido, J. Aranda, and P. Ruiperez, "Virtual and Remote Control Labs Using Java: A Qualitative Approach," *IEEE Control Syst.*, vol. 22, no. 2, pp. 8–20, 2002.
[6]   K. Kiili, "Digital game-based learning: Towards an experiential gaming model," *Internet High. Educ.*, vol. 8, no. 1, pp. 13–24, 2005.
[7]   M. Fedorova, G. Sin, and R. Gani, "Computer-aided modelling template: Concept and application," *Comput. Chem. Eng.*, 2015.
[8]   S. C. de las Heras *et al.*, "A Methodology for Development of a Pedagogical Simulation Tool used in Fermentation Applications," *Comput. Aided Chem. Eng.*, vol. 44, pp. 1621–1626, Jan. 2018.

Ricardo Fernandes Caroço

Phone:	+45 5270 3333
E-mail:	rcar@kt.dtu.dk

Supervisors:	Jakob K. Huusom
	Jens Abildskov
	Paloma Santacoloma, CP Kelco

PhD Study

Started:	September 2015
To be completed:	February 2019

Monitoring of Bioprocesses: Merging PAT, Kalman and Uncertainty

Abstract

The project focuses on assessing the challenges of implementing model-based monitoring strategies in industrial settings, exploring the development possibilities of a cross-(bio)industry workflow/guideline. A case-study focusing on the performance monitoring of a pectin batch extraction process is conducted in a way to take advantage of the first principle dynamic models, which describe the reactions and transport phenomena of the pectin extraction, that were developed for the considered critical quality attributes: pectin bulk concentration, degree of esterification (%DE) and intrinsic viscosity (IV). An wholesome procedure for a full-scale monitoring is envisioned, making use of state-of-the-art state estimation algorithms together with chemometric models, with the ultimate goal of providing the process operators with guidelines for process optimization and a decision making tool within a known uncertainty range.

Introduction

Monitoring and control strategies are crucial in several stages of a product/process life-cycle, from development to the optimization of an established process. These strategies are used to address a large number of objectives such as process understanding, troubleshooting, real-time control actions and continuous process optimization. Currently one of the major limitations in the biochemical industry is the multitude of disturbances that each process is subjected to, which can derive from processing biological feedstock. Nowadays the large segments of the industry operate in a heuristic recipe-driven way, dependent on rule-of-thumb experience which results too often in batch-to-batch discrepancies. These difficulties can be mitigated by an appropriate monitoring strategy and model building comes as an integral part of such a strategy. Models supply a representation of the underlying physical/chemical phenomena, allowing prediction and subsequent control decisions.[1]

Monitoring and control strategies applied in the biochemical industry have not reached the same level of maturity as the traditional bulk pharma & chemical industry, within the process analytical technology (PAT) initiative framework,. Furthermore the use of mechanistic models and online optimization algorithms is still new. There is an opportunity to explore state feedback algorithms which combined with PAT allow for the development of robust feed-forward monitoring and consequently a way to reduce process variations, improve product quality and lower the cost of operation.[2][3]

Workflow Formulation

The ultimate goal of the project is to develop a workflow/guideline that provides a knowledgeable and tailored approach to monitoring bio-process operations in plants using soft sensors.

Two types of soft sensors described in the literature: model-driven and data-driven: data-driven are based on chemometric models, informed by historical process data to predict other process variables on-line; and model-driven are mainly based on established models that describe mass and energy balances, known as the "First Principles", making use of Kalman filters or extended Kalman filters.

The work intends to provide a methodology for applying wholesome monitoring schemes within the PAT framework (including identification of critical quality attributes (CQAs) and critical process parameters (CPPs)), as well as to make use of Bayesian and Kalman techniques in order to monitor robustly the desired key performance indicators, and their uncertainty.

The focus will be set on the models, which have to be complex enough to be able to accurately predict the dynamics of the system, but still usable to day-to-day application of the strategies in the plants.

Some of the major questions raised by this effort are:

1) <u>Identifying what are currently the monitoring strategies employed in the industry.</u> Is there currently any systematic logic behind the selection of a given approach?

2) <u>Theory vs Industry reality.</u> What is feasible to implement in a settled industry? What is needed from a current process to develop a monitoring strategy? What needs to be abdicated from a theoretical optimal strategy, to fit with the real process possibilities?

3) <u>Relationship between type of process and monitoring strategy.</u> Is there any correlation between the type of process and a type of strategy, or is it a "case-by-case" scenario? Is it possible to construct a decision making tool based on the type of process, monitoring objective, available information, etc. This effort will be done in an iterative way and taking into account the projected case studies. The final goal is set on the development of a methodology, critically re-visiting what was previously done in the case-studies and testing it on a variety of different scenario cases.

Raw Material as a source of uncertainty – Pectin Extraction

Production comprises four core steps: extraction from the plant material, purification of the liquid extract, precipitation of pectin from the solution, and further de-esterification and/or amidation of the high methylester pectin with acid or alkali.[4]

This process is subjected to wide quality fluctuations in the raw material which result in production performance issues and undesired deviation of the critical quality attributes (CQA) of the end product: degree of esterification (%DE) and intrinsic viscosity (IV). Peel fingerprinting and determination of mechanistic model parameters that are inherent to each peel is a way to include this variability in the model. Figure 1 represents a partial least squares regression of the DE_0 (initial DE in peel) obtained using NIR spectra of the peels and an analytical reference.
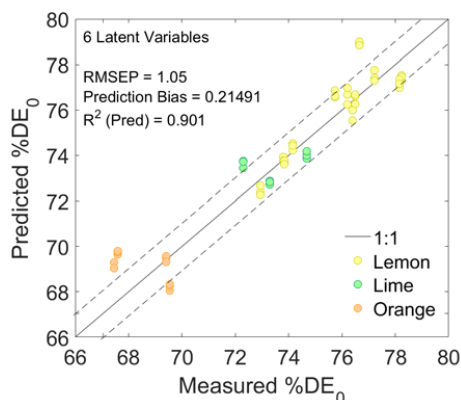
Figure 1: Externally validated PLS model for DE_0. The different colors represent different citrus fruits

The development of this PAT application allows us to obtain predicted values, and their uncertainties, for key parameters of the mechanistic model.

This project is continues as well previous efforts to model this process, and will try to reach plant scale implementation of an adequate monitoring strategy. The mechanistic model should be as such that describes the dynamics of the extraction that are immeasurable or that are not possible to measure, in a timely manner.

Work towards model robustness is key as the parameters that describe the models were tuned based pilot plant data and have now to be verified to describe production process behavior and validated to for a variety of different raw material and conditions, to ensure the which shows that the model is able to cope with the discrepancies in the raw material, allowing the product quality to hold consistently at the required standards despite variations. To take this into account the monitoring strategy has to be thought as whole and every step of that leads to the process (type of raw material, conditioning, handling, etc.) should be considered, as well as possible hybrid approaches, utilizing data obtained data-driven soft-sensors.
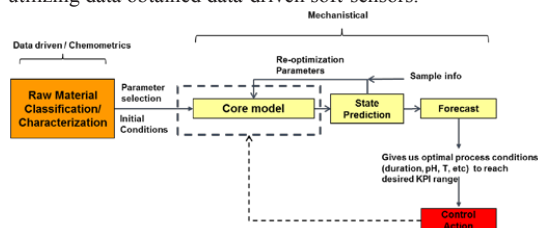
Figure 2: Representaion of an integrated monitoring strategy approach.

The integrated monitoring strategy will involve a combination of first principle models with chemometric data-driven models, supplemented with online process measurements such as volume, temperature, pH as well as discrete sampling for NMR analysis at-line (Figure 2).

References
1. D. Dochain (Ed.), Bioprocess Control, Control Systems, Robotics and Manufacturing Series, ISTE, London, UK., 2008, p. 11-16.
2. L. R. Formenti, A. Nørregaard, A. Bolic, D.Q. Hernandez, T. Hagemann, A.-L. Heins, L. Mears, M. Mauricio-Iglesias, U. Krühne, K. V. Gernaey. Challenges in industrial fermentation technology research. Biotechnology Journal, 9(6), 727–38.
3. J. K. Huusom. Challenges and opportunities in integration of design and control. Computers & Chemical Engineering, 81, 138–146.
4. CP Kelco. GENU® pectin Book. 2008.
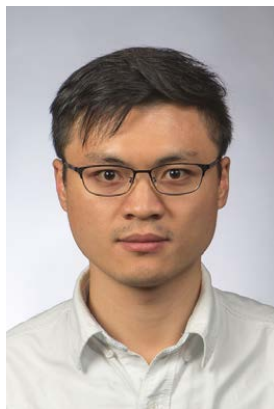
Yuqiu Chen

Phone: +45 5274 2015
E-mail: yuqch@kt.dtu.dk

Supervisors: John M. Woodley
                Georgios Kontogeorgis

PhD Study
    Started: November 2017
    To be   November 2020
completed:

Integrated ionic liquid and process design involving Separation Processes

Abstract

In the process industries, separation represents a fundamental step to reach the products quality and purity required by the market. Most separations involving mixtures with low relative volatilities as well as CO2 removal are energy intensive. Likewise, downstream separations from bioreactors are difficult because of relatively small amounts of products in large amounts of reactants and carriers such as water. Ionic liquids (ILs) based separation is being paid more attention as a potentially sustainable and energy efficient technology due to attractive features such as non-volatility, good solubility and selectivity. In this work, a systematic method that combines group contribution (GC)-based property prediction models and UNIFAC models for ILs (UNIFAC-IL) is presented, for use in computer aided molecular design (CAMD) and process design.

Introduction

As a fundamental step in the process industries, separation processes accounts for 10-15% of the world's energy consumption [1]. Its efficiency could drive the future development of the industry in terms of energy consumption and capital investment. Therefore, intensified separation alternatives are attractive, especially for those involved with energy intensive separation processes. In bio-processes, the downstream separations that contribute a major cost in manufacture are usually difficult because relatively small amounts of products should be recovered from dilute solutions [2]. Separation of close-boiling, azeotropic mixtures, and CO2 removal are examples of high energy consuming processes [3]. It is advantageous to investigate new technologies that allow energy efficient operation for such energy intensive or difficult separation processes.

Among many emerging separation technologies, the use of ionic liquids (ILs) as solvents is being considered because of their non-volatility and therefore low energy consuming solvent recovery operations [4]. Additionally, unlike organic solvents that may also be classified as volatile organic chemical (VOCs), which would escape into the atmosphere for their high volatilities, ILs exhibit attractive features such as almost negligible vapor pressure, low-melting point, and high thermal and chemical stability. Moreover, ILs have been found to provide good solubility and selectivity, which are important for separation processes. Therefore, ILs provide potential alternatives for the replacement of VOCs in many separation processes. A common IL-based extractive distillation process can be found in Figure 1, where the distillation column is used to separate the light key component, 1, from the heavy key component, 2, and the entrainer (IL); subsequently, the IL is regenerated by combining a flash drum and an air-operated, atmospheric stripper.
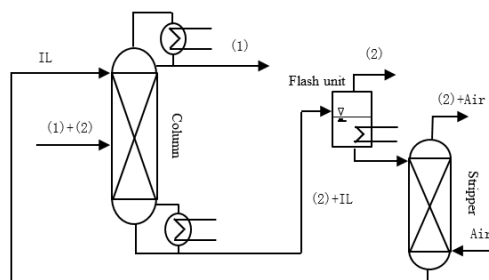
Figure 1. IL-based extractive distillation process

Generally, ILs consist of diverse organic cations which are attached to various substituents and organic or inorganic anions. This results in more than several thousand possible ILs. Finding optimal ILs for specific separation tasks by the usual trial-and-error approach can, therefore, be time consuming and expensive due to the numerous ILs that may be considered as potential solvents. To overcome the limitations of such selection

methods, CAMD, a systematic approach that integrates property predictive models and optimization algorithms to reverse engineer molecular structures with unique, is ideally suited. In this way, tailor-made ILs can be generated by adjusting the cations, anions, and substituents. Thus, the "generate and test" approach of generating candidate ILs by tailoring their properties and testing them on the desired separation task is suitable for the design of ILs, as well as for design-verification of their ability to perform specific separation tasks.

Usually, the properties of ILs directly or indirectly impact the performance of the process in which the IL is employed as solvent. However, the classical two-stage design method (molecular design followed by process design) cannot fully represent the strong interdependencies between solvent properties and process performance. Thus, some trade-offs are necessary between tailor-made solvent properties in the design of whole chemical processes. For example, in the context of an extraction process, the selected solvent must offer both high capacity, selectivity and easy recovery for the species to be extracted. Alongside, properties such as viscosity and surface tension should also be considered because of their impact on the process operation and the size of processing units. In this work, an integrated approach, where CAMD and separation process synthesis design problems are solved simultaneously, is proposed.

Framework
The overall framework of the proposed integrated IL and process design method is illustrated in Figure 2. First, the problem of detailed separation processes is defined, then two CAMD based synthesis and design options can be selected for solving this problem with the required associated tools, database, thermodynamic model (UNIFAC-IL) and property models (GC-based property models). Third, the solution of the formulated mixed-integer non-linear programming (MINLP) problem is further evaluated by means of process analysis or simulation. Finally, the optimal ILs and the corresponding optimal flowsheets with the best overall process performance can be identified.
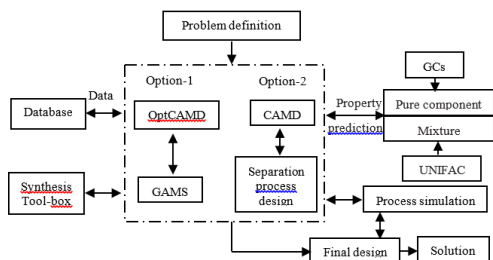
Figure 2. Framework of the integrated IL and process design

In our previous work [5], a comprehensive database has been created by collection of physical properties of ILs from numerous literature sources and also by apriori generation of new ILs. The database has 4960 ILs, out of which around 300 have been reported to exist. There are 7 cations and 16 anions.

Properties of ILs are essential for the design of products and processes containing ILs. To date, only a small number of ILs have been reported and the available experimental data on their properties is still scarce and limited to the well-studied ILs. Therefore, empirical or theoretical methods are promising and alternative ways to obtain the required information of their properties. In this proposed integrated method, two types of property model: GC-based pure component property models and GC-based mixture property models are considered. Because of the molecular structure of ILs, they are also regarded as "designer" solvents, similar rules of CAMD for traditional organic solvent are also introduced to IL design in this work. As well as VOCs, the predictions of solubility and phase equilibria are essential for the design of ILs as solvents in separation processes. In the present work, the UNIFAC-IL thermodynamic model is employed since it can provide desirable prediction results [6].

Integrated with UNIFAC-IL model and GC-based models for physical properties of ILs, a MINLP problem is formulated. By solving this problem, the main objective of this work that simultaneously to identify optimal IL and the corresponding flowsheet configurations with the best economic performance, subjecting to relevant constraints on molecular structure, IL properties and operating conditions, can be achieved.

Conclusion
A systematic method combining GC-based property models, UNIFAC-IL models, CAMD and process design has been developed. By using this integrated design method, the IL molecular structure and the process variables are optimized simultaneously by the formulation and solution of formulated MINLP problems.

Acknowledgements

References
1. D.S. Sholl, R.P. Lively, Nature, 532 (2016) 435-438.
2. J.M. Woodley, Computers and Chemical Engineering, 105 (2017) 297–307
3. R. Rooradi, M.-O. Bertran, R. Frauzem, S.B. Anne, R. Gani, Chemical Engineering Research and Design, 131 (2017) 440–464.
4. B.C. Roughton, B. Christianb, J. White, K.V. Camarda, R. Gani, Computers & Chemical Engineering, 42 (2012) 248–262.
5. Y. Chen, J J.M. Woodley, G.M. Kontogeorgis, R. Gani, Computer Aided Chemical Engineering, 44 (2018) 1045–1050.
6. Z.G. Lei, C.N. Dai, J.Q. Zhu, B.H Chen, AIChE Journal, 60 (2014) 3312–3329.

Valeria Chiaula

Phone: +45 4525 6813
E-mail: valchi@kt.dtu.dk

Supervisors: Anne Ladegaard Skov
Piotr Mazurek
Anders Christian Nielsen, Coloplast A/S
Jens Tornøe, Coloplast A/S

PhD Study
Started: August 2017
To be completed: August 2020

Advanced wound care adhesives with excellent moisture handling properties

Abstract
Chronic wounds, which are often manifested in elderly and diabetic patients, result from anomalies in the cellular and molecular wound repair mechanism. Such wounds can lead to significant disability, amputation and increased mortality. Here, we propose a novel, skin-friendly, industrially relevant glycerol-silicone hybrid adhesive with improved moisture handling due to the incorporation of emulsified glycerol. Various parameters will be taken into account in order to develop a relevant adhesive, in particular glycerol content, glycerol domain size and adhesive thickness to allow for a controlled moisture absorption.

Introduction

Broadly, for wounds to heal, a moist, clean and warm environment is required. A moist wound bed easily promotes growth factors and many cell types including epithelial cells to migrate, facilitating wound edge contraction. Thus, appropriate dressings play a significant role to create and maintain such an environment [1]. Silicone adhesives are silicone elastomers which are not fully crosslinked but remain close to the gelation threshold (i.e. with a low crosslinking degree) [2, 3].

Within the field of advanced wound care, silicone adhesives are currently the preferred, state-of-the-art adhesive system due to its gentle skin adhesion properties. However, due to their hydrophobic nature, current silicone adhesives for wound care are challenged when it comes to moisture handling. As fluid handling and transportation in silicones are normally limited and since silicone adhesives attach poorly to moist surfaces, basic perspiration from the user's skin can cause the dressing to lose their adhesive properties and eventually fall off. Furthermore, absorption through a silicone contact layer is usually low compared to "classic" adhesives, such as alginates or hydrofibers, which renders silicone incompatible with highly exuding wounds.

To minimize such effects, silicone adhesives with improved fluid handling would help transmitting fluid away from the interface between either skin and adhesive, or the wound and the adhesive. The consequence of fluid build-up in either type of interface can be failure of adhesion or local maceration. To overcome such scenarios, holes in the silicone layers are normally introduced in the products, which not only introduces an extra complication in the manufacturing process, but generally also provides less flexibility in the product design. Furthermore, the nature of the adhesives itself, if not properly cured, causes the adhesives to partially flow throughout the holes, therefore making those smaller.

Specific Objectives

The main objective of this project is to develop a novel, industrially relevant, skin-friendly glycerol-silicone hybrid adhesive with several new properties, including:

- Improved moisture handling due to the incorporation of emulsified glycerol;
- Beneficial skin care effects due to the incorporated glycerol.

Silicone elastomers do not provide any significant liquid transport through them, but they are permeable to water vapor, e.g. sweat. Contrarily to the hydrophobic silicone elastomer, glycerol droplets cause water to be absorbed in significant amounts. This allows for the glycerol content as a tunable parameter that directly affects the moisture handling capabilities of the hybrid adhesives since it determines the amount of water absorbed.

Experimental

In order to create the hybrid adhesives silicone and glycerol are speedmixed together and the resulting emulsion is cured. Desired amounts of silicone and glycerol were mixed at 3500 revolutions per minute (rpm) for 5 min using a dual asymmetric centrifuge

SpeedMixer DAC 150 FVZ-K. The obtained glycerol in silicone emulsions were coated with various commercial knives to obtain adhesives with thicknesses of around 0.2, 0.3 or 0.4 mm, respectively. The samples were subsequently cured at 80 °C for 1 h. The study of droplet size was performed by optical microscopy at t = 0 min and t = 60 min respectively. The images were analyzed by particle analyzer software in order to obtain the size distributions relative to glycerol domains. In water absorption experiments, specimens of glycerol-silicone hybrid adhesives of same area and thickness were immersed in distilled water. The water uptake was monitored gravimetrically over different time intervals. Samples name are formed using the pattern GX_SA, where G stands for 'glycerol' and X denotes glycerol content as phr (glycerol weight amount per hundred weight parts of silicone rubber) added to the silicone prepolymer. SA stands for "silicone adhesive".

Results and Discussion
Glycerol in silicone emulsions were prepared by applying high shear forces for a minimum mixing time, which provides sufficient shear forces for obtaining reasonably mono-dispersed emulsions for a broad range of glycerol incorporated into silicone [4]. High shear forces caused the glycerol to form discrete droplets distributed evenly within the silicone matrix. Subsequently, the emulsions were investigated with respect to the stability during 60 min using optical microscopy. Specifically, we studied changes in the size of the glycerol domains, which might occur due to agglomeration, coalescence or disproportion. Figure 1 shows G20_SA emulsions. The relative average glycerol domain sizes are reported in Figure 2. The results highlighted the stability of glycerol domain sizes over 60 min, since no changes were observed. The stability of the emulsions is a crucial parameter to control, because it directly affects the properties of the final adhesives. Since the glycerol content is a tunable parameter that influences the moisture handling properties, the droplet size may affect the moisture handling capabilities as well.
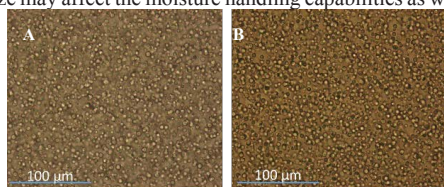
Figure 1: Optical microscopy images of G20_SA at (A) t = 0 and (B) t = 60 min after the formation of the emulsions, respectively. Scale bars correspond to 100 µm.
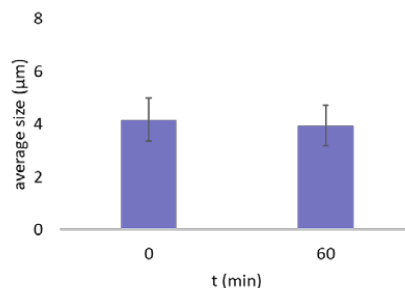
Figure 2: Average glycerol domain size of G20_SA in the emulsion as function of time.

Glycerol-silicone composites exhibit an ability to absorb water due to the hygroscopic nature of glycerol [4]. The water absorption is an effect of building up osmotic pressure. In fact, water driven by differences in osmotic pressure in the two different phases fills the glycerol domains embedded in the silicone. Therefore, four different glycerol-silicone hybrid adhesives were prepared and subsequently tested for their water uptake ability. Specimens of same area and thickness were immersed in distilled water. The water uptake was monitored gravimetrically over time. Results for the water absorption are presented in Figure 3. As expected, results showed that adhesives with higher amounts of glycerol absorbed more water than compositions with lower glycerol amounts. Furthermore, the results indicate that glycerol-silicone adhesives are versatile systems, which can be tuned according to the extent of wound exudates that need to be absorbed.
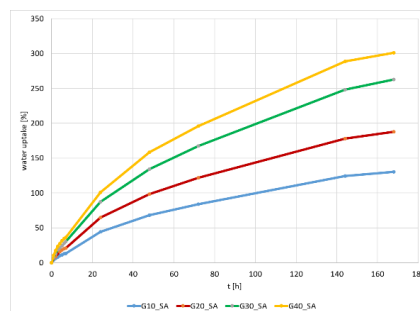
Figure 3: Water uptake profiles of adhesives with different glycerol loadings.

References

1. A. Sood, M. S. Granick, N. L. Tomaselli, *Adv Wound Care (New Rochelle)* 3 (2014), 511-529
2. S. M. G. Frankær, M.K. Jensen, A. G. Bejenariu, A. L. Skov, *Rheologica Acta* 51 (2012), 559-567
3. M. K. Jensen, A. Bach, O. Hassager, A. L. Skov, *Int. J. Adhesion and Adhesives* 29 (2009) 687-693
4. P. Mazurek, S. Hvilsted, A. L. Skov, *Polymer* 87 (2016), 1-7

Line Riis Christensen

Phone: +45 2896 0199
E-mail: linmads@kt.dtu.dk

Supervisors: Anne Ladegaard Skov
                  Ole Hassager

PhD Study
  Started: May 2016
  To be completed: April 2019

Simulation of thermal breakdown in a multi-layered stack of dielectric elastomers

Abstract
A dielectric elastomer (DE) is a thin elastomer film sandwiched between two compliant electrodes, and upon application of an electrical field the DE increases in area and decreases in height. DEs are soft transducers that can be used as actuators, generators, and sensors. When using DEs multiple types of breakdowns may occur, depending on the operating conditions. The scope of this project is to study the parameters that lead to thermal breakdown by modelling the performance of DEs during operation.

Introduction
Dielectric elastomers (DEs) are a promising group of materials that can convert electrical energy into mechanical energy and vice versa. Thus, they can serve multiple purposes as actuators, generators, and sensors. DEs are composed of a thin incompressible elastomer film sandwiched between two compliant electrodes. When an external voltage is applied to the electrodes, electrostatic forces are created between the two electrodes which cause the elastomer to decrease in height but increase in the planar directions as shown in Figure 1. When the applied voltage is switch off again, the elastomer regains its original shape. Usually a stack of DEs are used in products, such that the achievable mechanical force is increased.

Several types of breakdowns can occur during operation of DEs, and they can be categorized based on the required time until breakdown with aging mechanisms being slow mechanisms while breakdown mechanisms are somewhat instantaneously fatal. One of the most important breakdown mechanisms is thermal breakdown since this require less than 10^{-5} seconds for a breakdown to occur, and it occurs at low electric fields [2]. Thermal breakdown occurs when the energy

generated within the DE, i.e. from joule heating, is higher than the amount of energy dissipated away, which eventually leads to an exponential increase in temperature, either locally or macroscopically. The equation for Joule heating is specified as:

$$Q = \frac{V^2}{R} = E^2 \sigma(T)\, N\, d\, A \qquad (1)$$

where V is the applied voltage, R is the electrical resistance of the material, E is the electric field, $\sigma(T)$ is the electrical conductivity which follows an Arrhenius type equation with temperature, N is the number of layers in the stack, d is the thickness of each elastomer layers, and A is the cross-sectional area of the stack.

Thermal breakdown is more prone to occur in a stack of DEs than in a single layer of DE, since when DEs are stacked up, the volume increases without and an equal increase in surface area. Hence, more energy is generated while the amount of heat dissipated away is not increased significantly when DEs are stacked.

Specific Objectives
The aim of this project is to obtain a better understanding of the thermal breakdown mechanism that can occur in DEs, and furthermore investigate which parameters affect the ability of a breakdown to take place. The research will be based on modelling of the thermal breakdown mechanism of DEs using the commercially available finite element software COMSOL Multiphysics.

The stack of DEs studied is a multilayered cylindrical stack of DEs, with N layers of DEs, each having a
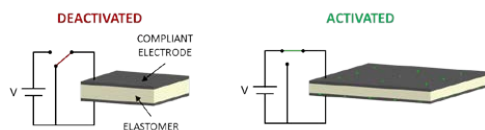
Figure 1: Illustration of the working principle of a dielectric elastomer during actuation [1].

thickness of 50 μm. The different electrical, thermal, physical and mechanical properties used as inputs to the model have been determined experimentally.

Results and Discussion
A 2D axisymmetric model of the cylindrical stack of DEs is setup in COMSOL using the Joule heating and Electromechanics multiphysics modules. It is specified that every second electrode layer is a ground electrode and the remaining electrode layers are terminals with an applied voltage (V_0) of 3.5 kV. Furthermore, heat transfer on every surface has been specified in accordance with the following equation:

$$h(T) = h_{const}(T - T_0)^{\frac{1}{4}} \tag{2}$$

where h_{const} is a heat transfer coefficient, T is the temperature at the surface of the stack, and T_0 is the temperature of the surroundings.

The influence of several parameters on the point of thermal breakdown, thus the number of layers it is possible to stack before thermal breakdown occurs, has been studied. The results from simulations with and without deformation of the stack have been compared.
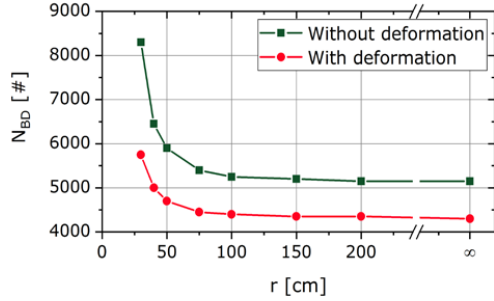
Figure 2: Possible amount of layers (N_{BD}) as a function of the radius in a stack of DEs.

The first parameter studied is the radius of the stack. From Figure 1 it is seen that when the radius increases N_{BD} decreases until a plateau value which is equal to the N_{BD} value that can be obtained when the curved surface of the stack is assumed thermally insulated ($r = \infty$). The remaining simulations are performed with thermal insulation on the curved surface. Additionally, it is found that, in theory, no thermal breakdown would occur if the radius is significantly small, due to the surface of the stack always being sufficiently large to dissipate the excess heat away.

When increasing the thickness of each layer, d, the breakdown point, N_{BD}, increases as shown in Figure 3. When d increases the electric field, E, decreases, and as seen from Equation (1) the amount of Joule heating produced in the stacked DE increases with d and E^2. Thus, the decrease in E has a bigger impact on the amount of Joule heating generated than the increase in d, leading to an increase in N_{BD} with d.

The third parameter studied is the voltage applied to the terminal electrodes, V_0. From Figure 4 it can be seen that the breakdown point, N_{BD}, decreases with increasing V_0. This may also be explained by looking at equation 1,
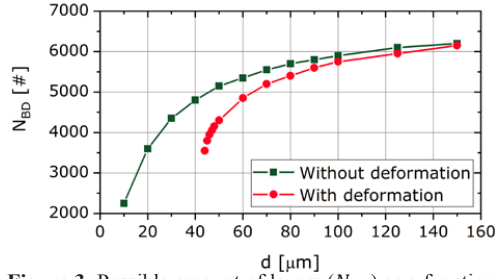
Figure 3: Possible amount of layers (N_{BD}) as a function of the thickness of the silicone layers in a stack of DEs.

since the amount of generated Joule heating increases with the applied voltage, thus the amount of layers possible to stack, before a thermal breakdown occurs, decreases.

Conclusion
An electro-thermal and –mechanical model of a multi-layered stack of DEs has been setup in COMSOL multiphysics, and from this the effect of various parameters on the point of thermal breakdown has been determined. In all cases it was found that N_{BD} for simulations including mechanical deformation was lower than for the simulations without deformation, due to the increase in electric field when including deformation.

Furthermore, it was found that when increasing the radius of the stack N_{BD} decreases, due to limiting heat transfer. Increasing the thickness of the elastomer layers leads to an increase in N_{BD} due to decrease in Joule heating. And lastly, increasing the applied voltage leads to a decrease in N_{BD} due to an increase in joule heating.

References
1. L. R. Madsen, O. Hassager, A. L. Skov, Dansk Kemi 10 (2017) 12-15.
2. L. A. Dissado, J. C. Fothergill, Electrical degradation and breakdown in polymers (1992) 1st ed. London, Peter Peregrinus Ltd.
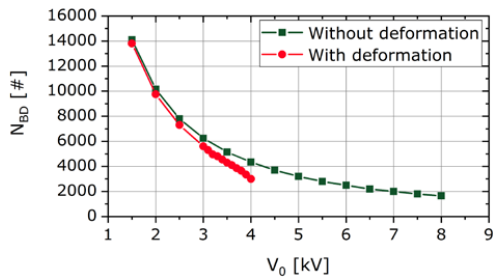
Figure 4: Possible amount of layers (N_{BD}) as a function of the applied voltage, V_0.
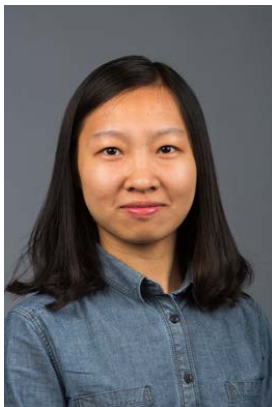
Yifan Du

Phone: +45 5290 9814
E-mail: yifandu@kt.dtu.dk

Supervisors: Peter Glarborg
Weigang Lin
Sønnik Clausen

PhD Study
Started: September 2017
To be completed: September 2020

Air-pollutant sensor system for wood stoves

Abstract
Wood stoves have been widely applied to the domestic heating system across Europe. However, wood smoke that consists of multiple gaseous pollutants and particulate matter (PM) was proved to be harmful to human health and the environment. Aiming at optimizing the batch-wise wood burning process and reducing pollutant emissions in wood stoves, a low-cost sensor-based automatic air control system for wood stoves is being developed and tested in this project. Combustion experiments and sensor tests are performed on a full-scale wood stove setup. Comprehensive emission measurements, especially advanced PM measuring methods, are conducted for the characterization of the stove emission profiles and the evaluation of the sensor performances.

Introduction

Residential wood combustion for heat supply has been used in many European countries due to the renewability and CO_2-neutrality of biomass [1], as well as the aesthetic appeal of stoves and fireplaces. However, small-scale wood combustion devices have been recognized as important sources of regional air pollution. In Denmark, the emissions of particulate matter ($PM_{2.5}$, particles with aerodynamic diameter below 2.5 micrometers) from small-scale wood-burning units have contributed to more than 60% of the total Danish PM emissions, resulting in approximately 400 premature deaths and health costs of over half a billion euros annually [2]. Besides, residential wood burning in Denmark is also one of the main sources of volatile organic compounds (VOCs) emissions and almost the exclusive substantial source of polycyclic aromatic hydrocarbons (PAHs), with many of the PAHs are known or suspected carcinogens [3], [4]. These carbonaceous particles and gaseous emissions from batch wise wood combustion are mainly the products of incomplete combustion. The adequate oxidation of combustibles only occurs with sufficiently high chamber temperature, good mixing with appropriate amounts of air, and sufficient residence time for the oxidation process [4]. For conventional wood stoves, it is hard to achieve optimal combustion by typically manual control. The combustion conditions and emission levels of conventional wood stoves are thus significantly affected by firing habits of users [5]. In order to improve stove performances and minimize harmful emissions, a novel

sensor-based air control system for wood stoves is being developed in this project, with a close collaboration between DTU and HWAM A/S. It is expected that the low-cost optical sensor system is capable of directly measuring multiple pollutants (e.g. soot and tar) in the stove chimney. The on-line signals may be implemented to the control system to further optimize the operation of the wood stove. With the automatic control system for the combustion process, the influence of inadequate user behavior is expected to be reduced.

Specific objectives

- Establishing comprehensive measuring methods for key combustion parameters and major air pollutants, especially for the PM.
- Characterizing different combustion phases and investigating the soot formation process during residential wood combustion.
- Testing the sensor prototype on the wood stove and evaluating the sensor performance by comparing the signals with measuring results of advanced instruments.
- Investigating the influence of air supply patterns on combustion conditions and emission characteristics of the wood stove, and providing a guidance for the design of control strategy.

Combustion experiments and sensor tests are performed on a full-scale wood stove setup that is integrated with air staging and an air control system, as shown in Figure 1. The number concentration, size distribution and emission factor of PM are determined through the Scanning

Mobility Particle Sizer Spectrometer (SMPS), Electrical Low Pressure Impactor (ELPI+) as well as the gravimetric method.

Figure 1: The wood stove setup

Results and discussion

The main compositions of the PM were estimated through the two-step thermal treatment of the total particles collected on quartz filters during the combustion. The measuring results from five consecutive combustion charges are shown in Figure 2. OC represents the organic carbonaceous compounds that could be easily burned out at 250 °C; EC represents the elemental carbon content (mainly the soot particles) that will be oxidized at a higher temperature of 550 °C; while the ash content is considered as the remaining residue after the two-step heating procedures. It can be seen from Figure 2 that the EC content of the PM was significantly higher than OC and ash contents. In fact, the average EC content of the five charges was 85.0%, while the average OC and ash contents were 11.2% and 3.8%, respectively. The findings indicate that soot particles are the dominant composition of the PM emitted from the wood stove.
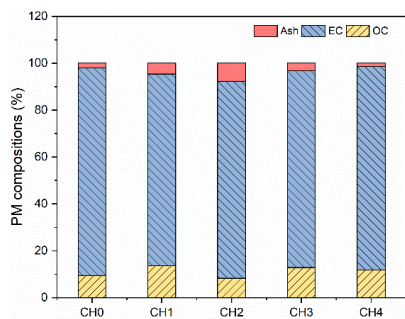
Figure 2: The main compositions of PM collected on filters (CH0-CH4 represent different burning charges)

Preliminary test results of the optical sensors for soot and tar are shown in Figure 3. Signals by the sensors are also compared with the measured particle number concentrations by the SMPS. In general, the varying trends of soot and tar signals agreed well with the measuring results by the advanced instrument.
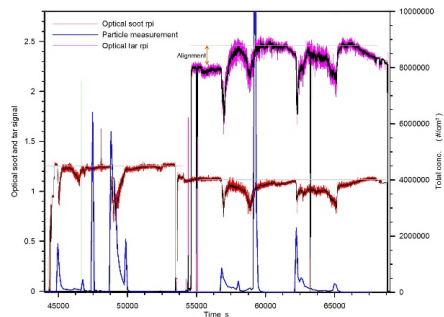
Figure 3: The comparison of sensor signals (soot and tar) with measurements by the SMPS during combustion

Conclusions and future work

As soot formation generally occurs at high temperatures in the fuel-rich zones, the PM compositions analysis indicates that the air supply patterns of the wood stove still need to be further optimized. Besides, it would be interesting to investigate the detailed soot formation mechanisms with regard to the wood log burning process in the stove. Preliminary sensor tests showed the promising application of the optical sensor system to automatically controlled wood stoves. Further modifications, adaptations and tests of the sensor system will be conducted in the future.

References

1. C. Pastorello, S. Caserini, S. Galante, P. Dilara, and F. Galletti, Atmos. Environ., vol. 45, no. 17, pp. 2869–2876, 2011.
2. T. B. Bjørner, J. Brandt, L. G. Hansen, M. G. Hjelmsø, and M. N. Källstrøm, Regulation of air pollution from wood-burning stoves, Report No. IFRO Working Paper 2016/11, Univeristy of Copenhagen, 2016.
3. M. Nielsen, O.-K. Nielsen, M. Plejdrup, and K. Hjelgaard, Danish emission inventories for stationary combustion plants: Inventories until 2008, NERI Technical Report No. 795, Aarhus University, 2010.
4. J. A. Peppers, Burn Cycle Emissions from a Wood Burning Stove, University of California Davis, 2013.
5. M. Wöhler, D. Jaeger, S. K. Pelz, and H. Thorwarth, Energy and Fuels, vol. 31, no. 7, pp. 7562–7571, 2017.

Karl Markus Jannert Enekvist

Phone: +46 738 17 51 11
E-mail: maene@kt.dtu.dk

Supervisors: Georgios M. Kontogeorgis
                      Kim Dam-Johansen
                      Xiaodong Liang
                      Xiangping Zhang

PhD Study
  Started: September 2018
  To be completed: September 2021

Computer-aided Product Design of Coatings

Abstract

To simplify the extensive process of formulating new coatings a combination of databases and models capable of estimating properties will be used to predict functionality in coatings. This prediction can improve formulation time and accuracy, and substitute unwanted ingredients while maintaining performance, which could be of great interest to an industry that relies heavily on experience. The approach is to create a computational framework by finding the relevant properties for each constituent, starting with pigments and polymers, and create databases or develop new group-contribution methods depending on available data and project needs.

Introduction

Paints and coatings are complex systems where the final application characteristics and the performance are complex functions of their many ingredients, properties, as well as interactions within the system and with the environment.

Currently, much of the functionality of coatings and paints are determined through experiments and graded on a scale visually. While these tests usually assess the final performance of a complete coating system well enough, they have a very low predictive capability, and formulation therefore depends mostly on experienced formulators and earlier formulations.

The development of a new paint starts with a problem statement. The formulator creates a sample for testing, which is later revised according to the results. This resource intensive cycle continues with increasingly small optimization steps as the difference between the paint properties and targeted specifications decrease. Computational aid for a property – performance relationship in coatings can significantly decrease the formulation time and costly experiments by finding a starting point that is closer to the initial specifications.

Computer-Aided Product Design

Computer-Aided Product Design (CAPD) consists of a combination of computational tools, algorithms, large databases and predictive methods for the estimation of different product properties. The aim is to be able to solve a large range of design problems in coating formulation within a systematic framework that is both flexible and practical [1].

This PhD Project will build upon earlier research by Elise Conte [2] who developed several methods and tools for product-design of consumer-oriented products, including sunscreen, insect repellants, and paints. The coating formulation was, however, highly simplified using only a preset pigment and binder and focused on the stability and design of binary solvent mixtures. The project is also related to an ongoing project of Spardha Jhamb, who focuses on CAPD of solvents in the coating system. The final aim of this combined research is an extensive product design framework for a broad range of coatings.

Property Estimations

As the complex paint systems have to be broken down into its more manageable constituents, the first area of interest for this project is pigments, and later polymers. The continuation of the project will then depend on the obtained results, as well as the outcome of other current research.

For paint pigments, some of the important properties that can affect the final coating characteristics can be seen in table 1. Product specific properties like particle size distribution, oil adsorption, particle shape, and pigment volume concentration has significant effect on the paint functionality.

Table 1. Paint characteristics and pigment properties.

Paint functionality	Pigment property
Tinting strength	Absorption index
Whitening power	Refractive index
Hiding power	Absorption index
	Refractive index
Reflectance	Absorption index
	Refractive index
Bleeding	Solubility (binder, solvents)
Wettability	Surface Tension
Dispersibility	Hansen solubility parameters
	Isoelectric point
	Specific gravity
	Molecular Weight
Heat resistance	Melting point
	Boiling point
	Decomposition temperature
Light resistance	Absorption index (UV)

Depending on the availability of data for each property, as well as the project needs, either databases or new models for property prediction will be created, as it is not feasible to measure the properties of large groups of compounds. For this purpose, group contribution models are preferred due to their high predictive capabilities. The choice of property model is of course of high importance, as the model strongly affects the reliability of the design, as well as availability of model parameters and uncertainties in the property estimations [3].

Results and Discussion

Currently the project is at an early stage, creating the knowledge base for pigments, which will become one of the critical pieces of the complete system.
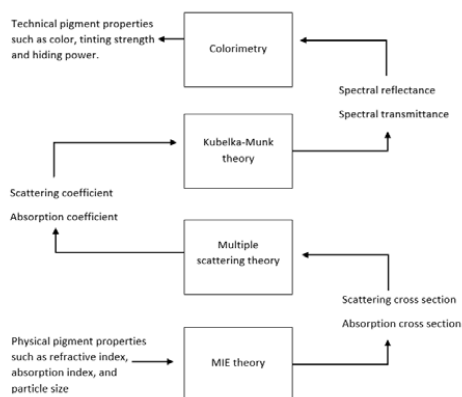
Figure 1. Relationship between optical properties of pigments, and the theoretical basis, modified from Buxbaum and Pfaff [4].

The most common use of computational methods for pigments in the industry today is color matching with the aid of optical properties and spectrometers, the basis of which can be seen in figure 1. Using functional pigments, however, seems to be almost entirely left to experience.

Conclusions and Future Work

While a number of group contribution methods are already available for certain pigment and polymer properties, additional methods for more accurate results will need to be developed, as well as comparison to measured data currently available.

Several property – performance relationships that are less clear may need to be explored, such as the factors influencing toxicity and resistance to light and chemicals. One of the challenges will be whether to include these special functionalities, as well many more, in the CAPD program.

While the full scope of product design extends beyond product problem specifications and product design through modelling and tools, further experimental planning and verification is not currently within the reach of this project. Application of the developed framework with property models, databases, methods and tools will instead be tested through a number of case studies that represents relevant problem statements.

References

1. Gani, R. Chemical Product Design: Challenges and Opportunities. *Computers and Chemical Engineering* 28(12) (2004) 2441-2457
2. Conte, E. 2010. *Innovation in Integrated Chemical Product – Process Design – Development Through a Model-based System Approach*. Ph.D. Technical University of Denmark (DTU).
3. Marrero, J. Gani, R. Group-contribution based estimation of pure component properties. *Fluid Phase Equilibria* 183(0) (2001) 183-208
4. G. Buxbaum, G. Pfaff, Industrial Inorganic Pigments, 3:rd Completely Revised Ed., Wiley-VCH Verlag, DE, 2005, p. 23.

Andreas Eschenbacher

Phone: +49 151 17868639
E-mail: aesc@kt.dtu.dk

Supervisors: Anker Degn Jensen
     Peter Arendt Jensen
     Ulrik Birk Henriksen
     Jesper Ahrenfeldt

PhD Study
  Started: February 2017
  To be completed: January 2020

Performance of Mesoporous HZSM-5 for the Upgrading of Wheat Straw Derived Pyrolysis Vapors in Bench Scale

Abstract
The performance and stability of post-synthesis desilicated ZSM-5 zeolites was screened in an *ex-situ* catalytic fixed bed for the upgrading of pyrolysis vapors generated in an ablative reactor system using wheat straw as feedstock. Steam treatment of the zeolites initially led to a pronounced loss in acidity, which then appeared stable for repeated reaction-regeneration cycles. A mild desilication approach preserving >85% of microporous volume indicated an improved performance as the oil yields and quality were improved compared to the parent zeolites.

Introduction
In order to allow processing of biomass derived fast pyrolysis oils in petroleum refineries, reduction of the oil`s oxygen content and acidity is required [1]. Deoxygenation can be obtained by direct upgrading of the pyrolysis vapors under atmospheric conditions over solid acid catalysts, among which ZSM-5 has shown high selectivity to aromatics and limited coke formation due to its shape selective micropores [2]. However, the coke produced by the oxygenate volatiles nevertheless causes rapid poisoning of active sites and pore blockage [3], requiring frequent regeneration to recover activity. In addition, the steam produced from the pyrolysis process, the dehydration of oxygenates, and the coke combustion may cause irreversible dealumination. Within this work, we aimed to extend the accessibility of active sites during the vapor upgrading despite rapid coking by introducing auxiliary mesopores, which were introduced by desilication followed by mild acid wash to remove any Al debris blocking pore entries [4].

Specific Objectives
While the majority of scientific work related to catalytic fast pyrolysis covers wood as feedstock due to higher oil yields, we utilized wheat straw as a representative fast-growing agricultural residue with a high ash content of 6 wt %. It was investigated how the introduction of mesopores changes the pore structure and acidity of the zeolite. The deoxygenation of pyrolysis oxygenates is assessed based on the oil`s yield and properties and correlated with the gas and coke formation. Hot gas filtration upstream the catalyst fixed bed is employed in order to prevent transfer of biomass indigenous alkaline and alkaline earth metals which would deactivate the zeolite`s acid sites.

Materials and Methods
Straw was fed at 200 g/h to an ablative fast pyrolysis unit, followed by gas filtration upstream the ex-situ located catalytic fixed bed containing 20 -150 g catalyst, staged liquid collection including an electrostatic precipitator (ESP) and gas analysis of non-condensables. Three parent ZSM-5 with Si/Al ratios between 16, 28, and 39 (abbr. CBV30, CBV55, CBV80) were tested along with their respective hierarchical counterparts (abbr. mesoCBV30, mesoCBV55, mesoCBV80), which were prepared by desilication, followed by acid wash, ion exchange and calcination. Prior to reaction, all catalysts were steamed for 5 h at 500 °C, 30 vol-% steam. Collected oil was analyzed for moisture, acidity (TAN), elemental analysis, size exclusion chromatography (SEC), GC-MS/FID, and selectively by ^{13}C, ^{1}H, and 2D HSQC NMR. Catalysts were characterized by XRF, NH_3-TPD, N_2 and high resolution Ar-physisorption, TEM and XRD.

Results and Discussion
The desilication resulted in solid yields of 50 - 80%, in accordance with the extent of created mesoporosity. Both the parent and mesoporous ZSM-5 lost ~50% of its initial acidity by the steam treatment, while their crystallinity was preserved. TEM investigations revealed differences in the location of mesopores, which were

better distributed for CBV30, whereas for CBV55 and CBV80 the mesopores formed preferentially in the crystal center. Mass balances for the pyrolysis experiments were ~95%. A thermal reference oil (phase separated from an aqueous fraction) was obtained over a SiC bed with 21.5 wt-%$_{d.b.}$ oxygen at 29% carbon yield and TAN = 54 mg KOH/g. For all catalysts, a change in product distribution occurred at increasing amounts of biomass pyrolyzed. Towards higher biomass-to-catalyst mass ratios (B:C), the yield of gas, reaction water, and coke showed a decreasing trend, while the yield of the phase separated oil fraction, but also the organics lost to the aqueous phase increased. At low B:C ratio, a highly aromatic and deoxygenated product was obtained with reduced TAN, however, at the expense of high carbon losses to coke (~9%) and gas (~35%). For both parent and mesoporous ZSM-5, the extent of coke formation but also the conversion of oxygenates was reduced at lower catalyst loadings (60 ml vs. 300 ml). The introduction of mesopores resulted in an increased coking propensity (Fig. 1). While no clear change in performance resulted for the mesoCBV30, an extended activity resulted for mesoCBV55 and mesoCBV80, as higher carbon recoveries of oil with less oxygen were obtained, especially towards higher amounts of biomass fed (Fig. 2).
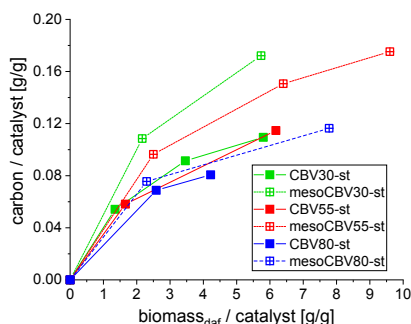
Figure 1: Coking propensity for parent ZSM-5 and its hierarchical version when upgrading straw pyrolysis vapors over ~300 ml catalyst.
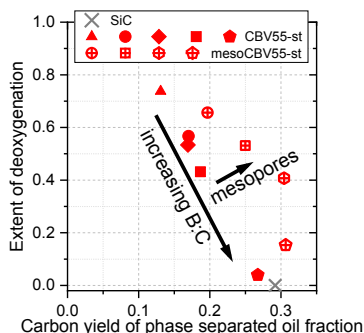
Figure 2: Extent of achieved deoxygenation (with respect to thermal reference of a SiC bed) against the carbon yield recovered in the oil fraction, here shown for CBV55.

Conclusion

The coking propensity increases upon introduction of mesopores, however, the accessibility of active sites appears prolonged. This is attributed to a better utilization of the bulk zeolite material by the created auxiliary mesopore network. The benefit is also apparent for mild desilication, which avoids significant loss of micropore volume that contains the majority of active sites.

Future work

The well performing mesoporous ZSM-5 catalysts of this study may be further modified by metal promotion for enhanced catalytic performance. In addition, improvements of the zeolite`s hydrothermal stability could allow faster regeneration under harsher conditions. Technical bodies of ZSM-5 extrudates are currently under investigation.

References

1. R. French and S. Czernik, Fuel Process. Technol., 91 (1) (2010) 25–32
2. J. Jae *et al.*, J. Catal., 279 (2) (2011) 257– 268
3. A. G. Gayubo, A. T. Aguayo, A. Atutxa, B. Valle, and J. Bilbao, J. Chem. Technol. Biotechnol., 80 (11) (2005) 1244 – 1251
4. D. Verboekend, S. Mitchell, M. Milina, J. C. Groen, and J. Pérez-Ramírez, J. Phys. Chem. C, 115 (29) (2011) 14193–14203

List of Publications

1. A. Eschenbacher, Graduate School Yearbook 2017
5. A. Eschenbacher, P. A. Jensen, U. B. Henriksen, J. Ahrenfeldt, A. D. Jensen, Book of Abstracts, Sustain 2017
6. A. Eschenbacher, P. A. Jensen, U. B. Henriksen, J. Ahrenfeldt, A. D. Jensen, Book of Abstracts, EUBCE 2018 - 26th European Biomass Conference and Exhibition
7. A. Eschenbacher, P. A. Jensen, U. B. Henriksen, J. Ahrenfeldt, U. V. Mentzel, A. D. Jensen, 18th Nordic Symposium on Catalysis (NSC), 2018
8. A. Eschenbacher, P. A. Jensen, U. B. Henriksen, J. Ahrenfeldt, U. V. Mentzel, A. D. Jensen, Thermal & Catalytic Sciences Symposium (TCS) 2018

Anna Burniol Figols

Phone: +45 45256195
E-mail: afig@kt.dtu.dk

Supervisors: Hariklia N. Gavala
                Ioannis V. Skiadas
                Anders E. Daugaard

PhD Study
  Started: February 2018
  To be completed: January 2020

Polyhydroxyalkanoate (PHA) Production from Crude Glycerol

Abstract
PHA are biodegradable and renewable bioplastics produced by bacteria. The objective of the PhD project is to produce PHA from crude glycerol (a by-product of the biodiesel industry) by using mixed microbial consortia (MMC) in order to achieve low PHA production costs. Several culture enrichment strategies have been investigated to increase the substrate conversion and carbon recovery of the process. Moreover, a sustainable and low cost purification method employing ammonia was developed.

Introduction
Plastic pollution, presence of microplastics in the environment and use of fossil resources are important topics in the current political agenda. Biodegradable plastics made from renewable resources, such as polyhydroxyalkanoates (PHA), could be a possible alternative to conventional fossil-based plastics.

PHA are a family of polyesters synthesized in bacterial cells as storage polymers in situations of unbalanced growth. Once extracted and purified from bacterial cells, they present similar properties to conventional plastics such as polypropylene or polyethylene (Fig. 1). Despite there are already PHA products in the market, its presence is limited, mainly due to the high production costs [1].

Fig. 1: PHA film

The project is based on three strategies to reduce production costs:

- The use of crude glycerol (a by-product of the biodiesel industry) as a substrate for PHA production.
- The use of mixed microbial consortia (MCC) instead of pure bacterial strains for PHA production. MMC do not require sterilization and are generally more tolerant to inhibitors present in waste substrates. These cultures can accumulate up to 90 % wt PHA when submitted to feast/famine cycles.
- The development of a sustainable and low-cost purification method.

Crude glycerol can be directly converted to PHA [2]. However, the PHA yield is limited by the side production of glycogen. This phenomena can be overcome by fermenting the original substrate into volatile fatty acids (VFA), recognized preferred substrates for PHA production [3]. However, the fermentation of glycerol in MMC often leads to the production of 1,3-propanediol (1,3-PDO). This alcohol has already many market applications, but has never been studied as a substrate for PHA production.

In regards to the purification method, PHA are currently purified with expensive and toxic solvents, and most alternatives developed until now lead to significant reduction of molar mass during the recovery and processing of the polymer.

Specific objectives
The main objectives of the phD are:

- Evaluate 1,3-PDO as a possible substrate for PHA production, by the application of different MMC enrichment strategies.
- Test the possibility of enriching MMC with selective consumption of VFA over 1,3-PDO with the objective of recovering 1,3-PDO while converting the volatile fatty acids into PHA.
- Assess different feeding strategies and bioreactor configurations in order to increase the PHA productivity.
- Investigate ammonia treatment as a method for PHA recovery and purification.

Results and discussion

Classical feast/famine enrichments are performed with nitrogen during the whole enrichment phase. This strategy did not lead to PHA production from 1,3-PDO during the accumulation phase. However, our results showed that by limiting the nitrogen during the feast phase, PHA production from 1,3-PDO could be attained (Fig. 2).
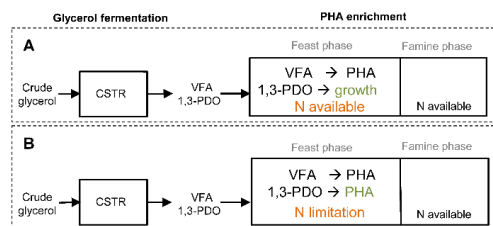
Fig. 2: PHA production from 1,3-PDO with nitrogen limitation during the feast phase.

However, maximum PHA yields from 1,3-PDO were much lower than from VFA (0.21 vs 0.74 Cmol PHA/Cmol Substrate, respectively). Given the low PHA yield from 1,3-PDO, and that this alcohol is also a high value product, a new enrichment strategy was set in order to avoid the consumption of 1,3-PDO. When the MMC enrichment was performed without 1,3-PDO in the medium, the enriched culture selectively converted VFA into PHA at a very high yield (0.99 C_{mol} PHA/C_{mol} Substrate), while leaving 1,3-PDO in the supernatant (99% recovery) (Fig. 3). At the end of the fermentation, PHA represented 76 % of the dry weight of the cells. Thus, the process converted fermentation by-products (VFA) into a high value product (PHA), that can be easily separated from the 1,3-PDO containing supernatant.
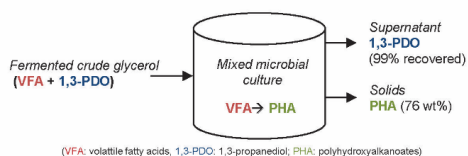
Fig. 3: Selective conversion of volatile fatty acids to PHA with recovery of 1,3-PDO.

After the PHA production, PHA were submitted to a purification process, in which dilute aqueous ammonia was used to digest non-PHA cell material. By using moderately elevated temperatures, around 90% PHA purity and recovery were attained. Moreover, the recovered polymers presented high thermal stability during melting at 170°C, with only 10% reduction of the molar mass. This value was much lower than with previously suggested methods not employing toxic solvents (Fig.4).
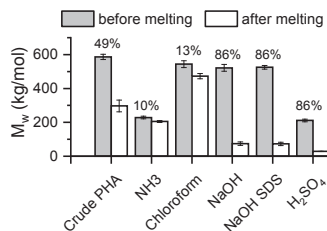
Fig. 4: Weight-average molar mass (M_w) of PHA before and after melting at 170°C using different purification methods. Values on top of the graph indicate percentage of M_w loss during melting.

Conclusions

The main conclusions obtained so far within the PhD project are:

- 1,3-propanediol from fermented crude glycerol can be converted to PHA by mixed microbial consortia with a suitable enrichment strategy.
- Nitrogen has an important role in the selection of PHA producing bacterial from 1,3-PDO.
- The overall carbon recovery of the process can be increased by selectively converting VFA in to PHA, while recovering 1,3-PDO.
- Purification of PHA with dilute aqueous ammonia solutions can lead to high purity and recovery of PHA, while maintaining the thermal stability of the polymer.

References

1. C. Kourmentza, J. Plácido, N. Venetsaneas, A. Burniol-Figols, C. Varrone, H.N.Gavala and M.A. Reis. Bioengineering 4.2 (2017) 55.
2. 2. A. Freches and P. C. Lemos. N. Biotechnol. 39 (Part A) (2017) 22–28,
3. L. S. Serafim, P. C. Lemos, M. G. E. Albuquerque, and M. A. M. Reis. Appl. Microbiol. Biotechnol 81 (4) (2008) 615–628.

List of publications

- A. Burniol-Figols, C. Varrone, S. B. Le, A. E. Daugaard, I. V. Skiadas, and H. N. Gavala. Water research 128 (2018) 255-266.
- A. Burniol-Figols, C. Varrone, A. D. Egede, S. B. Le, I. V. Skiadas, and H. N. Gavala. Water research 136 (2018) 180-191.
- C. Kourmentza, J. Plácido, N. Venetsaneas, A. Burniol-Figols, C. Varrone, H.N.Gavala and M.A. Reis. Bioengineering 4.2 (2017) 55.

Héctor Alexánder Forero-Hernandez

Phone: +45 4525 2910
E-mail: hafh@kt.dtu.dk

Supervisors: Bent Sarup, Alfa Laval Copenhagen A/S
              Gürkan Sin
              Jens Abildskov
              Anker Degn Jensen

PhD Study
Started: June 2016
To be completed: June 2019

Validation and Improvement of Property and Process Modelling for Oleochemicals

Abstract
While oilseed and vegetable oils, with an estimated output of 769 million metric tons per year (2017/2018 forecast), are small compared to primary petrochemicals, they are an important component in today's commodities market. To a large extent, this is due to the high technological standard of this mature industry. Generally speaking, vegetable oils are extracted from soybeans, palm fruit, sunflower, coconuts, rapeseed, cottonseed, olives, flax, castor seed and groundnuts, making them the most important renewable raw materials for the chemical industry. It furthermore has become possible to better respond to consumer needs by modifying the carbon chain and distribution of the oleoproducts and by understanding their behavior and properties. Nevertheless, reviewing the technical development of the oleochemicals manufacture one finds that some basic facts related the thermodynamic and kinetics have only been partly recognized because of the rather harsh physical conditions at what oleochemicals are exposed during their processing. The purpose of the project is the provision of a systematic methodology and framework to design and optimize selected oleochemical processes, in particular the fat-oil splitting process.

Introduction
This project is part of the Marie Sklodowska-Curie Innovative Training Network "ModLife: Advancing Modelling for Process-Product Innovation, Optimization, Monitoring and Control in Life Science Industries" in the Horizon 2020 Program of the European Commission (H2020-MSCA-ITN-2015 call, Project No.675251). It aims to collect, validate and improve properties and models of selected oleochemical processes (including recovery of high value added products) so as to optimize them.

Modelling the hydrolysis of vegetable oils
Vegetable oils are primarily triglycerides, i.e., triesters of long-chain saturated and unsaturated fatty acids combined with glycerol. Basic oleochemicals (chemicals derived from vegetable oil and animal fats) are free fatty acids, methyl esters, fatty alcohols, and fatty amines as well as glycerol as by product. Fatty acids of every chain length, saturated and unsaturated, have been produced through hydrolysis on an industrial scale for more than 130 years. The hydrolysis of fats and oils produces several important industrial chemicals including monoglycerides, diglycerides, and glycerol. The existing industrial and commercial process hydrolyzes oils to

fatty acids and glycerol at temperature and pressure of 250°C and 50 bar, respectively within two hours to achieve 96%–99% conversion. Kinetic modeling of biphasic reactions, specifically the hydrolysis of vegetable oils at high temperatures and pressure, is complicated due to the heterogeneous nature of the system. Hence, it is the aim of this particular document to present the development and validation with dedicated experiments of a biphasic model based on measurable properties of the overall hydrolysis reaction. As a result of its heterogeneous nature, the hydrolysis reaction is affected, not only, by the chemical kinetics but also by the rate of mass transfer between the oil and water as well as another observable variables with the process such as temperature, pressure, density, viscosity, geometry of reactor, etc. The general modeling objective followed in this work is that the model should be sophisticated enough to describe the complexities of the hydrolysis of vegetable oil, but the parameters should be based on measurable phenomena to the extent possible. The presented model is grounded in the biphasic nature of the process and includes expressions to describe both mass transfer and thermodynamic behavior of the system. However, not all the complexities of the system are incorporated. To identify the working bounds of the

proposed model, there were performed Monte Carlo simulations of the model outputs for uncertainty estimation along with a sensitivity analysis method based on regression. Further details and mathematical formulations can be found in publications made by the authors [1,2].

Experimental batch hydrolysis of rapeseed oil
Hydrolysis reactions were run in a 300 ml Hastelloy C-276 jacketed reactor with ceramic band heaters (Parker Autoclave Engineers, Model 300 ml HC EZE-Seal), including a cooling loop that allows rapid cooling of the contents in the reactor. The system is equipped with a controller to monitor and control temperature and agitation speed. The reactor has a sampling port for withdrawal of liquid samples during the reaction every 30 minutes. A scheme of the set-up used is depicted in Figure 1. 11 experiments were carried out based on a Box-Behnken design for three factors (temperature, oil-to-water ratio and agitation speed) with time fixed as 6h. Samples are analyzed using High-Performance Liquid Chromatography for triglycerides, diglycerides, monoglycerides and fatty acids.
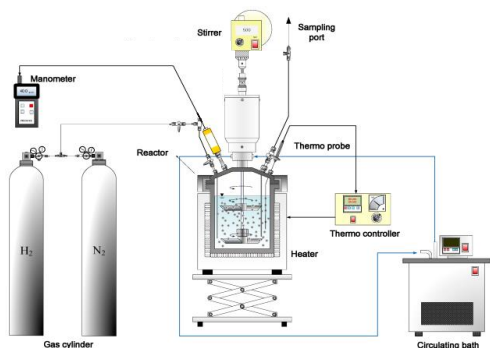
Figure 1. Reactor set-up used for the hydrolysis of oils

Model validation and uncertainty analysis
The performance of the model over the entire time course of the reaction is illustrated in Figure 2 and Figure 3, using selected validation data sets, where data is provided in terms of moles of species. Visually speaking the goodness of the model fits is quite remarkable. These fits were obtained from identification of 8 kinetic and 2 mass transfer parameters involved using non-linear regression. The proposed model captures the dynamics for the four analyzed components over the entire course of the reaction, although the prediction for diglycerides and monoglycerides shows some deviation from the experimental data. The model mismatches observed may be due to process phenomena not taken into account and for errors in the analytical measurements. Likewise, the uncertainty in the parameter estimates plays a part given that some of the parameter estimates are strongly correlated. This can be due to the model structure or the similarity of the parameters of the underlying chemical system.
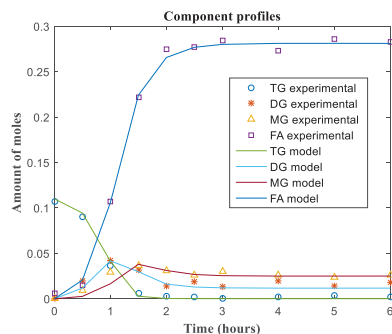
Figure 2. Reaction profiles for the hydrolysis
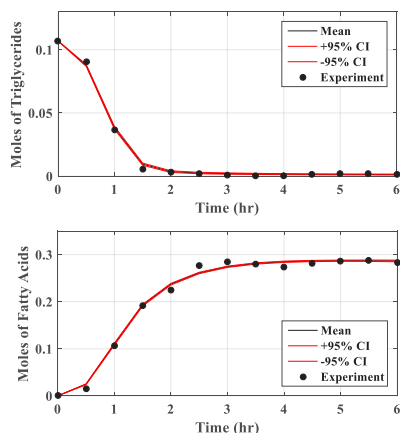
Figure 3. Uncertainty and bounds of the model

When the experimental values are overlaid on the uncertainty analysis, we can see that over the complete course of the reaction, most of the experimental values fall within the bounds of the plots. The narrow prediction bands reflect the robustness of the predictions for those model outputs over the entire course of the reaction. Through these plots it is possible to put bounds on the model predictions, which can give the modeler some insight into the reliability of the model to make predictions.

Conclusions
Developed models for process are able to validate accurately available experimental data with a narrow confidence interval. Sources of uncertainties and operation design spaces in the system have been identified.

References
[1] H. Forero-Hernandez, M. Jones, B. Sarup, J. Abildskov, A.D. Jensen, G. Sin, in: Proc. 27th Eur. Symp. Comput. Aided Process Eng. (Escape 27), 2017: pp. 1177–1182.
[2] H. Forero-Hernandez, M. Jones, B. Sarup, J. Abildskov, A.D. Jensen, G. Sin, Modelling, Uncertainty and Sensitivity Analysis of the Batch Thermal Hydrolysis of Vegetable Oils, (2018). Access through: https://goo.gl/FZ13U1

Jie Gao

Phone: +45 5020 8886
E-mail: jgao@kt.dtu.dk

Supervisors: Kim Dam-Johansen
Weigang Lin
Hao Wu

PhD Study
Started: May 2018
To be completed: May 2021

Flame Synthesis of Nanoparticles

Abstract

Flame synthesis is a highly diverse and scalable technique for the synthesis of nanostructural materials. The PhD project will focus on preparation, characterization and application of nanoparticles produced by flame synthesis.

Introduction

Flame aerosol technology is widely used in large-scale production of nanoparticles, such as single component SiO_2, Al_2O_3, TiO_2, their mixed composites TiO_2/SiO_2, Al_2O_3/SiO_2, and even non-oxide ceramic particles TiN, TiC and SiC[1]–[8].

As shown in Figure 1, flame aerosol technology can be classified into two sorts by the state of the injected precursor[6]: vapour-fed aerosol flame synthesis (VAFS) and liquid-fed aerosol flame synthesis (LAFS). In LAFS, evaporation of a liquid precursor process may be facilitated by other external heat supplier such as flame. The flame here is used as an ignition source and provide energy to support precursor combustion[9]. And this technique is called Flame Spray Pyrolysis (FSP). For an inorganic precursor, the flame is used as hot walls[10] of spray pyrolysis- Flame Assisted Spray Pyrolysis (FASP).

The current industrial applications of flame aerosol technology are mainly on the production of single component nanoparticles. To further develop the technology, it is desired to explore the production of functional composite nanomaterials. The advances that can be brought to this technology include but not limited to the following: developing processes that can produce composite nanomaterials with unique properties and significant application potential; reducing the production cost by using low-cost precursors and/or process optimization; developing modelling tools that can describe the aerosol formation process and be used in process up-scaling.
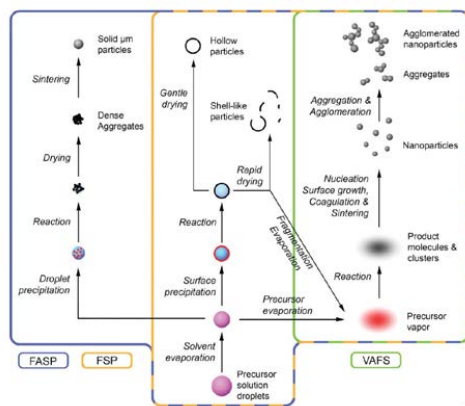
Figure 1. Schematic for particle formation in Flame Aerosol Technology[7].

Specific Objectives

The objectives of the PhD project are:

- Develop a flame aerosol technique that can produce composite nanomaterials;
- Improve and optimize the flame aerosol technique;
- Explore the application of the composite nanomaterials;

Methodology

In the start phase of the PhD project, an existing Flame Spray Pyrolysis (FSP) setup, shown in Figure 2, will be

used for synthesis of metal oxides or composites particles. In the FSP process, the precursor is fed through a capillary to the nozzle and atomized by high-pressure dispersion gas which fed through an annular aperture around the capillary tube. Methane-oxygen premixed gas is usually used to ignite the aerosolized precursor solution which typically contain metal elements and solvent. In the chamber, at high temperature, the metallic or semimetallic components of the precursor will go through evaporation, nucleation and condensation processes to form primary particles of metals or metal oxides. In the high temperature region, some aggregation will form initially, but rapidly quenching due to the radiation and convection effect. The formed particles are collected on a fibre filter using a vacuum pump.
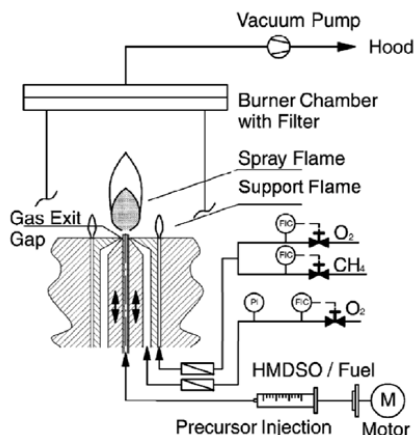
Figure 2. Experimental set-up of Flame Spray Pyrolysis[11]

The setup can be operated with different liquid precursors, flame conditions, gas pressure and flow rate to obtain particles with different chemical and physical properties. The particles collected can be further analyzed by ex-situ characterization tools, such as X-Ray Diffraction (XRD) for determination of crystalline phases, and Transmission Electron Microscopy (TEM) for particle size and morphology.

References
[1] P. Roth, Proc. Combust. Inst., 31(2)(2007) 1773–1788
[2] T. Hawa and M. R. Zachariah, Phys. Rev. B - Condens. Matter Mater. Phys., 69(3) (2004)1–9, 2004.
[3] M.R. Zachariah, Lecture Note, University of Maryland, 2010.
[4] R. Strobel, F. Krumeich, W. J. Stark, S. E. Pratsinis, and A. Baiker, J. Catal., 222(2)(2004) 307–314
[5] R. Strobel, "Aerosol flame synthesis of supported metal particles and their catalytic applications," phD Thesis, Switzerland:ETH, 2006.
[6] R. Strobel, A. Alfons, and S. E. Pratsinis, Adv. Powder Technol., 17(5)(2006) 457–480.
[7] R. Strobel and S. E. Pratsinis, J. Mater. Chem., 17(45)(2007)4743–4756.
[8] B. Schimmoeller, S. E. Pratsinis, and A. Baiker, Chem.Cat.Chem., 3(8)(2011)1234–1256.
[9] M. Sokolowski, A. Sokolowska, A. Michalski, and B. Gokieli, J. Aerosol Sci., 8(4)(1977)219–230.
[10] G. L. Messing, S.-C. Zhang, and G. V. Jayanthi, J. Am. Ceram. Soc., 76(11)(1993)2707–2726.
[11] H. Grobmann, Bachelor Thesis, Denmark Technical University, 2010

Nipun Garg

Phone: +45 91858604

E-mail: nipgar@kt.dtu.dk

Supervisors: John M. Woodley

                    Georgios M. Kontogeorgis

PhD Study

   Started: October 2016

   To be completed: October 2019

An extended methodology for Phenomena based synthesis-intensification

Abstract

Process Intensification (PI) is one of the ways that aims to drastically improve the process performance and bring improvements both in terms of sustainability and economics. It has emerged to be an important tool providing opportunities and solutions for more efficient and sustainable processes. A systematic intensification methodology generating innovative solutions by operating at lower scale i.e. phenomena [1] level is developed by Babi et al. [2]. In this methodology the phenomena are combined using connectivity rules to generate feasible alternatives that match the pre-defined performance criteria generating non-trade-off sustainable solutions. Previously, existing methodology was extended to solid-liquid phenomena to widen the application range [3]. In this research, the phenomena-based synthesis-intensification methodology is further extended to overcome the application limitation and generate wide range of solutions. New phenomena class and sub classes are introduced to expand the phenomena list and intensified equipment's translating to phenomena and vice versa are added to existing database. Furthermore, a new step by step framework is developed to carry out phenomena-based synthesis, generating more sustainable hybrid/intensified solutions.

Introduction

In recent years, a major focus is on hybrid/intensified and novel equipment that can dramatically improve the performance of chemical and biochemical processes. Therefore, methodologies, techniques and tools that potentially could transform the basics of process synthesis and design, generating novel, innovative and sustainable solutions are highly beneficial. The key attributes of such methods and tools should be that they are systematic, flexible in applicability & approach and should cover wide range of domains and scales ranging from molecular to process or from phenomena to unit operation scale. There are numerous approaches for process synthesis and design developed in past many decades mainly categorized into knowledge-based methods [4,5], methods on mathematical optimization techniques [6] and hybrid methods [2,7] that combines different approaches into one method. The objective of all these methods in one or other way is to generate better solutions. One of such methods is developed based on phenomena [1] that combines phenomena at the lowest level to generate novel hybrid/intensified solutions at the unit operations. This approach has been extended to process level by Babi et al. [2]. They developed a holistic 3-stage method consisting of synthesis, design & analysis and innovation. In

synthesis stage, a process flowsheet is identified which is then designed and analysed in detail in second stage to identify process bottlenecks. These are then translated to improvement targets being achieved in innovation stage. In this stage, the phenomena-based synthesis method is applied to generate sustainable solutions.

In this part of research, an overview of the new phenomena-based synthesis intensification framework is presented along with the new phenomena list (PBB's) to increase the search space of unit-op and generate more sustainable and innovative solutions.

Phenomena based synthesis-intensification

Most of the unit-operations constituting the chemical or a biochemical process can be represented in terms of mass, energy, momentum or transport phenomena. A list of such phenomena is developed by Lutze et al. [1] and further enhanced by Babi et al. [2]. These set of phenomena is further extended to incorporate a wider search space of unit operations. An extended set of phenomena assist in generating new and innovative solutions which might be missing from the intensified solutions generated using previous databse. The new set of phenomena along with the possible classes is shown in figure 1. Here, V represents vapor, L is liquid, S is solid, M is membrane while H, C and D within energy

supply phenomena denotes heating, cooling and direct energy supply. Here direct energy supply i.e. ES(D) may represent any alternate energy source for example microwave, ultrasound, centrifugal, electromagnetic other than cooling (C) or heating (H) that assists in enhancement of any task within a unit-op.

Phenomena Building block	Class
Mixing (**M**)	V, L, S, VL, LS, VS, LL
2 phase mixing (**2phM**)	LL, VL, LS, VS
Reaction (**R**)	V, L, S, VL, LS, VS
Energy supply (**ES**)	C, H, D
Phase contact (**PC**)	VL, LS, LL, VS
Phase transition (**PT**)	VL, LS, LL, VS, MVV, MLL, MVL
Phase Separation (**PS**)	VL, LS, VS, LL, VV, SS
Dividing (**D**)	-

Figure 1: Extended list of phenomena building block (PBB) along with different classes

Some of the examples of new added phenomena are shown in figure 2. Using M(L) i.e. mixing, R(L) i.e. reaction in liquid phase and ES(D) i.e. alternate energy source (microwave) phenomena, a microwave reactor can be represented. Similarly, a hybrid of microwave assisted distillation can also be generated combining phenomena shown in figure 2.
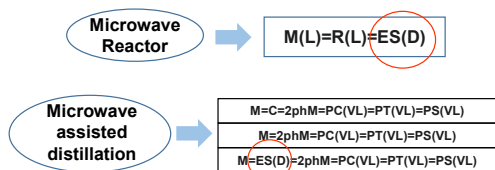
Figure 2: An example of hybrid/intensified unit-operations translated using extended list of phenomena

Overview of developed framework for Phenomena based synthesis-intensification

An overview of generic framework to carry out phenomena based synthesis-intensification is shown in figure 3. It mainly consists of 3 steps including 12 sub steps. In step 1, the main task is to identify the desirable tasks and phenomena that affect the driving force in the base case flowsheet and enables the methodology to have potential of generating new options. Here, an extensive list of unit-op translating to phenomena and process hotspots translating to phenome is used to carry out the respective sub steps. In second step, the feasible flowsheet alternatives are generated using several algorithms, combination rules and feasibility rules. Here, a list of feasible SPB's for a specific task is identified using thermodynamic based insights from Jaksland et al. [4]. The number of flowsheet options are further reduced using the feasibility rules. Further, a detailed model based analysis is performed to identify the feasible flowsheet alternatives. In the third step, feasible flowsheet alternatives are simulated and analyzed in terms of economics, sustainability and LCA. The results for all the intensified alternatives are then verified and compared with base case through a set of pre-defined performance parameters.

For an alternative to be non-trade-off and more sustainable, all the performance parameters have to be either same or better than the base case.
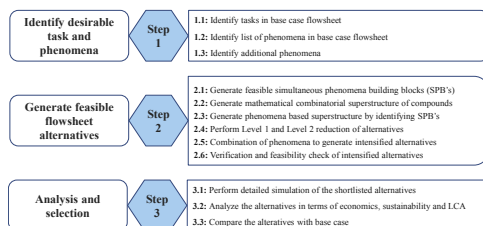
Figure 3: An overview of steps involved in new framework for phenomena based synthesis-intensification

Conclusion

In conclusion, a process intensification methodology is developed that can operate at lower level of aggregation (phenomena) and generate wide range of solutions. The extended list of phenomena, databases, algorithms provides an increased search space to come up with even better range of solutions. Further, an incorporation of logical and feasibility rules makes the methodology more robust and quick to generate feasible intensified flowsheet alternatives.

Current and Future Work

Currently, the new methodology is being applied to hydro de-alkylation of toluene case study to generate intensified and more sustainable alternatives. Future work includes application of the new framework to an industrially applicable case study and development of a generic mathematical model for the methodology to solve the phenomena-based synthesis-intensification problem quickly and efficiently.

References
1. P. Lutze, R. Gani, J.M. Woodley, Comp. & Chem. Eng. 36 (1) (2012), 189-207.
2. D.K. Babi, J. Holtbruegge, P. Lutze, A. Gorak, J.M. Woodley & R. Gani, Comp. & Chem. Eng., 81(2015), 218-244.
3. N. Garg, G.M. Kontogeorgis, J.M. Woodley and R. Gani, Comp. & Chem. Eng. 43 (2018), 875-880.
4. C.A. Jaksland, R. Gani, K.M. Lien, Chemical Engineering Science, 50 (1995), 511-530.
5. J.J. Siirola, Comp. & Chem. Eng., 20 (1996), S1637-S1643
6. K.P. Papalexandri, E.N. Pistikopoulos, AIChE J, 42 (4) (1996), 1010-1032.
7. S.E. Demirel, J. Li, M.F. Hasan, Comp. & Chem. Eng. 105 (2017), 2-38.

Peter Sams Hammershøi

Phone: +45 61926644

E-mail: Petersams.hammershoi@eu.umicore.com

Supervisors: Prof. Anker D. Jensen
Ton V.W. Janssens, Umicore Denmark

PhD Study
Started: May 2015
To be completed: October 2018

Reversible and Irreversible Deactivation of Cu-CHA NH₃-SCR Catalysts by SO₂ and SO₃

Abstract
The deactivation of a Cu-CHA catalyst for selective catalytic reduction (SCR) of nitrogen oxides with NH_3, by SO_2 and SO_3 (SO_x) was investigated. The catalytic performance was evaluated after exposure to SO_2 in presence and absence of SO_3 and H_2O, at 200 °C or 550 °C. The deactivation is partially reversible at 550 °C, and the irreversible part shows a 1:1 correlation with the S/Cu ratio, consistent with deactivation by formation of Cu-sulfates, whereas the reversible deactivation is much larger than the S/Cu ratios. The irreversible deactivation is enhanced at 200 °C or in presence of H_2O, and the deactivation is significantly increased in presence of SO_3 at 200 °C, but not at 550 °C.

Introduction
Combustion of diesel in automotive engines produces polluting compounds, which are removed to a certain extent in the diesel exhaust system. NO and NO_2 (NO_x) are removed by NH_3-SCR over a catalyst. State-of-the-art SCR catalysts are Cu-exchanged zeolites with the CHA topology [1]. The Cu-CHA materials are susceptible to poisoning by sulfur oxides [2], which are inevitably present in diesel exhaust. Therefore, SCR catalysts have to be regenerated or engineered to tolerate the amounts of SO_x in the exhaust, which is improved by a better understanding of the impact of the different operating conditions on the catalyst deactivation.

Specific objectives
The deactivation mechanism should be elucidated by comparison of the deactivation with the S-content after SO_x exposure and regeneration. The impact of H_2O and SO_3 on the deactivation, at 200 °C and 550 °C, was investigated by evaluating the SCR performance of a Cu-CHA catalyst in the SCR reaction before and after SO_x exposure, and after regeneration at 550 °C.

Experimental
The Cu-CHA catalyst had a Si/Al ratio of 16.6 and a Cu-loading of 2.5 wt% and was washcoated on a 300 cpsi cordierite monolith. SCR activity measurements were carried out on cylindrical samples of 20×27 mm (D×L) in a quartz flow reactor in the temperature range 130-250 °C, where steady state NO_x conversions are measured. The rate constant is used as measure of the activity, and

is calculated assuming first order kinetics in NO. The inlet SCR gas composition was 500 ppmv NO, 530 ppmv NH_3, 10 % O_2, 5 % H_2O in N_2-balance at 8 NL/min. The outlet gas was measured with an MKS MultiGas 2030 FTIR. The SO_x exposure conditions were at 8 NL/min with 100 ppmv SO_2 or a mixture of 70 ppmv SO_2 and 30 ppmv SO_3, and with 5 % H_2O or no H_2O at either 200 °C or 550 °C for 3 h. Regeneration was carried out for 4 h at 550 °C with the same gas and flow conditions as for SCR activity measurements. The S-content was estimated by measuring SO_2 desorption during regeneration and while heating to 900 °C in a pure N_2 flow after the last SCR activity measurement.

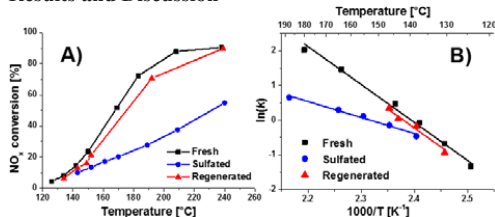**Results and Discussion**

Figure 1: A) NO_x conversions as functions of temperature, and **B)** Arrhenius plot, of the fresh, sulfated and regenerated states of the catalyst. SO_x exposure conditions: 100 ppm SO_2 and 5 % H_2O at 200 °C.

The low-temperature NO_x conversion of the sulfated state of the catalyst shown in Figure 1A, is significantly

lower than that of the fresh. After regeneration the NO_x conversion is almost restored to the same level as the fresh, but not entirely. Thus, there are, at least, two different forms of deactivation. The deactivation restored by regeneration is *reversible*, and is the difference between the sulfated and regenerated states of the catalyst, and the deactivation left after regeneration is *irreversible*, and is measured directly on the regenerated state of the catalyst. The relation is shown in Eq.(1).

$$Total\ deactivation = Reversible + Irreversible\ (1)$$

In Figure 1B, the slopes of the different states of the catalyst in the Arrhenius plot shows that the activation energy of the SCR reaction over the sulfated state is different to those of the fresh and regenerated states of the catalyst. The can be due to a different SCR mechanism over the sulfated state of the catalyst. The similar activation energy of the fresh and regenerated states is consistent with a deactivation that is due to a loss of sites. The trends observed in Figure 1A and B are similar for all the different SO_x exposure conditions.

Formation of Cu-sulfates is a possible reason for the deactivation [2]. In that case, a 1:1 correlation between the deactivation and S/Cu ratio would be expected. In order to investigate this, the amount of S-species on the catalyst were measured, which can be done from SO_2 desorption [2]. Therefore, SO_2 desorption was measured during regeneration, and used to quantify the amounts of S-species related to the reversible deactivation. Also, the S-species related to the irreversible deactivation were quantified by measuring SO_2 desorption during heating to 900 °C in pure N_2 flow, after the final activity measurements on the regenerated state of the catalysts. The reversible and irreversible deactivations and S/Cu ratios are compared in Figure 2 for each SO_x treatment. The reversible deactivations are surprisingly larger than expected from their S/Cu ratios, whereas the irreversible deactivation has a close to 1:1 correlation with the S/Cu ratio. Again this is consistent with the irreversible deactivation being due to loss of sites, whereas the reversible deactivation must be caused by something else.
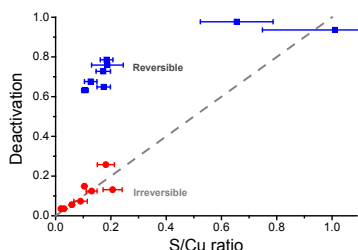
Figure 2: Reversible and irreversible deactivation for each SO_x exposure condition plotted as function of the molar S/Cu ratio. The grey dashed line shows the 1:1 correlation between deactivation and S/Cu ratio.

Due to the wide operating conditions of an SCR catalyst, it is important to know how the different conditions affect the deactivation. Therefore, the reversible and irreversible deactivations resulting from the 8 different SO_x exposure conditions are compared in Figure 3.
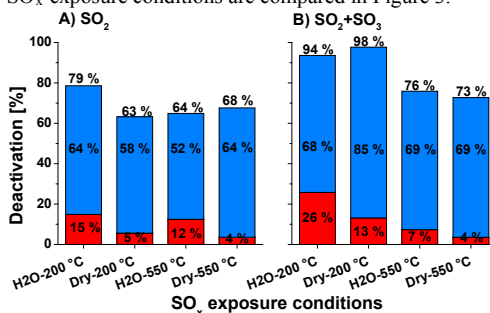
Figure 3: Reversible (blue bars) and irreversible (red bars) deactivation for each SO_x exposure condition. The percentages listed in each column are from the bottom: irreversible deactivation, reversible deactivation and the sum of the two being the total deactivation.

The irreversible deactivation is always larger when the SO_x exposure has been carried out at 200 °C, compared to at 550 °C, while there is no consistent trend for the reversible deactivation. Also in the presence of H_2O, the irreversible deactivation is always higher than at dry conditions. The presence of SO_3 has a large impact at 200 °C, where the deactivation is significantly enhanced by its presence, while at 550 °C the deactivations by SO_2 only and the mixture of SO_2 and SO_3 are similar.

Conclusions

By exposure to SO_x, a significant deactivation of a Cu-CHA NH_3-SCR catalyst is observed, which is partially reversible at 550 °C. The irreversible deactivation is directly proportional to the S/Cu ratio, consistent with formation of Cu-sulfates, while low S/Cu ratios infer disproportionally large reversible deactivations. The irreversible deactivation is slightly enhanced at 200 °C or in H_2O presence, while the presence of SO_3 greatly increases the deactivation at 200 °C, but has no apparent effect at 550 °C.

References

1. C. Paolucci, I. Khurana, A.A. Parekh, S. Li, A.J. Shih, H. Li, J.R. Di Iorio, J.D. Albarracín-Caballero, A. Yezerets, J.T. Miller, W.N. Delgass, F.H. Ribeiro, W.F. Schneider, R. Gounder, Science 357 (2017) 898-903
2. P.S. Hammershøi, P.N.R. Vennestrøm, H. Falsig, A.D. Jensen, T.V.W. Janssens, Appl. Catal. B 236 (2018) 377-383
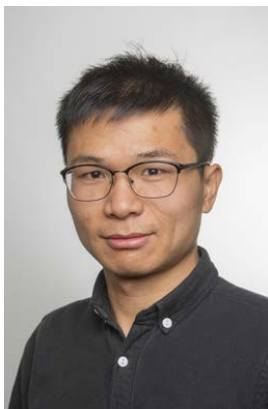
Pengpeng Hu

Phone: +45 50349473
E-mail: penghu@kt.dtu.dk

Supervisors: Anne Ladegaard Skov
                 Qian Huang

PhD Study
   Started: October 2018
   To be completed: September 2021

Supra-molecular assembly utilized in dielectric elastomers

Abstract
Silicone elastomers are promising dielectric materials applied in dielectric elastomer transducers. Developing silicone elastomer materials with high-permittivity and self-healing property is critical to realization of their full commercial applications. Recently, silicone elastomers functionalized with supra-molecular assembly show a great potential to achieve self-healing property, as well as possible increase of dielectric permittivity. The objective of this project is to prepare silicone elastomers with high dielectric permittivity and efficient self-healing property by introducing supra-molecular assemblies into silicone elastomer networks. Additionally, the project aims to investigate the linkages between multiple interactions (covalent bonds and noncovalent bonds) on molecular scale and macroscopic properties.

Introduction
Dielectric elastomer transducers (DETs) are promising for novel, advanced electromechanical applications such as actuators, generators, and sensors, due to their simple and flexible working principle combined with the advantage of light weight and low cost [1, 2]. The elastomer is one of the most important components of a DET. Silicone elastomers are often highlighted as the most suitable and promising elastomer material for DETs due to their high efficiency, reliability and fast response times. The drawback of the silicone elastomers is their relatively low dielectric permittivity, which means high driving voltages are often required to obtain a desired strain [3, 4]. Various methods aimed at enhancing the Dielectric permittivity of silicone elastomers have been performed, including silicone composites [5-8], silicone/polymer blends [9-11], chemically modified silicones [12], and systems with complex network structures [13]. In most cases, the enhancements of dielectric permittivity lead to the decreases of electrical breakdown, since high-permittivity materials often have higher degrees of imperfection and higher losses [13]. The solution is to develop high-permittivity and self-healing elastomer materials. This way, lower electrical fields are required to actuate the dielectric elastomer, and the elastomer is able to self-heal if a break occurs.

The self-healing property of the material can be realized by introducing dynamic bonds into the load-carrying molecular structure of the material. Once the damage occurs, these dynamic bonds will break and subsequently reestablish, thereby restoring the mechanical strength of the material [14]. Elastomers with self-healing property (even at room temperatures) were realized by introducing hydrogen-bonding interactions [15], ionic interactions [4], π–π interactions [16], and coordinative bond interactions [17] into the molecular networks, respectively. A supra-molecular assembly is a well-defined complex of molecules held together by such noncovalent bonds [18]. In previous work, interpenetrating polymer networks were developed by introducing ionic networks (from amino- and carboxylic acid-functional silicones) into silicone elastomer networks. The interpenetrating polymer networks were applied as dielectric elastomers, and high permittivity was obtained while dielectric breakdown strength and Young's modulus were not compromised from amino- and carboxylic acid-functional silicones [19]. Another example is a self-healing dielectric elastomer that additionally possessed high dielectric permittivity. It consisted of an interpenetrating polymer network of silicone elastomer and ionic silicone species that were cross-linked through proton exchange between amines and acids [4].

Although improvements on properties of DETs have been achieved by introducing dynamic bonds into silicone elastomer networks, the road toward the full commercialization of DETs still faces challenges.

Objectives, tasks and methods

As described above, development of high-permittivity and self-healing elastomer materials is a key solution to improve the properties of DETs. The objective of this PhD project is to prepare supra-molecular assemblies and introduce them into silicone elastomer networks. It is expected that the resulting polymer networks with double dynamics will have high dielectric permittivity, transient and self-healing properties, as well as permanent elasticity for overall product performance.

The specific tasks and methods are shown in figure 1. The first step is to prepare silicone elastomers by introducing selected types of non-covalent bonds into silicone elastomer networks. Secondly, the rheological properties of the desired silicone elastomers will be studied. The typical approaches include small amplitude oscillatory shear (SAOS) tests and extensional rheology tests. Additionally, the mechanical properties of the desired silicone elastomers will be investigated by performing tensile tests, and the corresponding sample structures will be analyzed by wide-angle X-ray scattering (WAXS) tests and microscopy tests. Based on the understanding of the properties above, the molecular parameters of the desired silicone elastomers will be identified. It is then possible to predict the rheological and mechanical properties as a function of molecular parameters through modeling, which provides a guidance to the synthesis step.
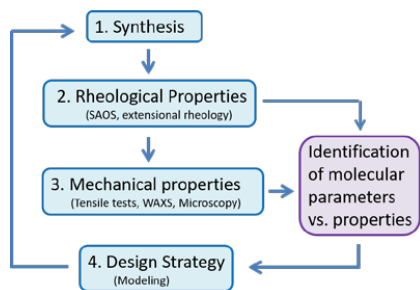
Figure 1 Tasks and methods of the project

Conclusions

Literature shows that various attempts to improve the properties (permittivity, Young´s modulus, dielectric loss, lifetime, etc.) of silicone elastomers have been successful to some extent, and development of silicone elastomers with high permittivity and efficient self-healing property is critical to apply silicone elastomers in commercial DETs. This project will utilize supra-molecular assembly in silicone elastomers to realize self-healing property and improve permittivity, and understand the linkages between the multiple interactions within supra-molecules and macroscopic properties.

References

1. Madsen, F. B., Daugaard, A. E., Hvilsted, S., & Skov, A. L., Macromol Rapid Commun 37(5) (2016) 378-413.
2. Brochu, P. and Q. Pei, Macromolecular Rapid Communications 31(1) (2010) 10-36.
3. Liu, Y. J., Liu, L. W., Sun, S. H., Zhang, Z., and Leng, J. S., 52(9) (2009) 2715–2723.
4. Madsen, F.B., L. Yu, and A.L. Skov, ACS Macro Letters, 5(11)(2016) 1196-1200.
5. Carpi, F. and D. De Rossi, Ieee Transactions on Dielectrics and Electrical Insulation, 12(4)(2005) 835-843.
6. Skov, A. L., Bejenariu, A. G., Bøgelund, J., Benslimane, M., and Daugaard, A. E., Conference on Electroactive Polymer Actuators and Devices (EAPAD). San Diego, 2012, CA.
7. Dang, Z.M., Xia, B., Yao, S.H., Jiang, M.J., Song, H.T., Zhang, L.Q., and Xie, D., Applied Physics Letters, 94(4)(2009) 042902.
8. Molberg, M., Crespy, D., Rupper, P., Nueesch, F., Manson, J.A. E., Loewe, C., and Opris, D. M., Advanced Functional Materials, 20(19)(2009) 3280-3291.
9. Benslimane, M. and P. Gravesen, Smart Structures and Materials 2002 Conference, San Diego, 2002. CA.
10. Gallone, G., F. Galantini, and F. Carpi, Polymer International, 59(3)(2010) 400-406.
11. Razak, A.H.A., P. Szabo, and A.L. Skov, Rsc Advances, 5(65)(2015) 53054-53062.
12. Duenki, S. J., Ko, Y. S., Nueesch, F. A., and Opris, D. M., Advanced Functional Materials, 25(16)(2015) 2467-2475.
13. Skov, A. L., and Yu, L., Advanced Engineering Materials, 20(5) (2018) 1700762.
14. Yan, T., Schroeter, K., Herbst, F., Binder, W. H., and Thurn-Albrecht, T., Supramolecular polymer network. Sci Rep, 6(2016) 32356.
15. Ogliani, E., Yu, L., Javakhishvili, I., and Skov, A. L., R S C Advances, 8(15)(2018) 8285–8291.
16. Liu, L., Yan, S., and Zhang, L., Macromolecular Rapid Communications, 39(20)(2018) e1800349, e1800349.
17. Li, C.H., Wang, C., Keplinger, C., Zuo, J.L., Jin, L., Sun, Y., and Bao, Z., Nature Chemistry, 8(6)(2016) 619–625.
18. Mattia, E. and S. Otto, *Supramolecular systems chemistry.* Nat Nanotechnol, 10(2)(2015) 111-119.
19. Yu, L., Madsen, F. B., Hvilsted, S., and Skov, A. L., RSC Adv., 5(61)(2015) 49739-49747.

Anders Jaksland

E-mail: andjaks@kt.dtu.dk

Supervisors: John M. Woodley
Manuel Pinelo
Wan Yinhua, UCAS

PhD Study
Started: September 2017
To be completed: September 2020

Economic Evaluation of the Biotechnological Production of Bulk Chemicals

Abstract
In-situ Product Removal (ISPR) is seen as a potential technology to overcome the problems of product inhibition in bioprocesses. The maximum feasible cost when implementing ISPR in a two-stage fermentation process has been calculated for varying separation factors. The maximum feasible cost of implementing ISPR shows an increasing trend for increasing separation factors, however with a diminishing return. The cost includes capital investment and operational costs.

Introduction
In-situ product removal is defined as the fast removal of product from the site of reaction as it is formed [1]. The role of ISPR in a bioprocess is to reduce the effect of product inhibition on cell growth and/or product formation, by continuously removing the product from the fermentation vessel. This means the concentration build-up in the reaction is stopped at a point lower than the saturation concentration caused by the inhibition. When the concentration is kept at a lower point, then the productivity of the process increases. If the removal of product is selective, a higher concentration than the saturation concentration can be achieved downstream at the same time. Thus ISPR has the potential to increase both productivity and product concentration for the downstream process. A lot of research has been done in ISPR in the last thirty years [2], however some important questions remain unanswered:

"Which products benefit the most from having implemented ISPR?"
"What is the design of a process with ISPR and how is it operated?"
"At what cost does the ISPR have to be available if the overall process economics are to be improved?"

The last question is especially critical to find the answer to, as the driver for developing and implementing ISPR is to improve the process economics. With the implementation the increased productivity leads to a smaller and cheaper fermentation vessel and the increased product concentration leads to a less expensive downstream, both in operational and capital expenses.

These benefits of course do not come for free, and the cost of implementing and operating ISPR has to be lower than those benefits. No information is easily available about the benefits of the improvement or the costs of the ISPR making the economic assessment time consuming and difficult.

Estimating the Cost of ISPR
To answer the above question the maximum economically-feasible cost of the ISPR technology is estimated. This is done by costing two process designs, where the difference of the cost evaluation will be able to predict the maximum ISPR cost. The first process design is a process without ISPR implemented. The second process design is a process with ISPR implemented. When costing the second process the costs related to the actual ISPR, both the capital cost and the operational cost, will be assumed to be free. This means the difference in cost between the two cases, will be an upper bound for when the ISPR is economically feasible to implement. The two designs are not fully costed and designed, but only the part of the process where ISPR significantly changes something is taken into consideration. In this work that means the design spans from the bioconversion to a product concentration of 300 g/L.

The Two Process Designs
The two processes are designed to be fed-batch two-stage fermentations. The two stage fermentation process is chosen as it is one of the most promising bioprocesses for the production of bulk chemicals [3]. The two-stage fermentation also shows many synergies with ISPR

resulting in no oversizing of the ISPR unit and simple operation. The first stage is costed by the biomass requirement for the second stage and the second stage is costed based on the productivity.

In the process without ISPR the two-stage fermentation is followed by a separation of cells, that are then recycled to the second stage. The liquid stream containing the product is passed to an evaporation unit where the product is concentrated to the final 300 g/L.

In the process with ISPR the second stage of the fermentation is couple to the ISPR and the product is continuously removed during the fed-batch. The product stream downstream of the ISPR unit is passed to an evaporation unit where the product is concentrated to 300 g/L. The two designs can be seen in figure 1 and figure 2 respectively.
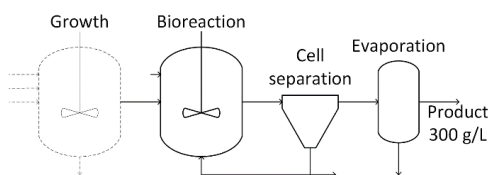
Figure 1: The process without ISPR.
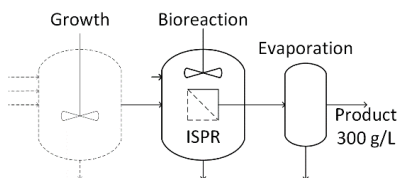
Figure 2: The process with ISPR.

Results and Discussion

For a variation in separation factor between 1 and 11, the optimal productivity and product concentration point of operation has been found and the corresponding cost difference calculated. The cost difference represents the maximum available cost of ISPR per kilogram product.
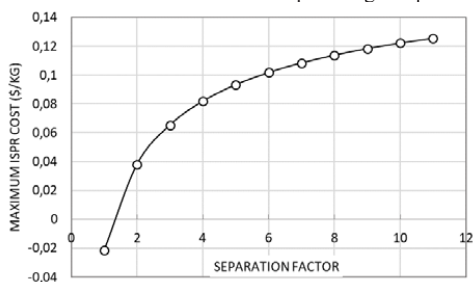
Figure 3: The cost difference between the two processes for varying separation factors.

In figure 3 the cost difference can be seen as a function of the separation factor for a specific case, where the base case design productivity was 2 g/l/h and the product concentration was 100 g/L. Any feasible implementation if ISPR has to be below the curve. The trend is that for an increased separation factor more money becomes available for the ISPR implementation. This follows the intuitive expectation of the cost of ISPR, the more selective the ISPR is, the more expensive it becomes. Another conclusion that can be made is that a simple in-situ recovery of the product, without any concentrating mechanism is not a feasible way of implementing ISPR as the process becomes more expensive compared to the normal design even before any money is spent on the ISPR.

To put the maximum ISPR cost into perspective the ISPR unit is now implemented as a membrane. If the membrane has a lifetime of 3 years, the cost per square meter can be calculated for varying total fluxes. This is shown in figure 4, where a feasible membrane price can be found below the curve. Be aware that the cost indicated is CAPEX and OPEX combined during 3 years.
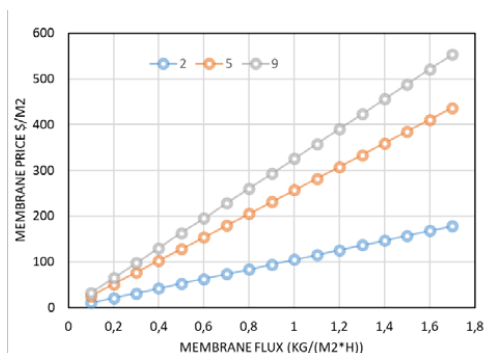
Figure 4: The combined CAPEX and OPEX cost in 3 years for a membrane for a variation of separation factors.

Conclusion

The maximum feasible cost of implementing ISPR in the two-stage fermentation has been calculated. The cost of ISPR shows an increasing maximum cost for an increasing separation factor, however with diminishing returns. Thee cost includes capital investment and operational costs.

References

1. J. M. Woodley, M. Breuer, D. Mink, Chem. Eng. Research and Design 91 (2013) 2029-2036.
2. W. V. Hecke, G. Kaur, H. De Wever, Biotech. Advances 32 (2014) 1245-1255.
3. J. M. Burg, C. B. Cooper, Z. Ye, B. R. Reed, E. A. Moreb, M. D. Lynch, Current Opinion in Chem. Eng. 14 (2016) 121-136.

Spardha Jhamb

Phone: +45 3062 8046
E-mail: spajha@kt.dtu.dk

Supervisors: Georgios M. Kontogeorgis
               Xiaodong Liang
               Kim Dam-Johansen

PhD Study
   Started: October 2016
   To be completed: September 2019

A Systematic Methodology for Property Model-Based Chemical Substitution and Solvent-based Coating Formulation Design

Abstract

A systematic model-based methodology for chemical substitution, which considers different problem definitions depending on the objective for substitution, has been developed. A general framework, which includes the algorithm steps of the methodology and corresponding data-flow, associated property models, activity coefficient models, property databases and modeling tools for generating and evaluating the substitute candidates, is presented here. The application of the developed methodology is tested through four case studies on substitution of chemicals used in chemical-based products and/or their corresponding manufacturing processes.

Moreover, the need of developing a systematic method for the selection of solvents in coating formulations is foreseen.

Introduction

Many hazardous chemicals are found in industrial processes, commodity products and consumer products. Both, mankind and environment are exposed to harmful properties of these chemicals, that have proven to be detrimental to human health and affect the smooth functioning of the ecosystem. Therefore, different legislations framed by the regulatory bodies have restricted the use of hazardous chemicals (e.g. Restriction of Hazardous Substances Directive by the European Chemical Agency, EChA [1]) and provided various degrees of incentives to substitute such chemicals used in manufacturing processes, equipment operations and formulated products, with environmentally benign and safe alternatives (e.g. EU Chemical Agents Directive, EU Carcinogens and Mutagens Directive [2]). Also, reputed organizations have already realized the importance of worker health and safety benefits and have experienced increase in productivity as well as have saved money by simply reducing the use of hazardous chemicals and implementing safer alternatives (U.S. Occupational Health and Safety Administration). Hence, besides the more noble objective of protecting humans and the environment from the dangers of unsafe chemicals, the regulations imposing chemical substitution have also provided the chemical industry with a monetary incentive.

Although several successful efforts to substitute hazardous chemicals have been made by both academia and industry (for example, Toxics Use Reduction Institute (TURI) at UMass Lowell, Substitution Support Portal developed through a collaborative effort of consultancy companies and non-profit organizations in Europe), a versatile methodology that can solve this problem in a systematic manner is required so that a viable solution can be reached by any user. Besides currently, substitution of hazardous chemicals from products, manufacturing processes and plant operations, is carried out either using time-consuming experimental procedures or using database search and predictive property models. But the use of property models is restricted to property prediction rather than alternative generation and design. A model-based method, therefore, can aid to quickly identify the reliable substitute candidates and consequently, the resources and time for experimental verification is focused only on a few chemicals.

Considering these reasons, the need for a generic and systematic model-based methodology for chemical substitution has been recognized. A chemical substitution methodology which can quickly and reliably identify the promising candidates through model-based techniques, check their economic feasibility and only then make use of experiments to verify their compatibility and applicability, has been developed and used to identify viable, safer chemical alternatives in four case-studies.

A Model-based Methodology and Framework

A systematic and generic framework, which incorporates model-based methods and tools that can solve a wide

range of chemical substitution problems has been developed. The framework comprises of methods, tools and databases that are required to chronologically perform a set of tasks. A workflow diagram for the methodology for substitution of hazardous chemicals available through this framework is shown in Figure 1.
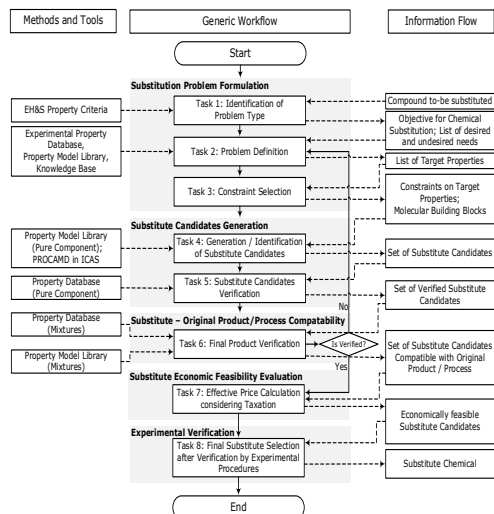

Figure 1: Workflow diagram for the methodology for chemical substitution

Results and Discussion

The developed substitution methodology has been explained below via one of the four solved case-studies.

Case-Study: Substitution of Methylene Chloride from a Paint and Epoxy Remover

The 'Jasco® Premium Paint and Epoxy Remover' is made up of 80% methylene chloride, 15 - 20% methanol and less than 5% of petroleum distillates (Whatsinproducts.com, 2001). However, methylene chloride is listed on the REACH 'Restricted Substances List' as it is a Volatile Organic Compound (VOC). In a study in Denmark [3], it was reported that, concentrations of methylene chloride in the breathing zone was found to be from 210 ppm (741 mg/m3) to 2025 ppm (7148 mg/m3) when liquid paint strippers were used indoors under general ventilation conditions. This value is considerably higher than the Permissible Exposure Limit (PEL) of 500 ppm (8h-TWA) established by the OSHA and 100 ppm (8h-TWA) established in most EU countries [4].

To identify a substitute for methylene chloride using Computer-aided Molecular Design, the needs are first translated to target pure component and mixture properties of the substitute candidate to-be-identified as given in Table 1. Constraints on these properties are supplied in the Pro-CAMD tool [5]. As a result of this step, nine substitute candidates are generated.

Additionally, to check if the substitute together with the other ingredients of the Jasco® stripper would give a similar performance as that of the original product, it has been assumed that the original product is a 20:80 % (v/v) mixture of methanol and methylene chloride. The substituted mixture, where the volume of methylene chloride in the original product is replaced with an equal volume of substitute candidate, should be able to dissolve an epoxy resin with a radius of solubility = 9 MPa½ and Hansen Solubility Parameters, δ_{d1} = 20 MPa½, δ_{p1} = 10 MPa½ and δ_{h1} = 8 MPa½.

Table 1: Needs and Target Properties of Substitute

Need	Target Property
Liquid phase	Normal Melting Point (NMP), Normal Boiling point (NBP)
Low volatility	Vapor pressure (VP)
Low flammability	Flash Point (FP)
Non-toxic in vapor phase	Vapor toxicity ($LC_{50,vapor}$)
Miscibility in original mixture (contains higher alkanes ($C_{14} - C_{15}$) and methanol)	Gibbs energy of mixing (ΔG^{mix}), Solubility Parameter ($\delta_{Hild,298K}$)
Ability to dissolve epoxy resin	Hansen solubility parameters ($\delta_{d2}, \delta_{p2}, \delta_{h2}$)

Out of the nine candidates, only the 20:80 (v/v) mixture of methanol and 2 – propanone could dissolve the polyester resin as this mixture has a solubility parameter distance, R_a of 8.89 MPa½.

Conclusion and Future Work

Hence, a systematic model-based methodology for chemical substitution has been developed and has been used to substitute environmentally hazardous and/or unsafe chemicals in liquid phase homogeneous formulations from various industrial sectors.

Besides, the need for a systematic methodology to select non-toxic and biodegradable solvents for a coating formulation is recognized. One of the foreseen application areas is, to select a solvent mixture for the wet dispersion of pigments before their size distribution is measured in a Master Sizer.

Acknowledgements

References

1. Echa.europa.eu, REACH Legislation - ECHA [online] Available at: https://echa.europa.eu/regulations/reach/legislation [accessed 8 Oct. 2018]
2. Osha.europa.eu. European directives on safety and health at work - EU-OSHA. [online] Available at: https://osha.europa.eu/en/safety-and-health-legislation/european-directives [accessed 8 Oct. 2018]
3. Miljøstyrelsen, Denmark. Miljø projekt nr 101 (1988)
4. OECD. Risk Reduction Monograph No. 2: Methylene Chloride, Background and National Experience with Reducing Risk, OECD Environment Monograph Series 101, 1994, Paris
5. R. Gani, G. Hytoft, C. Jaksland, A.K. Jensen. Comp and Chemical Eng. 21(10) (1997) 1135 - 1146.
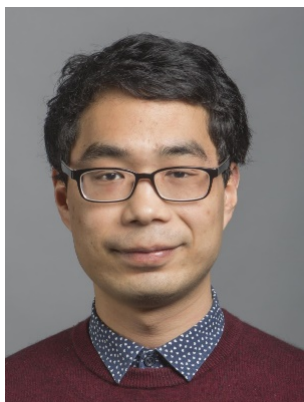
Mingbo Ji

Phone: +45 52909785
E-mail: minji@kt.dtu.dk

Supervisors: Manuel Pinelo
    Anders Egede Daugaard
    John Woodley

PhD Study
  Started: February 2018
  To be   January 2021
completed:

Effect of selected chemical treatments on the performance of commercial polymeric membranes

Abstract

Ultrafiltration (UF) membranes are widely used in industrial purification and concentration. However, conventional UF membrane separation cannot satisfy all industrial requirements due to membrane fouling or low selectivity in some applications. Membrane pretreatment with solvents/chemicals may be exploited to develop high performance UF membranes because of its simplicity and convenience. In the present work, we treated polysulfone (PSf) and regenerated cellulose (RC) membranes with an ethanol solution at certain conditions. Ethanol-treated PSf membranes shows much higher water permeability than the virgin membrane -about 7 times-, while ethanol-treated RC membrane displays little significant changes in terms of water permeability. Meanwhile, ethanol treatment decreased retention for both pepsin and BSA slightly for PSf membranes. However, it seems that ethanol-treated PSf membranes suffer more severe fouling during protein filtration, which need to be further studied.

Introduction

Previous research demonstrated that exposure to some solvents/chemicals would significantly change membrane properties and impact membrane performance. For instance, Ross et al. [1] reported that defluorination and oxygenation occurred on PVDF membranes under NaOH treatment, which would enhance the hydrophilicity of the membrane. Navarro et al.[2] suggested that significant hydrolysis only and partial hydrolysis alone on H_3PO_4 and HF treated membrane occurs, respectively. In addition, a HF treatment increases flux due to the resultant higher hydrophilicity without a significant change in pore size, while the H_3PO_4 treatment substantially increases flux due to the wider pores, even with a reduction in hydrophilicity. Zhang et al. [3] treated the PSf and PVDF membrane with NaClO. The results demonstrated that pore was enlarged, which was verified by dextran sieving experiments and the decreased HA rejection rate. Moreover, the increased negative charge on aged PSf membrane surface have a great impact on its sieving properties and fouling propensity.

Based on studies above, the general conclusion that can be drawn is that solvents/chemicals treatment change the membrane property, such as hydrophilicity, pore size, charge, etc. severely affecting the membrane performance. Thus, solvent/chemicals treatment may be a promising way to develop high performance UF membranes.

Specific objectives

The objective of the PhD project focuses on separating proteins (which possess similar molecular weight) with a high separation factor and further developing a novel, simple, universal and efficient modification protocol for membrane surface regulation to obtain high performance membranes. The scope of the PhD work includes:

- Membrane pretreatment with solvents/ chemicals such as ethanol, NaOH, NaClO, etc.
- Membrane performance in terms of water permeability, protein flux, retention, flux recovery ratio (FRR), pore size distribution, etc. will be studied in detail.
- Elucidating the mechanism of solvents/chemicals treatment with different membranes
- Based on mechanism of pretreatment, new modification methods will be developed, such as surface charge regulation, which is producing lots of charge groups on membrane surface. Different groups and immobilization methods will be studied.
- Investigating the effect of surface charge on membrane separation performance as solvents/chemicals treatment
- Evaluating the protocol of commercial membranes modification, such as stability, reuse, cleaning, etc.

Results and discussion

As shown in Figure 1 and 2, ethanol-treated membranes shows seven times higher water permeability than virgin PSf membranes. It can be seen that protein flux decreased tremendously during filtration and resulting low flux recovery ratio. It is interesting that there is no significant changes in pepsin retention, which needs to be further studied.
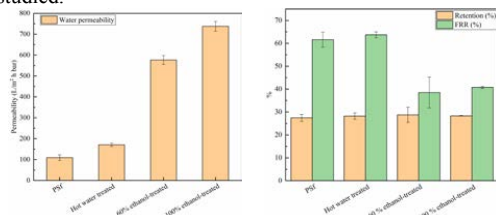
Figure 1: Water permeability, pepsin retention and flux recovery ratio (FRR) for pristine and ethanol-treated membranes, condition: 1 g/L, pH 4.7, stirring rate 100 rpm
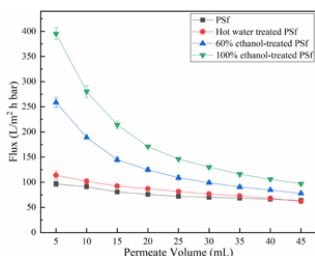
Figure 2: Pepsin flux for pristine and ethanol-treated membranes

To reduce concentration polarization on the membrane surface, we increased the stirring ratio to 500 rpm during filtration.   As shown in Figure 3, pepsin shows higher flux decline than BSA, which means that pepsin will foul membrane quickly. Furthermore, it shows that BSA and pepsin retention decreases slightly for ethanol-treated membranes, indicating that membrane pores are changed.
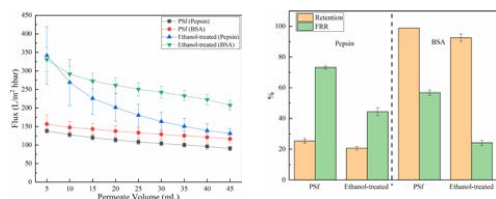
Figure 3: Flux, retention and FRR of pepsin and BSA filtration for pristine and ethanol-treated membranes, condition, 1 g/L, stirring rate 500 rpm

We further studied the protein retention performance from Figure.4, which shows the permeate volume dependent retention. We hypothesize that during the initial 0-10 mL, pepsin goes through the membrane by a sieving effect, leading to low retention; 10-25 mL, protein blocks membrane pores, leading to high retention; 25-45 mL, high concentration of residual solution results in more protein going through the membrane, leading to low retention.
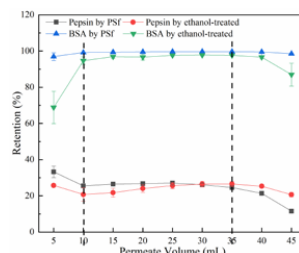
Figure 4: Permeate volume dependent retention of pepsin and BSA for PSf and ethanol-treated PSf membranes

As shown in Figure.5, ethanol treatment seems to have little effect on permeability and recovery for the RC membrane. The possible reason is that the RC membrane is hydrophilic intrinsically, leading to high flux recovery ratio. Furthermore, high FRR suggests that RC membrane mainly suffers surface fouling
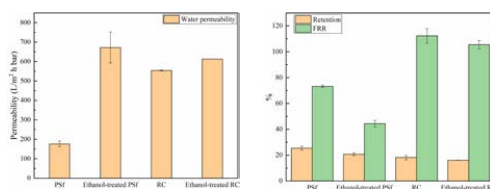
Figure 5: Water permeability, pepsin flux, retention and flux recovery ratio for PSf and regenerated membranes

Conclusions and Future work

Ethanol pretreatment significantly increases the water permeability of commercial PSf membranes, approximately 7 times higher than virgin membranes. Ethanol-treated PSf membranes suffer more severe fouling than virgin membranes. Ethanol treatment changes the membrane pores, which is verified by the retention of pepsin and BSA. However, due to intrinsic hydrophilicity, ethanol treatment has little effect on regenerated cellulose membrane.

Future work will mainly focus on the mechanism elucidation of solvents/chemicals on membranes and on developing other modification methods.

References

1. Ross, G. *Polymer (Guildf)*. **2000**, *41*, 1685.
2. Navarro, R.; González, M. P.; Saucedo, I.; Avila, M.; Prádanos, P.; Martínez, F.; Martín, A.; Hernández, A. *J. Memb. Sci.* **2008**, *307*, 136.
3. Zhang, Y.; Wang, J.; Gao, F.; Chen, Y.; Zhang, H. *Water Res.* **2017**, *109*, 227.

Mark Jones

Phone: +45 4525 2910
E-mail: Mark.Jones@alfalaval.com

Supervisors: Bent Sarup, Alfa Laval Copenhagen A/S
                Gürkan Sin

PhD Study
  Started: April 2016
  To be completed: April 2019

Multi-scale Framework for Design and Optimisation applied to Oleochemical Processes

Abstract

In this work we present a modular multi-scale framework where we provide tools ranging from property prediction to unit operation and flowsheet modelling up to the top-level superstructure optimisation. The framework has been applied to the domain of oleochemical processes where vegetable oils are hydrolyzed to give fatty acid mixtures which must be separated in specific saturated and unsaturated C-cuts and a sweet water mixture which needs to be purified to higher grade glycerol purity.

Framework

The developed framework builds on Fortran and Python being the main programming languages combined with free license and open-source packages. The different layers are connected with each other so that data can be exchanged between the engineering tasks with a high degree of automation. Each layer allows to be individually wrapped and made available for different analysis and optimisation methods such as sensitivity analysis, surrogate-based and derivative-free optimisation techniques.
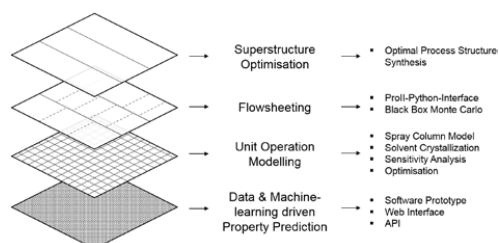
Figure 1: Modular multi-scale framework for design and optimisation

SAFEPROPS: Property Prediction Software Prototype with Machine-learning Methods and Confidence Intervals

SAFEPROPS (safeprops.io) is a property prediction prototype which allows the user to retrieve physical and thermophysical properties by accessing the web-interface or API of the server-based application. Machine-learning methods (Gaussian process regression and neural networks with drop outs) are being currently implemented to enhance group-contribution methods with a more data-driven approach.

Model Library

Apart from models available in the Pro/II process simulator (CSTR, distillation, evaporator, molecular distillation) we also implemented a finite volume model for a counter-current spray column and a solvent crystallization model. The model library layer allows to apply sensitivity analysis, surrogate modelling and derivative-free optimisation with the packages f90wrap [1], SALib [2], Chaospy [3] and scikit-learn [4].
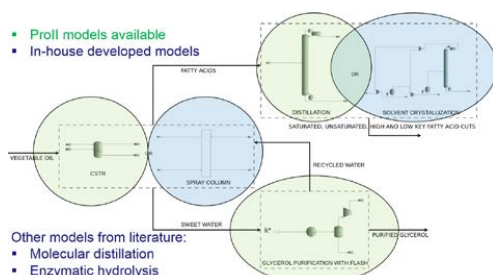
Figure 2: Models for the oleochemical process domain

Uncertainty and Sensitivity Analysis with ProII-Python-Interface

We developed an interface to connect the commercial process simulator Pro/II with Python or Matlab to apply Monte Carlo based methods which allows us to run black box evaluations of process flowsheets as seen in Figure 3 where we for example propagated the uncertainty in the parameters of the SRK equation of state (T_C, P_C and ω) through the process system and retrieved the uncertainty and sensitivity of the model output (in this example the coefficient of performance COP) subject to these property uncertainties.
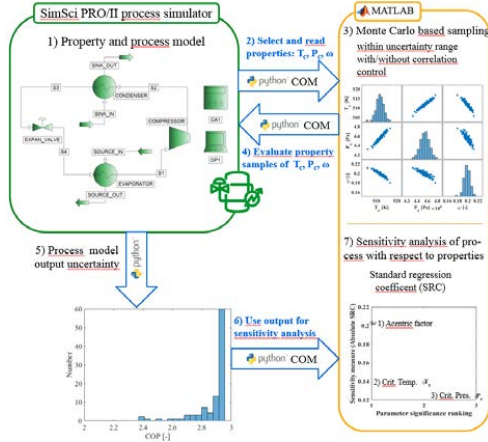
Figure 3: Uncertainty and sensitivity analysis with the ProII-Python-Interface [5]

Superstructure Optimisation with General Disjunctive Programming and Surrogate Models

On the superstructure optimisation layer we use surrogates derived from unit operations or entire sub-process flowsheets to include them in the formulation of a general disjunctive program (GDP) [6]:

$$
\begin{aligned}
\underset{x}{\text{minimize}} \quad & Z = \sum_{u \in U} c_u + f(x) \\
\text{subject to} \quad & h(x) = 0 \\
& g(x) \leq 0 \\
& \begin{pmatrix} Y_u \\ h_u(x) = 0 \\ r_u(x) \leq 0 \\ c_u = \gamma_u \end{pmatrix}, \forall u \in U^P
\end{aligned}
$$

$$\Omega(Y) = True, \quad Y_u \in \{True, False\}, \quad x \in X, \quad c_u \geq 0$$

Figure 4: Equation system for general disjunctive programs and permanent unit operations

$$
\begin{bmatrix} Y_u \\ h_u(x) = 0 \\ r_u(x) \leq 0 \\ c_u = \gamma_u + \sum c_{uv} \\ \begin{bmatrix} Y_{u,v} \\ h_u(x) = 0 \\ r_{uv} \leq 0 \\ c_{uv} = \gamma_{uv} \end{bmatrix} \vee \begin{bmatrix} \neg Y_{u,v} \\ B^{uv}x = 0 \\ c_{uv} = 0 \end{bmatrix}, \forall v \in U^C_{FE} \end{bmatrix} \vee \begin{bmatrix} \neg Y_u \\ B^{u}x = 0 \\ c_u = 0 \end{bmatrix}, \forall u \in U^C
$$

Figure 5: Disjunction with finite element disjunctions for conditional unit operations [7]

The superstructure problem implemented in Pyomo [8] solves the disjunction between a spray column or a series of CSTRs for the hydrolyzing step of vegetable oil to fatty acids and glycerol in respect to minimizing total annual cost (TAC) subject to the global constraints being the minimum and maximum product demand, overall mass balances around the two processes and closing equations. The fixed parameters were product sales price, raw material and utility costs. The GDP is first transformed via convex-hull relaxation into a mixed integer nonlinear problem (MINLP) and then solved with IPOPT. Other solvers such as GDPopt and Couenne were also tested.

Conclusions

A modular framework has been established with Fortran, Python and additional packages such as Pyomo. Results [9] [10] show that we can perform research on all key issues such as optimisation of the steam inlet distribution to the spray column, sensitivity analysis of (sub-) process models and determining optimal process structures.

Acknowledgements

References

[1] https://github.com/jameskermode/f90wrap
[2] https://salib.github.io/SALib
[3] https://github.com/jonathf/chaospy
[4] https://scikit-learn.org
[5] J. Frutiger, M. Jones, N. Ince, G. Sin; Computer Aided Chemical Engineering, 44 (2018) 1489-1494
[6] M. Mistry, A. D'Iddio, M. Huth, R. Misener; Computers & Chemical Engineering, 133 (2018) 98-114
[7] B. Pahor, Z. Kravanja, N. Bedenik; Computers & Chemical Engineering, 25 (2001) 765-774
[8] https://pyomo.org
[9] M. Jones, H. Forero-Hernandez, A. Zubov, B. Sarup, G.Sin; Superstructure Optimization of Oleochemical Processes with Surrogate Models; Computer Aided Chemical Engineering, 44 (2018) 277-282
[10] M. Jones, H. Forero-Hernandez, B. Sarup, G. Sin; Computer Aided Chemical Engineering 40 (2017) 1885-1890

Alena Jurásková

Phone: +45 50174558
E-mail: alejur@kt.dtu.dk

Supervisors: Anne Ladegaard Skov
              Kim Dam-Johansen
              Stefan Møller Olsen, Hempel A/S

PhD Study
 Started: February 2018
 To be completed: February 2021

Challenges of thin silicone condensation curing films with well-defined structure

Abstract

In this study, preparation of thin films (~100µm) of condensation-curing silicones is investigated. It is found that behavior of typical condensation curing system consisting of OH terminated poly(dimethylsiloxane) (OH-PDMS), tin catalyst and methyltrimethoxysilane (MTMS) or tetraethoxysilane (TEOS) cross-linker is highly dependent on the sample thickness. High volatility of the cross-linkers that becomes enhanced with decreasing sample thickness is reported. The high volatility does not allowed for proper curing of thin silicone films, even though the cross-linker is used in excess. In addition, reliability and reproducibility of such system becomes an issue.

Introduction

Silicone elastomers are materials known for good thermal and oxidation stability, flexibility, hydrophobicity, low surface energy, etc. This makes them the first choice for many applications in electronic, medical, automobile, aerospace and many other industrial fields. Nevertheless, the use of silicone elastomers is limited by their rather poor mechanical properties. The improvement of mechanical properties by addition of fillers or by chemical modification comes often together with deterioration of some of the properties mentioned above [1]. One way to improve mechanical properties without influencing other desirable properties is by changing the network structure. Several studies regarding the structure-property relationship have been done in addition curing silicones [2, 3]. Nevertheless, not much work has been done in the more economically friendly, room temperature curing condensation type of silicone elastomers [4]. In addition, no study was conducted with respect to the long-term properties of the networks. Therefore, preparation of condensation curing type of silicone elastomers with well-defined structure and stable properties over time remains a challenge, especially when thin films are required.

Materials & Methods

Silicone elastomers were prepared by condensation curing reaction between methoxy groups of the cross-linker and OH groups of the OH terminated PDMS in a high humidity oven at 25°C (Figure 1). The stoichiometric ration between functional groups of MTMS cross-linker (f = 3) and OH-PDMS (f = 2) was kept equal to r = 5.
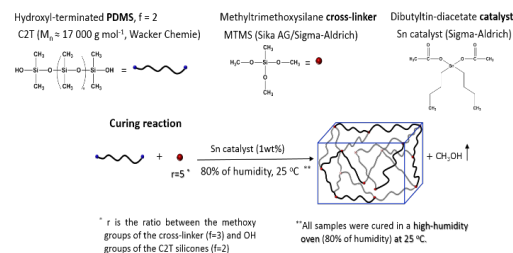
Figure 1: Materials and curing reaction used to synthetize condensation curing silicone elastomers.

Results and Discussion

The influence of sample thickness on condensation curing reaction of silicone elastomers has been investigated. From Figures 2 and 3 can be see that weight loss of the sample over time is highly dependent on the sample thickness. The weight loss during condensation curing reaction is a typical feature caused by alcohol release (Figure 1). Nevertheless, if only alcohol (in this case methanol) and eventually the catalyst would be realized from the system, no difference in the final weight loss percentage of the samples should be seen, because the composition stays the same for all tested thicknesses. In addition, the films of thickness $\leq 0,6$ mm are not cured

and samples with thickness ≥ 1.5 mm remain sticky on the surface, if methyltrimethoxysilane (MTMS) from new bottle is used (Figure 2). This signifies uncompleted curing of the samples even thought, the MTMS was used in high excess (r=5).
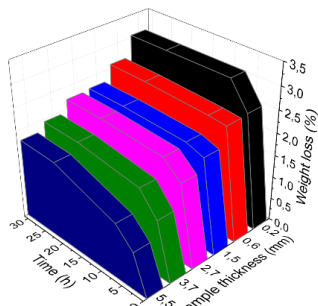
Figure 2: Weight loss (%) of the samples consisting of C2T, MTMS (new bottle, 2.57 wt%) and dibutyltin diacetate (1.14 wt%) over time. Thickness of the samples was varied from 0.2 to 5.5 mm.

The results above indicate high volatility of MTMS cross-linker, if it is used in high purity without any trace of hydrolyzation. Therefore, the weight loss presented in Figure 2 is a combination of the MTMS evaporation, methanol release and eventually catalyst evaporation. Such cross-linker is then not suitable for condensation curing, especially if thin films are required. The same features were observed if tetraethoxysilane (TEOS) was used as the cross-linker.
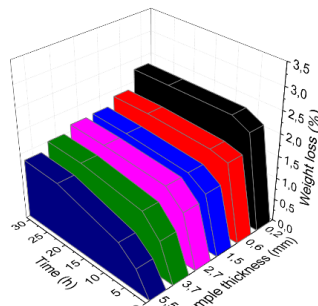
Figure 3: Weight loss (%) of the samples consisting of C2T, MTMS (old bottle, 2.55%) and dibutyltin diacetate (1.17 wt%) over time. Thickness of the samples was varied from 0.2 to 5.5 mm.

The evaporation is significantly decreased if old bottle of MTMS product is used as can be seen in Figure 3. Samples of all thicknesses were cured within few hours, without leaving the surface sticky. This is probably due to partial hydrolyzation and subsequent condensation of the MTMS, resulting to a mixture of hydrolysis product, which are less volatile compare to pure MTMS and therefore are able to cross-link the system. This means that attention has to be paid if MTMS and TEOS cross-linkers are used for condensation curing of the silicone

elastomer. As due to the high volatility of the cross-linkers, the system is sensitive to the thickness of the sample, time required for the mixing of the components and temperature and humidity during the sample preparation. In addition, the cross-linkers are prone to hydrolyzation, which limits the reproducibility of the curing reaction.

Figure 4 summarize long term stability of the silicone networks cross-linked by partially prehydrolyzed MTMS represented by Young´s modulus and elongation at break. The measurements were done using ARES-G2 rheometer. It can be see that both, elongation at the break and the Young´s modulus are not stable over time.
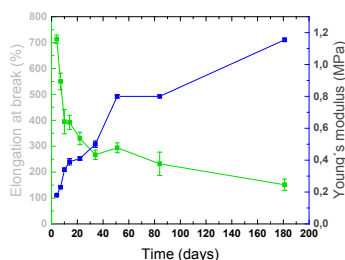
Figure 4: Long-term properties of silicone elastomer (thickness 100 µm) consisting of C2T, MTMS (old bottle, r=5) and dibutyltin diacetate (~1 wt%) represented by elongation at break (%) and Young´s modulus (MPa).

Conclusion

For preparation of thin condensation curing silicone elastomer films, special attention has to be paid to the choice of the cross-linker. Cross-linkers, typically used for condensation curing of silicone elastomers, MTMS and TEOS, suffer from high volatility and are therefore unable to take part in the curing reaction if the required film thickness decrease under certain level. The volatility is decreased if the cross-linkers mentioned above are partly pre-hydrolyzed. Nevertheless, even though partly hydrolyzed MTMS allowed the curing of thin silicone elastomer layer, the mechanical properties of the film are not stable over time. Therefore, different, more stable cross-linkers have to be considered in the future.

References
1. F. B. Madsen, A. E. Daugaard, S. Hvilsted, A. L. Skov, Macromol. Rapid Commun. 37 (5) (2016) 378–413.
2. A. G. Bejenariu, L.Yu, A. L Skov, Soft Matter. 8 (14) (2012) 3917–3923.
3. F. B. Madsen, A. E. Daugaard, C. Fleury, S. Hvilsted, A. L. Skov, RSC Adv. 4 (14) (2014) 6939–6945.
4. R. W. Winter, G. B. Shah, Macromol. Chem. Phys. 2208 (2002) 1-8.

Kasper Martin Jønck

Phone: +45 6194 6425

E-mail: kasmj@kt.dtu.dk

Supervisors: Peter Arendt Jensen

Peter Glarborg

Hao Wu

Lars E. Hansen, ROCKWOOL International A/S

Haosheng Zhou, ROCKWOOL International A/S

PhD Study

Started: April 2018

To be completed: June 2021

CFD-based Optimization of High Temperature Melting Cyclones used in Stone Wool Production

Abstract

The main focus of this PhD project is the development of a Computational Fluid Dynamics (CFD) model for simulation of melting cyclones used in the production of stone wool. The validated CFD model will be applied to evaluate the influences of fuel properties and operating conditions on melting cyclone performance, and to optimize the operation and design of melting cyclones.

Introduction

Stone wool is produced by melting raw materials and subsequently spinning the 1500 $^{\circ}$C melt into fibers using a cascade spinner [1].

Traditionally the melting of the raw materials has been done in a cupola furnace with the necessary heat obtained through the combustion of coke.

This PhD study focuses on a new cyclone based melting technology developed by Rockwool; the Integrated Melting Furnace (IMF).

In the IMF, raw materials and stone wool waste is blown tangentially into a melting cyclone along with pulverized coal, air, oxygen and natural gas. This generates a swirling motion inside the cyclone in which combustion of the fuel and heating of the feed takes place. The cyclone motion results in the separation of molten particles and the flue gas.

The impact of molten particles on the walls results in the formation of a melt layer that flows down the cyclone and forms a melt bath in the bottom. A sketch of the melting cyclone is shown in Figure 1.

The technology has an increased energy efficiency and reduced CO_2 emission compared to the cupola ovens.

However, there is pressure to further increase the efficiency and reduce the emissions (e.g. CO_2, NO_X). To achieve this better understanding of the process is needed.

Specific Objectives

The aim of the project is to improve the understanding of the physical and chemical processes in the melting cyclone. This will be done through the following steps:

- An integration of fluid dynamic modelling, solid fuel combustion modelling and melting models in a melting cyclone simulation.
- Verification of model performance with experimental data and evaluate melting cyclone performance.
- Investigation of the influence of applying biomass to substitute coal in a melting cyclone and how this influences cyclone performance.
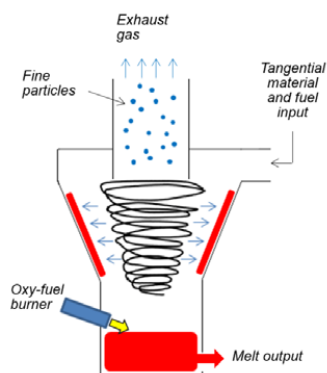
Figure 1: Conceptual sketch of the IMF Melting Cyclone

Experimental activity

In order to verify the CFD simulations experimental data of the process is needed however no experimental studies on cyclones with combustion and melt collection have been found in the peer reviewed literature.

Measurements are therefore performed on full-scale installations at ROCKWOOL factories. The possible measurement types are limited by the hostile environment (i.e. very high temperatures and slagging) in the furnace. Currently, measurements of the flue gas temperature and composition and the heat flux have been performed or are planned.

Modelling methodology

The commercial software ANSYS Fluent is used to perform the CFD simulations of the melting cyclones.

To capture the multiphase reacting particulate flows, a combination of Eulerian and Lagrangian approaches will be used where the Eulerian method is used for the fluid flows and a coupled Lagrangian method is used for raw materials, wool waste and pulverized fuels.

Part of the work will be to test the different existing models for turbulence, radiation, and chemical reactions to determine where the need for development is greatest. The existing models in the software will be modified or extended when needed using User Defined Functions.

Current Results

Melting cyclones are employed in several fields most notably within metal production e.g. for the smelting of copper. However, a literature study has revealed a dearth of published knowledge on melting cyclones.

The lack of published data and limited possibilities for measurements will likely lead to separate validation of different physics and models needed in the simulations.

A lot of work has been performed for slagging coal combustion that is also relevant for this project, e.g. see [2].

Simple CFD calculations have been performed with each case capturing only a few of the relevant physical phenomena.

Conclusions and future work

Additional measurement data are needed and means of acquiring these will be investigated.

The complexity of the CFD simulations will increase by gradually combining more and more physics in the same simulations. These simulations will serve as a proof-of-concept and to evaluate the feasibility of full scale simulations encompassing the full physics. Based on the outcome of these tests the modelling strategy will be adapted.

Acknowledgements

References

1. B. Sirok, B. Blagojevic, P. Bullen, Mineral wool: production and properties, Elsevier, 2008
2. L. Chen, A. F. Ghoniem, Fuel 113, (2013) 357–366.

Adam Paul Karcz

Phone: +45 4525 2830

E-mail: adkr@kt.dtu.dk

Supervisors: Kim Dam-Johansen
              Anne Juul Damø
              Martin P. Andersson

PhD Study
  Started: May 2016
  To be completed: April 2019

Surface Characterization of Activated Chalcopyrite Particles

Abstract
The world's most abundant copper mineral, chalcopyrite ($CuFeS_2$), is difficult to extract in atmospheric leaching using traditional ferric sulfate lixiviants, because of its unique physical properties. FLSmidth® has devised a novel approach, which utilizes a mechanochemical Rapid Oxidative Leach (ROL) assisted by a Stirred Media Reactor (SMRt). Due to the reduction of surface passivation problems associated with atmospheric leaching, this process is able to achieve copper recoveries >97% in under 6 hours. An important contribution to this is a preconditioning step, which uses a few percent or less of copper (II) ions to dope the mineral and thereby "activate" chalcopyrite. Because this activation plays a major role in accelerating the leach kinetics, it is critical to understand the associated phenomena and their part in the ROL. The project aims at using characterization techniques to study the mechanisms of the activation process. Design and conduction of relevant activation/leaching experiments will be supported by density functional theory (DFT) modelling of physical changes in the mineral. Through a better understanding of the mechanisms at play during the activation and subsequent leaching, methods to improve the process will be developed that maximize the efficiency of atmospheric leaching.

Introduction

Due to the near-term transitioning of a large number of mine sites from heap leaching and smelting of high-grade copper oxide ore to abundant, low-grade copper sulfide (i.e. chalcopyrite) ore processing, there is high interest in finding a cost-effective copper extraction method that is compatible with current industrial infrastructures [1]. However, the atmospheric leaching of chalcopyrite has proven to be arduous [2]. Most copper sulfide minerals require the application of both an acidic environment and an oxidizing agent to leach copper as Cu^{2+}. These conditions are achieved using oxidizers such as ferric (Fe^{3+}) ions, as either a sulfate or chloride:

$$CuFeS_2 + 4Fe^{3+} \rightarrow Cu^{2+} + 5Fe^{2+} + 2S^0$$
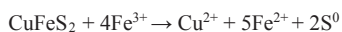
However, atmospheric leaching of chalcopyrite concentrates using such leaching aids is well known to suffer from slow kinetics and poor copper recoveries, due to (a) the semiconducting properties of chalcopyrite and (b) the formation of a passivation layer (i.e. sulfur species) on the surface of the particles [1].

To account for the slow kinetics, FLSmidth® has developed the ROL process, which is compatible with existing extraction processes and is cost-effective.

The ROL approach is two-stage process, which consists of the following:

1. Reductive activation through Cu^{2+} doping of chalcopyrite to form an intermediary copper sulfide ($Cu_X S_Y$) surface for enhanced reactivity.

2. Oxidative leaching of copper in a batch or continuous leach circuit comprised of a continuous stirred tank reactor (CSTR) assisted by a stirred media reactor (SMRt), which mitigates the passivation of the particles by cleaving new, active surfaces.

The main advantage of the ROL process is that it can complete leaching within 6 hours and with much lower energy consumption compared to competition (<100 kWh/t for ROL process vs. >1,000 kWh/t for competitors [3]).

Specific Objectives

The main challenges of the PhD project are to elucidate the mechanisms involved in the surface reactions of activated and leached chalcopyrite particles. Important studies that require attention include the bulk (chalcopyrite) structural changes that occur to the particles after activation, the role of pH and redox potential during the reaction, an understanding of the

degree of activation and its relation to leaching kinetics, and the effect of high-energy mixing creating transitory surface states (and the relaxation time of these states).

In particular: (1) the structural details, such as lattice parameters and crystal structure, and (2) chemical/ electronic property identification/determination of the activated and leached chalcopyrite particles will be investigated; therefore, the application of advanced (nano-scale) characterization is needed. The project will aim at using surface and bulk materials characterization techniques, i.e. x-ray diffraction (XRD), transmission electron microscopy (TEM), and x-ray photoelectron spectroscopy (XPS), to explore – and to better understand – the structural details of activated and leached chalcopyrite particles. These results will be supported with appropriate quantum mechanical and reaction engineering models, particularly density functional theory (DFT).
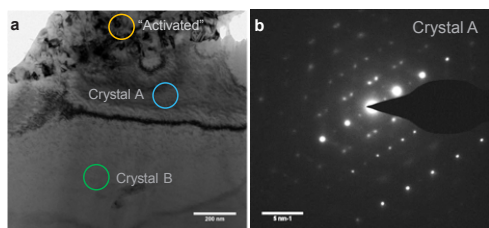
Figure 1: a TEM image a chalcopyrite slab where diffraction patterns were taken. Scale bar is 200 nm. **b** Select area diffraction pattern of the area indicated as Crystal A. Scale bar is 5 nm^{-1}.

Results and Discussion

Since lattice restructuring can have such a dramatic influence on semiconductor reactivity, we investigated the relationship between chemical activation and deformation of the chalcopyrite crystal through the use of electron microscopy [4]. Although the extent of conversion was about a few mol%, the lattice was found to be strained throughout the particle. To substantiate these observations, we plan to elucidate the electrochemical effects of activation by studying the experimental conditions through spectroscopy and atomistic modeling, e.g., DFT calculations via FHI-aims software [5] in Fig. 2. For instance, it can be used to understand the strain in the crystal lattice due to copper doping as a bulk change, or it can be seen through surface effects by comparing interactions with different ionic species (Fig. 3).

Conclusions

The results so far provide insights into the complex mixture of physical phenomena that come together to explain the difficulty of leaching (tendency of sulfur to form on the surface) and improved kinetics due to activation (improved conduction at the surface and increased strain in chalcopyrite particles).
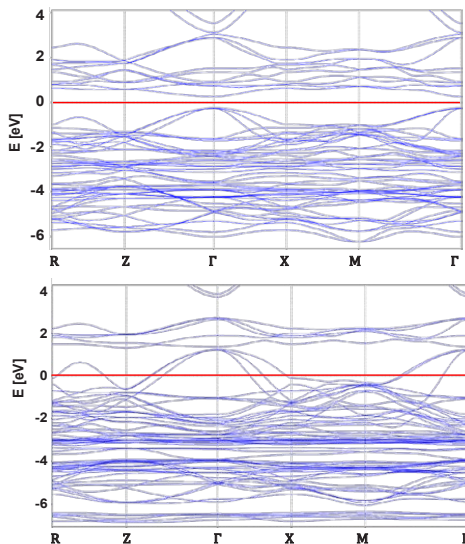
Figure 2: The band structure of chalcopyrite using unmodified structure (top) and 50% of iron replaced with copper, i.e. highly activated (bottom). Red line is the Fermi level, in which bands below are valence and above are conduction. A gap represents a (semi-) insulator (top) while overlap leads to metallic behavior (bottom). Hence, copper doping has a clear trend toward making the mineral more conductive and improving the electrochemistry.
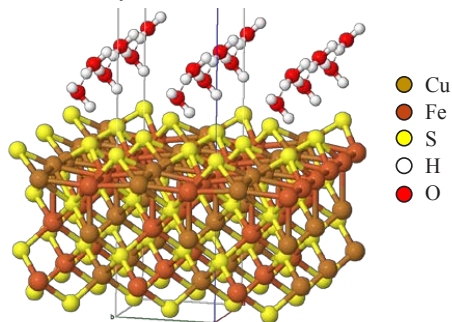
Figure 3: Relaxation of chalcopyrite with an initially metal-terminated surface in the presence of water shows restructuring of the sulfur atoms to migrate to the surface and cause hydrophobic behavior.

References

[1] C. Eyzaguirre, S.S. Rocks, R. Klepper, F.A. Baczek, D. Chaiko, in:, Hydroprocess, Antofagasta, Chile, 2015.
[2] K. Osseo-Asare, Hydrometallurgy 29 (1992) 61–90.
[3] J.R. Cobble, C.E. Jordan, D.A. Rice, Hydrometallurgical Production of Copper From Flotation Concentrates. USBM RI 9472, USBM RI 9472, 1993.
[4] A.P. Karcz, A.J. Damø, J.B. Illerup, S. Rocks, K. Dam-Johansen, D. Chaiko, J. Mater. Sci. (2017).
[5] V. Blum, R. Gehrke, F. Hanke, P. Havu, V. Havu, X. Ren, K. Reuter, M. Scheffler, Comput. Phys. Commun. 180 (2009) 2175–2196.

Sara Krpović

Phone: +45 5019 9187
E-mail: sarakr@kt.dtu.dk

Supervisors: Anne Ladegaard Skov
Kim Dam-Johansen

PhD Study
Started: February 2018
To be completed: January 2021

Coating with inherent sensing functionality based on dielectric elastomer

Abstract

Dielectric elastomers (DEs) are soft transducers that can be used as actuators, generators and sensors, due to their ability to convert electrical energy into mechanical energy and vice versa. In this project we propose the use of DE as capacitive tactile sensor for the detection of biofouling and barnacles, on the synthetic surface exposed to the aqueous environment.

Introduction

Biofouling and barnacles accumulation on synthetic surfaces, which are exposed to the natural aqueous environment, presents serious problems in the marine industry [1]. High cost of registrations of antifouling coatings containing toxic ingredients, ecological awareness and high cost of cleaning damaged coatings, led to substantial interest in the development of coatings with sensing and selfcleaning functionality.

Current antifouling approaches and technologies include coatings with controlled release of biocides in order to detach biofouling from the surface, and systems where intentional deformation of DE can be employed to detach biofouling species [1, 2]. This intentional deformation of DE is a consequence of the applied voltage to the electrodes sandwiching the dielectric material. Columbic force created between opposing charges causes the decrease of thickness and increase in planar area of incompressible elastomer.

However, the detection of biofouling and barnacles on the synthetic surfaces exposed to the aqueous environment, is still visual only. Hence, a need is to develop a new approach that enables more effective detection of biofouling and thus easier cleaning of fouled surfaces.

Objectives

The objective of the PhD project is to fabricate a sensor based on DE, which actively and effectively detects and detaches biofouling from the synthetic surface exposed to the aqueous environment. This sensitive and active surface will be made from materials, which are already used in the coating industry. The sensor will be made as a system with two compliant electrodes and intermediate silicone based DE between them, where the change of the capacitance of the sensor will indicate the presence of biofouling and barnacles on the surface of the sensor. This change of the capacitance of the sensor is caused by a change of the thickness and surface area of the DE in response to external stimuli. The capacitance of the sensor (Figure 1(a)) can be estimated by following equation (1).

$$C = \varepsilon_r \varepsilon_0 \frac{A}{t} \tag{1}$$

Where C is capacitance, ε_r is the relative permittivity of the dielectric material between the electrodes, ε_0 is the vacuum permittivity ($8,85 \times 10^{-12}$ F/m), A is the overlapping surface area of the electrodes on the opposite sides of the dielectric material and t is the thickness of the dielectric material [3].

The schematic illustration of the working mechanism of the sensor and actuator for the detection and detachment of biofouling and barnacles, is presented on Figure 1, and the detection mechanism can be explained following the equation (1) [4].

When water pressure (Figure 1(b)) is applied to the surface of the sensor, the soft system is undergoing deformation causing a decrease in thickness and increase in planar area. This deformation causes an increase of the capacitance from C to C′. Further, when the biofouling and barnacles are attached to the surface of the sensor, and the water pressure is again applied (Figure 1(c)), the deformation will be different, thus the capacitance change. When the biofouling has been detected, the last step is to have it detached from the surface, by applying the high voltage to the sensor. This will cause larger deformation of the sensor and in that way detachment of

the biofouling species, which are removed by water waves (Figure 1(d)).
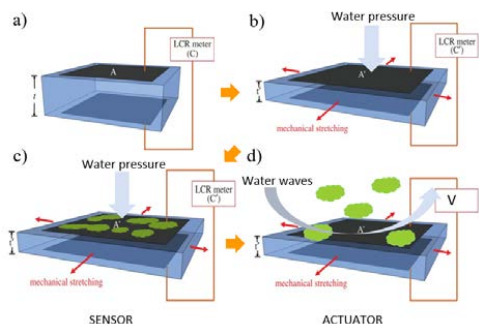
Figure 1: Schematic illustration of the sensor working principle for the biofouling and barnacle detection and detachment. a) Schematic illustration of the trilayer structure of the sensor. b) Schematic illustration of the deformation of the sensor when force (water pressure) is applied to the surface. c) Schematic illustration of the deformation of the sensor, which is covered with biofouling, when water pressure is applied to the surface. d) Schematic illustration of the detachment of biofouling from the surface when sensor works like an actuator. [4]

Results and Discussion

Commercially available platinum catalyzed two-part addition curing polydimethylsiloxane (PDMS) (Elastosil® RT 625 A/B, Wacker Chemie AG, Germany) was used as dielectric material in the sensor.

Stretchable conductive composite (CB_S184) was prepared by dispersing carbon black nanopellets (CB) (Ketjenblack EC-300J nanopellets, AkzoNobel, Netherlands) in the commercially available platinum catalyzed two-part addition curing PDMS (Sylgard 184, Dow Corning), silicone oil (1000 cSt, Sigma-Aldrich), and n-heptane (Sigma-Aldrich). CB dispersion was achieved by sonication using a sonication probe (UP200S, Hielscher – Ultrasound Technology, Germany, 200 W, 24 kHz) for 20 min. Prepared mixture was then mixed with the Sylgard 184 curing agent in a SpeedMixer™ (DAC 150 FVZ, Hauschild Co., Germany).

Electrical properties of dielectric material and composite were investigated. Figure 2 shows the storage permittivity ($\varepsilon'=\varepsilon_r$) of Elastosil RT 625 A/B, as a function of frequency at 25 ⁰C. It is clear from the Figure 1 that the storage permittivity in not changing with the frequency. The average storage permittivity obtained at 1kHz is 2,37.

As it can be seen from Figure 3, the AC conductivity (σ') of the CB_S184 composite across the entire frequency range is linear and not changing with the frequency. Since the alternating current (AC) conductivity of the composite is in the range from 10^{-4} to 10^{-3} S/cm the composite can be considered sufficiently conductive to be used as electrode.
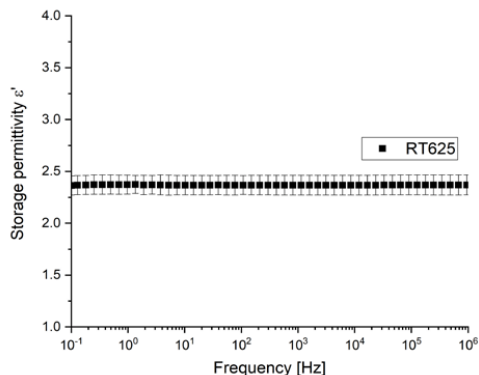
Figure 2: Relative permittivity or storage permittivity as a function of frequency for Elastosil RT625 A/B at 25 ⁰C.
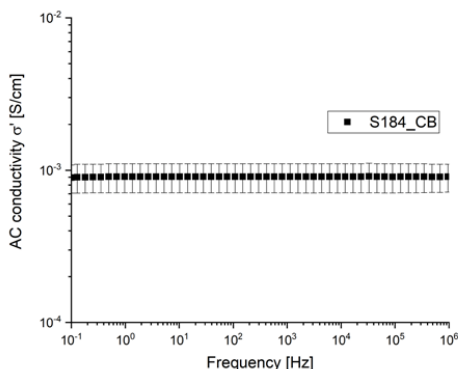
Figure 3: AC conductivity (σ') as a function of frequency for CB_S184 composite at 25 ⁰C.

Trilayer flexible structure sensor is fabricated by coating 200 µm thick Elastosil RT 625 A/B, and 100 µm thick CB_S184 conductive composite, on 2 mm thick stainless steel plate. The capacitance change (ΔC) between two states, when there is 685 g load applied on the surface of the sensor (C') and when there is no load (C), was measured with Impedance Analyzer Aligent 4294 A (40 Hz – 110 MHz).

Figure 4 shows the change of ΔC of the Sensor_1, as a function of frequency at 25 ⁰C. As it can be seen from Figure 4, ΔC is decreasing with the frequency.
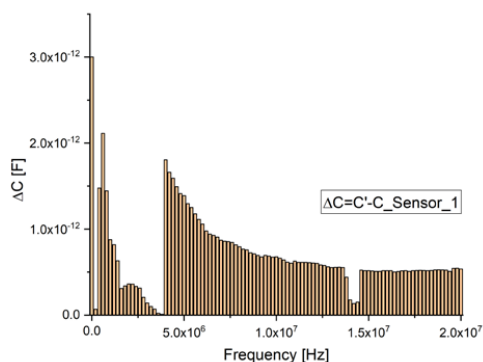
Figure 4: The ΔC of the Sensor_1 as a function of frequency at 25 ºC.

One of the characteristics of the capacitors is that their capacitance is decreasing with the frequency when AC voltage is applied to the circuit. It can be seen that in case of Sensor_1 the change of ΔC with the frequency when AC voltage of 500 mV is applied, follows that trend. The highest ΔC is at low frequencies, this means that all real time measurements of the capacitance should be performed at low frequencies.

Conclusion and Outlook

Although the Sensor_1 showed sensitivity to pressure load, the capacitance change of the Sensor_1 is unfortunately extremely low. Therefore, the sensitivity of the sensor needs to be improved.

It was noted that dielectric material used for the sensor fabrication should be much softer in order to achieve higher sensitivity. The preliminary tests with a new softer dielectric material showed increased sensitivity of 7,0 %. Experiments will be carried out to further increase the sensitivity of the sensor by increasing the relative permittivity of the dielectric material, and increasing the conductivity of stretchable electrode.

References

1. P. Shivapooja, Q. Wang, L.M. Szott, B. Orihuela, D. Rittschof, X. Zhao, G.P. Lopez, Biofouling 21 (3) (2015) 265-274.
2. P. Shivapooja, Q. Wang, B. Orihuela, D. Rittschof, G.P. Lopez, X. Zhao, Adv. Mater. 25 (2013) 1430-1434.
3. S. Laflamme, M. Kollosche, J.J. Connor and G. Kofod, Struct. Control Health Monit. 19 (2012) 70-81.
4. T. Wang, M. Farajollahi, Y.S. Choi, I.T. Lin, J.E. Marshall, N.M. Thompson, S.K. Narayan, J.D.W. Madden, S.K. Smoukov, Interface Focus 6 (4) (2016) 00-26.

Francois Kruger

Phone: +45 4525 2983
E-mail: fkru@kt.dtu.dk

Supervisors: Nicolas von Solms
Georgios M. Kontogeorgis
Even Solbraa, Equinor

PhD Study
Started: April 2016
To be completed: March 2019

Thermodynamics of Petroleum Fluids Relevant to Subsea Processing

Abstract
Subsea processing is transitioning into a new era where multiple qualified technologies will be combined into fully fledged subsea factories. In our on-going collaboration with Equinor, we are measuring new phase equilibrium data, improving the description of the mixture thermodynamics and applying these gains in process simulations – in order to make these subsea factories a reality.

Introduction
The need for improved efficiency and recovery in offshore oil & gas production are driving the development of subsea processing facilities, which include separation systems, boosting and injection. Other advantages of subsea processing (as opposed to topside processing) include decreased costs and extended operational lifetimes.

With the separation, boosting and injection already qualified technologies, one possibility is to develop a subsea dehydration or dew point control process [R1], where gas-dominated well streams can be treated directly, allowing for export into the distribution system.

Robust design and operation of these units requires new experimental equilibrium data and improved thermodynamic modelling to formulate a detailed understanding of the properties of reservoir fluids over a broad range of temperatures and pressures.

Objectives
As part of a research collaboration between the Centre for Energy Resources Engineering (CERE) at DTU and Equinor, this PhD project has the following objectives:

1. Generate new equilibrium data
2. Thermodynamic model evaluation
3. Determine process design implication

Experimental data measurement
During this project, phase equilibrium measurements were conducted in two different laboratories. Data measured during an external research stay at Equinor's

R&D facility in Trondheim (Norway) resulted in publications for CH_4-H_2O-MEG [P1] and NG-H_2O-MEG [P2] data. A sample of the results are shown below:
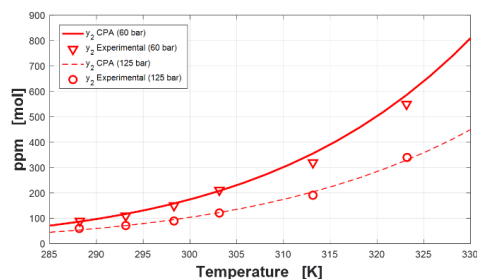
Figure 1: H_2O in gas for ternary MEG + H_2O + CH_4, with 90 wt% MEG, T = 288-323 K and P = (60, 125) bar.

In **Figure 1**, modelling was performed using literature 4C parameter set for MEG, yielding an error of 5.2%. Amongst many conclusions from the two papers it was shown that the Cubic-Plus-Association (CPA) [R2] equation of state is suitable for use in the design of dehydration units. However there are still opportunities for improvement e.g. when both MEG and CO_2 are in the system.

In parallel with our studies in Trondheim, measurements are being made in a three-phase VLLE cell (see **Figure 2**) at DTU CERE. In 2018 a new gas chromatograph (Agilent 7890B) has been commissioned for improved quantification of the phase distributions and the generation of new experimental data has commenced.

Figure 2: Three-phase VLLE cell located at DTU.

Thermodynamic model development

The CPA equation of state was developed specifically for developed specifically for describing mixtures of hydrocarbons and associating compounds e.g. H_2O/MEG. While describing the experimental data from Objective 1 of this study, we also aim to improve the thermodynamic modelling of these systems further. To this end, three new association schemes for MEG (see **Figure 3**) were proposed in a publication in Fluid Phase Equilibria [P3] where the 4F scheme showed potential in the description of ternary CH_4-H_2O-MEG data.
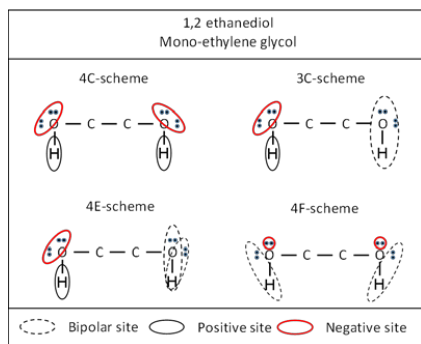
Figure 3: Association schemes for MEG. [P3]

Within the scope of the association scheme development, parameter uncertainty analysis was applied. Using the Bootstrap Method, the confidence intervals of the model parameters (and by extension, the model predictions) can be calculated and implemented in subsequent process designs.

Process design of subsea dehydration systems

The first step in the process design is to develop an accurate process simulation. Using tools developed at CERE, we are able to run simulations of dehydration units in both AspenPlus and Matlab. Already we have begun with case studies to determine the optimum MEG quality and recycle rate for different gas mixtures, and developed operating curves in terms of temperature and pressure (see **Figure 4**).
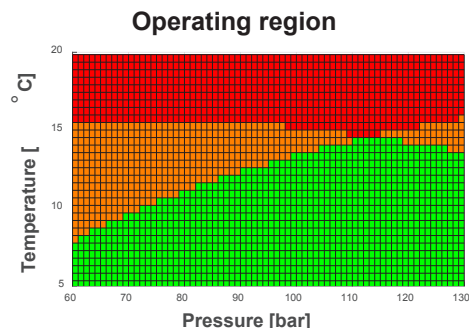
Figure 4: Case study of the safe operating region for the removal of water from methane using 90 wt% MEG.

Conclusions

Several new phase equilibrium data have been measured for systems relevant to subsea dehydration of natural gas. Along with the proposal of new association schemes, uncertainty analysis has been applied to improve the thermodynamic description of these systems. Although the process design element of this study is on-going, the combination of the thermodynamic modelling and uncertainty analysis in process simulation presents the opportunity for improved fidelity in both design and current operations.

Abbreviations

CPA   Cubic-Plus-Association
MEG   Mono-ethylene glycol
NG   Natural gas
VLLE   Vapour-liquid-liquid equilibrium

References

R1. Fredheim A.O., Johnsen C.G., Johannessen E., Kojen G.P., Gas-2-Pipe™, A Concept for Treating Gas to Rich Gas Quality in a Subsea or Unmanned Facility. Houston: OTC, 2016.

R2. Kontogeorgis G.M., Yakoumis, I.V., Meijer, H., Hendriks, E., Moorwood T., Fluid Phase Equilib. 201 (1999) 158-160.

List of Publications

P1. Kruger, F.J., Danielsen, M.V., Kontogeorgis, G.M., Solbraa, E., von Solms, N., J. Chem. Eng. Data 63 (2018) 1789-1796.

P2. Kruger, F.J., Kontogeorgis, G.M., Solbraa, E., von Solms, N., J. Chem. Eng. Data 63 (2018) 3628-3639.

P3. Kruger, F.J., Kontogeorgis, G.M., von Solms, N., Fluid Phase Equilib. 458 (2018) 211-233.

Kristian Krum

Phone: +45 27509740

E-mail: krkkru@kt.dtu.dk

Supervisors: Peter Glarborg

Hao Wu

Songgeng Li

Thomas Norman

PhD Study

Started: September 2017

To be completed: August 2020

NOx Control in Combustion of Alternative Fuels

Abstract

Combustion of solid waste fuels in waste-to-energy (WtE) plants is a competitive method for conversion of waste to electrical energy and heat. The emission of nitrogen oxides (NO_x) from WtE plants continuous to be a major environmental concern. Additionally, the ash formed during combustion of waste causes severe practical issues due to deposition and corrosion in the boiler. In this project, it is of interest to study techniques for the simultaneous reduction of NO_x emissions, deposition and corrosion in the boiler section of WtE plants. A technique of interest is the commonly used selective non-catalytic reduction (SNCR) process using alternative additives, e.g. ammonium sulphate, ammonium phosphate and cyanuric acid. It is also of interest to study the impact of inorganic elements, released from the waste during combustion, on the SNCR process.

Introduction

The handling of municipal solid waste (MSW) that is produced daily in large amounts has become a significant challenge. An alternative to traditional landfilling is extraction of energy through combustion in waste-to-energy (WtE) plants.

Most of the waste fractions in MSW are nitrogen containing materials, and thus form nitrogen oxides (NO_x) during combustion. The emission of NO_x continuous to be a major environmental concern, as NO_x participates in the formation of acid rain and photochemical smog.

In Denmark, the most common technique to reduce NO_x emissions from grate-fired WtE plants is selective non-catalytic reduction (SNCR) using ammonia or urea as reducing agent. The SNCR process is governed by the overall reactions using ammonia and urea, respectively:

$$4NH_3 + 4NO + O_2 \rightarrow 4N_2 + 6H_2O \qquad (1)$$

$$NH_2CONH_2 + 2NO + \tfrac{1}{2}O_2 \rightarrow 2N_2 + CO_2 + 2H_2O \quad (2)$$
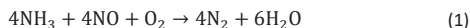
The SNCR process is known to be very temperature dependent, and has a narrow temperature window of efficient NO_x reduction. It is therefore of practical interest to investigate the effect of different operating parameters, in order to study how the temperature window of effective NO_x reduction can be broadened.
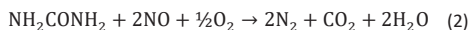
The ash species formed from combustion of MSW have a high tendency to form sticky and corrosive ash deposits in the boiler, due to high amounts of inorganic elements and chlorine in MSW. In previous studies, it has been shown that addition of sulphur containing additives can reduce the extent of deposition and corrosion in the boiler [1]. Therefore, the use of alternative additives in the SNCR process, for simultaneous reduction of NO_x, deposition and corrosion, has recently become of interest. Potential additives include e.g. ammonium sulphate, ammonium phosphate and cyanuric acid. However, fundamental research on the decomposition behaviour of the additives, and their behaviour and performance in the SNCR process, is required in order to evaluate the viability of the additives.

Specific Objectives

The overall objective of this project is to obtain an improved understanding of the NO_x formation and reduction mechanisms during waste combustion. It is of interest to evaluate the use of alternative SNCR additives, such as urea, ammonium sulphate, ammonium phosphate and cyanuric acid, for simultaneous reduction of NO_x, deposition and corrosion. It is also desired to investigate the impact of inorganic elements released from MSW combustion on SNCR chemistry.

Experimental Investigation of the SNCR Process with Ammonium Sulphate as Reducing Agent

The SNCR performance of ammonium sulphate was studied in a bench-scale setup. The setup, shown in Figure 1, consists of a homogeneous flow reactor surrounded by an electrically heated oven, an FTIR analyzer and a novel feeding system capable of feeding micron sized liquid droplets. The feeding system consists of a storage tank for the aqueous solution of the additive of interest, in which a nebulizer is placed in order to create a fine mist of micron sized droplets from the

aqueous solution. A carrier nitrogen gas flow is used to transport the mist from the storage tank to the flow reactor.

SNCR experiments were performed for three aqueous ammonium sulphate solutions (2.5 wt%, 5 wt% and 10 wt%) at low and high oxygen concentration (1.25% and 8%). The typical water concentration was 3-5%. The temperature in each experiment was varied between 973 K and 1173 K. The inlet NO concentration to the flow reactor was approximately 370 ppm for each experiment. The residence time in the hot zone of the reactor was around 5-6 s depending on the flow rate and reactor temperature.
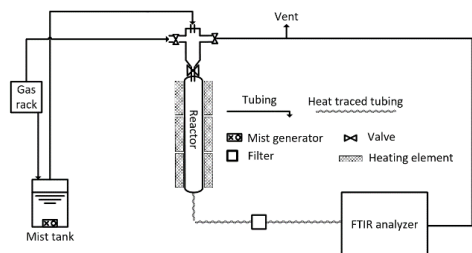
Figure 1: Schematic illustration of the bench-scale setup.

Kinetic Modeling of the SNCR Process with Ammonium Sulphate as Reducing Agent

A detailed chemical kinetic model (DCKM) has been developed for the SNCR process using ammonium sulphate as reducing agent, and Chemkin 17.1 has been used as modeling tool. The model is based on the mechanism developed by Glarborg et al. [2], consisting of a total of 150 species and 1389 reactions. The mechanism is constituted by different subsets for nitrogen chemistry, including subsets for NH_3, amine, H_2/O_2, H_2S/O_2, and S/N. In order to imitate the use of ammonium sulphate as reducing agent, the expected decomposition products from ammonium sulphate suggested by Halstead [3] has been implemented as inlet conditions in the model:

$$3(NH_4)_2SO_4 \rightarrow 4NH_3 + 3SO_2 + 6H_2O + N_2 \qquad (3)$$

The model was further modified by introducing a newly developed NH_2SO_2 subset constituted by 7 reactions, in an attempt to describe an observed inhibiting effect of SO_2 on NO reduction.

Results and Discussion

Through experiments with the developed bench-scale setup, it was generally observed that ammonium sulphate as an additive in the SNCR process yields comparatively low NO_x reductions compared to reference gas experiments using NH_3 gas, as reflected in Figure 2. The optimum temperature was typically observed to be around 1125 K. The low optimum temperature, as compared to other studies [4,5], may be explained by the significantly longer residence time in the present setup. The experimental results shown in Figure 2 indicate a strong dependency of SO_2 on the SNCR chemistry.

However, the model does not capture this dependency satisfactorily.

The general trend of increasing the O_2 concentration was observed to be a downwards shift in the optimum temperature, while the NO reduction efficiency was decreased, which is in line with observations from other studies [6].
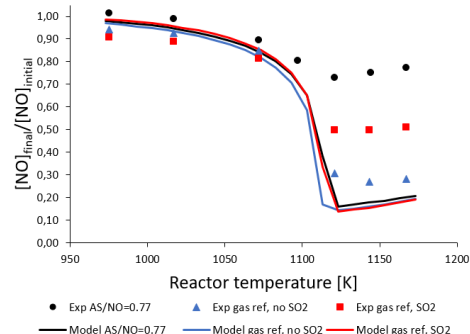
Figure 2: Comparison of experimental and simulation results of SNCR with ammonium sulphate (AS) with reference SNCR experiments using $NH_3/NO=1.05$ with an O_2 concentration of 1.25%.

References

1. M. Hupa et al., Proceedings of the Combustion Institute 000 (2016) 1–22.
2. P. Glarborg et al., Progress in Energy and Combustion Science 67 (2018) 31-68.
3. W. D. Halstead, Journal of Applied Chemistry 20 (1970) 129-132.
4. T. Nguyen et al., Chemical Engineering Journal 152 (2009) 36-43.
5. W. Hall, P. Williams, Waste Management & Research 24 (2006) 388-396.
6. Z. Lu, J. Lu, Combustion and Flame 156 (2009) 1303-1315.

Kasper Hartvig Lejre

Phone: +45 2020 6568

E-mail: kasphal@kt.dtu.dk

Supervisors: Søren Kiil

Peter Glarborg

Philip Fosbøl

Henrik Christensen, MAN Energy Solutions

PhD Study

Started: October 2015

To be completed: December 2018

Mathematical Modelling of Sulfuric Acid Accumulation in Lube Oil in Diesel Engines

Abstract

Slow-steaming operation and an increased pressure in the combustion chamber have contributed to increased sulfuric acid (H_2SO_4) condensation on cylinder liners in large two-stroke marine diesel engines, thus causing increased corrosion wear. The scope of this project is to investigate how H_2SO_4 is formed, transported, and neutralized in the lube oil film on the cylinder walls. The conditions inside the cylinders will be reproduced in laboratory experimental setups, where the different subprocesses are studied separately.

Introduction

Slow-steaming became popular during the recession in the last part of the 2000s. This meant that the large two-stroke marine diesel engines were now operated at a lower engine load in order to save fuel. To ensure optimal specific fuel oil consumption the engines were further optimized in this new part load range. This resulted in increased cylinder pressures and colder cylinder liners at part load among others. The lower liner surface temperature, in combination with an increased operating pressure, has led to increased water and acid condensation in the cylinder lube oil film on the cast iron liner surfaces, which promotes "cold corrosion" [1]. The phenomenon is a mixture of chemical corrosion from acid and mechanical wear. It is generally thought that the cold corrosion phenomenon originates mostly from corrosion by condensed sulfuric acid (H_2SO_4), due to the sulfur-rich fuel used in marine diesel engines [2]. Expensive lube oil with limestone ($CaCO_3$, present as nanosized reverse micelles) is continuously added to the cylinder liners to neutralize the H_2SO_4 formed, but the efficiency of this procedure is not always optimal [3]. A small degree of corrosion is, however, beneficial on the cylinder liners, making the liner surface a little rough. This means that the cylinder liner surface can better maintain a protective oil film. However, uncontrolled cold corrosion destroys the liners and piston rings [4].

Specific Objectives

This PhD project is a part of a large research project (SULCOR) in corporation with MAN Energy Solutions,

DTU Chemical Engineering (KT), and DTU Mechanical Engineering (MEK), where the combined output from the different projects should lead to new engine designs and/or new operational engine procedures, which will improve the existing lubrication strategy. The main core of this PhD project is to develop a mathematical model that can predict conditions prevailing at the oil-cylinder liner interface, where corrosion takes place. The cast iron tribo-corrosion process is handled in another PhD project at KT, where this PhD project provides the boundary condition data required. Other PhD/postdoc projects at DTU-MEK will provide valuable information on e.g. oil flow pattern, gas phase composition, and the actual formation and condensation of H_2SO_4 on an oil film under laboratory conditions (lube oil test rig). The project objectives cover the following:

- A literature study on diesel engines, lube oils, and the chemistry of a selected running engine.
- Collection and analysis of spent lube oil from selected full-scale diesel engines.
- Development of the analysis technique.
- Design and construction of reactor setups for H_2SO_4/SO_2-lube oil experiments.
- Mapping and quantification of acid generation, transport, and neutralization mechanisms in a running diesel engine.
- Mathematical modelling of sulfuric acid accumulation in lube oil in diesel engines.
- Recommendations for practical use of the results from the different subprojects.

Results and Discussion

The neutralization reaction between H_2SO_4 droplets and $CaCO_3$ reverse micelles in lube oil has been investigated both experimentally and by modeling. Experimentally, the reaction was investigated in a mixed flow reactor (MFR) setup, studying the effect of stirrer speed, H_2SO_4 concentration, residence time, and Ca/S molar ratio on reactant conversion. Experimental results showed that the reaction rate was significantly reduced when reaching a critically low Ca/S molar ratio. A certain degree of stirring was needed to initiate and maintain the reaction. Also, no apparent effect of varying the residence time was found. Diluting inlet H_2SO_4 flow decreased the conversion of $CaCO_3$. Furthermore, the results indicated that the limiting step in the mechanism is adsorption of reverse micelles onto the much larger H_2SO_4 droplets. A mathematical model was developed, describing the reaction between H_2SO_4 droplets and $CaCO_3$ reverse micelles in lube oil under well-mixed conditions. The outcome of the modeling was extraction of a reaction rate expression by fitting of the model to the experimental MFR data. Exploration of the model showed that reaction rate increases significantly with lube oil temperature. The $CaCO_3$ concentration in lube oil and H_2SO_4 droplet concentration have only minor impacts at a fixed Ca/S molar ratio. The validated mathematical model was also used to predict conversion of H_2SO_4 at the cylinder liner surface for conditions relevant for a full-scale application, see Figure 1.
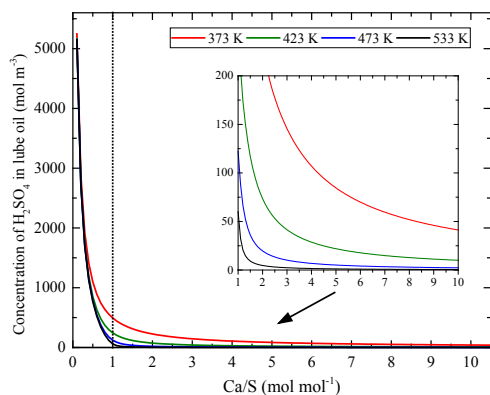
Figure 1: Model simulations showing the average concentration of H_2SO_4 in the lube oil film as a function of Ca/S at varying temperature. Model parameters are: radius of H_2SO_4 droplets = 0.5 μm, residence time = 0.5 s, $CaCO_3$ content in lube oil = 0.089 kg kg^{-1}, and initial concentration of H_2SO_4 droplets = $18 \cdot 10^3$ mol m^{-3}. The horizontal dotted line represents Ca/S=1.

Calculations indicated that H_2SO_4 may reach the liner surface regardless of how well-wetted the cylinder liner surface is. The concentration of H_2SO_4 in the lube oil film is significantly increased for conditions with a local molar excess of H_2SO_4 compared to $CaCO_3$ reverse micelles (Ca/S<1 in Figure 1). Therefore, to control the corrosion rate practically, it is important to ensure that sufficient lube oil is provided in the critical regions, particularly at the upper part of the cylinder liner where the most pronounced wear is found.

It is also of interest to investigate, if SO_2 has a role on the consumption of $CaCO_3$ in the lube oil, since SO_2 is highly present in the gas phase for sulfur-rich fuel. This may happen either by direct reaction between SO_2 and $CaCO_3$ or by absorption of SO_2 by the lube oil followed by reaction to H_2SO_4 [5]. The significance of SO_2 consuming $CaCO_3$ reverse micelles in lube oil was studied in a batch reactor setup at relevant full-scale conditions. The reaction showed a weak temperature dependence and a high initial water dependence. Reaction products included both $CaSO_3$ and $CaSO_4$, depending on the reaction conditions employed. A mathematical model was developed and kinetic parameters were determined by fitting the model to the experimental $CaCO_3$ conversion data. The model was then used to predict $CaCO_3$ conversions in lube oil from SO_2 at worst-case conditions relevant for a full-scale application. Simulations show that consumption of $CaCO_3$ from SO_2 is insignificant in a two-stroke marine diesel engine application and that the H_2SO_4-$CaCO_3$ reaction outmatches the SO_2-$CaCO_3$ reaction.

Conclusion

It is crucial understanding the underlying processes in the lube oil-acid system inside engines to optimize the lube oil strategy. This project contributes to increased knowledge about neutralization mechanisms in lube oil. The rate expressions derived can be used in models describing spatial and temporal formation and condensation of H_2SO_4 in engines. In combination with a model describing the wear rate of the cylinder liner from H_2SO_4 concentration in lube oil emulsion, it would allow optimization of the lube oil feeding with respect to achieving low levels of corrosion.

References

1. MAN Diesel & Turbo, "Service Letter SL2014-587/JAP", 2014.
2. C. Amblard, *J. Japan Inst. Mar. Eng.* 50 (6) (2015) 54–62.
3. A. K. van Helden, M. C. Valentijn, H. M. J. van Doornt, *Tribol. Int.* 22 (3) (1989) 189-193.
4. D. Atkinson, *11th Int. Conf. Cond. Monit. Mach. Fail. Prev. Technol. C.* 5 (2) (2014) 17-22.
5. H. Nagaki, K. Korematsu, *JSME Int. J. Ser. B.* 38 (3) (1995) 465-474.

List of Publications

K. H. Lejre, S. Kiil, P. Glarborg, H. Christensen, S. Mayer, ASME ICEF, Seattle, 2017, paper ICEF2017-3580.
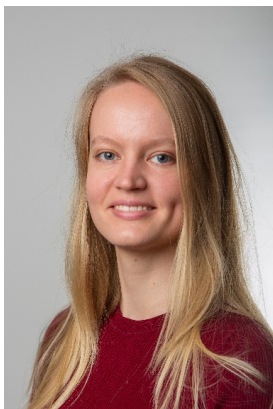
Anna Leth-Espensen

E-mail: annlete@kt.dtu.dk

Supervisors: Peter Glarborg
Peter Arendt Jensen
Kim Dam-Johansen

PhD Study
Started: May 2016
To be completed: April 2019

Application of Improved Computational Fluid Dynamic Simulations for Pulverized Biomass Combustion

Abstract

The need for an environmentally justifiable energy production has increased the interest in combustion of pulverized biomass particles in suspension firing boilers. The aim of this project is to provide computational fluid dynamics (CFD) simulations, which can aid in the process of understanding the physical processes taking place in swirl stabilized biomass flames. The project includes development of a char yield model and a single particle biomass pyrolysis model, which can both be used as inputs to CFD flame simulations. The pyrolysis model is a shell model, which can account for drying and devolatilization concurrently.

Introduction

In Denmark, the energy sector is currently changing from coal-based energy production to pulverized biomass combustion for environmental reasons. The implementtation of biomass particles as the primary fuel entails challenges with regard to the design and operation of the combustion facilities. In this project, the focus is on suspension firing. The process of biomass suspension firing is not yet fully understood, which causes challenges with regard to ensuring flame stability, full conversion of the particles, and minimizing emittance of harmful substances. Biomass particles differ from coal, because they have larger diameters, a wider size distribution, and a higher volatile content, which causes a different conversion and flow pattern for the particles.

Also of interest in this project is how the combusting biomass particles influence the stability and geometry of the flames in suspension fired boilers. Computational fluid dynamic (CFD) can aid in the process of understanding the pyrolysis process' influence on swirling jet flames better.

Specific Objectives

The aim of this PhD project is to make a model for pyrolysis of biomass particles at suspension firing conditions and conduct CFD simulations of a suspension firing unit. The project is divided into three subparts, a char yield model, a pyrolysis model, and CFD simulations; evaluating the effects of the models.

The char yield model should be able to determine the char yield after pyrolysis for biomass particles subjected

to suspension firing conditions. These conditions include high heating rates (> 1000 K/s), high ambient temperatures (> 1000 K), and particle sizes in the range of 20-2000 μm. The char yield is an important parameter in most suspension firing CFD models and also necessary in pyrolysis and combustion models. The char yield is typically estimated from proximate analysis, but they yield too high a char values. Conducting experiments at high heating rates to determine the char yield under relevant conditions is time consuming and a simple model is hence favorable. The model presented here is an empirical model building on the principles of the partial least squares (PLS) regression method. The model is based on data obtained by Trubetskaya[1] and evaluated against additional experimental data.

The biomass pyrolysis model is developed in collaboration with the Department of Energy and Process Technology at NTNU and builds on work by Thunman et al.[2]. The model divides the particle into three shells. The innermost layer is the moist layer, then a dry layer, and the outermost layer is the char layer. By considering the energy equations applicable to each individual layer and assuming that all reaction and/or phase change happens at the boundaries between the layers it is possible to formulate a sharp interface model (SIM). This is the case in this model except for the pyrolysis process, which takes place both in the wet and the dry shell. The three phases can exist concurrently, which is necessary to account for the phenomena taking place in thermally thick particles (Bi > 0.1). The model is produced as a standalone model in order to compare it to experimental

data before it is implemented into CFD. To ensure reasonable computational time and smooth operation in the CFD simulations, there is a limit to the complexity of the model.

The CFD simulations conducted as part of this PhD are on a suspension firing unit located at Amagerværket. The aim is first to test the char yield model and the devolatilization model and establish whether they enhance the accuracy of already existing simulations. A large part of this evaluation of the simulations is the comparison to previously obtained measurements made by Johansen et al. [3]. The final objective is to determine which operation parameters are important for control of the combustion process, and see if design improvements can be made in order to establish a stable flame at different loads levels.

Results and Discussion

The char yield model [4] is made using PLS regression and is limited by the amount of available experimental data for fully pyrolized particles devolatilized under suspension firing conditions. Currently the model is made for woody and herbaceous biomass for particles with the following parameters: Diameter 0.125 - $0.925 \cdot 10^{-3}$ m, final temperature $873 - 1673$ K, heating rate $0.1-12 \cdot 10^3$ K/s. The model is thus only valid within these intervals, and more experimental data is necessary in order to expand the model to the full range of possible parameters for suspension fired particles. The model is evaluated against additional experimental data from literature. The evaluation show that the model on average predicts the char yield with ± 0.9 percentage points of the char measured in weight percentage on a dry ash free basis (wt% daf). This is just above the uncertainty level of the experiments, which is the lower value of accuracy that can be obtained. The analysis of the parameters included in the model work additionally shows that the size of the particles is negligible when calculating the final char yield for fully pyrolyzed particles. This is possibly because the size is already included as it influences the heating rate parameter, and there is no need to account for the size effects twice, or possibly because for particle sizes relevant to suspension firing conditions a finite fraction of the particle is pyrolyzable regardless of size when full pyrolysis is ensured. Furthermore, the analysis shows that the most important parameters for the char yield are the potassium content and the heating rate, whereas the final temperature is of minor importance. The model shows that a high potassium content gives a higher char yield, whereas a high heating rate and/or high final temperature gives a lower char yield. For a woody biomass particle with parameters in the intervals mentioned above the char yield in wt% daf can be estimated using equation (1).

$$\text{Yield} = 10^{(3.4370 + 0.6852 \cdot KC - 0.6598 \cdot \log(FT) - 0.2130 \cdot \log(HR))} \quad (1)$$

Where FT is the final temperature in K, HR is the heating rate in K/s, and KC is the potassium content in wt% db.

The focus of the work on the biomass pyrolysis model has been to establish the importance of particle morphology, since biomass particles are typically elongated, but often modeled as spheres for reasons of simplicity. The model presented here can account for cylindrical particles and the effects of volume to surface ratio can thus be studied. The morphology of particles of the same volume is significant and the devolatilization time almost halves for a cylinder with aspect ratio (AR) = 10 compared to a sphere of the same volume; an example can be seen in figure 1. The model is validated against experimental data.
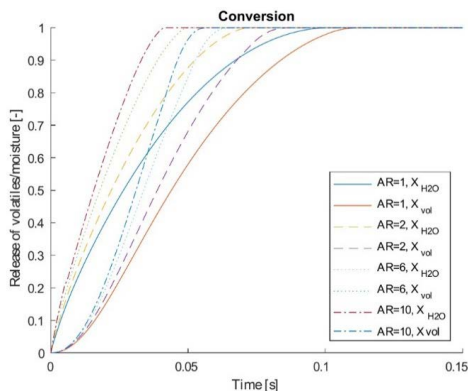
Figure 1: Devolatilization times for one spherical (AR=1) particle and three cylindrical particles of the same volume. The diameter for the spherical particle is 722 μm. T_{gas} = 1373 K, ρ = 60 kg/m^3, 6 wt% a.r. H_2O.

References

[1] A. Trubetskaya, Fast Pyrolysis of Biomass at High Temperatures, Ph.D. DTU, 2015
[2] H.Thunman, B. Leckner, F. Niklasson, F. Johnsson, Combustion and Flame 129 (2002) 30-46
[3] J.M. Johansen, Power Plant Burners for Bio-Dust Combustion, Ph.D. Thesis, DTU, 2015
[4] A. Leth-Espensen, P. Glarborg, P.A. Jensen, Energy & Fuels, 32 (2018) 9572-9580

Rowan Malan Lindeque

Phone: +45 6166 3141

E-mail: rmalin@kt.dtu.dk

Supervisors: John M. Woodley
Ulrich Krühne
Kim Dam-Johansen
Tommy Skovby, H. Lundbeck A/S

PhD Study
Started: November 2017
To be completed: October 2020

Accelerating the implementation of biocatalytic processes for pharmaceutical production by standardization in continuous flow reactors

Abstract

The use of biocatalysis to assist in the synthesis of optically pure chiral pharmaceuticals is well established, particularly for the production of optically pure alcohols and amines. Nevertheless, most of these processes use fed-batch technology. Recently, a significant number of API synthesis and production processes have started to be converted into continuous processes and it is clear that biocatalysis also needs to embrace this. Indeed, if carried out in the right way, this will also capitalize upon the particular ability of enzymes to enable highly selective conversions. However, this also highlights a recurring problem, which is that, as an emerging field, biocatalysis still suffers from the need for case-by-case development. Therefore, in order to accelerate the development and implementation of new biocatalytic processes, more standardized methods are needed. The overall objective of this work is to determine whether multiphase biocatalytic systems, such as biooxidations, can be operated with a continuous, modular, once-through approach to achieve industrially feasible performance targets.

Introduction

Enzymes as biocatalysts are increasingly gaining attention in the pharmaceutical industry because they are often highly enantio-, regio- and stereoselective, which greatly reduces the need for protection and de-protection steps that make conventional chemical syntheses more complex. [1] They also operate at mild conditions, avoiding spontaneous side reactions that can occur at elevated temperatures and pressures often necessary for chemocatalysis. [2] In addition to this, recent advances in the field of protein engineering are allowing biocatalysts to be modified to have high activities towards a wide variety of industrially attractive, non-native substrates. [3] Despite these advantages, biocatalysts are only rarely implemented at large scales and, when they are, operation is typically limited to batch or fed-batch, as is the case in the pharmaceutical industry. The use of batch technologies makes integration of biocatalytic steps into existing production processes challenging and causes research and development of new processes to be more time-consuming, since design must often be done on a case-by-case basis. This is especially problematic in the pharmaceutical industry, where long times-to-market already greatly restrict the periods of market exclusivity for novel pharmaceuticals. [4] As such, it is clear that, to accelerate the implementation of biocatalysis for commercial production of pharmaceuticals, a new standardized methodology for development and operation of biocatalytic systems is required.

Industry specific requirements

To be effective, any standardized approach will have to satisfy the unique requirements of the highly regulated pharmaceutical industry. For instance, in order to maintain high product qualities, production processes should be precise and reliable. For this reason, continuous operation is becoming more attractive for the industry as it allows much greater control and automation than batch or fed-batch operation. [5] Reducing the complexity of industrial production processes also makes them easier to control and regulate. Therefore, a standardized process should avoid recycling substrates and enzymes as far as possible and instead, focus on maximizing substrate conversion in a single pass. Although the cost contribution of enzymes can be significant, the high prices of pharmaceutical products should permit this once-through approach and, as the costs of enzymes continue to drop, a similar approach may become feasible for lower-priced products in future. Finally, a standardized approach should accommodate the desire for flexible equipment in industry and combined chemo- and biocatalytic reaction paths. Therefore, all unit operations should be modular to allow production sequences to be easily rearranged for the

production of multiple intermediates or Active Pharmaceutical Ingredients (APIs). Figure 1 shows a conceptual diagram of the proposed standardized process. Nonetheless, it is likely that some enzyme/substrate combinations will have unique challenges that necessitate a more tailored and traditional process design approach.
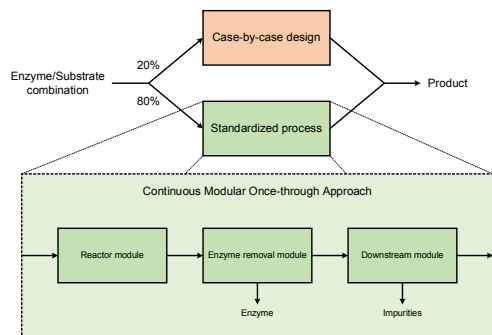
Figure 1: Proposed standardized approach to accelerate industrial implementation of biocatalysis for pharmaceutical production

Biooxidations

Oxidation reactions are common in pharmaceutical syntheses. For this reason, oxidases, which use molecular oxygen instead of harsh chemical oxidants to catalyze such reactions, are highly attractive in industry. However, due to their need for a gaseous substrate, these multiphase systems present many new challenges for process design. For instance, if these enzymes are to be applied industrially in a once-through approach, it is essential that the enzymes be used as effectively as possible while they are in the reactor. This means ensuring that mass transfer of oxygen from the gas phase to the liquid phase does not limit reaction rates. [6] Many reactor technologies have recently been developed to achieve high interfacial areas and improve gas-liquid mass transfer, such as segmented flow reactors or tube-in-tube reactors. [7] However, although these microreactors have been shown to have exceptional performance at laboratory scale, they are difficult to scale up without severely compromising performance. As such, these reactors are ill-suited towards a standardized approach. Instead, to accelerate the implementation of biooxidations in industry, it is necessary to demonstrate whether they can feasibly be operated in mature reactor technologies that are flexible and scalable, such as continuously stirred tank reactors (CSTRs). [8] Of course, CSTRs also have downsides for pharmaceutical production, namely broad residence time distributions, which reduce their precision. However, operation of multiple CSTRs in series, as shown in Figure 2, to achieve pseudo plug-flow behavior could resolve this.
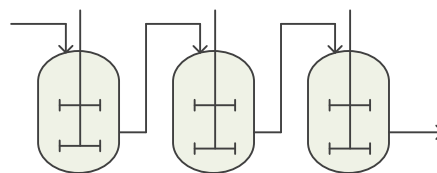
Figure 2: CSTRs operated in series to approximate plug-flow behavior for multiphase biooxidation reactions

Specific Objectives

The aim of this project is to determine whether industrially feasible yields, productivities and product concentrations can be achieved when operating biooxidation reactions in a series of CSTRs, according to the proposed continuous, modular, once-through standardized approach. Biooxidations should serve as a good case study to identify the limitations of the standardized approach due to the challenges presented by multiphase biocatalytic systems.

References

1. J. Albarrán-Velo, D. González-Martínez, V. Gotor-Fernández, Biocatal. Biotransform. 36 (2018) 102-130.
2. L. Martínez-Montero, V. Gotor, V. Gotor-Fernández, I. Lavandera, ACS Catal. 8 (2018) 2413-2419.
3. J.M. Woodley, Curr. Opin. Chem. Biol. 17 (2013) 310-316.
4. R.A. Sheldon, D. Brady, Chem. Commun. 54 (2018) 6088-6104.
5. J.M. Vargas, S. Nielsen, V. Cardenas, A. Gonzalez, E.Y. Aymat, E. Almodovar, G. Classe, Y. Colon, E. Sanchez, R.J. Romanach, Int. J. Pharm. 538 (2018) 167-178.
6. A.T. Pedersen, T.M. de Carvalho, E. Sutherland, G. Rehn, R. Ashe, J.M. Woodley, Biotechnol. Bioeng 114(6) (2017) 1222-1230.
7. R.H. Ringborg, A.T. Pedersen, J.M. Woodley, ChemCatChem 9 (2017) 3285-3288.
8. J. Price, M. Nordblad, H.H. Martel, B. Chrabas, H. Wang, P.M. Nielsen, J.M. Woodley, Biotechnol. Bioeng. 113(8) (2016) 1719-1728.

Xinyan Liu

Phone: +45 45256180
E-mail: xlin@kt.dtu.dk

Supervisors: Georgios M. Kontogeorgis
                Xiaodong Liang
                Xiangping Zhang
                Suojiang Zhang

PhD Study
   Started: September 2016
   To be   August 2019
completed:

Model Development for Ionic Liquid Design and Process Synthesis for Shale Gas Separation

Abstract

Shale gas usually goes through serious of separation process to obtain the upgrading commercial gas. Traditional technologies for shale gas separation are distillation for hydrocarbon gases and solvent separation for acid gas. Ionic liquid, because of its unique properties of being non-volatile and flexibility in design, could be used for the shale gas separation. However, the numerous number of potential ILs makes it difficult to find the specific IL to absorb the gas. In order to solve the problem, a framework is systematically developed from the initial model-based ILs to the final gas separation process synthesis. Firstly, experimental solubility database and thermodynamic models, including COSMO-RS and UNIFAC-IL, are developed and applied to predict the activity coefficient of some gases in various ILs. The optimal ILs are screened through two methods: experimental database and computer aided method which based on the predicted models. Based on the screened results, the gas separation schemes are designed and simulated after verification of the rigorous thermodynamic model. The important design issues are determined through sensitivity analysis. Finally, the gas separated results are compared with traditional technologies. In this work, a five-gas shale gas model is assumed and related separation process is designed and simulated.

Introduction

Shale gas, considered as the clean energy and a substitute for coal, has attracted increasing attention in recent years. It needs to go through a series of processing units to obtain the upgrading commercial gas which could be supplied into pipeline or used as feedstocks for petrochemical plants to produce value-added chemicals.

Traditional common technologies for shale gas separation include energy intensive distillation and solvent based absorption. Distillation is usually applied for light hydrocarbon gas separation in which the separated gas is recognized as an important raw gas for synthesizing many industrial chemicals. The process includes columns with large numbers of trays to get a high purity product at low temperatures and high pressures resulting in a high energy consumption and negative environmental impact. The solvent based absorption technology is widely used for separating gases such as CO_2, H_2S which need to be removed in order to satisfy the emission standard of air pollutants.

Having some advantages of non-volatility, flexible designing, ionic liquid (IL) has been paid much attention. It is reported that different ILs can be used for different gases absorption [1]. Therefore, a strategy for a five-gas shale gas model separation process synthesis where both

traditional distillation and IL-based absorption are employed has been developed. However, the numerous combinations of cation and anion make it a challenging task to search for the optimal one for this shale gas separation. Then selection-screening methods are proposed first. Then related process synthesis and evaluation are conducted.

Methodology

In this work, we first establish an experimental database on gas solubility and Henry constant in various ILs. Then database is applied for the predicted models development including corrected COSMO-RS model and UNIFAC-IL model. The activity coefficients of gas in ILs are calculated based on these predicted models so that the gas solubility in new ILs which is not included in experiments could be predicted [2]. Thus a three-stage methodology proposed for the shale gas separation process design and evaluation will be highlighted. The first stage involves IL screening, where two methods are applied. One is only based on the experimental database. The other is a computer-aided method which could be used to automatically obtain the optimal IL on the group contribution basis. The second stage is process design, where the important design issues are determined and

overall separation scheme is generated. The third stage is process simulation and evaluation. Rigorous process simulation is conducted after the development and verification of related thermodynamic model. Here, a model shale gas containing five gases is assumed as a case study to highlight the application of this methodology.

Corrected COSMO-RS Model

The COSMO-RS model is first developed by Klamt et al. As a predictive method, the COSMO-RS calculation only requires molecular structure information. Many researches have applied it for ILs screening. However, high deviations between experimental and the predicted properties make it can only provide qualitatively results. Here, aimed to three light hydrocarbon gases (CH_4, C_2H_4, C_2H_6) which have high deviations, linear corrected COSMO-RS based model is proposed, as seen in Table 1.

Table 1 Corrected COSMO-RS model for the infinite dilution activity coefficient of three light hydrocarbon gases in ILs

Gas	Corrected model, T in K	AARD with experimental γ^{∞}	
		Before correction	After correction
CH_4	$\gamma^{\infty}_{cor} = 0.771\gamma^{\infty}_{cosmo} + 2.687 - 0.0087T$	123.4%	50.6%
C_2H_4	$\gamma^{\infty}_{cor} = 1.582\gamma^{\infty}_{cosmo} + 1.268 - 0.00466T$	29.5%	6.3%
C_2H_6	$\gamma^{\infty}_{cor} = 1.149\gamma^{\infty}_{cosmo} + 2.410 - 0.006699T$	19.5%	8.9%

UNIFAC-IL Model

The UNIFAC model is considered to be a predictive model based on the concept of group contribution. Due to this character, it can be applied for solvent screening for many purposes. Its development should be based on sufficient activity coefficient data of gas in various ILs. As main components of shale gas, there are sufficient experimental data for CO_2 and CH_4, but less for C_2H_4 and C_2H_6, which need the pseudo data generated based on the COSMO-RS model. Therefore, a UNIFA-IL model among the four gases (CO_2, CH_4, C_2H_4, C_2H_6) is developed. The IL is divided into several groups including alkyl chains, skeleton of cation and anion. 37 pairs of group interaction parameters are fitted for 23 IL-CO_2 and 8 IL-CH_4 systems. And another 23 pairs of group interaction parameters are fitted for 10 IL-C_2H_4 and 10 IL-C_2H_6 systems.

ILs Screening

Based on the experimental database, one optimal IL ([thtdp][phos]) which has the lowest Henry constant of CO_2 and a higher selectivity of CO_2/CH_4 has been selected. The predicted solubility of other gases C_2H_4 and C_2H_6 in this IL has been calculated with a low solubility based on the corrected COSMO-RS model, indicating the IL can be only used for decarbonization process. Through the computer-aided screening method, another IL ([MMPy][eFAP]) has also been generated. Based on the calculation of the predicted models, it has a little lower solubility of CO2 than [thtdp][phos], but a higher selectivity of CO2/ CH4. Both these two ILs are applied for further simulation to be evaluated.

Shale Gas Separation Scheme

For a five-component shale gas model, which consists of 80% CH_4, 7% CO_2, 7% C_2H_6, 3% C_2H_4, 3% H2, a hybrid separation strategy combining the screened IL-based absorption with distillation has been proposed, as seen in Fig. 1. Since the screened IL only has a high solubility on CO2, the solvent absorption method is first applied for CO2 removing purpose, while other light hydrocarbon gases are separated through traditional distillation. The simulation results for the first screened IL ([thtdp][phos]) show a good purity and recovery rate on the four gases. This can regarded as a base case to be compared with the process of computer-aided screened IL as well as traditional technology based process. Further detailed analysis will also be conducted.
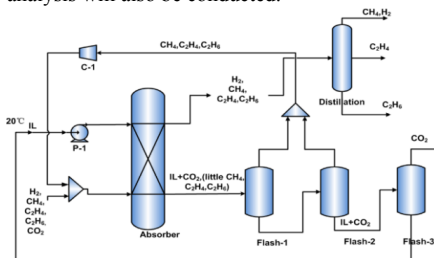
Figure 1 Hybrid IL-based shale gas separation

Conclusion and future work

This work proposes a framework for a model based IL design and further application on shale gas separation process. A database containing sufficient experimental data for Henry's law constant and solubility of several gases in ILs is established and then used for development of predicted COSMO-RS and UNIFAC-IL models. Then two optimal ILs are screened based on experimental database and computer-aided method respectively. One separation scheme is proposed and related simulation is conducted to get different products for multi-utilization.

Future work is necessary to apply the IL screened based on the group contribution basis UNIFAC-IL model. Then rigorous gas separation simulation and evaluation will be also developed and compared between these two IL-based processes.

Acknowledge

References

[1] Z. Lei, C. Dai, B. Chen, Gas Solubility in Ionic Liquids, Chem Rev 114 (2014) 1289-1326.
[2] X. Liu, T. Zhou, X. Zhang, S. Zhang, X. Liang, R. Gani, G.M. Kontogeorgis, Application of COSMO-RS and UNIFAC for ionic liquids based gas separation, Chemical Engineering Science 192 (2018) 816-828.

Xue Liu

Phone: +45 5273 1868
E-mail: xuli@kt.dtu.dk

Supervisors: Anne Ladegaard Skov
Suojiang Zhang
Yi Nie

PhD Study
Started: December 2017
To be completed: November 2020

Screening of ionic liquids for keratin dissolution by means of COSMO-RS and experimental verification

Abstract

Wool keratin, which is polar, hydrophilic, biodegradable, is expected to enhance interaction responses between implantations and cells. However, wool keratin is hard to reuse because it is difficult to dissolve in conventional solvents. An increasing interest has been manifested in the use of ionic liquids (ILs) as solvents for dissolution of wool keratin due to their tunable and excellent properties. However, it is nevertheless a challenge to identify the best ILs for keratin dissolution. Experimental measurement assesment of all these systems is not practically feasible; hence a rapid and a priori screening method to predict the keratin solubility capacity for ILs is needed. Herein, three keratin models and 621 ILs, including 27 cations and 23 anions, were used to evaluate keratin dissolution capability via a screening method based on COSMO-RS. From the prediction results of logarithmic activity coefficients (lnγ) for the three keratin models, it can be concluded that anions play a leading role in keratin dissolution, while cations only have a moderate effect on the dissolution process. The hydroxyl group on the cation side chain has a significant effect on the keratin dissolution capability of ILs. In addition, the experimental solubility of wool keratin in ten ILs was used to verify the theoretical predictions. Experimentally determined keratin solubility agrees well with the predicted lnγ. Ac^-, Dec^-, $HCOO^-$, Cl^-, BEN^-, DMP^-, DEP^-, DBP^-, TOS^- and Br^- with various cations studied in this work exhibited particularly good properties for keratin dissolution. The excess enthalpy calculations indicated that the main forces in the keratin dissolution in ILs are H-bonds, while the contribution of misfit forces and van der Waals forces are secondary.

Introduction

Dielectric elastomers (DEs), which are often referred to as "artificial muscles", possess many excellent properties, such as large strains, high-energy densities, and fast responses [1]. Polydimethylsiloxane (PDMS) elastomers are one of the most used materials for DEs [2]. Unfortunately, most PDMS used in tissue engineering applications are nonpolar, inert and highly hydrophobic，which lead to the low biocompatibility and interaction responses between implantations and cells [3].

Keratin, which is polar, hydrophilic, and biodegradable, is expected to enhance interaction responses between implantations and cells [3]. The biofunctions of silicone /keratin composites for tissue engineering could be achieved due to the special amino acid sequence in keratin [4]. Moreover, keratin can improve the mechanical properties of composites, which probably results from the formation of a common spatial network between keratin and silicone elastomer [3].

Wool, consisting of approximately 95 wt% pure keratin, is a kind of degradable natural biopolymer. It also contains about 11-17% cysteine, which serves as crosslinking sites to form water-stable fibers [5]. However, wool keratin is difficult to dissolve in conventional solvents, due to the tight packing of the secondary structures in the polypeptide. So efficient dissolution of keratin is the basis for the research of elastomer–keratin compositions [5].
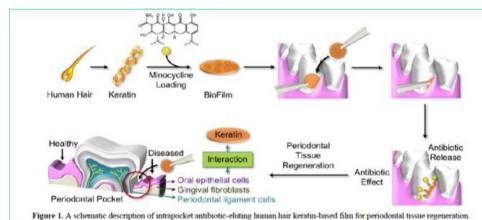

Fig.1 A schematic description of intrapocket antibiotic-eluting human hair keratin film for periodontal tissue regeneration.

As a new design solvent, ILs can dissolve a large number of biopolymers with high efficiency, due to their unique properties like high thermal stability, tunable properties, and good dissolving ability [5]. Although

there have been extensive studies for dissolution of keratin in ILs, it is still a challenge to identify the best ILs for keratin dissolution. Experimental measurement of all these systems is not practically feasible; hence a rapid and a priori screening method to predict the keratin solubility capacity for ILs is needed. In this work, we designed three models containing disulfide bonds for describing wool keratin, and 621 ILs formed from 27 cations and 23 anions were selected for evaluation of their ability to dissolve wool keratin by COSMO-RS. It lays a foundation for the research of keratin elastomer composites later.

Specific Objectives

The objectives of this work were to design three keratin models based on our previous work and to select the best keratin model from three keratin models, and use COSMO-RS to screen the best ILs for keratin dissolution.

Results and discussion

Predicting the logarithmic activity coefficient (lnγ)

We selected 621 ILs formed from 27 cations and 23 anions for evaluation of their ability to dissolve wool keratin by using COSMO-RS. The structure of cations and anions employed in this work can be seen in Fig.2 and Fig.3.
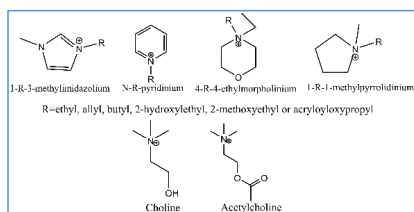
Fig.2 Structure of cations
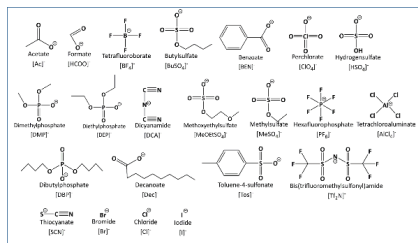
Fig.3 Structure of anions

Keratin has a complex structure, and there are a large number of inter- and intra-molecular strong hydrogen bonds and disulfide bonds. Moreover, keratin molecules have no regular repeating units, which led to it difficult to design a suitable model to describe keratin. In this work, three models containing disulfide bonds for describing wool keratin were designed. The chemical structures and charge surface regions are displayed in Fig. 4.

The predicted logarithmic activity coefficients (ln γ) of the three keratin models in each of the 621 ILs are depicted in Fig.5. The cations and anions are listed

according to their keratin dissolution ability. The ILs with high keratin dissolution capacities according to the
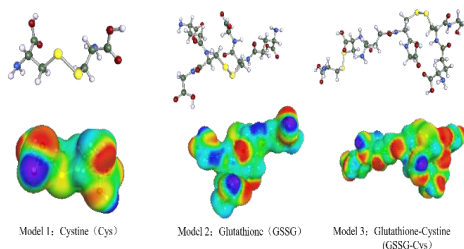
Fig.4 Chemical structures and charge surface regions of keratin models

predicted logarithmic activity coefficients are located to the left, while the ILs with lower keratin dissolution capacities are located to the right. From the prediction results of lnγ of the three keratin models, it can be concluded that the ILs with the methylpyrrolidinium cation have a lower predicted lnγ than the others, while ILs with anions Ac⁻, Dec⁻, HCOO⁻, Cl⁻, DEP⁻, DMP⁻, DBP⁻, BEN⁻, Br⁻ or TOS⁻ also have a lower lnγ, thereby suggesting that they have high keratin dissolution capability. Furthermore, the lnγ of these three keratin models in different ILs with varying cations matches closely; however, the structures of ILs are different. The slight difference in lnγ is due to the effect caused by the cations. Conversely, there is a big difference between the lnγ of these three keratin models in different ILs with varying anions, thus indicating that the keratin dissolution capacity of ILs is indeed affected by cations and anions, albeit the anion plays a leading role in this regard

Fig.5 The logarithmic activity coefficients (lnγ) prediction of the CYS keratin model in 621 ILs at 120°C.
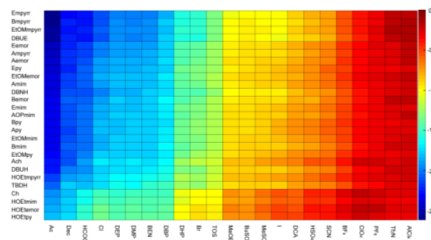
Fig.6 The logarithmic activity coefficients (lnγ) prediction of the GSSG keratin model in 621 ILs at 120°C.
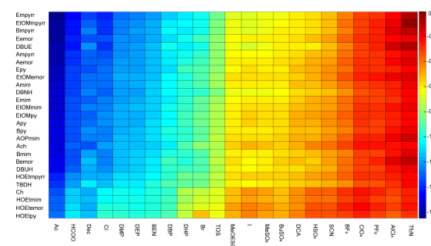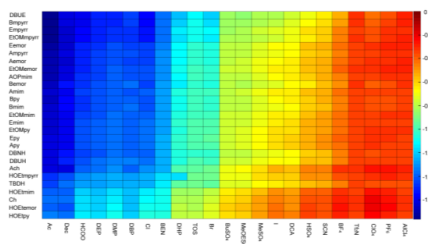
Fig.7 The logarithmic activity coefficients prediction of GSSG-CYS in 621 ILs. Conditions: the mole fraction of model was 0.5, the mole fraction of IL cations and anions was 0.25 each. The calculation temperature was 120 °C.

Verification experiments

The solubility of keratin in ten ILs was measured at 120°C to validate the COSMO-RS prediction results. In these ten ILs were the functional groups ethyl, allyl, butyl or 2-hydroxyethyl, along with methylimidazolium, methypyrrolidinium and pyridinium selected as cations, and Ac⁻, DEP⁻, Cl⁻, DCA⁻ or SCN⁻ as anions. From Table 2, it is evident that the keratin solubility trend in ILs is almost the same as in the logarithmic activity coefficient (lnγ). We also compared our data with the literature values.

Table 1: Experimental solubility of wool keratin in ten ILs and lnγ prediction results for three keratin models

No.	ILs	Solubility (wt%)	Temperature ˚C	lnγ prediction results at 120°C		
				CYS model	GSSG model	PP model
a	EmimAc	38	120	-2.35	-1.53	-1.63
b	EmimDEP	22	120	-1.82	-1.18	-1.41
c	AmimCl	13	120	-1.89	-1.27	-1.40
d	EmimCl	14	120	-1.86	-1.26	-1.37
e	BmimCl	11	120	-1.85	-1.25	-1.41
f	HOEtmimCl	3	120	-1.46	-1.03	-1.14
g	BmimDCA	1.5	120	-0.79	-0.55	-0.66
h	BmimSCN	< 1	120	-0.67	-0.49	-0.56
i	BmpyrrCl	40	180	-2.10	-1.38	-1.56
j	BpyCl	36	180	-1.83	-1.25	-1.41
k	BmimCl	35	180	-1.85	-1.25	-1.41

Keratin model effect. In order to check whether these keratin models are able to describe the keratin, the residual sum of squares (RSS) and R square (R²) between the lnγ of the three keratin models and keratin solubility were analysed further. Figure 6 shows that the R squares (R²) were 0.71, 0.66, 0.65 by using CYS, GSSG and PP as the keratin model, and the residual sum of squares (RSS) were 0.68, 0.32 and 0.37, respectively. The R squares (R²) of the three keratin models were similar, while the residual sum of squares for CYS was higher

than for the other two models. These findings suggest that the lnγ of GSSG and PP are better correlated with the experimental keratin solubility results than that of CYS. As illustrated in the predicted lnγ of the three keratin models, the values of lnγ when using CYS are lower than for other two models, which might be due to the fact that the CYS model is too simple to represent keratin.
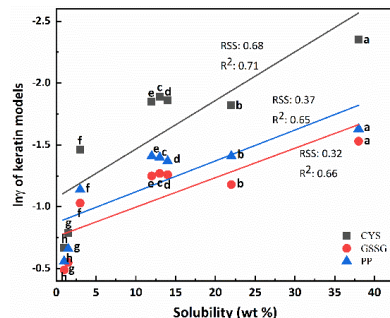
Fig.6 Experimental keratin solubility in ten ILs plotted against lnγ at 120°C

Predicting excess enthalpy
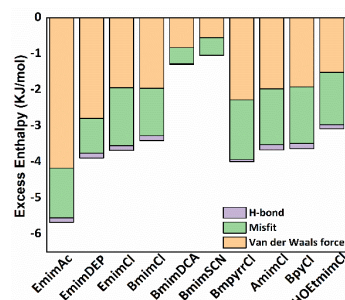
Fig.7. Excess enthalpies between the CYS keratin model and ten ILs
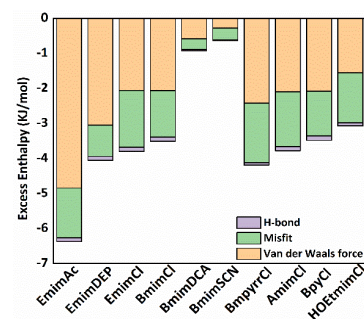
Fig.8 Excess enthalpies between the GSSG keratin model and ten ILs
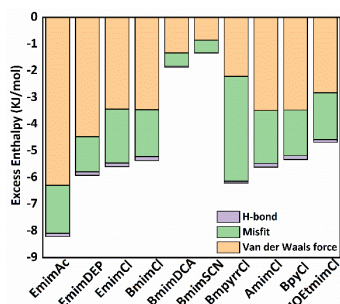
Fig.9. Excess enthalpies between the GSSG-CYS keratin model and ten ILs

Excess enthalpies between three keratin models and ten ILs were calculated, in order to explain further the possible interactions of keratin molecules and ILs structures. Combining the results presented in Fig. 7-9, it is evident that the main forces in the keratin dissolution process in ILs are H-bonds, while the contributions of misfit forces and van der Waals forces are secondary. Moreover, the excess enthalpies of ILs with the same cations and different anions exhibit a big difference, which can be proven by the excess enthalpy differences between EmimAc, EmimDEP and EmimCl. This conclusion can also be drawn from the excess enthalpy differences between BmimCl, BmimDCA and BmimSCN, albeit there is a slight difference between those of ILs with the same anions and different cations, such as the six ILs with Cl$^-$ shown in Figs. 7-9. This is in agreement with the deduction that anions play a crucial role in disrupting chemical interactions and therefore dissolution.

Conclusions

In summary, three keratin models were selected to represent keratin, and a screening method based on COSMO-RS was used to evaluate the keratin dissolution capability of ILs. Prediction results for the logarithmic activity coefficient (lnγ) indicate that anions play a major role in the keratin dissolution process, while cations have a moderate effect on the keratin dissolution capability of ILs. In particular, the hydroxyl group in cations has an important influence on the solubility of keratin in ILs. Ac$^-$, Dec$^-$, HCOO$^-$, Cl$^-$, BEN$^-$, DMP$^-$, DEP$^-$, DBP$^-$, TOS$^-$ and Br$^-$, with the various cations studied in this work, exhibited particularly good properties for keratin dissolution.

The experimental solubility of ten ILs was in accordance with that of the prediction lnγ, thereby indicating that the prediction value of lnγ via COSMO-RS can effectively reflect the keratin dissolution capability of ILs. Furthermore, the GSSG and GSSG-CYS keratin models are better at describing keratin than the CYS options. Finally, our excess enthalpy calculations indicated that H-bonds play a main role in the keratin dissolution process, followed by misfit forces and van der Waals forces.

References

1. R., Pelrine, R., Kornbluh, Q., Pei, J., Joseph, Science 287 (5454) (2000) 836-839.
2. C., Löwe, X., Zhang, G., Kovacs, Advanced engineering materials 7 (5) (2005) 361-367.
3. M., Van Dyke, U.S. Patent 2004, Application No. 10/606,279.
4. H., Lee, Y., Hwang, H., Lee, S., Choi, S., Kim, J., Moon, H. Bae, Macromolecular Research 23 (3) (2015) 300-308.
5. X., Liu, Y., Nie, X., Meng, Z., Zhang, X.,Zhang, S., Zhang, RSC Advances 7 (4) (2017) 1981-1988.

Petter Lomsøy

Phone: +45 2889 7086

E-mail: plom@kt.dtu.dk

Supervisors: Kaj Thomsen

Philip Loldrup Fosbøl

PhD Study

Started: September 2017

To be completed: August 2020

Kinetics of Scale Formation in Oil and Gas Production

Abstract

Scale formation poses a major challenge for the oil and gas industry, due to loss in production. Substantial deposition may result in stop of production or failure in critical components. The target system for this project is iron carbonate, which is commonly found in production equipment, and often as corrosion product in production tubing. The kinetics of Iron Carbonate is to be investigated, for improved prediction of fouling layer forming in production equipment. An in situ experimental method is designed in order to reveal the kinetic behavior of the different stages of formation.

Introduction

In the search for understanding the behavior of scale precipitation kinetics, a series of different methods have been used in the past. The most common method is "bulk jar test", which is a static system with decreasing saturation as precipitation occurs. Representation of relevant properties found in hydrocarbon production are therefore sparsely reported [1].

Challenges in experimental design and embodiment, are specially associated to kinetic mechanisms. Where the early stages of nucleation, are highly dependent on the sensitivity of analytical method.

The focus have been towards the mechanism of bulk precipitation throughout the reported literature. The perception of surface scale formation, has been leading towards the deposition of crystals already present in the bulk solution. However, lately there has been several studies suggesting otherwise. It seems that bulk precipitation and surface deposition are separate mechanisms, with its respective separate kinetics ([2], [3], and [4]). This development in the field reveals a need for further improvement of experimental methods and techniques.

Specific objectives

Development of an in situ method for investigation of $FeCO_3$ scale formation kinetics. With the aim to address the conditions found in production of hydrocarbons in relation to scale formation.

The coherence between kinetics of surface scale precipitation and bulk precipitation are to be evaluated.

Experimental conditions

The following conditions pose as the frame for the experimental campaign:

- CO_2 Partial pressure 0-150 kPa
- Temperature 25-80°C
- Varying supersaturation
- Anoxic conditions
- Laminar and turbulent flow conditions

Experimental setup and design

The investigation of the kinetics of $FeCO_3$ is challenging. Especially when the aim is to introduce relevant production conditions, found in the production of oil and gas. The setup need to have the ability to supply a range of CO_2 partial pressure, temperature, flow velocities and saturation. In addition, the system has to maintain an anoxic environment, while investigating scale formation in situ.

In order to meet the challenges reported, a new method is applied to the field of scale formation kinetics. Nano X-ray CT accompanied with image analysis, are to be introduced as a way of describing kinetics of scale formation on a solid surface. A flow cell containing a stainless steel sample, will resemble the behavior of production tubing and casing. The method will give information on both the early stages of nucleation, crystal growth, and the formation of porous scaling layers. The computed tomography technique will supply information
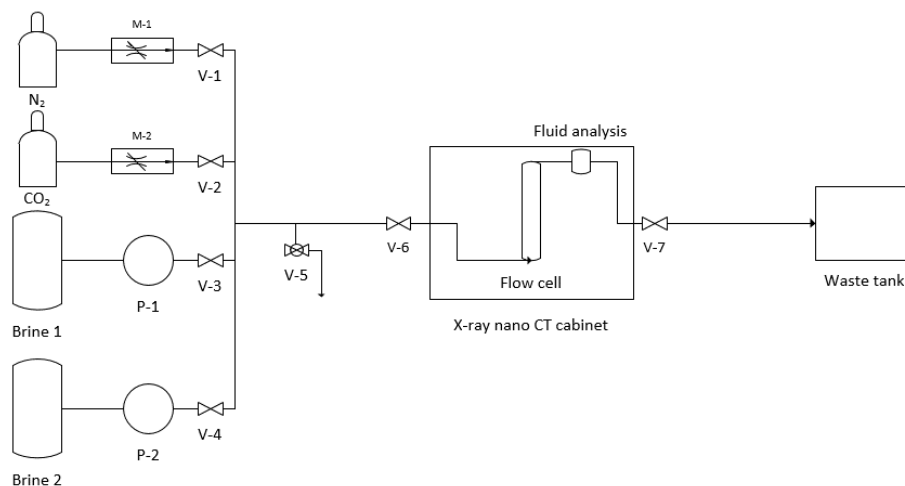
Figure 1 Diagram of the experimental setup

that is not commonly described by static tests. In addition to detection of the early stages of nucleation and growth rate, layer thickness and its porosity will be evaluated. Particles precipitated in the bulk fluid is to be detected, in order to correlate the relation between surface and bulk precipitation kinetics.

Figure 1 shows the flow diagram of the experimental setup, where two brines are mixed and surpassing a carbon steel sample within the flow cell, situated in a nano X-ray CT cabinet. For $FeCO_3$ investigation $FeCl_2$ and $NaHCO_3$ brines will be prepared. As the figure shows, the setup is a "once through" system, which allows for a constant solution chemistry during experiments. Figure 2 shows the design of the in situ flow cell, which will be mounted into the nano X-ray CT setup. This cell allows scale formation on a carbon steel sample, as a function of the before mentioned conditions. A 3d volume can be reconstructed from several radiographs, recorded on different angles of the sample.

It has been an important aspect of the cell design to model the capabilities regarding flow velocity, and thus the ability to produce turbulent flow regime. This is to strengthen the knowledge regarding scale formation kinetics as a function of turbulent flow. This is especially relevant for production of oil and gas, due to the complex geometry and flow regime throughout a producing well.

Conclusion

This study address the kinetics of iron carbonate scaling, which are a substantial challenge to the flow assurance and integrity of wells and equipment. Quantifying the rate of $FeCO_3$ scale surface deposition and bulk crystallization, with a new approach, will strengthen the knowledgebase regarding the system in question.

References

1. Sanjuan, B. and Girard, J.: 1996, Review of kinetic data on carbonate mineral precipitation, BRGM, Report R39062, p. 91.
2. Morizot, A., Neville, A. et al.: 2001, Using an electrochemical approach for monitoring kinetics of $CaCO_3$ and $BaSO_4$ scale formation and inhibition on metal surfaces, SPE Journal 6 (02), 220–223Chen, T., Neville, A. and Yuan, M.: 2005, Calcium carbonate scale formation—assessing the initial stages of precipitation and deposition, Journal of Petroleum Science and Engineering 46(3), 185–194.
3. Sanni, O., Charpentier, T., Kapur, N., Neville, A. et al.: 2015a, Study of surface deposition and bulk scaling kinetics in oilfield conditions using an in-situ flow rig, NACE-International Corrosion Conference Series, Vol. 2015, Leeds

Figure 2 Flow cell design

Vicente T. Monje López

Phone: +45 52 76 26 76

E-mail: vtml@kt.dtu.dk

Supervisors: Krist V. Gernaey

Xavier Flores Alsina

Helena Junicke

Kasper Kjellberg, Novozymes

PhD Study

  Started: February 2018

  To be completed: January 2021

Gradients of pressure in anaerobic digesters:
Effect on gas solubility, (bio)reaction thermodynamics, and minerals precipitation.

Abstract

The height of the water column in tall bioreactors causes severe differences in hydrostatic pressure along the vertical axis of the tank, and may significantly affect gas solubility and dissolved gas concentrations at a given height in the reactor. In anaerobic digesters, many of the biochemical reactions occur close to thermodynamic equilibrium. Therefore, even slight changes in the concentration of reagents and products can have profound impact on reaction feasibility. Another consequence of the pressure gradient is the altered solubility of carbon dioxide in the liquid phase, which causes a pH gradient in the bioreactor. This pH gradient possibly affects mineral precipitation.
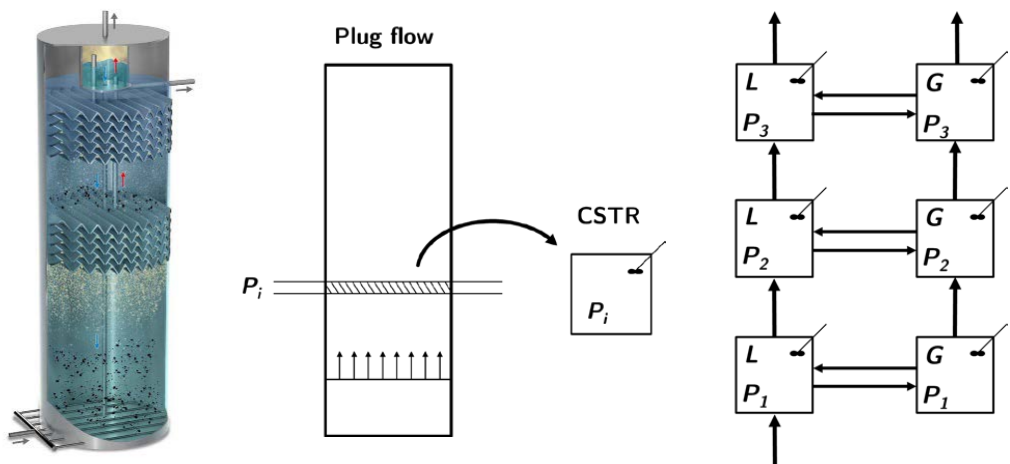
Figure 1. From left to right; Anaerobic digester scheme (BIOPAQ®IC), conceptualization of gradients of pressure along the reactor, proposed structure for model implementation. P_i stands for total pressure at a certain point. L and G for liquid and gas phases in the anaerobic digester.

Introduction

Wastewater treatment has undergone a profound development in the last few decades, in short, from aerobic to anaerobic technologies. The three major driving forces leading this transformation are increased carbon removal capacity per volume unit, reduction of operating costs, and the possibility to perform resource recovery from the wastewater in form of biogas (methane plus carbon dioxide) and precipitated minerals such as struvite (NH_4MgPO_4).

The anaerobic digester

In this project, efforts are focused on the study of the anaerobic digester installed in the wastewater treatment plant at the Novozymes production site in Kalundborg (Denmark), treating wastewater from both, Novozymes and Novo Nordisk.

Fig. 1 (left) gives a schematic overview of the anaerobic digester used in this case study [1]. In this reactor configuration, wastewater containing organic carbon enters through the bottom of the reactor and rises together with the generated biogas. Thanks to the up-flow in the tank, granular biomass is suspended, creating a fluidized bed that provides contact surface area between biomass and substrate while ensuring biomass retention in the reactor.

The water column has a maximum height of 30 meters, causing a hydrostatic pressure of 4 bar at the bottom of the bioreactor.

Theoretical approach

The anaerobic digester can be regarded as a plug-flow reactor in terms of operating pressure (Fig. 1, middle). For modelling purposes, we compartmentalize the reactor volume into a series of continuously stirred tank reactors (CSTRs), each of them under a different operating pressure.

The change in operating pressure causes changes in gas solubility according to Henry´s Law:

$$c_{A,L}^* = H^o \cdot x_{A,G} \cdot P_{Total}$$

$c_{A,L}$ stands for solubility of compound A in the liquid phase, $x_{A,G}$ stands for the molar fraction of compound A in the gas phase, H^o stands for the Henry coefficient, and P_{Total} stands for total pressure.

It is expected that solubility of gaseous compounds changes with total pressure along the vertical axis of the bioreactor. This influences the actual Gibbs energy change (ΔG^1) of the (bio)reactions taking place in the digester:

$$A + B \rightarrow C + D$$

$$\Delta G^1 = \Delta G^o + R \cdot T \cdot ln\left(\frac{[C][D]}{[A][B]}\right)$$

ΔG^1 and ΔG^o stand for Gibbs free energy change of the evaluated reaction conditions and in standard conditions, respectively; R stands for the ideal gas constant; T stands for temperature; A, B, C, D stand for the concentration of the involved chemical species.

Since many anaerobic bioconversions proceed close to thermodynamic equilibrium, changes in metabolite concentration can make a certain reaction work in one direction in one zone of the bioreactor and in the opposite direction in another zone. The aim of this project is to investigate if that is the case in the full-scale digester and to understand the implications of this on the system performance.

Besides affecting reaction thermodynamics, changes in pressure also affect the amount of dissolved CO_2. The bicarbonate buffer system is one of the key regulators of the pH in anaerobic digesters and therefore changes in CO_2 solubility influence the pH in the liquid phase. Mineral precipitation is highly sensitive to pH [2], which is a generally undesired process inside the anaerobic digester since salt crystals compete with biomass for space in the granules and cause a decrease of carbon removal capacity [3].

Modelling

The IWA anaerobic digestion model no 1 [4] will be used as starting point for the mathematical modelling of the anaerobic digester. Specific modifications will be performed to include the effect of solubility changes on thermodynamics.

Acknowledgments

References

1. Paques (2018, November 1). BIOPAQ®IC. Retrieved from www.paques.nl
2. Flores-Alsina, X., Solon, K., Mbamba, C. K., Tait, S., Gernaey, K. V., Jeppsson, U., & Batstone, D. J. Water Research 95 (2016) 370-382.
3. Feldman, H., Flores-Alsina, X., Ramin, P., Kjellberg, K., Jeppsson, U., Batstone, D. J., & Gernaey, K. V. Water research (2017) 126 488-500.
4. Batstone, D. J., Keller, J., Angelidaki, I., Kalyuzhnyi, S. V., Pavlostathis, S. G., Rozzi, A., ... & Vavilin, V. A. Water Science and technology (2002) 45(10), 65.

Hao Luo

Phone: +45 4525 2853
E-mail: haol@kt.dtu.dk

Supervisors: Kim Dam-Johansen
    Hao Wu
    Weigang Lin

PhD Study
    Started: October 2016
    To be completed: September 2019

CFD Simulation of Biomass Combustion in Fluidized Beds

Abstract

The project aims at developing an efficient and reliable computational fluid dynamics (CFD) model to simulate biomass combustion in fluidized bed systems. A comprehensive single-particle model has been developed and validated to describe devotalilization and char combustion. Based on the comprehensive single particle model, a heat transfer corrected isothermal model has been developed for CFD simulation of devolatilization of large biomass particles in a fluidized bed.

Introduction

Biomass combustion in a fluidized bed involves reaction and hydrodynamic behaviors. CFD is considered as a useful tool to simultaneously describe the hydrodynamic and reaction behaviors. However, the following challenges remain in current CFD modelling of biomass combustion in a fluidized bed：

(1) Particle-scale: current CFD modelling neglects the particle internal heat and mass transfer, which have significant effects on the combustion of for large biomass particles [1].

(2) Meso-scale: the meso-scale structures (e.g. cluster or bubble) have significant effects on momentum, and heat and mass transfer between gas and solid phase [2,3]. Current meso-scale structure model should be validated.

(3) Reactor-scale: CFD modelling coupled with comprehensive particle model and detailed kinetics is computational demanding for a large-scale fluidized bed. It is essential to develop reliable and efficient approaches to couple CFD models with chemical reaction kinetics.

Objectives

The overall objective of this project is to develop an efficient and reliable approach to simulate biomass combustion in fluidized bed systems. The specific objectives include:

– Develop and validate a comprehensive single particle model for biomass combustion.
– Validate meso-scale model for biomass combustion in fluidized bed.
– Develop a reliable and efficient approach to CFD modelling large-scale fluidized bed.

Particle-scale model

A comprehensive single particle model for biomass devolatilization has been developed. The model includes both internal and external heat transfer. The modelling results were compared with our single particle combustion experiment.

Fig.1 compares the experimental and predicted devolatilization time of pine wood particles with different apparent density (dry basis) and moisture content (6.9 % to ~53.0%). Both the modelling and experimental results show that the devolatilization time increases with the increase of moisture content, and the devolatilization time increases linearly with the increase of the apparent density of dry particle. Therefore, particle dry apparent density and moisture content are two critical parameters to determine the devolatilization time, besides particle size and shape, and operating temperature. The model predicted devolatilization time are generally in a good agreement with experimental data in ±25%.

Fig.2 compares the experimental and predicted char conversion time of pine wood particles at 1487K with varying O_2 concentration of 0.0 % to ~10.5% and H_2O concentration of ~26.0%. The predicted char conversion time are in good agreement with the experimental data, when O_2 concentration is 4.4% and 10.5%. However, the char conversion time at 0.0% O_2 is not well predicted, suggesting an improvement of the model, especially the kinetics for steam gasification, is needed.
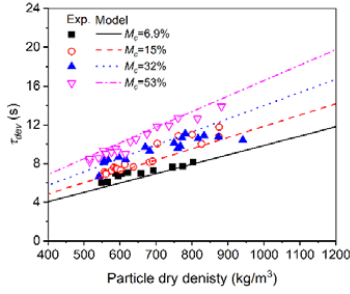
Figure 1: A comparison between the experimental and predicted devolatilization time of pine wood particles with different moisture content and dry apparent density (d_p=4.0 mm, T_g=1496 K, T_w=1296 K)
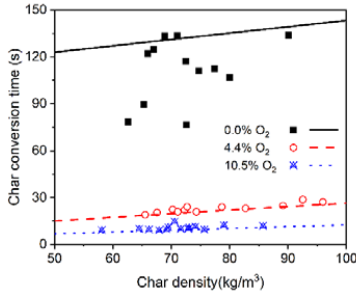

Figure 2: A comparison between the experimental and model predicted char conversion time with variation of oxygen concentration (d_p=4.0 mm, T_g=1487 K, T_w=1287 K, 26% H_2O)

A heat transfer corrected isothermal model for CFD simulation of biomass devolatilization

Coupling the developed comprehensive devolatilization model with CFD is computational demanding. The conventional isothermal particle model commonly used in CFD modelling is only reasonable for small particles. To develop a model with high accuracy and computational efficiency for both large and small particles, a heat transfer corrected isothermal model is developed and more details can be found in Luo et al. [4]. Both the conventional and corrected isothermal models were implemented into ANSYS Fluent® to simulate biomass devolatilization in a batch fluidized bed.
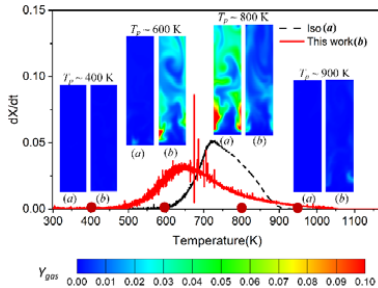
Figure 3: Comparisons of CFD modeling devolatilization rates versus particle temperature and contour plot of volatiles mass fraction (Y_{gas}). (d_p=10.0 mm, T_g=1173 K, T_w=1173 K, Air)

Fig. 3 shows a comparison of biomass devolatilization rate predicted in CFD simulations. At lower particle temperatures, (T_p~600 K), the corrected isothermal model shows a higher devolatilization rate than the conventional isothermal model. At higher particle temperatures (T_p~800 K), the devolatilization rate predicted by the conventional isothermal model is larger than that of corrected isothermal model. The result is consistent what we observed in single particle modeling.

Table 1. compares the computational efficiency of the conventional and corrected isothermal model. The computational speed of the two models is in the same order of magnitude, suggesting the heat transfer corrected isothermal model can be used with high computational efficiency.

Table 1. A comparison of computational efficiency by using the conventional and corrected isothermal model

Particle size	Computational efficiency (s/time step)	
	Isothermal	corrected
d_p=1, mm	0.92	0.88
d_p=3, mm	0.97	0.92
d_p=6, mm	0.95	0.98
d_p=10, mm	0.93	1.15

Conclusion

A comprehensive single-particle model for biomass devolatilization and char combustion was developed and validated. Then, a heat transfer corrected isothermal model was developed based on the comprehensive devolatilization model to model devolatilization of large biomass particles. The model was validated by experimental data and implemented in a CFD software. The results show that the corrected isothermal model can be used to model both large and small particle with high computational efficiency.

Future work

The comprehensive single-particle char combustion will be simplified as sub-model for CFD simulations. The current meso-scale model (e.g. drag model, heat transfer model etc.) will be tested for CFD modelling biomass combustion in fluidized bed. Finally, the development of a reliable and efficient approach to model large-scale fluidized by coupling CFD and chemical engineering models.

References

1. A. Gómez-Barea, B. Leckner, Prog. Energy Combust. Sci. 36 (2010) 444–509.
2. W. Wang, B. Lu, N. Zhang, Z. Shi, J. Li, Int. J. Multiph. Flow. 36 (2010) 109–118.
3. K. Hong, Z. Shi, W. Wang, J. Li, Chem. Eng. Sci. 99 (2013) 191–202.
4. H. Luo, H. Wu, W. Lin, D.J. Kim, in: Nordic Flame Days, Stockholm,Sweden, 2017.

Enrico Mancini

| Phone: | +45 50298515 |
| E-mail: | enrmini@kt.dtu.dk |

Supervisors:	Manuel Pinelo
	Seyed Soheil Mansouri
	Krist V. Gernaey
	Jianquan Luo

PhD Study
| Started: | June 2018 |
| To be completed: | July 2021 |

Sustainable and cost-effective downstream routes for separation of bio-fermentation products

Abstract

Downstream processes constitute a major cost for production of valuable bio-chemical such as bio-succinic acid. Process optimization and identification of critical factors favouring technological advances in membrane technologies for bio-succinic acid production would contribute developing cost-effective downstream routes for large-scale production of bio-products. A developed computer-aided framework will be used to investigate potential downstream membrane-based routes exploiting molecular physio-chemical properties of fermentation products. The production of one of the most important bio-building blocks, bio-succinic acid, will be used as a study case. A starting literature study will help identify the most sustainable, available and potentially significant feedstocks, fermentation and separation techniques. The results of the previous assessments will be tested in lab.

Introduction

Biorefinery is a promising concept that can contribute overcoming the petrol-era, especially with respect to sustainable fine chemical production, addressing at the same time several problems: the depletion of petroleum resources (with the associated consequences), human sustainability, waste management and political concerns [1]. Production and separation of valuable products from biomass have indeed been successfully achieved and implemented at full scale [2]. However, the lack of cost-effective downstream processes is largely preventing biorefinery products to become economically competitive, and membranes are one of the fundamental technologies for separation of fermentation products such as succinic acid [3]. Therefore, critical factors such as pH, pressure, steric effect etc. in downstream processes must be identified and grade for a potential technological breakthrough and biochemical bulk production. The model fermentation product bio-SA has gained increasing interest [2], since more than 30 commercially valuable products can be currently synthetized from it, including solvents and lubricants, synthetic resins and biodegradable polymers such as PBS and polyamides, cosmetics, food and pharmaceuticals [2].

Objectives

Fermentation is a biotechnology from which many valuable bio-products can be obtained. However, to economically compete with petrol-based products, cheap feedstocks must be used and, most importantly, both technological advances and process optimization further developed. Typically, cheap feedstocks may require pretreatment to break down the structure, such as for the lignocellulosic matter, and application of fermentation and separation processes. Further processing and know-how will be required in order to divert fluxes from unwanted products, obtain near-theoretical yields, lower potential inhibitory processes and obtain the purest product. The hand in hand growth of technologies and processes requires iteration between the model and real values. Therefore, lab experiments will be carried out according to the process optimization results using succinic acid as the model fermentation product. Succinic acid has been selected from both the E.U. and the U.S. department of energy, among the most important blocks. This work will begin with a literature study to identify which are the potential feedstocks, fermentation and separation techniques for large-scale production of succinic acid. Inexpensive, sustainable and available feedstock will be pinpointed, together with the identification of fermentation strategy and microbial strain with the highest records so far. These, will be then study through a techno-economic analysis, which will be focused on membrane separation techniques. Thus, a computer-aided framework will be used to assess and rank the critical parameters in downstream technologies, which will be subsequently tested through an experimental validation of bio-SA production (Figure 1).
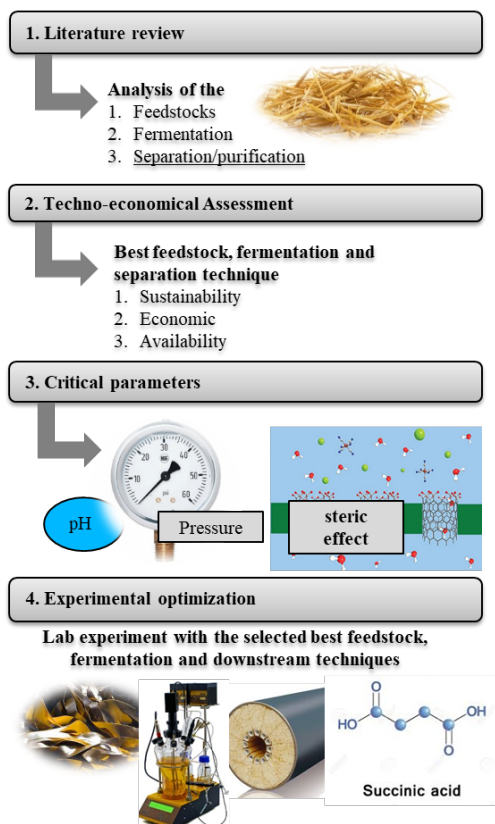
Figure 1. Illustration of the four objectives and their related application upon the case study: bio-succinic acid.

Potential experimental configuration

According to the literature study, a potential scenario for both the techno-economic study and the experimental work is configuring, and some collected data are reported in Table 1.

1. **Feedstock.** To date, large-scale production of succinate has primarily focused on starch-based sugars for bio-SA. However, not to compete with food production, cheap lignocellulosic sugars should be extracted from non-food crops [4]. Furthermore, bio-SA bulk production is expected to be from processing lignocellulosic feedstock material [5].

2. **Pretreatment.** For lignocellulosic feedstocks, typical thermochemical followed by enzymatic-based pretreatment are considered the less complex and more efficient and sustainable than those non-enzymatic [6]

3. **Fermentation.** Among the potential configuration, simultaneous saccharification and fermentation (SSF) has been reported as the optimal for large-scale production of bio-SA [7].

4. **Downstream.** Currently, three major steps are used to separate bio-SA: (1) cell removal by membrane filtration, (2) removal of impurities with, among others,

molecular sieve or ion exchange resin, and finally (3) evaporation or crystallization [8].

Table 1. Some collected data for succinic acid production. Used feedstocks, fermentation strategy, productivity and yield.

Feeds -tock	Ferment. strategy	Conc. (g/L)	Product. (g/l/h)	Yield (g g^{-1})
CB	AB	120	1.65	0.805
WM	SSF	62.1	0.91	0.087
WS	AB	2.02	$\approx$ 22.5	$\approx$ 0.03
CS	AB	61		0.92
BK	SSF	24.8	0.79	0.28

Abbreviations
Feedstock: cane bagasse (CB); wheat milling by-products (WM); wheat straw (WS); corn stalk (CS); bakery waste (BK). Fermentation strategy: anaerobic batch (AB); solid-state fermentation (SSF).

References
1 F. Cherubini, Energy Convers. Manag., (2010), 51, 1412–1421.
2 R. K. Saxena, S. Saran, J. Isar and R. Kaushik, Curr. Dev. Biotechnol. Bioeng. Prod. Isol. Purif. Ind. Prod., (2016), 601–630.
3 Pacific Northwest National Laboratory (PNNL), T. Werpy and G. Petersen, US Dep. Energy, (2004), 36–38.
4 D. Salvachúa, A. Mohagheghi, H. Smith, M. F. A. Bradfield, W. Nicol, B. A. Black, M. J. Biddy, N. Dowe and G. T. Beckham, Biotechnol. Biofuels, (2016), 9, 1–15.
5 C. S. K. Lin, et al., Energy Environ. Sci., (2013), 6, 426–464.
6 A. K. Chandel, V. K. Garlapati, A. K. Singh, F. A. F. Antunes and S. S. da Silva, Bioresour. Technol., (2018), 0–1.
7 S. González-García, L. Argiz, P. Míguez and B. Gullón, Chem. Eng. J., (2018), 350, 982–991.
8 K. K. Cheng, X. B. Zhao, J. Zeng, R. C. Wu, Y. Z. Xu, D. H. Liu and J. A. Zhang, Appl. Microbiol. Biotechnol. (2012), 95, 841–850.

Marvin Masche

Phone:	+45 9351 1606
E-mail:	marv@kt.dtu.dk

Supervisors:	Jesper Ahrenfeldt
	Maria Puig Arnavat
	Peter Arendt Jensen
	Sønnik Clausen
	Ulrik Birk Henriksen
	Jens Kai Holm, Ørsted

PhD Study

Started:	January 2016
To be completed:	December 2018

Morphology and Grindability Study of Wood and Combustion Characterization at Pulverized-Fuel Firing Conditions

Abstract

Wood pellets contribute significantly to the green transition of Danish coal-fired power stations. Before firing in the existing boilers, pellets need to be comminuted. The literature review shows that the comminution and pelletization of wood is a complicated process influenced by the chemical, physical, mechanical, and fracture properties of wood and the applied equipment. A study was performed focusing on the mechanical processing pathway of European beech (hardwood) and Austrian pine (softwood), including pellet feedstock comminution, pelletization, and pellet comminution. The results of the present research suggest that milling beech requires less energy, leads to a higher size reduction ratio, and produces finer particles than pine. Furthermore, the pelletizing process appears to be more decisive for the evolution of the particle shape than pellet milling.

Introduction

Increasing environmental concerns have resulted in higher energy production from biomass in Denmark. This is especially true for wood pellets because of their favorable properties compared to unprocessed biomass. The largest Danish energy company, Ørsted, will phase out all its coal-fired power plants by 2023. Thus, the biomass consumption for energy production in Denmark is expected to increase from 136.5 PJ in 2012 to 173 PJ in 2020 [1].

In the field of pelletization, feedstock comminution is an important step, as it changes the physical biomass properties (e.g., particle size, shape, flowability, bulk density). These are important properties for suspension-firing, as they affect the particle heat and mass transfer. Fig. 1 shows the downsizing pathway of pellet feedstock, which includes several comminution steps. However, pellet producers will not comminute the feedstock more than needed, as grinding biomass to smaller particles requires more energy [2].

Generally, the energy consumption for biomass grinding depends on feed size, feed moisture, density, biomass type, material feed rate, and milling equipment. The chemical structure of biomass influences its pelletizing performance and pellet quality. Softwoods with greater extractives require less power for pelletizing than hardwoods due to the lubricating effect of extractives that reduces the friction in the pellet die channels [3].

Aim and Scope

We performed a study that follows the complete mechanical processing pathway of European beech (hardwood) and Austrian pine (softwood), including pellet feedstock comminution, pelletization, and pellet comminution. To the best of our knowledge, this is the first study that focusses on all of these steps consecutively. This study provides an understanding of how pelletization and comminution operations alter the physical properties of wood particles. The results of this study will be of benefit to pellet producers and power plant managers, who want to improve the overall boiler efficiencies for wood suspension-firing.

Material and Methods

European beech (*fagus sylvatica*) and Austrian pine (*pinus negra)* from Central Zealand (Denmark) were used in this study. First, debarked logwood was chipped. Then, the fresh wood chips went through a two-stage milling process in a semi-industrial hammer mill, including fine and coarse milling. Pellets were produced from the fine grinds. The pellet quality parameters were assessed according to ISO 17225-2:2014. Finally, produced pellets were comminuted in the same hammer mill that was used for fine milling. Physical properties, e.g., particle size distribution (PSD), and particle shape of different wood samples were analyzed by sieve analysis for size analysis and digital image analysis

(DIA) for size and shape analysis, as well as the wood sample bulk density. The grinding and pelletizing performance of beech and pine pellets were assessed by determining the specific energy demand for grinding (SGEC) and pelletizing, respectively.
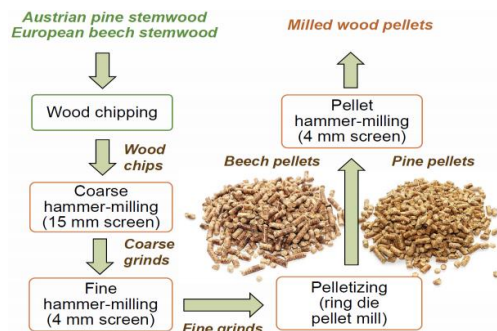

Figure 1: Major processing steps of converting stemwood to milled wood pellets for suspension-firing.

Results and Discussion
Beech presented fewer extractives than pine that led to higher pelletizing energy consumption due to the lubricating effect of extractives in the press channel. Figure 2 shows that pelletization modifies the internal pellet particle length ($d_{Fe,max}$) probably by shearing of wood particles between the rollers and rotating die in the pellet press. The particle breaking effect was more dominant for beech particles, which produced a larger amount of fines than pine during milling operations.
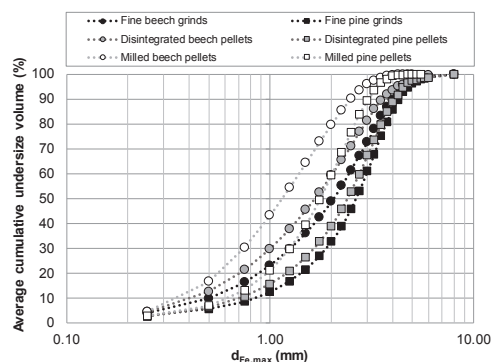
Figure 2: Particle length ($d_{Fe,max}$) analysis by DIA.

For pellet producers and power plant operators, the energy for mechanical processes (i.e., comminution and pelletization) has to be minimized to achieve optimal process efficiencies. Figure 3 shows a strong power law relationship between SGEC and the size reduction ratio. Milling beech requires less energy and leads to a higher size reduction ratio than pine. For pellet producers, fine milling represents the most energy-consuming milling process. Switching to beech pellets will slightly improve the overall power plant efficiency and provide finer fuel particles for suspension-firing.
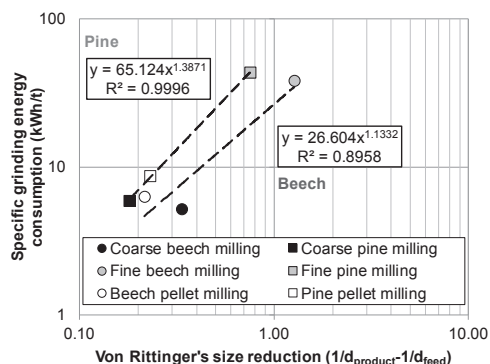
Figure 3: SGEC vs. Von Rittinger's size reduction ratio.

Conclusions
The following conclusions can be drawn from recent research:
- For practical milling operations, beech wood requires less energy for milling than pine.
- Pelletization improves the wood grindability. Thus, pellet comminution is more energy efficient than fine grinding when using the same hammer mill.
- The pelletizing process in the pellet mill alters the shape and length of the wood particles. There is an important reduction in the particle length, which results in higher particle circularity and elongation ratio values.

References
[1] From sustainable biomass to competititve bioenergy, State of Green. (2015). https://stateofgreen.com/en/uploads/2015/11/From-Sustainable-Biomass-to-Competitive-Bioenergy.pdf (accessed May 24, 2018).
[2] M. Temmerman, P.D. Jensen, J. Hébert, Von Rittinger theory adapted to wood chip and pellet milling, in a laboratory scale hammermill, Biomass and Bioenergy. 56 (2013) 70–81. doi:10.1016/j.biombioe.2013.04.020.
[3] T. Filbakk, G. Skjevrak, O. Høibø, J. Dibdiakova, R. Jirjis, The influence of storage and drying methods for Scots pine raw material on mechanical pellet properties and production parameters, Fuel Processing Technology. 92 (2011) 871–878. doi:10.1016/j.fuproc.2010.12.001.

Xianglei Meng

Phone: +45 52909586
E-mail: xmen@kt.dtu.dk

Supervisors: Nicolas von Solms
Xiaodong Liang
Suojiang Zhang, IPE (Beijing, China)
Xiangping Zhang, IPE (Beijing, China)

PhD Study
Started: December 2015
To be completed: February 2019

Biological Porphyrin Ionic Liquids as Photocatalysts for Conversion of CO$_2$ to Carbonates

Abstract
A series of biological porphyrin ionic liquids (BPILs) that combine the advantages of ionic liquid and porphyrin were design and synthesized by different method. The structure and surface appearance of these BPILs were investigated. These BPILs catalysts have multiple active sites and a good capacity of visible light absorption due to the advantages of functional ionic liquids and metal porphyrin part, thus can reduce the energy inputs greatly by using the visible light. They were successfully used in conversion of atmospheric CO$_2$ to carbonate with a visible light.

Introduction
Carbon dioxide (CO$_2$), a global warming gas, is also regarded as an abundant, nontoxic and renewable C1 resource. The utilization of CO$_2$ as raw materials for production of energy carriers and chemicals has been widely demonstrated.[1] One of the typical feasible routes is the synthesis of five-membered cyclic carbonates by cycloaddition of CO$_2$ with epoxides. [2] This process is a very attractive atom economical reaction with no formation of by-products.

Ionic liquid, well known as a green solvent, has been wildly used in the synthesis of cyclic carbonates from CO$_2$ and epoxides because its structure can be easily designed. [3] Although most of the ionic liquid catalyst systems show a good yield to produce carbonates, high temperatures and high CO$_2$ pressures are always needed, which makes this process not so "sustainable". [4] Recently, much of the focus has been on metal based porphyrin. As the main effective component of heme, chlorophyll, etc, metal based porphyrin could not only activate CO$_2$ at atmospheric CO$_2$ conditions, but also have a good capacity of visible light absorption. They have been widely used to conversion of CO$_2$ under mild reaction conditions. [5]

Specific Objectives
Inspired by these works, we designed a series of biological porphyrin ionic liquids (BPIL) to combine the advantages of ionic liquid and porphyrin (Figure 1). These BPIL catalysts can activate the epoxide and make the key step much easy. The activation of CO$_2$ supported by the ionic liquid part and metal center of porphyrin

helps to react with epoxide at atmospheric CO$_2$ conditions. Furthermore, BPIL have a good capacity of visible light absorption, thus can reduce the energy inputs greatly by using the visible light, and realize the efficient conversion of atmospheric CO$_2$ to carbonate at very mind conditions with a visible light.
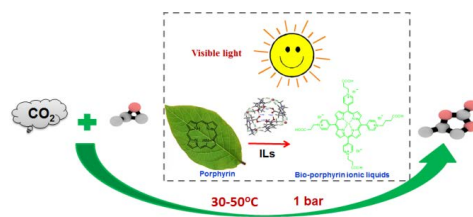
Figure 1: Picture shows the synthesis of carbonates catalysted by bio-porphyrin ionic liquids

Reaction process
The coupling reaction of carbon dioxide and epoxide is carried out in photo-catalytic glass reactor equipped with a magnetic stirrer and an automatic temperature control system. In a typical reaction, appropriate amounts of epoxide and catalyst are charged into the reactor at room temperature. Then, a balloon of CO$_2$ is connected to the reactor to maintain an atmospheric pressure. The reaction system will be irradiated by the visible light (λ= 420nm). Control the temperature within the desired range afterwards. After the reaction, the remaining CO$_2$ was

vented out slowly. The products were analysed by H NMR spectra using CDCl$_3$ as an internal standard.

Results and Discussion
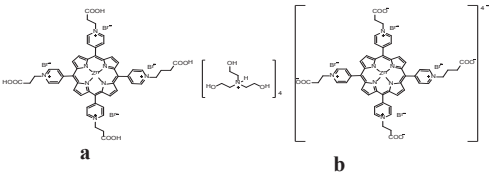
Figure 2: Catalysts used in this study.

We have been proved that Br$^-$ is an excellent nucleophilic ion for the cycloaddition reaction in our previous work. [6-8] Hence, Br- is chosen as the model anion. At the initial of our study, we prepared the BPILs by self-assemble method. The structure was shown in Figure 2. The surface appearance of the BPILs was analyzed by SEM (Figure 3). We can see that the BPILs **a** is a long flatter ribbon-like fibre. But BPILs **b** has a very different sharp with **a**. The capacity of visible light absorption of BPILs **a** was studied by UV spectrum. There was a strong signal at 420nm as shown in Figure 4.
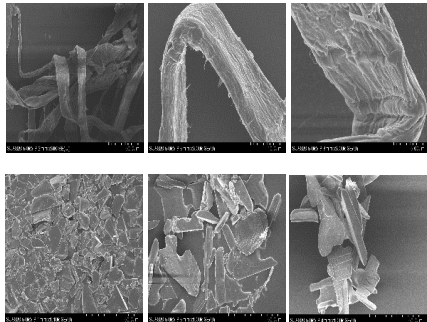
Figure 3: SEM of the bioporphyrin ionic liquids (**a** and **b**).
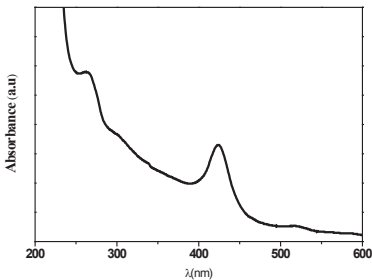
Figure 4: UV spectrum of the bioporphyrin ionic liquids **a**.

Then, the catalytic activity of various BPILs was carried out with epichlorohydrin and a balloon of CO$_2$. The results were shown in Table 1.

Table 1: Catalysts screening for the synthesis of carbonates

Entry	Catalyst	Temperature (°C)	Light	Yield[b] (%)
1	BrC$_2$COOH	80	No	Trace
2	TPP	80	No	Trace
3	ZnTPP	80	No	Trace
4	TPPC$_3$OOH	80	No	29
5	**a**	80	No	92
6	**b**	80	No	12
7	**a**	50	No	29
8	**a**	50	Yes	95

[a]Reaction conditions: epoxide (0.5ml), catalyst (0.1mol%), CO$_2$ (balloon), Time (8h) [b]Determined by ^{1}H NMR.

Conclusions

In summary, a series of biological porphyrin ionic liquids (BPILs) were designed and synthesized. As compared to enzymic catalytic reactions, biological porphyrin ionic liquids can be worked in a harsh temperature conditions, and when compared to traditional catalyst systems, BPIL can have a high efficient under a visible light. The BPIL were successfully used as photocatalysts for cycloaddition of CO$_2$ with and realize the efficient conversion of atmospheric CO$_2$ to carbonate at very mind conditions.

References

[1] X.B. Lu, D. J. Darensbourg, *Chem. Soc. Rev.* 41 (2012) 1462-1484.

[2] P. Jessop, T. Ikariya, R. Noyori, *Chem. Rev.* 95 (1995) 259-272.

[3] C. Bruckmeier, B. Rieger, W. A. Herrmann, F. E. Kühn, *Angew. Chem. Int. Ed.* 50 (2011) 8510-8537.

[4] B. Schaffner, F. Schaffner, S. P. Verevkin, A. Borner, *Chem. Rev.* 110 (2010) 4554-4581.

[5] J. W. Comerford, I. V. Ingram, M. North, X. Wu, *Green Chem.* 17 (2015) 1966-1987.

[6] B. H. Xu, J. Q. Wang, J. Sun, Y. Huang, J. P. Zhang, X. P. Zhang, S. J. Zhang, *Green Chem.*, 17 (2015) 108-122.

[7] X. L. Meng, Y. Nie, J. Sun, W. G. Cheng, J. Q. Wang, H. Y. He, S. J. Zhang, *Green Chem.* 16 (2014) 2771-2778.

[8] X. L. Meng, H. Y. He, Y. Nie, X. P. Zhang, S. J. Zhang, J. J. Wang, ACS Sustainable Chem. Eng., 5 (2017) 3081–3086

Frederico Montes

Phone: +45 4525 6194

E-mail: fmon@kt.dtu.dk

Supervisors: Gürkan Sin

    Krist Gernaey

PhD Study

Started: April 2016

To be completed: April 2019

Radial Basis Function control strategy for cooling crystallization processes

Abstract

Pharmaceutical industry faces several challenges and barriers when implementing new or improving current pharmaceutical processes. Moving faster from the laboratory scale to industrial production can be a profitable strategy, but brings many uncertainty to the upstream processes. The objective of this work is to develop and validate control strategies that rely only on online measurements and data, while optimizing and exploring the whole spectrum f possible outcomes. To this end, a Radial Basis Function strategy has been applied to a two dimensional cooling crystallization population balance model in order to control and stabilize the uncertainties and process disturbances coming from the upstream synthesis.

Introduction

For traditional pharmaceutical industry, separation processes and strict time schedules are two common discussed topics. The former topic usually takes place in the form of batch units, mainly composed by distillations, filtrations and crystallizations amongst others. These operations are rather complex, expensive, and generate waste (such as solvents). Moreover, some of these steps might propagate deviations/disturbances for the next consecutive process unit, commonly referred as uncertainty in the process variables. New strategies are needed to the process understanding and drug development, such as the as the usage of principles of chemistry, engineering, material science, and quality control [1]. In addition, as encouraged by the U.S. Food and Drugs Administration (FDA), the use of Process Analytical Technology (PAT)tools to certify and control the end product quality and requirements is of major importance for the whole process risk assessment. This leads to a necessity of implementing fast, reliable and easy to use control strategies and online monitoring, that takes into account or counters previous uncertainty. This is especially important when moving from lab-scale to mini-plant or pilot-plant, where time schedules are tight, and every day before a patent expiration is important, and valuable.

For this purpose, a control-strategy based on Radial Basis Functions Networks [2] is applied to a population balance Ibuprofen crystallization unit. This cooling crystallization operates in discontinuous mode, and the modelling parameters are adapted from available

literature. The model construction and simulation is based in a Matlab/Simulink interface (The MathWorks®, Natick, MA), and the outputs are used to simulate the control strategy, that uses a reference trajectory of the mean size crystal to predict and actuate on the temperature profile, over the simulation time. The mean size is predicted using different Radial Basis Functions, evaluating them, and then re-simulate the system, with uncertainty in different parameters.

Specific objectives

The control strategy here presented has an advantage for processes and cases in which the understanding of the process (namely crystallization) is not broad or complete. By having on-line measurements on diverse variables (to be controlled, manipulated, and disturbances) and a desired trajectory (crystal mean size), the RBF NN trains its model with each update and predicts the future behavior of the process. Each radial node can be described as:

(eq.1) $\qquad y(x) = \sum_1^i \lambda_i \Phi(x - x_i) + p(x)$

where λ_I stands for the weight of the network nodes (or weights), $p(x)$ is an optional low order polynomial, and Φ is the radial basis function chosen. These RBF can range from multiple choices, such as binomial, multiquadratic, exponential, and many others. By training the weights, extrapolations and interpolations of the system can be used for predicting and acting on the system.

Case study: Ibuprofen crystallization
Figure 1 shows the uncertainty in the crystal size distribution of Ibuprofen while under upstream deviations (both parameter uncertainty and process deviations) [3-6].
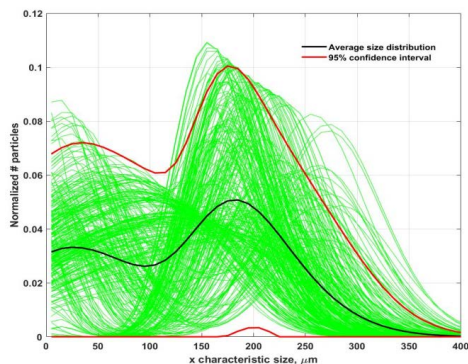

Figure 1: Uncertainty in Ibuprofen crystal size distribution while under upstream deviations, after 5 hours of crystallization.

Using the trajectory followed by the initial seed, the target size was set to be $240\mu m$, and to follow the same growth [7]. Different strategies can be applied relatively to which strategy to with the training data:

- Golden batch: data from a previous process exists and can be used
- Moving window: amount of data used to train the RBF is limited, and earlier dynamic points are being replaced for earlier ones
- Growing window: Training data constantly grows, no data is erased.

For the case of Golden batch, figure 2 shows the final uncertainty in both closed and open loop crystallizations. The average final crystal mean size is of $238\mu m$.

Table 1: Open and closed loop mean and deviation

Case	Mean size (μm)	Deviation (μm)
Open loop	238.7	7.4
Closed loop	240.3	1.4

The uncertainty is, overall, almost nullified, as the RBF is able to correlate and create its own neural network as the process evolves.
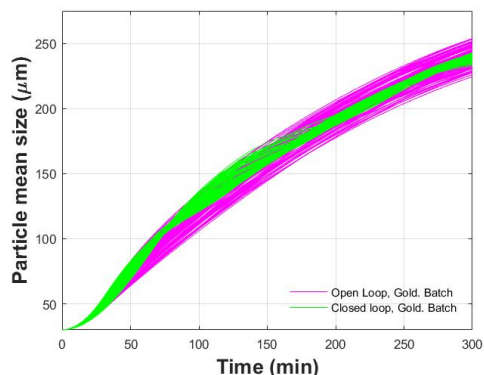
Figure 2: Time evolution of the crystal mean size uncertainty for closed and open loop, with Golden Batch strategy.

Conclusion – Upcoming work
The use of RBF strategy produced its first promising results. Although secondary nucleation is not avoided (and not presented here), the solution for such problem will be attempted with a secondary source of RBF neural networks, that tracks the nucleation of the system whit online measurements.

References
1. M. S. Escotet-Espinoza, R. Singh, M. Sen, T. O'Connor, et al., 2015, Pharmaceutical Technology, 39, Issue 4.

2. M. Orr, 1996, Introduction to Radial Basis Function Networks, Centre for Cognitive Science.

3. A. Rashid, E. White, I. Marziano et al., 2010,Proc chemeca, Adelaide, paper 377

4. A. Rashid, E. White, I. Marziano et al., 2011, Proc chemeca, Sydney, paper 107

5. F. Montes, K. Gernaey, G. Sin, 2017,ESCAPE 27, Barcelona,

6. F. Montes, K. Gernaey, G. Sin, 2018,PSE, San Diego

7. F. Montes, K. Gernaey, G. Sin, 2018, I&CE, 57(30), pg. 10026-10037

Gisela Nadal Rey

Phone: +45 4525 2993

E-mail: gnre@kt.dtu.dk

Supervisors: Krist V. Gernaey
Sjef Cornelissen, Novozymes A/S

PhD Study
Started: March 2017
To be completed: February 2020

Systematic scale-down approach for bioprocesses

Abstract

Scale-down simulators are great tools to study the behavior of microorganisms under heterogeneous conditions. Nevertheless, their design can be rather challenging since there are not clear guidelines to define their operational settings. Thus, we have defined a systematic scale-down strategy that combines both fluid dynamic and microbial kinetic models to achieve more realistic designs of scale-down experiments. This approach consists of three steps, starting with the performance of computational fluid dynamics (CFD) simulations to obtain detailed information of the reactor environment. This is followed by the compartmentalization of this environment, which is done by identifying zones with a certain homogeneity. Finally, experimental constraints are taken into account and a multi-compartment system is set up. In this contribution, our systematic scale-down strategy is thoroughly explained and applied to an industrial case study, the fed-batch aerobic fermentation process of baker's yeast.

Introduction

It is well known that gradients in reactor conditions occur when increasing scale in bioprocesses, due limitations in the mixing and the mass transfer capabilities of the systems. These heterogeneities can lead to the occurrence of the so-called scale-up issues, which yield to reduced productivity, product titer and quality [1,2]. The reason is that the organism does not perform at the operational settings but at suboptimal conditions, since cell performance strongly depends on the environment. Thus, understanding the cell mechanisms consequence of the presence of gradients is needed if we want to improve the process and its scale-up.

If we want to study the physiology of microorganisms under gradient-like conditions, we need to use scale-down simulators. These are lab-scale setups that can resemble full-scale conditions [3]. Although these systems are already used for strain characterization, their design is still a challenge. There are no clear guidelines to establish important operational parameters such as the volume ration between tanks, recirculation rate, pulse-feeding rate, etc. Seeing that, we decided to develop a systematic scale-down approach for bioprocesses.

The scale-down strategy

The systematic scale-down approach (Figure 1) is model-based in order to capture the on-going phenomena that leads to a certain occurrence and degree of gradients. To this end both fluid dynamic and kinetic models are used to describe the dynamics of the bioprocess environment and the reactions taking place. The best manner to combine such models is by using computational fluid dynamics (CFD). Based on these CFD results, we can identify homogeneous volumes with respect to a set of specified parameters, such as substrate concentration, pH, etc. Then, we obtain a compartment map, which is a collection of ideal-mixed compartments with such volumes, connections and flows between them that are able to represent the operation of a large-scale reactor. Finally, by considering experimental constraints, we should be able to design and operate the scale-down experiment.
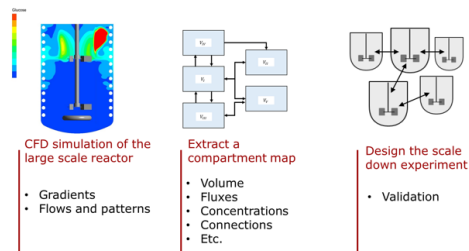

Figure 1: Systematic strategy to scale-down bioprocesses.

Case study: *Saccharomyces cerevisiae* **fed-batch fermentation process (100 m^3)**

Two-phase (liquid and gas) computational fluid dynamics (CFD) simulations were performed in a 100 m^3 reactor. The fermenter contains cooling coils, baffles and the agitation is performed with 4 Rushton turbines. Glucose was fed on top of the reactor to simulate the fed-batch operation. Furthermore, air was sparged in the bottom. The CFD model was extended with a microbial kinetic model from literature [4-6] for *S. cerevisiae* (Figure 2). It considers the presence of three different metabolic regimes (aerobic, overflow and oxygen-limited) depending on the glucose and oxygen concentrations and establishes critical concentrations of these substrates for the instant switch between regimes. Growth follows Monod kinetics and stoichiometry is used to determine glucose and oxygen uptake rates. Kinetic constants and yield coefficients might differ between regimes.
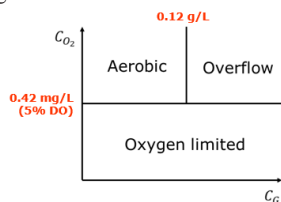

Figure 2: Metabolic regimes of the kinetic model for *S. cerevisiae*, depending on the glucose and oxygen concentrations. The critical concentrations of these substrates are included in red.

After performing the CFD simulations, we observed that both glucose and oxygen shifts occurred, meaning that significant gradients for glucose and oxygen are likely to happen under these conditions. We used this information to build the glucose- and oxygen- based compartment maps, where the critical switch concentrations were used as boundaries. These were further overlapped, resulting in a three-compartment map (Figure 3) in which each compartment corresponds to one different metabolic regime. From the compartment map, information regarding the operational conditions of the scale-down system such as volumes, flow rates, concentrations and connections between compartments was extracted. Then, by applying the adequate experimental constraints, the scale-down design was built. This consists of a three-reactor setup with a different metabolic regime in each reactor. The reactors have different working volumes and recirculation flows, as seen in Figure 3.

Finally, there are several experimental restrictions to be taken into account. On the one hand, it is important to consider which are the possible maximum pumping rates and minimum volume ratios. On the other hand, we might encounter challenges regarding process control, since working with several tanks at different process conditions that are connected between them might not be trivial.
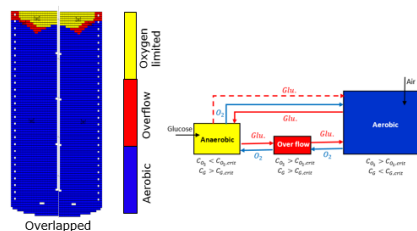
Figure 3: On the left, overlapped compartment map of glucose- and oxygen-based compartment maps, with three compartments that correspond to the different metabolic regimes. On the right, scheme of the scale-down system which would result from the compartment map.

Conclusions

The main outcome of this work is the introduction of a systematic scale-down approach to study gradients in bioprocesses. Furthermore, this work evidences the need to understand the connection between fluid dynamics and microbial kinetics to design more representative scale-down models. To this end, we conclude that computational-based approaches that combine both models can aid to do that.

References

1. F. Bylund, E. Collet, S.O. Enfors, G. Larsson, Bioprocess Eng. 18(3) (1998) 171-180
2. G. Larsson, M. Törnkvist, E. Ståhl Wernersson, C. Trägårdh, H. Noorman, S.O. Enfors, Bioprocess Eng. 14(6) (1996) 281-289
3. P. Neubauer, S. Junne, Curr Opin Biotechnol 21(1) (2010) 114-121
4. R.A. Weusthuis, W. Visser, J.T. Pronk, W.A. Scheffers, J.P. Van Dijken, Microbiology 140(4) (1994) 703-715
5. C. Verduyn, E. Postma, W.A. Scheffers, J.P. Van Dijhken, J Gen Microbiol 136(3) (1990) 395-403
6. E. Postma, W.A. Scheffers, J.P. Van Dijken, Yeast 5(3) (1989) 159-165

Kasper Rode Nielsen

Phone: +45 2552 9479

E-mail: karon@kt.dtu.dk

Supervisors: Jakob Munkholt Christensen
Anker Degn Jensen
Poul Erik Højlund Nielsen, Haldor
Topsøe A/S

PhD Study
Started: September 2018
To be completed: August 2021

Novel Catalysts and Reaction Pathways to Complex Nitrile Molecules

Abstract

Nitriles are used in many different industries both as solvents, feedstock for the synthesis of other compounds and monomers in various polymers. Three important nitriles are hydrogen cyanide (HCN), acetonitrile (CH_3CN, ACN), and acrylonitrile (CH_2=CHCN, AN) and this project focuses on developing new processes for producing these chemicals. It was found recently that bimetallic carbides and nitrides could be suitable catalysts for the synthesis of nitriles. This project explores how these catalysts can be improved to ensure a viable conversion to nitriles with single-carbon molecules and simple nitrogen containing molecules as starting points.

Introduction

The production of acrylonitrile (CH_2=CHCN, AN) is one of the world's most important processes in terms of scale and energy consumption. The annual production has surpassed 6 million tons [1] with the main purpose of using it in polymers such as ABS (acrylonitrile-butadiene-styrene) and SAN (styrene-acrylonitrile). There are many methods of producing it but only a few have or have had industrial importance. Today, most AN comes from the so-called SOHIO process (for Standard Oil of Ohio). This process uses propylene as feedstock for the reaction. However, propylene constitutes approximately 70% of the entire production cost of AN and therefore there is a big incentive towards finding new and cheaper synthesis routes [2]. Furthermore, the supply of propylene is declining and the process for producing it has a high carbon footprint [1,3]. There are thus both potential economic and environmental reasons for changing to a new production method.

The SOHIO process is also special because it produces large amounts of acetonitrile (CH_3CN, ACN) and hydrogen cyanide (HCN) as byproducts. The global supply of these chemicals is thus highly dependent on the demand and production of AN.

If a new catalyst and reaction pathway to AN is developed, there is a need to look into the synthesis of HCN and ACN as well, since these are not necessarily produced as byproducts to a significant extent by the new process. HCN is used as starting material for a wide range of chemicals [4] and ACN is an important solvent [5].

HCN is produced as the main product in a number of processes. Among them is the Andrussow process that uses an expensive platinum catalyst. So also here, there is a potential to find cheaper alternatives to an already existing technology. Considering the fact that HCN is highly toxic, it would be desirable to develop a process that is not dependent on a big centralized production with subsequent need for transportation of the chemical. If a more decentralized process can be developed so that HCN can be made available on-site and on demand, many health risks can be avoided.

Haldor Topsoe A/S (in collaboration with the Technical University of Denmark) has already looked into the syntheses and generated some preliminary results. These studies focus on using single-carbon molecules and simple nitrogen containing compounds as feedstock for the reactions. This means that the process can rely on synthesis gas-derived reactants potentially coming from sustainable sources.

The preliminary experiments explored the use of bi-metallic alloys and their corresponding carbides and nitrides. The results showed that HCN could be synthesized from ammonia and methane [6, 7, 8] but even more interesting, it was found that the catalysts were able to catalyze the formation of a carbon-carbon bond. This was a crucial finding because it forms the foundation for synthesizing ACN as well. Other experiments have shown that this can indeed be accomplished and even with a high selectivity.

The next step is now to develop these catalysts and processes so that the optimum conditions for making HCN and ACN can be found. Subsequently, the formation of an additional carbon-carbon bond needs to

be explored in order to synthesize the important molecule, AN.

Current and Envisaged Production Methods
As described in the introduction, a number of industrial processes are currently running. The most widely used method of producing acrylonitrile is the SOHIO process and the reaction proceeds as in Equation 1 [9].

$$C_3H_6 + NH_3 + 1.5\ O_2 \rightarrow CH_2 = CHCN + 3\ H_2O \quad (1)$$
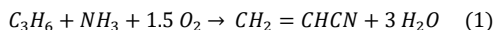
The reaction uses a heterogeneous catalyst with molybdates or antimonates and happens at approximately 400 to 510 °C.

Along with Equation 1, the side reactions are Equation 2 and Equation 3, which produces HCN and ACN, respectively [9].

$$C_3H_6 + 3\ NH_3 + 3\ O_2 \rightarrow 3\ HCN + 6\ H_2O \quad (2)$$

$$C_3H_6 + 1.5\ NH_3 + 1.5\ O_2 \rightarrow 1.5\ CH_3CN + 3\ H_2O \quad (3)$$

HCN is also produced independently through the Andrussow process. This proceeds through Equation 4 [4].

$$CH_4 + NH_3 + 1.5\ O_2 \rightarrow HCN + 3\ H_2O \quad (4)$$

The reactions happens at more than 1000 °C and uses a platinum-ruthenium gauze as catalyst.

This project aims to look into other reactants. This could for example be via methanol (Equation 5, 6 and 7) [8].

$$CH_3OH + NH_3 \rightarrow HCN + H_2O + 2\ H_2 \quad (5)$$

$$2\ CH_3OH + NH_3 \rightarrow CH_3CN + 2\ H_2O + 2\ H_2 \quad (6)$$

$$CH_3OH + CH_3CN \rightarrow CH_2 = CHCN + H_2O + H_2 \quad (7)$$
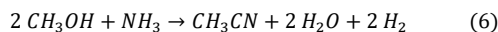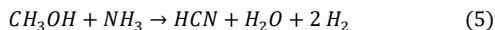
Molecules such as formaldehyde or formamide are also interesting.

Specific Objectives
The objectives for the project are:
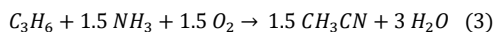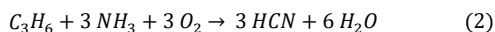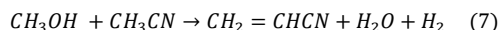- Improvement of the carbide/nitride catalysts in terms of catalytic activity, selectivity and stability.
- Elucidation of the structural and compositional properties that govern the catalytic behavior and gaining insight into the mechanisms of the HCN, ACN, and AN syntheses.
- Development of kinetic expressions for the reactions.
- Economic evaluation of the findings.

Experimental
Most of the experiments will be performed at Haldor Topsoe which has designed a setup dedicated to this project. The reactor is a u-tube quartz reactor with an inner diameter of 4 mm. The reactants will be continuously fed to the reactor and the reactor effluent will be characterized with online gas chromatography.

References
1. D. Cespi, F. Passarini, E. Neri, I. Vassura, L. Ciacci, F. Cavani, J. Clean. Prod. 69 (2014) 17-25.
2. D. Cespi, F. Passarini, F. Cavani, E. Neri, I. Vassura, Chem. Eng. Trans. 36 (2014) 169-174.
3. E. G. Rightor, C. L. Tway, Catal. Today 258 (2015) 226-229.
4. E. Gail, S. Gos, R. Kulzer, J. Lorösch, A. Rubo, M. Sauer, R. Kellens, J. Reddy, N. Steier, W. Hasenpusch, in: B. Elvers (Ed.), Ullmans's Encyclopedia of Industrial Chemistry, Electronic Release, Wiley-VCH, Weinheim, 2011.
5. I. F. Convey, D. Woods, M. Lewis, Q. Gan, P. Nancarrow, Org. Process Res. Dev., 16 (4) (2012) 612-624.
6. B. T. Mckenna, P. E. Højlund Nielsen, US Patent 2017/0246617A1 (2017), to Haldor Topsøe A/S.
7. B. T. Mckenna, P. E. Højlund Nielsen, WO Patent 2016/062551A1 (2016), to Haldor Topsøe A/S.
8. P. E. Højlund Nielsen, R. M. Nielsen, B. K. Olsen, WO Patent 2018/141826A1 (2018), to Haldor Topsøe A/S.
9. J. L. Callahan, Grasselli, E. C. Mihlberger, H. A. Strecker, Ind. Eng. Chem. Prod. Res. Dev., 9 (2) (1970) 134-142.

Niels Dyreborg Nielsen

Phone:	+45 4525 2952
E-mail:	ndni@kt.dtu.dk

Supervisors:	Jakob Munkholt Christensen
	Anker Degn Jensen

PhD Study
Started: November 2017
To be completed: November 2020

Catalytic Methanol Synthesis

Abstract
Methanol synthesis is a large-scale process (80 million tons demand in 2016, 7% annual growth rate), where H_2 and CO_2 react over a $Cu/ZnO/Al_2O_3$ (CZnA) catalyst and form methanol. Despite more than 50 years of research, the origin of CZnA's active sites is still intensely debated. This project aims at elucidating the active sites by focusing on Cu-oxide interactions explained by electron transfer phenomena. The surface coverage of formate (θ_{HCOO}) on Cu-oxide catalysts after methanol synthesis at reaction conditions is quantified by the CO_2 desorption in a subsequent temperature programmed desorption (TPD) experiment. Verification of this method is presented, though some catalysts exhibit significant CO_2 desorption from the oxide component, which calls for further work. The methanol turn-over frequency (TOF: rate per Cu surface atom) is found to increase with θ_{HCOO} for catalysts, where CO_2 desorption is attributed solely to HCOO desorption. This project is part of the Villum Center for the Science of Sustainable Fuels and Chemicals.

Introduction
Several studies investigating Cu-oxide catalysts report linear relations between the Cu specific surface area (m^2 Cu/g_{cat}) and the methanol rate ($g_{MeOH}/g_{cat}/h$) [1+2]. The ratio between methanol rate and Cu surface area is termed TOF, which differs depending on the oxide in the Cu-oxide catalyst. We hypothesize, that electron transfer phenomena can explain this oxide effect on the methanol TOF. Upon contact between an n-type semiconductor (e.g. oxide) and a metal, the Fermi levels of the metal and oxide must align, which causes (high energy) oxide electrons near the interface to transfer to the metal resulting in the formation of a Schottky barrier (Φ_B). This barrier depends on the metal work function and the electron affinity of the oxide and promotes oxide conduction band electrons to flow to the metal. Heating and/or reducing (in e.g. H_2) the oxide can cause removal of oxygen atoms. This creates oxygen vacancies (V_0) and free electrons, which may be trapped in V_0 or move to the lower energy state in the metal [3].
A key reaction intermediate for methanol synthesis is HCOO, which exhibits electron-withdrawing nature [4+5]. Electron donation through Cu to HCOO may therefore promote higher θ_{HCOO}. Consequently, our model predicts, that Cu experiences oxide dependent electron donation or withdrawal, which regulates the

θ_{HCOO} with potential influence on the methanol TOF. A linear relation between methanol TOF and θ_{HCOO} regardless of the oxide is expected, because the oxide effect on the electron donation is incorporated into variations in θ_{HCOO}.
Infrared spectroscopy is applied to identify the CO stretching frequency (v_{CO}) for CO adsorption on Cu, because CO adsorption on metallic Cu yields $v_{CO} < 2100$ cm^{-1}, whereas $v_{CO} > 2100$ cm^{-1} is associated with oxidized Cu (e.g. Cu^+) [6]. Oxide induced electron donation to Cu affects the nature of Cu measurements of v_{CO} for different Cu-oxide catalysts provide knowledge about the electron donation capacity of the catalysts.

Project Objectives
➢ Synthesis of Cu-oxide catalysts

➢ Cu surface area by N_2O-Reactive Frontal Chromatography (RFC) after H_2 reduction

➢ Methanol activity in $H_2/CO/CO_2 = 68/29/3$ at 250°C, 50 bar followed by θ_{HCOO} quantification

➢ Evaluate HCOO desorption temperature using diffusive reflectance IR spectroscopy (DRIFTS)

➢ Determine v_{CO} for CO adsorbed on Cu

- Analyze V_0 formation post H_2 reduction by electron paramagnetic resonance (EPR) and N_2O pulse experiments

Results and Discussion

Presented results address only some of the project objectives, as two more years still remain in the project. Prior to all experiments, the Cu-catalysts are reduced in H_2 to reduce CuO to Cu. H_2 reduction followed by diluted N_2O oxidation is used to determine the Cu surface area, which is applied in the methanol activity experiments to determine the methanol TOF. After measuring the TOF at reaction conditions, the catalysts are rapidly cooled with liquid N_2 to "freeze" the configuration of surface species existing at reaction conditions. After pressure release and He flush, a TPD experiment is conducted to measure the desorption of CO_2, H_2 and CO. Because two adsorbed HCOO molecules desorb as two CO_2 and one H_2 molecule, integration of the H_2 and CO_2 signals during heating should provide θ_{HCOO}. Studies conducting similar IR experiments report HCOO desorption from Cu-HCOO to occur at around 140°C identified by desorption of $\nu_{Cu-HCOO}$ = 1600 and 2850 cm^{-1} [4+7]. Significant H_2 desorption from the oxide necessitates, that the (apparent) θ_{HCOO} is quantified by integration of desorbed CO_2. Figure 1 shows, that Raney Cu and Cu/ZnO catalysts, which yield relatively sharp CO_2 desorption profiles at the characteristic desorption temperature for HCOO, indicate a relation between the apparent θ_{HCOO} and the TOF, but for the remaining catalysts a higher than expected θ_{HCOO} ($\Delta\theta_{HCOO}$) is measured. CO_2 desorbed from oxide(s) and other surface species may explain $\Delta\theta_{HCOO}$. Future experiments measuring the Cu surface area with and without HCOO are designed to determine the true θ_{HCOO} on catalysts incl. Cu/Al$_2$O$_3$ and Cu/SiO$_2$.
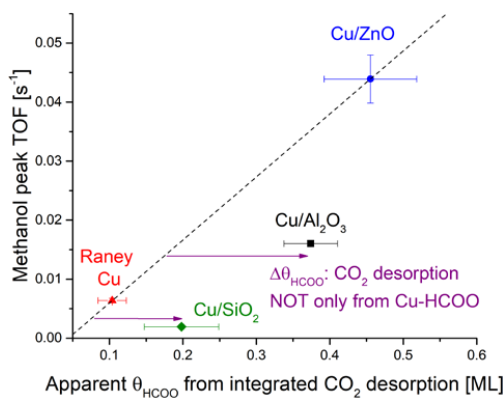
Figure 1: Methanol TOF (250°C, 50 bar in syngas) as function of integrated CO_2 signal post reaction.

Validation of the quantitative method, where CO_2 and HCOO desorption are related, is provided by DRIFTS.

After synthesizing formate at atmospheric pressure in syngas at around 100°C, the catalysts are cooled and flushed with He before performing a TPD experiment. Figure 2 shows, how the relative intensity (I/I_0) of $\nu_{Cu-HCOO}$ (blue and red curves) and the CO_2 signal (green curve) vary with temperature upon heating the partially HCOO covered surface. Concurrent desorption of CO_2 and HCOO (decreasing $\nu_{Cu-HCOO}$) in the temperature range characteristic for HCOO desorption from Cu validates the applied method to quantify θ_{HCOO}.
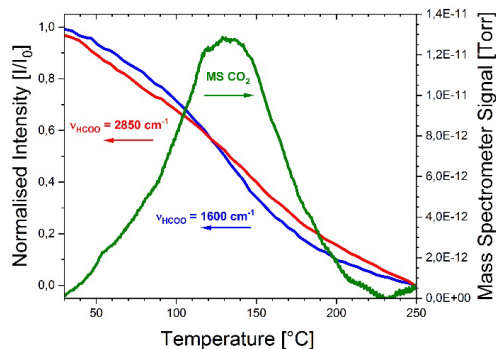
Figure 2: Combined MS and DRIFTS during TPD on a partially covered HCOO surface show concurrent CO_2 and HCOO desorption (decreasing $\nu_{Cu-HCOO}$).

Conclusion

θ_{HCOO} is quantified by CO_2 desorption after forming HCOO at reactions conditions. Future experiments are required to distinguish between CO_2 originating from HCOO desorption and CO_2 from other surface species. Further work will evaluate the Cu-CO interaction by EPR, N_2O pulse and infrared spectroscopy experiments. The aim of these studies is to quantify the concentration of V_0 and determine ν_{CO} for different Cu-oxide catalysts to analyse the suggested electron transfer model accounting for the oxide effect on the methanol TOF.

Acknowledgements

References

1. C. Baltes et al., J. Cat. 258 (2) (2008) 334-344
2. M. Kurtz et al., Cat. Lett. 86 (1-3) (2003) 77-80
3. M. Allen et al., App. Phys. Lett 92 (12) (2008) 1-4
4. S. Neophytides et al., App. Cat., 86 (1992) 45-64
5. L. Dubois, et al. Chem. Phys. Lett. 120 (6) (1985) 537-541
6. N. Topsøe et al., J. Mol. Cat., 144 (1999) 95-105
7. D. Clarke et al. J. Cat. 154 (2) (1995) 314-328

Rasmus Fjordbak Nielsen

Phone: +45 45 25 29 10
E-mail: rfjoni@kt.dtu.dk

Supervisors: Krist V. Gernaey
                 Seyed Soheil Mansouri

PhD Study
  Started: September 2018
  To be completed: August 2021

Novel Strategies for Control and Monitoring of Bio-Processes using Advanced Image-Analysis

Abstract

This project aims to facilitate the use of real-time imaging in bioprocesses, by generating a framework for utilizing images in generic particle processes, targeting monitoring and control. The framework will be model-based, and will include three stages: model creation, model verification including model uncertainty and model predictive control, all based on data obtained by the means advanced image-analysis.

Introduction

During the past two decades, bioprocesses have become an increasingly important part of many food, chemical and pharmaceutical industries. This has had an impact on both upstream and downstream processing, where fermentation, flocculation and crystallization have become often-occurring means for separation and purification of products. A common denominator for these processes is that they all contain particles in some form, whether it is cells, aggregates or crystals.

Process optimization in mainstream chemical engineering has been under development and used for more than half a century whereas the application in bioprocess has been somewhat lacking behind. The reasons for this are many, but mainly origins in the lack of process understanding.

Thus, today's operation of bioprocesses is typically based on heuristics, using a range of sensors that primarily origins from classical chemical engineering. Here, the focus has been mainly on measuring liquid and gas phase properties, and not on solid/particle properties. As the particles play a big role in these types of systems, this has led to difficulties in obtaining constant product qualities in production.

To accommodate this, FDA has stressed the need for more control of Critical Quality Attributes (CQA), by the introduction of a regulatory framework of Process Analytical Technology (PAT) back in 2004 [1]. Here they suggested that this could be obtained by using additional real-time process sensors (both physical and soft-sensors), but also by the use of model based control [2].

At the same time, there has been significant advances within the application of image-analysis. With the increased computational power and developments in image acquisition hardware, it is now possible to capture high-resolution images and carry out fast image analysis in real-time. This technology is relatively cheap, and commonly used in many everyday use products, including face-recognition, Optical Character Recognition (OCR) and many more.

With the increasing maturity of this technology and its availability, there is a significant opportunity for using this in monitoring particles in bioprocesses, where it may form a cheap measuring technique that can provide with better insights of various processes. Here, particle properties like size, surface structure, shape, opacity etc. can be measured in real-time, by the means of only a single process sensor. To date, very limited research has been carried out on the use of image-analysis in monitoring and control of bioprocesses and has been very case-specific[3].

Specific Objectives

This project aims to facilitate industrial implementation of image based monitoring and control. A generic model-based framework will be generated, that will consist of three stages: modeling, model verification and implementation of control structure. In the modelling phase, a process-model is built based on features obtained from an advanced image-analysis. In the model verification, the predictive features of the process model are verified, where the process model uncertainties can estimated. Lastly, based on the built process model, a model-predictive control approach is to be suggested.
The framework will be tested through a range of case studies to show the applicability of this framework and to present its strengths and weaknesses.

Result and Discussion

The suggested framework is based on population balance modelling, and consists of a range of modules, that can be used to estimate the rates of different phenomena like particle birth, particle growth, agglomeration and particle breakage. The outline of the framework can be seen in Figure 1.
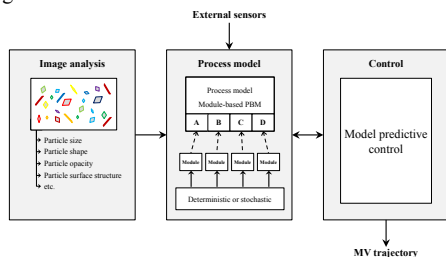

Figure 1: Outline of suggested modelling and control framework.

Each of these modules can either be white-box models, taking into account specific particle properties that can be measured by the means of image-analysis, or black-box models like random forest, neural networks etc.

The presented framework was used for modelling of the crystallization of lactose, where images were taken continuously of the crystallization broth every 3-4 minutes. An example of the segmented microscopy image, of the forming lactose crystals can be seen in Figure 2.
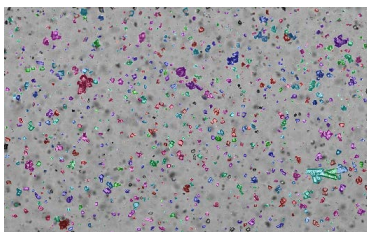

Figure 2: Segmented microscopy image of lactose crystallizing from a pure lactose solution.

The dimensions of the particles in each image were obtained by image analysis algorithms, and divided into 40 linearly distributed size-bins based on the mean Feret diameter, ranging from 25µm to 250µm.

These data were used to fit to a generic population balance model, with three modules to explain the following phenomena: primary nucleation, secondary nucleation and crystal growth. All of these modules were in this case study white box models, with a range of kinetic parameters to be fitted to the experimental data. The fitted model, compared to the experimental data can be seen in Figure 3.
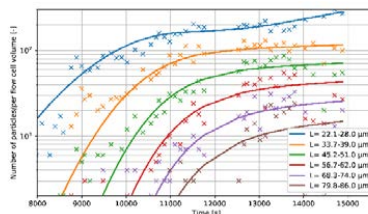
Figure 3: Calibrated crystallization model vs fitted data.

Furthermore, the predictive features of the calibrated model were verified by comparing the model prediction to a second experiment. The model prediction and the measured data for the verification experiment can be seen in Figure 4.
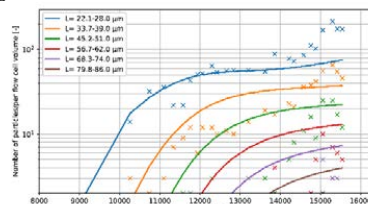
Figure 4: Verification experiment data vs model prediction.

From Figure 4, it can be seen that the generated model is fitting good with the measured data, which means that the model is in fact predictive. The nucleation rate is however not entirely precisely predicted, and it may therefore be worth looking into correlating this phenomenon to more particle properties that can be obtained from the image analysis.

Conclusions

Based on initial studies of lactose crystallization, it has been shown possible to model particle processes with an good precision, by the means of particle properties that can be extracted from advanced image analysis. It has furthermore been shown that the generated model is predictive to a certain extent. For future work, it will be examined whether extra measured particle parameters, can be used in the rate-estimations, using black box modelling.

Acknowledgements

References

1. FDA, Guidance for Industry PAT: A Framework for Innovative Pharmaceutical Development, Manufacuring, and Quality Assurance, 2004
2. J. Glassey, K. Gernaey, C. Clemens, T. Schulz, R. Oliveira, G. Striedner, C. Mandenius, Biotechnol. J. 6 (4) (2011) 369-377.
3. Á. Borsos, B. Szilágyi, P. Ş. Agachi, Z. Nagy, Org. Process Res. Dev. 21 (4) 511-519, 2017

Elisa Ogliani

Phone: +45 91485400
E-mail: eliogl@kt.dtu.dk

Supervisors: Anne Ladegaard Skov
     Liyun Yu
     Piotr Mazurek

PhD Study
     Started: January 2017
     To be completed: December 2019

Designing Reliable Silicone Elastomers for High Temperature Applications

Abstract

In this work, the thermal degradation mechanisms of silicone elastomers are investigated, with a strong focus on the role of network reactant stoichiometry in the thermal degradation behavior. Consequently, silicone elastomers with different stoichiometric ratios were synthesized to vary the relative fractions of elastic, dangling and sol structures. Thermogravimetric analysis (TGA) was performed to investigate the thermal degradation behavior and thermal degradation products of the silicone elastomers synthetized with different cross-linking densities.

Introduction

Silicone elastomers find application in fields ranging, for instance, from soft robotics and electronic skin, to the automotive and the aerospace industries. In addition, the high dissociation energy and the low energy barrier to rotation of the siloxane bond make silicone elastomers suitable for high temperature applications [1, 2]. Reliability and durability are strict requirements for silicone elastomers employed in high temperature applications, and significant effort has been invested by the industrial and the scientific communities into improving their thermal stability. Exploiting traditional methods, such as adding heat-resistant fillers or chemical modifications, still suffer from remarkable shortcomings. Therefore, developing cheap and easy solutions to improve thermal stability of silicone elastomer is a major challenge. This study focuses on determining the role of network structure on the thermal degradation of silicone elastomers [3]. Here, we demonstrate how to optimize the stoichiometric ratio used to prepare silicone elastomers in order to enhance their thermal stability by simple means.

Materials

Silicone elastomers were synthesized via a hydrosilylation reaction (Fig. 1) between the vinyl-terminated polydimethylsiloxane DMS-V35 (denoted V35, M_w = 52900 g/mol, as determined by SEC) and the hydride-functional crosslinker HMS-301 (f=8, M_w = 1900 g/mol, as determined by NMR and SEC, respectively), catalyzed by platinum (Karstedt's catalyst, 511). Samples were cured in oven at 80°C for 3 days, to ensure the maximum conversion. Three formulations

with different stoichiometric imbalances (molar ratio of hydrosilane groups over vinyl groups, r =1, 1.5, 2) were prepared, in order to obtain silicone networks with different crosslinking densities. Subsequently, unreacted PDMS (sol fraction) was removed from the silicone elastomers by extraction in heptane for 24 hours.
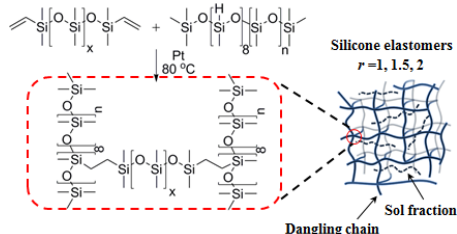
Figure 1: Hydrosilylation reaction used to synthetize the silicone elastomers with different stoichiometric ratios.

Specific Objectives

Firstly, TGA was performed from room temperature to 700°C under a nitrogen atmosphere, to inspect the general thermal degradation behavior of the silicone elastomers, before and after removing the sol fraction by extraction. Subsequently, long-term isothermal treatment (12 hours) of the silicone elastomers was performed, in order to collect and analyze the degradation products and to compare the effect of degradation on networks with different structures. Two reference temperatures were chosen, namely 300 and 400°C. Real-time TG-FTIR (Fourier-transform infrared spectroscopy) was used to detect the released volatile degradation products.

Results and discussion

TGA results indicated an increase in thermal stability induced by the removal of the sol fraction, since the onset of degradation for all the extracted silicone elastomers shifted toward higher temperatures than the corresponding non-extracted elastomers. Differential thermogravimetric analysis (DTG) clearly indicated how the removal of the sol fraction drastically affected the thermal degradation behavior of the samples, which, before extraction, occurred through a two-stage process taking place at different temperatures, depending on the elastomers' stoichiometric imbalances. After extraction, all elastomers degrade thermally via a single-step process occurring in a similar range with a maximum peak temperature of ~500˚C.

Weight loss curves of the non-extracted and extracted elastomers, obtained from the isothermal treatment at 300˚C, are illustrated in Fig. 2. Extracted elastomers showed higher thermal stability than non-extracted elastomers. The non-extracted networks and the linear PDMS (V35) showed the same degradation trend. It can be assumed that long-term thermal treatment at 300˚C of the non-extracted elastomers affects the sol fraction, which is mainly composed of linear PDMS (V35). In contrast, the residual weight of the extracted elastomers recorded after thermal treatment increased from the elastomer with r =1 towards r =1.5 and 2, proving that crosslinking density has a significant beneficial effect on thermal stability. It was also observed that the elastomer with the lowest crosslinking density—and thus the higher amount of dangling chains—degraded faster compared to the elastomers with r = 1.5 and 2. Therefore, for extracted elastomers, thermal degradation by random chain scission involves dangling chains, since the sol fraction is absent.
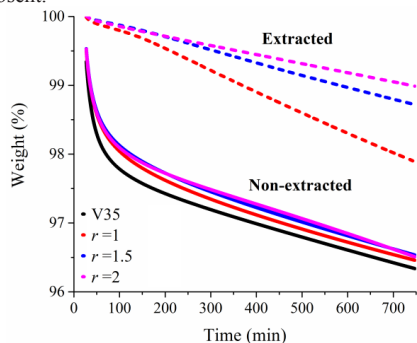
Figure 2: Weight loss curves of linear polymer V35, non-extracted, and extracted silicone elastomers during the isothermal treatment at 300˚C.

Isothermal treatment at 400˚C (Fig. 3) resulted in a considerably high extent of silicone elastomer volatilization. Removing the sol fraction induced an increase in thermal stability for all elastomers, as also observed after thermal treatment at 300˚C. Nevertheless, residual weight decreases from the elastomer with r =1 towards r =1.5 and 2, meaning that highly crosslinked

networks possess lower thermal stability than networks with lower crosslinking density. TG-FTIR data reveals that the extent of volatilization over time increases in line with the increasing stoichiometric ratio of the elastomers.
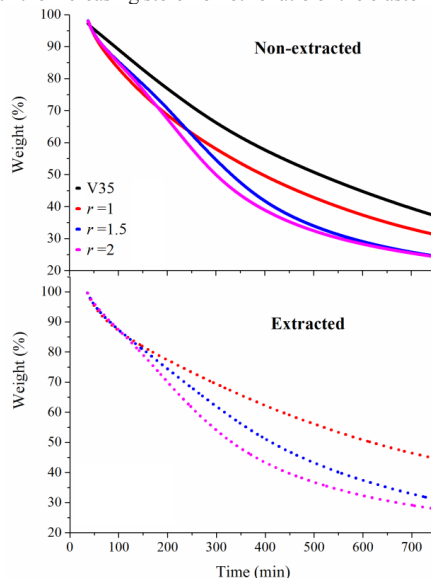
Figure 3: Weight loss curves of linear polymer V35, non-extracted, and extracted silicone elastomers during the isothermal treatment at 400˚C.

Conclusions

In this work, we present a cheap and facile way of boosting the thermal stability of silicone networks that does not involve adding fillers or chemical modification. It is established that the reliability and performance of silicone elastomers used in high-temperature applications are affected strongly by the stoichiometric imbalance used to synthesize the network. Our results prove that an overall improvement in the thermal stability of silicone elastomers can be achieved simply by removing the sol fraction. The results of this work can be used to guide the preparation of robust silicone elastomers for high-temperature applications.

Acknowledgements

References

1. N. S. Tomer, F. Delor-Jestin, L. Frezet, J. Lacoste, Open J. Org. Polym. Mater. 2 (2) (2012) 13-22.
2. J. S. kim, S. Yang, B. S. Bae, Chem. Mater. 22 (11) (2010) 3549-3555.
3. E. Ogliani, L. Yu, P. Mazurek, A. L. Skov, Polym. Degrad. Stab. 157 (2018) 175-180.

Merve Öner

Phone: +45 91849864

E-mail: meon@kt.dtu.dk

Supervisors: Gürkan Sin

Jens Abildskov

Stuart M. Stocks, LEO Pharma A/S

PhD Study

Started: January 2017

To be completed: December 2019

Modeling of a Large-Scale Pharmaceutical Crystallization Process

Abstract

This research project aims to develop a model of a large scale pharmaceutical batch cooling crystallization process via a compartmentalization approach. In this work, computational fluidic dynamics (CFD) is used to study the mixing behavior in the large-scale system. The compartmental volumes, location and flux connections are extracted from CFD data analysis to define the interconnected compartment network. The scaled-up process model containing multiple compartments coupled with crystallization kinetics is implemented and simulated in MATLAB/Simulink. The influence of the fluid dynamics on the simulated process performance in terms of crystal size distribution and final average crystal diameter is investigated.

Introduction

Prediction of the influence of the crystallizer scale on the process behavior and process performance is one of the major challenges in the design of industrial crystallization processes. Fluid dynamic conditions of industrial scale crystallizers are far from well-mixed behavior. This leads to spatial variations of critical crystallization process variables such as temperature, super-saturation, particle concentration, etc. within crystallizer geometry [1]. Consequently, crystallization process models based on the assumption of well-mixed behavior are not representative for a scaled-up process, and therefore not credible for the use in supporting optimal design of industrial crystallizers. Therefore, a more detailed insight into mixing conditions and its consequences for local crystallization phenomena must be taken into account in order to achieve reliable process design and scale-up [2, 3].

Specific Objectives

The main objective of this study is to develop a predictive model of a large scale pharmaceutical batch cooling crystallization process based on a compartmentalization appproach.

Methodology

Compartmental modeling is a reduced-model approach, in which the detailed mixing and the fluid dynamic information obtained from non-reactive CFD simulation is coupled with the process kinetics in a simpler simulation environment [4]. Application of the compartmental modelling requires the division of the large scale crystallizer into a finite number of compartmental volumes, in which minimized or negligible gradients e.g. in temperature, crystal distribution, super-saturation and energy dissipation exist. To determine the compartmental zones within the volume of pilot-scale crystallizer equipment, primarily the mixing is studied by means of CFD simulations. The results of CFD simulations are processed through both a manual or automatic zoning technique in order to identify the compartments [5]. In both zoning approaches, three components of the average flow velocity in 3D space are chosen as base criterion, since the mixing in the system significantly is linked to the velocity fields. The compartmental volumes, location and flux connections are extracted from data analysis to be used as input in the compartment model simulation together with crystallization the kinetics.

Seeded-batch cooling crystallization of paracetamol (active pharmaceutical ingredient – API) from ethanol (solvent) [6, 7] is chosen as a case study in this work. In the model, a linear cooling with a cooling rate of 0.4 ºC/min is applied to the initial solution, which has an initial concentration of 0.2617 kg paracetamol / kg ethanol and an initial temperature of 40 ºC, for 50 min. The liquid volume in the crystallizer is 218 L and impeller stirrer speed is 100 rpm. The obtained compartmental map form data analysis is shown in Figure 1. The crystallization process modelling based on
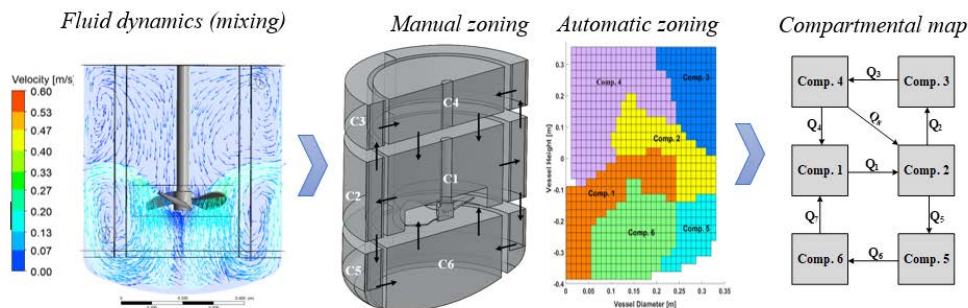
Figure 1: Fluid mixing and identification of compartmental zone map.

compartmental approach is implemented in MATLAB/Simulink, where every individual compartments are modelled as Mixed Suspension and Mixed Product Removal (MSMPR) crystallizer (Figure 2).
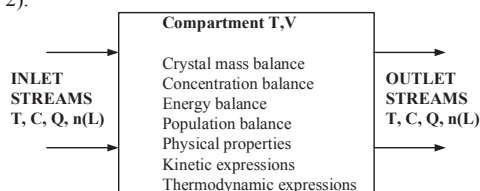
Figure 2: Single compartmental model [8].

Results and Discussions

The performance of the pharmaceutical batch cooling crystallization process has been analyzed using both compartmentalization approaches in terms of crystal size distribution (Figure 3) and time evolution of the primary and secondary nucleation rates (Figure 4). The results reveal that nucleation rates based on both approaches show a relatively small deviation between the predicted rates, which does not have a big impact on the obtained final crystal size distribution. It can be concluded that predictions based both zoning approaches are in accordance with each other. Besides, this approach provides a unique opportunity to study the effects of non-
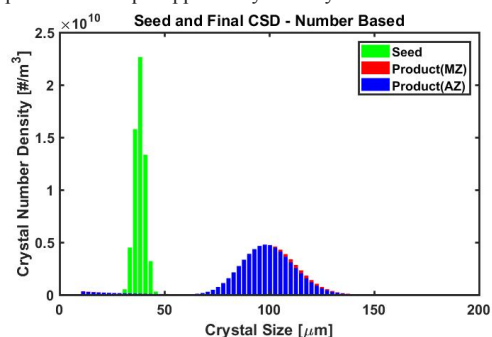
Figure 3: Final crystal size distribution in multi-compartment model.

homogeneous mixing on the process performance in many other applications as well *e.g.* process control and sensitivity analysis.
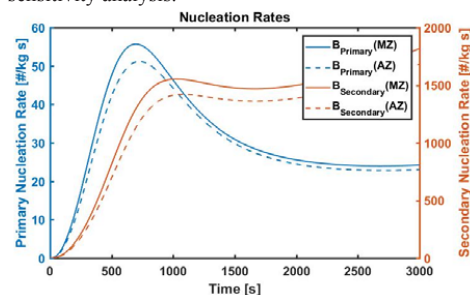
Figure 4. Primary and secondary nucleation rate change over time.

References

1. H.J.M. Kramer, S.K. Bermingham and G.M. van Rosmalen, *Journal of Crystal Growth,* 198/199 (1999) 729-737.
2. H.J.M Kramer, J.W Dijkstra, P.J.T Verheijen, and G.M van Rosmalen, *Powder Technology*, 108 (2-3) (2000) 185-191.
3. D. Green. *Handbook of Industrial Crystallization,* Butterworth-Heinemann, 2002, p. 181-199.
4. G.J. Wells and W.H. Ray, 2005, Methodology for modeling detailed imperfect mixing in complex reactors. *AIChE Journal*, 51:1508-1520.
5. F. Bezzo, S. Macchietto and C.C. Pantelides, *Computers & Chemical Engineering*, 28 (2004) 501-511.
6. C. Fernandes. Effect of nature of the solvent on the crystallization of paracetamol, accepted for 14th *International Symposium on Industrial Crystallization* (*ISIC 14*), 1999.
7. N.A. Mitchell (2013), Numerical Modeling of Cooling Crystallisation. PhD thesis.
8. E. Kougoulos, A.G. Jones and M. Wood-Kaczmar*, Chem. Eng. Comm.,* 193 (2006) 1008-1023.

Jyoti Shanker Pandey

Phone: +45 9194 2357
E-mail: jyshp@kt.dtu.dk

Supervisors: Nicolas von Solms
                  Alexander Shapiro
                  Niels Lindeloff, Total Denmark

PhD Study
  Started: July 2018
  To be completed: June 2021

Carbon Neutral Energy Production by Hydrate Swapping

Abstract

Gas hydrates are traditionally studied and seen as a problem in subsea oil and gas with the potential to block and damage flow lines. However vast amount of methane-rich gas hydrate reserves, discovered in permafrost and deep ocean sediments, are started to be considered as a source of cleaner energy and alternative to fossil fuels. Presently, Methane production from such deposits is considered technically challenging and commercial unattractive due to high-cost factor and risk of hydrate destruction. Recently, hydrate swapping is proposed as a potential method to recover methane from hydrate deposits. This method is a carbon neutral method as it produces Methane and stores carbon dioxide in hydrates at the same time without destabilizing the hydrates. This method is less understood and many unknowns yet to be studied. In this Ph.D. project, we propose to conduct different sets of experiments to investigate the kinetics as well as study the mechanism behind hydrate swapping.

Introduction

Natural gas hydrates occur abundantly in permafrost regions and deep oceans sediments. Known methods to produce methane gas from gas hydrates deposits are unviable and risky due to possible destruction to hydrates deposits coupled with the catastrophic release of a large amount of methane gas. The idea of this Ph.D. project is to investigate the possibility of methane production with simultaneous storage of CO_2 by injecting carbon dioxide and flue gas. In Swapping process, methane gas is produced from natural gas hydrate by injecting and storing CO_2 without affecting the stability of the solid hydrates. The key driver for hydrate swapping is the difference in the thermodynamic stability of CH_4 and CO_2 hydrates as CO_2 hydrates are more stable than CH_4 hydrates. [1] This stability difference (fugacity/chemical potential difference) means that a spontaneous swapping reaction should occur. A demonstration of the viability of the project will have enormous scientific and societal effects. Safe production of methane gas natural gas from hydrates while also storing CO_2 will address two significant issues of future supply of cleaner energy fuel and mitigating the effect of global warming. Validation of the hypothesis (successful production and storage) would result into increase attention to hydrate deposits as

an energy resource, help to advance the science of gas hydrates and increase industry interest in this area.

Specific Objectives

The project aims to develop a viable and safe method to produce methane gas from naturally occurring reservoirs of gas hydrates by injecting CO_2 or gas mixtures containing CO_2 (such as power plant flue gas) into hydrate reservoirs. Swapping process has many unknown and in this Ph.D. we seek to find answers to questions such as how fast is the process, the recovery rate of methane and storage percentage of CO_2 (kinetics), how stable the hydrates are? (Thermodynamic stability), is there any structural change (spectroscopy), using in-house expertise in core flooding, Imaging and spectroscopy experiments.

This Project will be conducted with the following objective.

- To study the effect of different porous medium properties on CH_4 recovery rates and CO_2 storage potential after swapping.
- To investigate the stability of the hydrate deposits after swapping

- To develop and test different techniques to enhance the swapping mechanism and improve methane recovery

Methodology

To find the answers of unknown connected with the simultaneous production of methane and storage of CO_2, following experimental methodology will be used

- Kinetics of CH4-CO2 swapping will be studied at the core scale level using modified core flooding setup to mimic gas production technique at pressure and temperature similar to gas hydrate deposits followed by swapped gas analysis using gas chromatography. Experiments will be carried out using readily available porous media (such as sandstone) with different properties ([2], [3]). This study will allow us to quantify how much gas can be produced from hydrate deposits in cores and how much CO_2 can be stored and the effect of different properties of cores on the swapping process.

- An essential component of this work will be to assess the thermodynamic stability of the hydrates before and after swapping with CO_2 as well as CO_2 containing flue gas (CO_2+N_2). Additional experiments will be carried out to study the effect of different impurities on stability before and after swapping. These experiments will be performed on a high-pressure micro differential calorimeter ([4] [5]) to obtain heats of dissociation of hydrates before and after swapping at pressure similar to actual conditions.

- The information about structural change happened with in gas hydrate structure during the swapping would be a key to understand swapping mechanism. This would assist in determining both the amount of gas that can be produced (and stored) as well as the stability of the newly formed mixed CH_4+CO_2 hydrate. Available spectroscopy techniques such as NMR will be used to study this process. Information about hydrate structure and cage occupancy will be correlated with stability analysis to explain the swapping mechanism. [6][7][8][9]

References

1. P. J. Herslund, K. Thomsen, J. Abildskov, and N. Von Solms, "Phase equilibrium modeling of gas hydrate systems for CO2capture," J. Chem. Thermodyn., vol. 48, pp. 13–27, 2012.
2. M. Ring, "Production of natural gas from hydrates with and without CO2 capture," no. January, 2014.
3. L. Mu and N. von Solms, "Methane Production and Carbon Capture by Hydrate Swapping," Energy & Fuels, vol. 31, no. 4, pp. 3338–3347, 2017.
4. L. Mu and N. von Solms, "Hydrate thermal dissociation behavior and dissociation enthalpies in methane-carbon dioxide swapping process," J. Chem. Thermodyn., vol. 117, pp. 33–42, 2018.
5. N. Daraboina, C. Malmos, and N. Von Solms, "Investigation of kinetic hydrate inhibition using a high pressure micro differential scanning calorimeter," Energy and Fuels, vol. 27, no. 10, pp. 5779–5786, 2013.
6. Y. Park, M. Cha, J. Cha, K. Shin, and H. Lee, "Swapping carbon dioxide for complex gas hydrate structures," Proc. 6th Int. Conf. Gas Hydrates, no. Icgh, 2008.
7. Y. Zhao, J. Zhao, D. Shi, Z. Feng, W. Liang, and D. Yang, "Micro-CT analysis of structural characteristics of natural gas hydrate in porous media during decomposition," J. Nat. Gas Sci. Eng., vol. 31, pp. 139–148, 2016.
8. K. A. Birkedal, L. P. Hauge, A. Graue, and G. Ersland, "Transport mechanisms for CO2-CH4 exchange and safe CO2 storage in hydrate-bearing sandstone," Energies, vol. 8, no. 5, pp. 4073–4095, 2015.
9. J. M. Schicks, M. Luzi, and B. Beeskow-Strauch, "The conversion process of hydrocarbon hydrates into CO2 hydrates and vice versa: Thermodynamic considerations," J. Phys. Chem. A, vol. 115, no. 46, pp. 13324–13331, 2011.

Tiago Pinto

Phone: +45 4525 5510
E-mail: tiapi@kt.dtu.dk

Supervisors: Krist V. Gernaey
Helena Junicke
Xavier Flores-Alsina

PhD Study
Started: January 2018
To be completed: December 2020

Ecological Control Strategies for Biobutanol Production

Abstract

New national and international policies are pushing for a more sustainable production landscape. Once seen as waste, many resources are now the focus of valorization and recovery. Mixed culture biotechnology is held as a promising solution for producing valuable biofuels and chemicals from such low-value substrates and waste streams. In this context, butanol is a biofuel of particular interest. With an energy density that is higher than ethanol and properties similar to gasoline, it is a qualified substitute for fossil transport fuels. Biobutanol is currently produced by *Clostridia* pure cultures with strict glucose requirement. However, recent reports suggest an alternative production pathway using butyrate and hydrogen as the sole substrates and with an improved environmental balance.

Introduction

Much focus has been given to alternative solutions for petrol-based chemicals and energy over the past decades. This interest arises from the need to achieve a more sustainable and environmental friendly production landscape, reducing our footprint on the planet.

Accounting for nearly 65% of the world´s consumption [1], liquid fossil fuels are the major target of such research. The search for renewable liquid fuels capable of replacing e.g. gasoline and diesel have in many cases focused on biorefinery approaches. Here, different generations of renewable feedstocks have been used but recently, in an effort to go even further, many resources that were once seen as waste are now the focus of valorization and recovery [2].

Bioethanol and biobutanol are the two top contenders for liquid fossil fuel replacement. But of the two, biobutanol is a much more interesting biofuel, with a higher energy density, can be blended with gasoline to any ratio without engine modification, low solubility in water, and higher boiling and flash point making it safer than bioethanol [3].

The most common process for biobutanol production is the Acetone-Butanol-Ethanol (ABE) fermentation (Fig.1) by anaerobic bacteria, mostly belonging to the *Clostridia* family. Although pure cultures of *Clostridium* can achieve high yields, they have strict glucose requirements. In this context, mixed microbial biotechnology is seen as a promising solution over pure strain culture due to its many advantages: non-sterile conditions, mixed and/or waste substrates, ecological selection, and continuous operation processes [4].
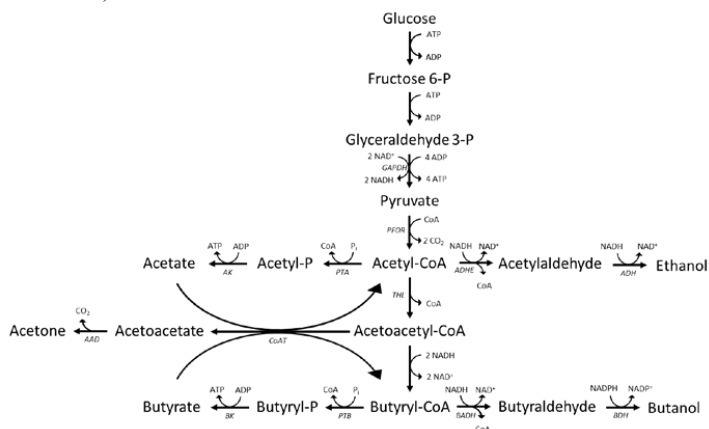

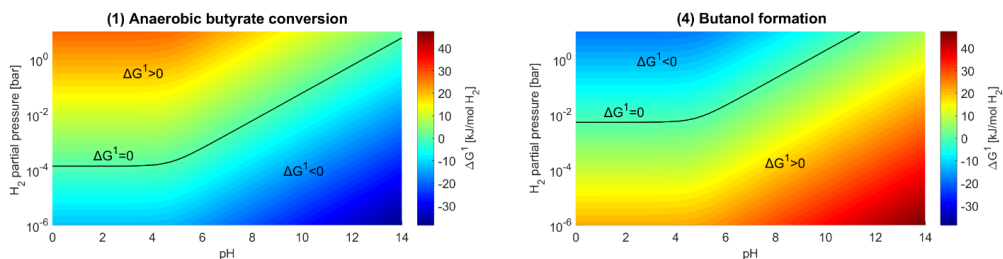**Figure 1** – ABE fermentation pathways in *Clostridium Acetobutylicum*.

Figure 2 – Gibbs free energy for (1) anaerobic butyrate conversion and (4) butanol formation from butyrate.
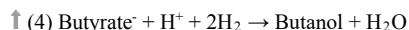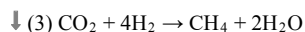
Recent reports [5], [6] lead to suggest an alternative production pathway using butyrate, a previous waste to many industries, and hydrogen as the sole substrates for biobutanol production.

Specific Objectives

The focus of the project is to enrich butanol-producing microorganisms through directed ecological selection in a continuously stirred tank reactor, starting from non-defined methanogenic communities fed on butyrate and hydrogen. By engineering the environment rather than the organism, we move towards the use of low-value feedstock for the production of a valuable chemical such as butanol, as opposed to the use of higher value substrates e.g. glucose, contributing to the progress of circular bioeconomy.

Enrichment Strategy

Operating at high H_2 partial pressure (p_{H_2}) of 1.0 to 1.5 bar, (1) anaerobic butyrate conversion becomes thermodynamically unfavorable (Fig. 2, left), and thus also (2) acetoclastic and (3) hydrogenotrophic methanogenesis, reducing the amount of CH_4 and CO_2 produced as by-products.

(1) Butyrate + $2H_2O \rightarrow 2$ Acetate + H^+ + $2H_2$

(2) Acetate + $H^+ \rightarrow CO_2$ + CH_4

(3) CO_2 + $4H_2 \rightarrow CH_4$ + $2H_2O$

(4) Butyrate$^-$ + H^+ + $2H_2 \rightarrow$ Butanol + H_2O
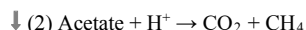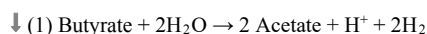
However, only high H_2 partial pressure is not sufficient to promote butyrate reduction to butanol (Fig. 2, right). Butanol formation at pH 7 and p_{H_2} of 1 atm the Gibbs free energy is -6.8 kJ/mol-H_2. As such, by controlling the fermentation at pH 5 we will further inhibit (1) anaerobic butyrate conversion while favoring (4) butanol formation.

Acknowledgements

References

1. Key world energy statistics. Int Energy Agency 2017.
2. S.S. Mansouri, I.A. Udugama, S. Cignitti, A. Mitic, X. Flores-Alsina, K.V. Gernaey, Current Opinion in Chemical Engineering, 18 (2017) 1-9.
3. N. Abdehagh, F. Tezel, J. Thibault, Biomass and Bioenergy, 60 (2014) 222-246.
4. R. Kleerebezem, M.C. van Loosdrecht, Current Opinion in Biotechnology, 18 (3) (2007) 207-212.
5. S.Y. Lee, J.H. Park, S.H. Jang, L.K. Nielsen, J. Kim, K.S. Jung, Biotechnology and Bioengineering, 101 (2) (2008) 209-228.
6. H. Junicke, M.C. van Loosdrecht, R. Kleerebezem, Applied Microbiology and Biotechnology, 100 (2) (2016) 915-925.

Katrin Pontius

Phone: +45 4525 6194
E-mail: kpon@kt.dtu.dk

Supervisors: Anna Eliasson Lantz
Ivan Hundebøl
Krist Gernaey

PhD Study
Started: December 2015
To be completed: January 2019

Auto-sampling and Monitoring of Bioprocesses

Abstract
Fermentations provide a highly demanding environment for reliable, stable and noise-free measurements and the measurements must provide demonstrable benefits without compromising the process. Consequently, fermentation production reactors are normally rather sparsely instrumented and typically only involve standard sensors such as pH, temperature and dissolved oxygen. Furthermore, robust, automatic sampling systems maintaining a sterile barrier and including a sampling preparation unit facilitating real-time analysis by more advanced methods like flow cytometry and NMR are increasingly under development on the market today. In order to allow further optimization of industrial fermentations, this project investigates and evaluates tools for process on-line monitoring devises that will supplement traditional on-line process data. It focuses on spectroscopy and image analysis as rapid and rather uncommonly used techniques acquiring real time fermentation data with respect to two different case studies.

Introduction
The establishment of economically viable processes through increasing product yields and reducing operating cost are one of the primary objectives of industrial bioprocess research and development. Industry is focusing increasingly on the development of more efficient and less time-consuming methods to monitor and control their fermentation processes at optimal conditions. By supplementing the standard monitoring tool-box only including pH, temperature and oxygen sensors with generic, robust and easy to use and apply monitoring devices it is possible to gain profound control regarding productivity and product quality. In order to select among the huge variety of potential on-line monitoring strategies proposed in literature including spectroscopy (IR, NIR, Raman, Fluorescence, NMR), flow-cytometry, image analysis and HPLC, two industrial production processes demonstrating state of the art protein production via recombinant microorganisms are considered as particular cases: a protease production process by *Bacillus* sp. as well as an insulin production process by yeast.

Specific objectives
The two particular case studies under investigation are:

Case study 1: Monitoring of phosphate and ammonium in the fermentation broth of an enzyme production process by *Bacillus* evaluating vibrational spectroscopic techniques (IR, IR, Raman) in combination with partial least-square modelling.

Case study 2: Monitoring of the physiological state of an insulin producing yeast strain combining digital time-lapse microscopy and image analysis.

Case study 1
Phosphates and ammonium are central nutrients in media for Bacillus fermentations and need to be present in relevant levels to promote growth and enzyme production. Besides, there are also major challenges associated with phosphate and ammonium. Both species impose additional costs on downstream wastewater treatment if more is added to the medium than needed by the microorganism during the fermentation. Spectroscopic techniques are increasingly used for the monitoring of fermentation processes due to their ability to monitor a wide array of organic species including biomass, nutrients, metabolites, proteins and cofactors [1-5].

This case study focuses on the determination of phosphate and ammonium concentrations in a *Bacillus* enzyme production process. IR, NIR and Raman spectroscopy in combination with partial least square regression (PLS) are being employed in this work. Finally, the spectroscopic technique leading to the best results regarding both analyst will be selected and developed into an at-line set up for fermentation

monitoring. To minimize the complexity associated with spectroscopic measurements on fermentation broth and decouple natural correlations of parameters, synthetic samples spiked with phosphate or ammonium in addition to real fermentation samples where applied in the model development process. Thereby, regions of IR, NIR and Raman spectra tied to phosphate and ammonium were appropriately identified and selected. Exemplary the spectral region correlated with phosphates in varying concentrations is shown in figure 1.
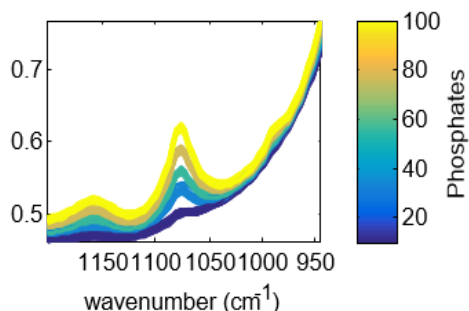

Figur 1: Section of an IR spectrum corresponding to different phosphate concentrations colored from blue (10 mM) to yellow (100 mM).

Case study 2

We want to take advantage of the recent advances in microscopy image analysis and evaluate its potential for on-/ at-line monitoring of yeast morphology during an insulin production process. In yeast cultures, cell size (distribution) has been shown to be correlated with cell viability (dead/alive[6], osmotically stressed[7]) and growth rate[8]. Furthermore, the cell size was recently correlated to the accumulation of an internal product (fatty acids) in microalgae[9]. Consequently, image analysis seems to be a promising tool for getting a snapshot of the physiological state of a yeast culture during a production process.

The lately developed oCelloScope instrument[10] enables rapid imaging and image analysis of a growing yeast culture. An example image with yeast cells identified is presented in figure 2. By analyzing images over the cultivation time we investigate the distribution dynamics of single cells, budding cells and cell aggregates, aiming at correlations between these morphological features and process performance. Reference data sets stating process performance are traditional fermentation data obtained by HPLC measurements (glucose, ethanol, glycerol, acetate, insulin) and off-gas anlysis (CO_2). The method developed in case study two is taken into account to supplement this data set further with information about phosphate and ammonium uptake. We want to develop a real-time monitoring tool that may be used in industrial bioprocess set-ups. Within this approach,

methodologies for automatic distinction between image objects (single cells, budding cells, cell aggregates) are developed and first time trends of the morphology dynamics of an insulin production process have been achieved.
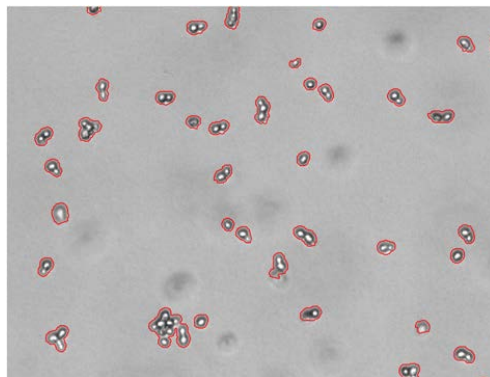
Figur 2: Image of a yeast culture showing with different objects (single cells, budding cells, cell aggregates) identified (red boundaries) by the image analysis software.

References

1 Harry L.T. Lee ,Vibrational Spectroscopy 35: 131–137 (2004)

2 Marose S, Lindemann C, Ulber R and Scheper T, Trends Biotechnol 17: 30–34 (1999).

3 Vaccari G, Dosi E, Campi AL, Gonzalezvara A, Matteuzzi D and Mantovani G, Biotechnol Bioeng 43:913–917 (1994).

4 Boehl D, Solle D, Hitzmann B and Scheper T, J Biotechnol 105:179–188 (2003)

5 Ronnest NP, Stocks SM, Lantz AE and Gernaey KV, J Ind Microbiol Biotechnol 38:1679–1690(2011).

6 Tibayrenc, P., Preziosi-Belloy, L., Roger, J. M. & Ghommidh, C. J. Biotechnol. (2010). doi:10.1016/j.jbiotec.2010.06.019

7 Camisard, V., Brienne, J. P., Baussart, H., Hammann, J. & Suhr, H. Biotechnol. Bioeng. (2002). doi:10.1002/bit.10178

8 Tyson, C. B., Lord, P. G. & Wheals, A. E. Dependency of Size of Saccharomyces cerevisiae Cells on Growth Rate. J. Bacteriol. 138, 92–98 (1979).

9 Marbà-Ardébol, A.-M., Emmerich, J., Neubauer, P. & Junne, S. Process Biochem. 52, 223–232 (2017).

10 Fredborg, M. et al. J. Clin. Microbiol. 51, 2047–2053 (2013).

Carlos Eduardo Ramírez-Castelán

E-mail: cara@kt.dtu.dk

Supervisors: Jakob K. Huusom
                  Anker D. Jensen
                  Angélica Hidalgo-Vivas, Haldor Topsøe
                  Jacob Brix, Haldor Topsøe

PhD Study
  Started: November 2014
  To be completed: February 2019

Optimal Model-based Monitoring of Tubular Reactors

Abstract

Achieving high quality information online is a challenge for a large range of processes in the chemical and biochemical industry. Even if it is possible to implement online sensors on the process, it constitutes a cost which requires the companies to optimize the sensor selection. This is especially true for processes with spatial variations as for the concentration and temperature in tubular reactors. Such processes are examples of nonlinear processes which require that the operator can get information of the nonlinear transient and profile in the system. Real time information of the state of the process is paramount in terms of online optimization through control and for ensuring product quality as well as a safe and reliable process operation.

Introduction

Modern refinery operations cover a wide and complex variety of processes, since the crude stills are the first major processing units, distillation processes are used to separate the crude oils by into fractions according to boiling point so that each of the processing units following will have feedstocks that meet their particular specifications. Higher efficiencies and lower costs are achieved if the crude oil separation is accomplished in two steps: first by fractionating the total crude oil at essentially atmospheric pressure; then by feeding the high-boiling bottoms fraction (topped or atmospheric reduced crude) from the atmospheric still to a second fractionator operated at a high vacuum.

Nevertheless, specific chemical reactions are vital for further refining stages such as hydrotreating, catalytic cracking, hydrocracking, hydroprocessing and hydrodesulfurization; terms that are used rather loosely in the industry because, in the processes hydrodesulfurization and hydrocracking, cracking and desulfurization operations occur simultaneously and it is relative as to which predominates.

Despite that, hydrotreating refers to a relatively mild operation whose primary purpose is either to saturate olefins, reduce the sulfur and nitrogen content of the feed, or both. It refers to a process in which petroleum products are catalytically stabilized and/or objectionable elements are removed from products or feedstocks by reacting them with hydrogen. Stabilization usually involves converting unsaturated hydrocarbons such as olefins and gum-forming unstable diolefins to parafins.

Objectionable elements removed by hydrotreating include sulfur, nitrogen, oxygen, halides, and trace metals. Hydrotreating is applied to a wide range of feedstocks, from naphtha to reduced crude. When the process is employed specifically for sulfur removal it is usually called hydrodesulfurization. Catalytic hydrotreatment is essential to obtain fuels with improved quality and low polluting compounds content (sulfur, nitrogen, aromatics). Catalytic cracking is the most important and widely used refinery process for converting heavy oils into more valuable gasoline and lighter products over 1 million tons/day of oil processed in the world [1].

In the case hydrotreating, and other large scale processes, it is not always possible to directly measure the important state variables online which are needed by the operator to judge if the plant is behaving as planned or not. If these cannot be determined by indirect measurements, then the information can be constructed by means of a state estimator using a process model and the available measurements from the system. Examples of such systems are the spatial concentration and temperature profiles inside tubular reactors, more specifically trickle-bed reactors that play an important role in the overall refinery flow.

Trickle bed reactors

A unique characteristic of trickle-bed reactors compared to other types of three-phase reactors is, in general, the catalyst particle is filled with liquid while the outer surface may not be completely wet or covered by the

flowing liquid which leads to a more direct contact between the gas phase and the catalyst [2].

The operation conditions of trickle-bed reactors are too hostile or fouling for sensors to work. In such cases, the system measurements must be made whether by sampling and lab analysis, which results are issued with significant delay, or using state estimators that may also incorporate information of known disturbances from feed mixture analysis or upstream data. For these reasons, trickle-bed reactors are difficult to operate due to the coupling between transfer phenomena, non-linear kinetics and their distributed nature which can lead to temperature hot spots in the catalytic bed or formation of an undesired compound. In that sense, online information of the current state of the process is important for the operator or any model based control algorithm for process optimization. Especially when a system may be operated close to a process constraint or the operator needs to avoid an unstable region which may lead to run away or undesired reactions.

Given known process inputs the model can predict online what the state of the process is and what the sensors should measure. By comparison between actual and predicted measurements, corrections in the model predictions can be made through a systematic algorithm which utilizes the statistical uncertainty of the measurements. Linear state estimators such as the Kalman filter is in wide-spread use but advanced monitoring of nonlinear process behavior in tubular reactors by nonlinear state estimators could reduce the risk of having a product that does not meet specifications significantly or conditions that reduce the performance of the catalytic bed.

For that reason, if the reaction rate depends on the liquid reactant, the wetting efficiency leads to reduced global reaction rates, on the other hand, if the reaction rate is controlled by the gas phase, the global reaction rate is higher since the resistance to mass transfer in the non-wetted surface is lower than in the covered surface [3]. Figure 1 shows the concept of trickle flow.
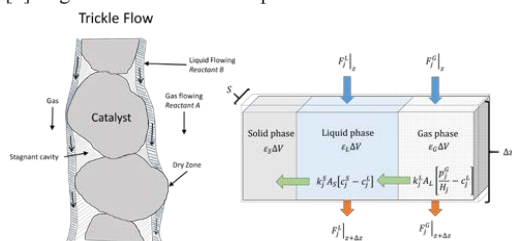

Figure 1: Trickle flow in fixed bed reactors

A model of the trickle-bed reactor is derived from the mass and energy equations according to the law of conservation to a small element of volume. The focus of interest is the nonstationary volume element, fixed in space, through which a fluid and gas are flowing and chemical reactions taking place only in the solid phase. The model of a trickle-bed reactor can be validated with

experimental data [4], and will allow to develop the state estimation of representative real case studies aiming towards the implementation of optimal model-based monitoring.

Current status
The petroleum feedstock contains a complex mixture of hydrocarbon compounds, therefore the phase distribution must be addressed to accurately describe the temperature and concentration profiles in the reactor. The model, solved using a finite differences scheme in MatLab, is able to describe the dynamic concentration and temperature profiles along the reactor. In order to describe the phase change, the simulation of the system is achieved by developing a framework that allows the information exchange between MatLab and ProII. Using the database available from ProII for petroleum streams, the framework consists in a dynamic model of a trickle-bed reactor, solved in Matlab, coupled with a flash calculation carried out in also ProII. This approach reduces the complexity of the numerical solution compared to the solution of a model that considers vaporization of complex petroleum Feedstocks. The objective is to apply this simulation framework to a real large-scale hydrotreating process.

Objectives
The aim of this project is to develop a generic optimal-model based monitoring framework suited for a wide range of tubular reactor applications of industrial relevance but the results may also be extended to other process system with similar characteristics.

References
1. James H. Gary, Glenn E. Handwerk, Mark J. Kaise Petroleum Refining: Technology and Economics, Fifth Edition, 2007.

2. AlDahhan, M. H.; Larachi, F.; Dudukovic, M. P.; Laurent, A. High-Pressure Trickle-Bed Reactors: A Review. Ind. Eng. Chem. Res. 1997, 36 (8), 3292-3314.

3. Herskowitz, M. Trickle-Bed Reactors: A Review. AlChE Journal (Vol. 29, No. 1) January, 1983.

4. Mederos, Fabián. Ancheyta, Jorge. Mathematical modeling and simulation of hydrotreating reactors. Applied Catalysis, 332 (2007) 8-12.

Giulia Ravenni

Phone: +45 93511592

E-mail: grav@kt.dtu.dk

Supervisors: Ulrik B. Henriksen
Jesper Ahrenfeldt
Zsuzsa Sárossy
Benny Gøbel, Ørsted

PhD Study
Started: November 2015
To be completed: December 2018

Upgrading of biomass producer gas by using residual char from gasification

Abstract

This project investigates the recycling of residual gasification char to clean and upgrade biomass producer gas. The performance of gasification char for adsorption and cracking of model tar compounds has been evaluated preliminarily with laboratory tests. Promising results with model tar species (toluene and naphthalene) have led to the design of a char-based gas upgrading unit for the treatment of biomass producer gas with high tar load (25-30 g/Nm^3). The unit was tested on the gas generated by the 100kW$_{th}$ Low Temperature-Circulating Fluid Bed (LT-CFB) gasifier at DTU, Risø. Several successful runs of the gas upgrading unit confirmed the effectivity of residual char as a tar reforming substrate. Future work should be done for optimization and upscaling of the gas upgrading system.
.

Introduction

The Low Temperature-Circulating Fluidized Bed (LT-CFB) gasifier, is a staged process operating at moderate temperature (up to 750˚C). It was conceived to convert a variety of fuels with a high content of low-melting ashes, such as wheat straw and sewage sludge [1]. The drawback of this technology is the quality of producer gas, which has a high tar load (up to 30 g/Nm^3). Improving the gas quality is critical for integrating gasification into the energy system. For example, pure syngas derived from biomass can be used for the synthesis of fossil-free biofuels and bio-chemicals.

The solid residue of gasification, char, is a porous material and a promising support to assist the reforming of tar into combustible gases (H$_2$, CO). The use of residual char from gasification represents at the same time an opportunity to improve the producer gas quality while reusing an inexpensive waste material. The effectivity of char for conversion of tar has been proven by several laboratory-scale studies [2–4]. However, only a few authors have reported the application of char-based gas treatments to actual gasifiers.

The aim of this project was to demonstrate the effectiveness and the feasibility of using residual gasification char in a gas upgrading unit. The char used in this study was produced at DTU in a TwoStage fixed-bed gasifier (also known as "Viking" gasifier) from gasification of wood chips. The specific surface area of this material exceeded 1000 m^2/g, while the pore volume was as high as 0.8 cm^3/g. Inorganic species (mainly Ca, Si, K) were well dispersed on the surface. In addition, the size of particles was suitable for fixed operation (with particles up to 1-2 cm). Thanks to these properties, this char was deemed particularly suitable as a support for reforming of tar.

Specific objectives

Preliminary laboratory experiments have been run in collaboration with the Institute for Energy Technology at Technical University of Berlin. Gasification char from the Viking gasifier was compared with other carbonaceous materials for the adsorption and decomposition of tar model compounds (toluene and naphthalene). The promising performance of gasification char led to the design the char-based gas upgrading unit. The unit was operated with a flow of producer gas extracted from the LT-CFB gasifier. A diagram of the reactor is shown in Figure 1.
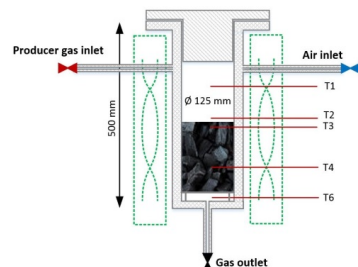

Figure 1: Diagram of the gas upgrading reactor

The residual gasification char used as bed material was collected from the ash container of the TwoStage,

"Viking" gasifier and sieved with a 3.15 mm sieve to remove small particles and powder. The cylindrical reactor contained a grate to support the char bed ($\approx$ 300 g) and had one inlet for the raw producer gas and one inlet for injection of air. The reactor was maintained at 800°C by an electric furnace. The flow of producer gas through the unit was guaranteed by a downstream gas pump, delivering a constant flow of 30 ± 2 l/min. The quality of the producer gas, before and after the passage through the unit, was assessed in terms of tar content and gas composition. Gas composition was monitored with an online gas analyzer (ABB, Denmark), while a Petersen Column was used to quantify the total tar concentration. The performance of the char bed was evaluated in combination with sub-stoichiometric oxidation through air injection. The consumption of the char bed was evaluated in different conditions, to verify the feasibility of this gas treatment method.

Results and discussion

Table 1 presents the gas composition measured on the untreated producer gas (PG) and after two gas upgrading tests. Test A was run with partial oxidation, with air injection above the bed (9.5 l/min). Test B was run without any air addition. Both tests were run for 120 minutes.

Table 1: Average gas composition measured before and after the passage through the gas treatment unit

Gas composition (Vol%)	N_2	O_2	CO_2	CO	CH_4	H_2
PG	61.8	0.15	18.8	11.9	3.1	4.2
Test A	54.8	0.11	14.4	13.3	2.7	14.8
Test B	49.1	0.10	14.7	15.1	5.1	15.9

Test A and test B reduced the tar content in the raw producer gas by 96 and 98%, respectively. Tar conversion resulted in an increased concentration of H_2 in the product gas. In Test B, without air, CH_4 concentration also increased. However, in these conditions the tar concentration in the exit gas was increasing over time, while the quality of the gas composition was declining. The effect was ascribed to the gradual deactivation of the char surface. On the contrary, when air was injected above the char bed, the gas composition at the outlet was stable throughout the test and the tar conversion remained very high. After Test A, the bed had lost about 15% of the original volume. After Test B, the volume of the char bed was unchanged.

Conclusions

Residual char from TwoStage gasification of wood chips was tested for the removal and conversion of tar. Laboratory tests with tar model compounds gave encouraging results. Therefore, a char-based gas upgrading unit was tested on actual producer gas derived from straw gasification in the LT-CFB gasifier at DTU, Risø. Gas analysis and tar measurements before and after the unit showed that the char-based gas treatment is able to significantly reduce the tar load (up to 98%) while increasing the H_2 content of the gas phase. Addition of air was found to assist the removal of tar, but it also decreased the heating value of the gas and it accelerated the consumption of the char bed. However, the synergy between the char bed and partial oxidation appeared to deliver higher and more durable gas quality. Further tests should address the optimization and upscaling possibilities for this gas upgrading concept.

References

[1] Thomsen TP, Hauggaard-Nielsen H, Gøbel B, Stoholm P, Ahrenfeldt J, Henriksen UB, et al. Waste Management 2017;66:145–54.
[2] Klinghoffer NB, Castaldi MJ, Nzihou A. Fuel 2015;157:37–47.
[3] Hervy M, Berhanu S, Weiss-Hortala E, Chesnaud A, Gérente C, Villot A, et al. Fuel 2017;189:88–97.
[4] Abu El-Rub Z, Bramer EA, Brem G. Fuel 2008;87:2243–52.

List of publications

Ravenni G, Sárossy Z, Ahrenfeldt J, Henriksen UB. "Activity of chars and activated carbons for removal and decomposition of tar model compounds – A review". Renewable and Sustainable Energy Reviews, 2018;94:1044–56

Ravenni G. Henriksen U.B., Ahrenfeldt J., Sárossy Z. "Tar Removal from Biomass Producer Gas by Using Biochar". Proceedings of European Biomass Conference (EUBCE) 2017.

Ravenni G., Sárossy Z., Ahrenfeldt J., Henriksen, U.B. "Residual char from gasification integrated in a tar removal system". Proceedings of European Biomass Conference (EUBCE) 2018.

Ravenni G., Elhami H.O., Neubauer Y., Ahrenfeldt J., Henriksen U.B. "Comparison of wood chars from gasification and pyrolysis for adsorption and conversion of tar model compounds". Proceedings of the International conference in Engineering for Waste and Biomass valorization (WasteEng) 2018.

Łukasz Ruszczyński

Phone: +45 4525 2912

E-mail: lrus@kt.dtu.dk

Supervisors: Jens Abildskov

                    Gürkan Sin

                    Alexandr Zubov

PhD Study
  Started: May 2016
  To be completed: April 2019

Thermodynamic modelling and data evaluation for life sciences applications

Abstract

In the case of available experimental data for the systems containing biomolecules, there is a strong need for reliable data as well as for validation of their consistency. It has been shown that for solid- and liquid-liquid equilibria data, validation using fluctuation solution theory (FST) could be applied. Substantial part of work is devoted to the development of the methodology for data validation, which includes development of the correlation models, production of initial guesses for parameter estimation and evaluation of the model parameters, including their uncertainty as well as criteria for discrimination among reliable and questionable data. We have reported steps for validating binary and ternary LLE.

Introduction

The knowledge of reliable thermodynamic properties of multicomponent systems is of the central importance in chemical engineering. Solid- and liquid−liquid equilibria (SLE and LLE, respectively) are important thermodynamic phenomena in a wide range of downstream separations and formulated products. Hence, over past decades much research has led to useful thermodynamic models for prediction of properties from limited data. However, most models require determination of a number of physical properties and several model parameters, compared to the available data. Moreover, the measured values are often uncertain and many measurements are required to build reliable data sets for parameter identification. Lack of interaction parameters between biomolecules (such as drugs) and solvents, as required in group contribution methods, makes the conductor-like screening (COSMO)-based activity coefficient models [1, 2] attractive. Predictions can be made prior to as well as in the absence of experimental data, which renders this class of models fully predictive. Although and because many relevant data are published, there is a strong need for reliable data as well as their evaluation [3, 4]. We have explored and refined a methodology for correlation and validity checks for binary and ternary solid- and liquid-liquid equilibria, SLE [5] and LLE [6] based on the fluctuation solution theory. We have formulated LLE with the unsymmetrical convention for normalizing activity coefficients of dilute species. An inherent part of the method is the estimation of initial guesses for parameter estimation and evaluation of obtained parameters. For that purpose, graphical representation method as well as the molecular predictive models like COSMO-SAC [1] model was applied, since parameters in the model are connected to the other measurable thermodynamic properties.

Specific objectives

The focus of this PhD project is a thermodynamic modelling of systems containing biomolecules or in general organic compounds whose structure includes more than one functional group such as active pharmaceutical ingredients (APIs) and equilibria between them and molecular solvents or ionic liquids.

Crucial part of the work is the improvement database of measurements including solid-liquid and liquid-liquid equilibria with systems relevant for life sciences (e.g. pharmaceuticals) including uncertainty analysis. Therefore, there is a need for reliable data as well as their evaluation. It was shown that for SLE data validation using FST (fluctuation solution theory) could be applied [5, 7]. In the developed FST model for SLE parameters are 2-parameter temperature dependence for activity coefficients at infinite dilution and 1-parametr expression for solute non-ideality relative to infinite dilution. Important and inherent part of this task is the estimation of initial guesses for parameter optimization and evaluation of obtained model parameters. The natural extension is the development of the FST model to LLE validation. Model for binary and ternary LLE

correlation and validation outside the critical region has been formulated.

Modelling methodology

The LLE problem consists of solving a set of n (number of components) equilibrium equations (isofugacity criterion).

We use different standard states for the components in both phases α and β. We assume that phase α is rich in one component and phase β is rich in another component and introduce unsymmetrically normalized activity coefficients γ_i^*.

The final binary LLE model (with potentially six parameters in total) is represented by the following equations:

$$\ln x_1^{\alpha} - \frac{c^{\alpha}}{T}(1 - x_1^{\alpha})^2 = \ln x_1^{\beta} + \frac{c^{\beta}}{T}\left[2x_1^{\beta} - (x_1^{\beta})^2\right] + a^{\beta} + \frac{b^{\beta}}{T}$$

$$\ln(1 - x_1^{\alpha}) + \frac{c^{\alpha}}{T}\left[1 - (x_1^{\alpha})^2\right] + a^{\alpha} + \frac{b^{\alpha}}{T} = \ln(1 - x_1^{\beta}) - \frac{c^{\beta}}{T}(x_1^{\beta})^2 \quad (1)$$

Later, we have focused on modelling type I liquid-liquid systems of one partially miscible binary (components 2 and 3) and two completely miscible binaries (1+2 and 1+3) when the liquid phases are rich in one component (' is rich in 2 and " is rich in 3). The model is proposed for distribution of the components in the liquid phases. The excess Gibbs energy models for the both liquid phases are based on the FST. The model requires experimental VLE data for the completely miscible binaries and LLE data for partially miscible binaries to obtain most of the model parameters, i.e. binary interaction parameters and temperature-dependent Henry's constants. The remaining binary interaction parameters are regressed from ternary LLE data. The proposed model is a natural extension of the binary model; it means the ternary LLE model reduces to binary case when the mole fraction of the single component vanishes.

Results and discussion

The developed model has been tested in more than 100 binary and type 1 ternary LLE cases including systems with ionic liquids and water or classical solvents commonly used in downstream separations. The overall performance in data fitting (absolute average relative deviation) was found to be approximately 5%.

The developed models constitute a basis for data validation procedure. We have considered some criteria for data evaluation:

1. 95% confidence intervals on the predicted by the model phases compositions,
2. outliers detection measures (e.g. COVRATIO),
3. comparison with experimentally measured calorimetric, solution properties (excess enthalpy and entropy at infinite dilution) since the model parameters are directly connected to those.

Experimental points, which satisfying the assumed criteria are considered as recommended. High quality data must be consistent with the solution properties.

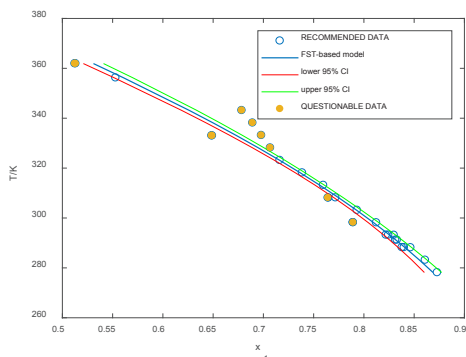Otherwise, data are assigned as questionable and further investigation has to be made.

Figure 1: LLE data validation in [bmim][PF$_6$] (1) / butan-1-ol (2) binary system [8].

Conclusions

Models have been constructed and tested for the correlation of binary and ternary LLE data. A range of criteria for binary LLE data validation, based on the goodness-of-fit, prediction intervals based on the parameters uncertainties, influence of outliers, parameter identifiability measures and identification of derivatives of solution properties directly from measured data have been addressed.

References

1. S.T. Lin, S.I. Sandler, *Ind. Eng. Chem. Res.,* **2002**, *41*, 899.
2. A. Klamt, *J. Phys. Chem.,* **1995**, 99, 2224.
3. M. Frenkel, *J. Chem. Thermodynamics*, **2015**, 84, 18.
4. V. Diky, J.P. O'Connell, J. Abildskov, K. Kroenlein, M. Frenkel, *J. Chem. Eng. Data*, **2015**, 60, 3545.
5. L.P. Cunico, R. Ceriani, B. Sarup, J.P. O'Connell, R. Gani, *Fluid Phase Equilibria*, **2014**, 362, 318.
6. Ł. Ruszczyński, A. Zubov, J. P. O'Connell, J. Abildskov, *J. Chem. Eng. Data*, **2017**, 62, 2842.
7. Ł. Ruszczyński, A. Zubov, G. Sin, J. Abildskov, *Proceedings of the 27th European Symposium on Computer Aided Process Engineering - ESCAPE 27,* **2017**, 247.
8. Ana B. Pereiro, A. Rodriguez, *J. Chem. Eng. Data*, **2007**, 52, 1408.

Max Schumann

Phone: +45 53336877
E-mail: maxsch@kt.dtu.dk

Supervisors: Anker Degn Jensen
Jakob Munkholt Christensen
Jan-Dierk Grunwaldt (KIT)

PhD Study
Started: January 2017
To be completed: January 2020

Sustainable Production of Higher Alcohols from CO

Abstract

C_2-oxygenate (C_2-O) formation from syngas has been studied over supported metallic Rh catalysts. Catalyst preparation was carried out through wet impregnation of $Rh(NO_3)_3$ on different metal oxides (SiO_2, TiO_2,). Catalytic activity tests for the CO hydrogenation reaction confirm a strong support dependence for the formation of C_2-O on the support material whereby the activity in producing target products follows $Rh/ZrO_2 \gg Rh/SiO_2$. Elevated reaction gas pressure conditions show a favorable impact on the selectivity towards C_2-O.

Setting the scene

The high energy density of liquid alcohols (e.g. EtOH) and the possibility to integrate those into existing energy systems are big advantages over other sustainably producible energy carriers, e.g. CH_4 or H_2. Conversion of H_2 with CO or concentrated CO_2 streams towards higher alcohols is a highly favorable reaction in that context. Single-metal supported Rh catalysts are known for their ability to produce C_2-oxygenate compounds [1] (mainly acetaldehyde and ethanol) from CO/H_2 and are chosen as starting point of this project.

Background

Rhodium is a good single metal catalyst for CO hydrogenation since it allows CO to adsorb in both, a molecular and a dissociative way. Both steps are required for the production of C_2-O compounds. Narrow product distribution and high selectivities for AcH and EtOH are advantages over other catalyst systems and make metallic Rh an attractive model system for this reaction [2]. In H_2-containing reaction atmosphere, the synthesis of C_2-O competes with the complete hydrogenation, which mainly produces CH_4. This limits the CO conversion range wherein moderate C_2-O selectivity levels are gained (up ca. 70 %) to 5 – 10 %. For any commercial application, it will be necessary to push beyond the limitation of low conversion ranges while keeping low metal Rh loadings.

Mechanistic introduction

There are two common viewpoints onto the reaction mechanism that can explain the observation of Rh to either behave like a pure methanation catalyst or like a selectively C_2-O products forming system.

One approach which is widely followed in Density-Functional Theory calculations is based on the distinction between the different Rh crystal facets. Rh(211) step sites have a high activity for the CO dissociation whereas Rh(111) terrace sites cannot break the C-O bond but show a high selectivity in forming C_2-O compounds [3]. From this point, it would be assumed that the Rh step sites dominate and CH_4 evolves as main product. One approach to explain the observed ability of Rh to form AcH is a selective blocking of the Rh step sites (via doping or support interaction). This can shift the product distribution from methane as main product towards high selectivity levels for the formation of C_2-O at the expense of overall activity.

Another approach focuses on the interplay of Rh with support metal oxide sites and the involvement of different surface intermediates within the catalytic cycle. Herein, the insertion of a CO species into C_1-compounds that originate from CO dissociation is widely assumed as the rate determining reaction step. Different species, e.g. acetate, formyl and carbene, were suggested as kinetic relevant intermediates based on isotopic labelling and chemical trapping experiments [4-6]. A mechanism that involves active composite centers which consist of interfacial sites between partially oxidized Rh and metal cations connected via support oxygen atoms, $Rh^{\delta+}$-O-Me, was proposed by Liu et al. [6]. These sites may stabilize intermediates that can then be hydrogenated to acetaldehyde (see Figure 1).
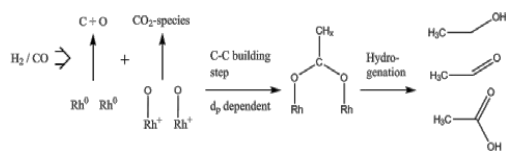
Figure 1: Key steps in reaction mechanism.

Tailoring a catalyst that provides the right balance between metallic Rh^0 which can dissociate CO and vicinal interfacial $Rh^{\delta+}$-O-Me islands that enable CO-insertion into CH_x, is hypothized to lead to an optimum C_2-O yield. The addition of dopants (e.g. Fe, Mn and Ce) can significantly shift the product distribution. Different effects, e.g. selective blocking of Rh(211) step sites or providing Lewis-acid sites that assist the build-up active composite centers are related hereto. This PhD project aims to merge the different models on active sites into one consistent image and to identify the optimum synthesis and operational conditions that favor the formation of described interfacial active site centers.

Specific objects

1) Investigation of the reaction mechanism (see last years epsidoe)
2) Catalytic CO hydrogenation reaction tests
3) Utilization of colloidal Rh nanocrystal synthesis

Catalytic CO hydrogenation reaction testing

Catalytic reaction testing was carried out at a high pressure set-up in CO/H_2 (1:2) atmosphere. The product distribution was investigated as a function of the CO/H_2 reaction atmosphere gas pressure. Operating the reaction at elevated gas pressure around 20 bar was observed to lead to a selectivity maximum of desired C_2-O products (EtOH, AcH, acetate esters) with an increasing fraction of acetate ester products (see Figure 2). While a similar trend for the product distribution was observed in the case of SiO_2 supported Rh, the level of CO conversion significantly dropped to ca. 0.3 %. Further elucidation of speculated differences in the interaction of the active Rh component and support metal oxide is part of this research project.

Rh nanocrystals via colloidal synthesis

Catalyst preparation via wet impregnation is the predominantly reported synthesis route in the literature. Hereby, an aqueous metal precursor salt solution is impregnated onto the support material. The mean particle size can to some extent be controlled by the metal loading. One main constrain of this method is, that mean particle size and the weight loading, which determines the level of CO conversion, cannot be decoupled. An alternative synthesis route constitutes colloidal synthesis of metal nanocrystals. Hereby, the nanocrystals are not formed on the support (wet impregnation), but separately in a by organic surfactants assisted reduction reaction. In a next step, synthesized nanocrystals can be impregnated with a desired loading content onto the support material. Synthesis of such monometallic Rh and bimetallic cobalt-rhodium alloy-nanocrystals is currently on going

and reaction testing of these catalysts under catalytic reaction conditions will be a main part of future work in this PhD project.
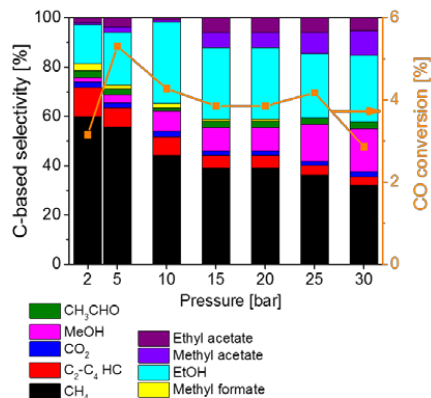
Figure 2: Product selectivity of $CO-H_2$ reaction as a function of the CO/H_2 (1:2) reaction gas pressure for 1 % Rh/ZrO_2 (37 NmL/min, 225 °C, 2.00 g catalyst).

References

[1] M. Ichikawa, Bull. Chem. Soc. Jap. 51 (8) (1978), 2273-2277.
[2] H. Luk et al., Chem. Soc. Rev. 46 (5) (2017), 1243-1636.
[3] N. Yang et al., JACS 138 (2016), 3705-3714.
[4] A. Takeuchi et al., J. Phys. Chem. 86 (13) (1982), 2438-2441.
[5] A. Kiennemann et al., J. Chem. Soc., Faraday Trans. 1 83 (1987), 2119-2128.
[6] J. Liu et al., Proc. 9th Int. Congr. Catal. V2 (1988), 735-742.
[7] M. Cargnello et al., Science 341 (2013), 771-773.

Lars Schwarzer

Phone: +45 4525 2837
E-mail: laschw@kt.dtu.dk

Supervisors: Peter Arendt Jensen
Peter Glarborg
Kim Dam-Johansen
Jens Kai Holm (Ørsted A/S)

PhD Study
Started: December 2015
To be completed: January 2019

Biomass Particle Ignition in Mill Equipment

Abstract

Spontaneous ignition of biomass presents a threat to its reliable and economic use in combined heat and power plants. Existing models to predict fires that occur in storage facilities or in fuel mills are often inaccurate. This study aims at developing a more reliable, predictive model. By implementing reactions and heat transfer in a 1D-, time-stepping solver for mass and enthalpy balances, self-ignition of biomass in lab-scale experiments can be predicted with reasonable accuracy. By resolving the relevant transport and reaction processes, the model developed in this study is expected to scale better and involve less experimentally tuned parameters than existing approaches.

Introduction

Biomass may spontaneously ignite when stored or processed at elevated temperatures. One example is milling of wood pellets in pulverized fuel combined heat and power plants (CHP). Danish CHP-units originally designed for coal combustion are being converted to biomass as a fuel, and fires have occurred both in mills and storage facilities. Prediction of self-ignition according to the relevant industry standard EN 15188 is based on scaling laws originally developed for explosive gas mixtures [1,2]. While the main benefits of these models are their numeric simplicity, they require extensive testing of materials to determine the parameters of the scaling laws, transport and reaction kinetics are convoluted into the same parameters. Application of these scaling laws has been shown to lead to erroneous predictions of thermal runaway [3, 4].

Objectives

As engineering software is widely available, the numerical simplicity of Semenov/Frank-Kamenetskii [1,2] models no longer outweighs the disadvantages outlined above. Objective of this PhD study is to develop a model that can predict self-heating and incipient ignition in biomass. A model that treats reaction and heat transfer separately is developed and tested against lab-scale experiments.

Experimental

Four different pulverized biomasses (beech and pine wood, wheat straw, and sunflower husk pellets) were investigated. For each experiment, a cylindrical wire mesh basket was filled with the sample to be tested and placed in a tube oven. The atmosphere during the experiment was controlled by mixing oxygen and nitrogen streams. Heating rates were set to 1 K/min from ambient temperature to up to 300 °C. Details of the experimental procedure have been presented in [5].

Reaction kinetic data were determined by thermogravimetric analysis (TGA). The temperature program of the TGA-experiments consisted of six isothermal stages between 150–250 °C, which were held for one hour each. Oxygen concentration was varied to differentiate between oxidative and purely thermal degradation.

Modelling

The biomass is modelled as a porous solid surrounded by a gas flow. Mass and enthalpy balances are solved to describe reaction progress and heat release. Species balances are solved mainly to account for consumption of oxygen in the gas phase, but can also be used to model change in composition of the reacting solid. The main goal is then to find appropriate descriptions for the transport and source terms in the balances.
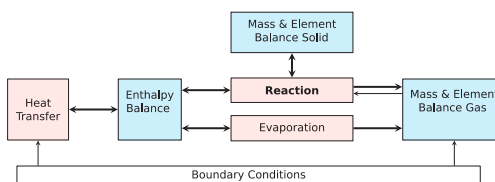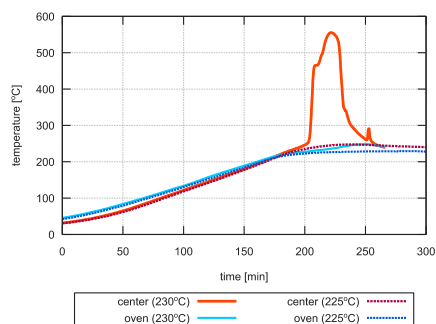

Figure 1: Model structure

Figure 2: Fixed bed experiments with pine (12g), 50–200 μm particle size, 20% oxygen give a critical ambient temperature for ignition of 227.5±2.5 °C.

Figure 3: Modelling the experiments shown in Figure 2 yields a critical temperature of 212.5±2.5 °C.

Figure 1 shows the conceptual structure of the model, highlighting the central position that the reaction mechanism has. Two reactions were considered here, one for heterogeneous oxidation of the solid and one for pyrolysis. Mass loss kinetics were modelled based on the TGA-data. Heat release rates were coupled to the mass loss kinetics. The heat of reaction was based on the mass-specific lower heating value, corrected for incomplete combustion. It was assumed that the fuel-carbon oxidizes to CO and CO_2 at a ratio of 1:2. The organic fraction for each material was modelled by assuming a single $C_xH_yO_z$-species for each fuel. The coefficients (x, y, z) were found from elemental analysis. An additional inert fraction (ash) and evaporation of moisture were included.

Heat is exchanged between solid and gas phase as well as gas phase and surrounding walls by convection, and directly between walls and solid by radiation. Heat transfer correlations and material properties can be found in reference works, e.g. [6].

The model was implemented as a one-dimensional, time-stepping solver in GNU Octave/Matlab. The reacting solid can be divided into an arbitrary number of cells. The gas-phase is modelled as a single continuously stirred reactor.

Results and Discussion

Experiments were carried out to determine critical ambient temperatures that would lead to thermal runaway. Figure 2 shows such an experiment for the example of pine in a 20% oxygen atmosphere. While the experiment at 225 °C oven temperature shows only a mild overshoot of the sample center temperature (dotted curves), heating to 230 °C oven temperature leads to thermal runaway of the sample (solid lines). The same effect can be seen in the model, Figure 3. The critical ambient temperature for thermal runaway is slightly lower (213.2 °C). Calculations were stopped once thermal runaway was reached in the model (at ca. 205 minutes).

Further experiments comparing different materials were carried out by heating at 1 K/min to 300 °C in oxidative atmosphere. The sample is initially colder than the oven, but eventually undergoes thermal runaway. The point at which oven wall and sample temperatures are equal was used as an onset criterion for thermal runaway,
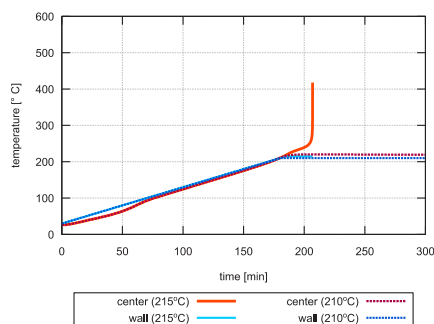
and was similarly slightly underestimated by the model. Comparing production rates of CO and CO_2 for experiment and model showed that the major trends were captured (Figure 4).

Conclusions

Model and lab scale experiments were in good agreement. Further improvements can be achieved by implementing a more refined reaction kinetic model and considering mass transfer limitations (diffusion) of oxygen.

References
1. N.N. Semenov, Zeitschrift für Physik 48 (1928) 571–582.
2. D.A. Frank-Kamenetskii, Diffusion and Heat Transfer in Chemical Kinetics, 2nd revised edition, Plenum Press, New York, 1969.
3. J.C. Jones, Fire and Materials 23 (1999) 239–243.
4. B.F. Gray, J.F. Griffiths, S.M. Hasko, J. Chem. Tech. Biotechnol. 34A (1984) 453–463
5. L. Schwarzer, P.A. Jensen, P. Glarborg, J.K. Holm, K. Dam-Johansen. Biomass ignition in mills and storages – is it explained by conventional thermal ignition theory? Nordic Flame Days 2017, Stockholm
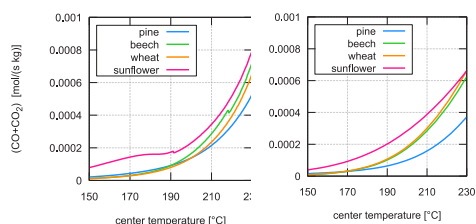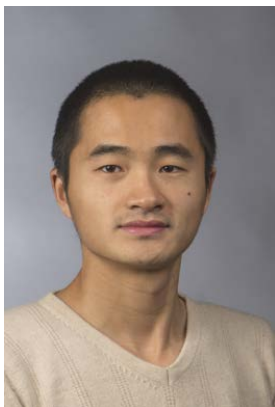6. VDI-GVC (editor), VDI-Wärmeatlas, 10th edition, Springer, Berlin/Heidelberg, 2006.

Figure 4: Combined CO and CO_2-emissions, experimental (left) and modelled (right) show acceptable agreement. The scaling is identical on both plots.

Jiang Shao

Phone: +45 52699368

E-mail: jshao@kt.dtu.dk

Supervisors: Anders E. Daugaard

              Anne Ladegaard Skov

PhD Study

Started: January 2018

To be completed: December 2020

Stretchable conductive elastomers

Abstract

Flexible electronics have become a fast growing industry and it is the future trend of development of electronic products. Stretchable conductive materials, as the key materials in the flexible electronics, can maintain a high level of electrical performance and reliability when they have large deformation. A new method has been developed to prepare stretchable conductive elastomers with high conductivity and stretch ability. The electrical results shows that the materials with this special structures can undergo large scale deformations without a significant loss in conductivity.

Introduction

In recent years, flexible electronics have become a mainstream direction in electronic products [1]. Flexible electronics based on elastic substrates have many special abilities when compared to traditional electronics, such as the ability to be stretched, bent, and twisted [2]. In particular, flexible electronics can maintain a high level of electrical performance and reliability, even under considerable deformation [3]. Stretchable conductive materials, which is essentially required for flexible electronics, have been a research hotspot over the past years and have become an attractive goal in materials science and engineering [4].

When developing flexible electronics, one of the major challenges from conventional electronics is the inherent stiffness of traditional conductor materials. Compared with conventional conductor materials, stretchable conductive materials have considerable advantages, for example, large strain endurance, high conductivity, and especially the exceptional conductivity retention capability during repeated deformations [5].

Silicone elastomers are one of the most widely used matrix materials for stretchable conductive materials, because of their low cost, high efficiency, environmentally friendliness, extensibility and mechanical flexibility [6,7].

Although silicones have many advantages, they have poor conductivity, and therefore requires large amounts of fillers to become conductive. In addition, such conductive silicones cannot maintain a constant conductivity at high strains (>30%), which restricts large scale applications [8]. Recently, many methods have

been developed to modify the properties of silicone to cater to flexible electronics, for example, surface patterning of silicone. However, methods like this need special processing, such as imprinting, and also have a negative effect on the extensibility of the silicone elastomer [9]. Methods like surface patterning only provide limited extensibility of the conductive system, which limits a broader applicability in advanced fields where high elongation and maintained good electrical conductivity is a requirement. For large scale applications in flexible electronics, new processing methods, which can combine high stretchability and conductivity in silicone materials, is a high demand.

In this project, a new method has been developed to prepare stretchable conductive elastomers. The electrical performance and stretchability have been investigated to demonstrate the practical value of such strategy.

Specific Objectives

This project aims at developing new methods to prepare stretchable conductive elastomers, which can undergo large levels of strain while maintaining electrical performance.

Methodology

Stretchable conductive composites based on bimodal networks have been prepared. Firstly, multi-walled carbon nanotubes (MWCNTs) were entrapped in a hyperbranched short chain poly(dimethyl siloxane) (SC-PDMS) to form high conductive domains. Secondly, hyper-branched long chain poly(dimethyl siloxane) (LC-PDMS) has been introduced as the surrounding matrix.

Additional MWCNTs were added into LC-PDMS as the "bridge" to connect the highly conductive domains. Thirdly, entrapped MWCNTs and hyper-branched LC-PDMS were mixed together and cured under high temperature to prepare the final composites.

Results and Discussion

Figure 1 shows the influence of adding free MWCNTs in the matrix. As it can be seen, even with a very small amount of free MWCNTs in the matrix (0.05wt%), the conductivity of transgressed from a non-conductive to a percolated system.
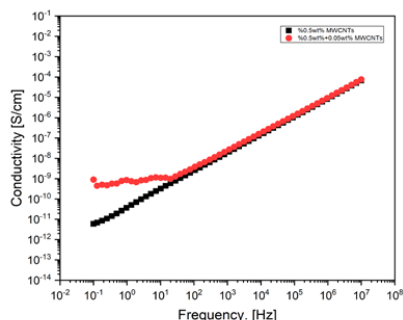

Figure 1: The influence of extra MWCNTs in matrix on the conductivity.

This shows that conductive systems can be prepared through "bridging" of the isolated domains. When there is no extra MWCNTs in the matrix, those high conductive areas are isolated and cannot form an effective conductive path. With additional MWCNTs in matrix, the extra MWCNTs in matrix can act as the "bridges" and connect the high conductive domains, which can improve the conductivity dramatically.
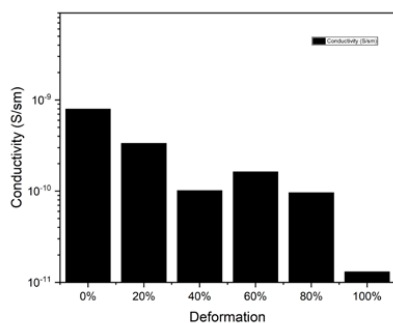

Figure 2: Conductivities of sample with extra MWCNTs under different strains.

Figure 2 shows the changes of conductivity when samples undergo deformations. It can be observed that the conductivities decrease initially, where after they remain almost stable until the deformation is >80%, where there is a significant decrease in conductivity.

This could be explained with the inhomogeneous structure of the materials. At first, when the deformation is only 20%, the initial conductive paths are destroyed, causing a decrease in conductivity. When the deformation is between 40% and 80%, although the initial conductive paths have been destroyed because of the deformation, the width and thickness of samples decrease, reducing the distances between those high conductivity areas. This thereby compensates for loss of the initial conductive paths by establishment of new pathways stabilizing the conductivity. When the deformation is 100%, there is a considerable loss of conductivity, which is attributed to the deformation exceeding a threshold, where the distances between the high conductive areas again have become too big, which lead to the ultimate loss of conductivity.

These experiments therefore demonstrate that the bimodal structures formed in the materials can, not only improve conductivity, but also maintain a stable conductivity under large scale deformations, which is the ultimate goal of the PhD project.

Conclusions

The current work has shown that it is feasible to prepare stretchable conductive elastomers with high conductivity and stretchability. With this method, the future work will be focused on optimizing mechanical and electrical properties of the materials.

References
1. M. F. De Volder, S. H. Tawfick, R. H. Baughman, & A. J. Hart, science 339(6119) (2013) 535-539.
2. J. Song, J. Li, J. Xu, & H. Zeng, Nano letters 14(11) (2014) 6298-6305.
3. J. T. Muth, D. M. Vogt, R. L. Truby, Y. Mengüç, D. B. Kolesky, R. J. Wood, & J. A. Lewis, Advanced Materials 26(36) (2014) 6307-6312.
4. J. A. Fan, W. H. Yeo, Y. W. Su, Y. Hattori, W. Lee, S. Y. Jung, Y. H. Zhang, Z. J. Liu, H. Y. Cheng, L. Falgout, M. Bajema, T. Coleman, D. Gregoire, R. J. Larsen, Y. G. Huang & J. A. Rogers, Nature communications 5 (2014) 3266.
5. B. C. Kim, J. Y. Hong, G. G. Wallace, & H. S. Park, Advanced Energy Materials 5(22) (2015) 1500959.
6. T. Sekitani, H. Nakajima, H. Maeda, T. Fukushima, T. Aida, K. Hata & T. Someya, Nature materials 8(6) (2009) 494.
7. Y. Zang, F. Zhang, C. A. Di & D. Zhu, Materials Horizons 2(2) (2015) 140-156.
8. T. Cheng, Y. Zhang, W. Y. Lai & W. Huang, Advanced Materials 27(22) (2015) 3349-3376.
9. G. Kofod & P. Sommer-Larsen, Sensors and Actuators A: Physical 122(2) (2005) 273-283.
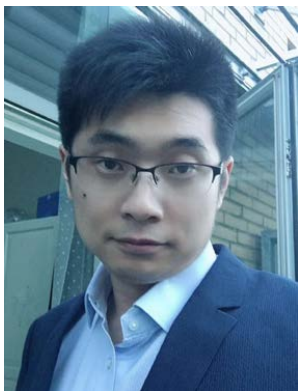
Peng Shen

Phone: +45 5039188

E-mail: psen@kt.dtu.dk

Supervisors: Peter Szabo

             Anders Egede Daugaard

             Qian Huang

PhD Study

Started: December 2016

To be completed: December 2019

Preparation and characterization of Hard-Soft Thiol-ene Alternate Materials with strong interface

Abstract

Thiol-ene materials are a series of materials that can easily be crosslinked using a suitable photo-initiator and a UV light source. An advantage of thiol-ene materials is that they can be tailored to have specific mechanical properties by controlling the stoichiometry of the mixtures. The alternating hard and soft thiol-ene material with a sharp solid interface was prepared. The rheological measurements were carried out using a filament stretching rheometer with a strain rate of $0.001s^{-1}$, the interface of the materials was strong enough to not crack.

Introduction

The layer-by-layer (LBL) technique has received tremendous scientific and technological interest as an effective and powerful approach to prepare materials with specific properties[1-3]. It has been widely used in different applications such as for biomedical materials[4], eco-materials, energy materials[5] to mention a few. Polymer materials with LBL structure are composed of two polymers with different physical and chemical properties that combine the advantages of both systems, which results in improved performance and extension of the application area compared to the respective homopolymers.

Thiol–ene materials can be obtained through traditional thermal conditions with common azo-species such as 2,2-azobis(isobutyro-nitrile) (AIBN) or via with little or no added photo-initiators photochemical thiol–ene reaction methods. During the last century, thiol-ene materials are global focus because of the highly efficient reactions of thiols with reactive C=C bonds, has widely application in hydrogel drug delivery, coatings, adhesives, optical applications, dendrimer synthesis, all-solid-state electrolyte, high strength laminates, dental resins and electroluminescent films. In particular, two thiol reactions emerged, thiol–ene free-radical addition to electron-rich/electron-poor C=C bonds, and the catalyzed thiol Michael addition to electron-deficient C=C bonds. Unlike typical chain-growth free-radical polymerizations or step-growth condensation polymerizations, thiol-ene polymers form in a stepwise manner but their formation is facilitated by a rapid, highly efficient free-radical chain-transfer reaction.

Thus, crosslinked thiol-ene polymerizations proceed very rapidly but will not reach the gel-point until relatively high functional group conversions.

Specific Objectives

In this project. We intend to prepare the new homogeneous thiol-ene materials with drastically different mechanical proportion, which is formed via a base Michael addition reaction. Products will show the different mechanical proportion by controlling the kind of reaction compound (thiol and ene with different average molecular functional groups).

Among the different reaction compound, we choose the 3:4 PETMP/TATATO ratio thiol-ene material as the hard segment, replace TATATO with some linear divinyl or multi-arm-PEG compounds as the soft segment.
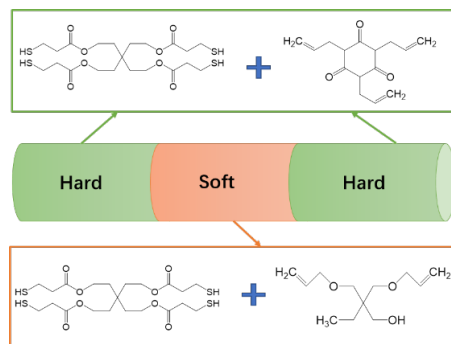

Figure.1 Artificial fingers with hard-soft alternate thiol-ene materials

Step-by-step preparation

The two chemicals were mixed by a SpeedMixer at the speed of 3000r/min for 2 mins; in addition, all processes were completed in total darkness for preventing the mixture from premature polymerization. The soft liquid was obtained in the same way except for replacing the TATATO with PMDPE.

It is very important that the first two steps polymerization process should strictly control the reaction time, the hard polymer liquid and soft polymer liquid are mix together in a shorter illumination time, however, the longer illumination time lead to the interface of hard and soft not strong enough to complete the next stretching process.
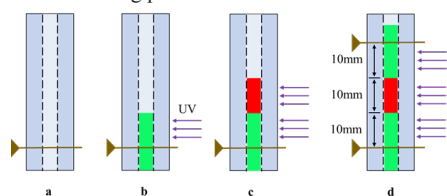

Figure 2. The production process for a hard-soft alternate sample (10mm soft segment)

Fracture experiments

The rheological and mechanical properties of polymers are intimately related to their molecular structure. The rheological measurements were carried out using a filament stretching rheometer (VADER 1000 from Rheo Filament ApS) with a strain rate of $0.001s^{-1}$. Meanwhile, a high-speed camera (Photron Mini UX100 with a Navitar Zoom6000 lens) was used to capture the fracture process; and the captured optical images were used to measure the local strain of the deformed sample accurately during the crack propagation.
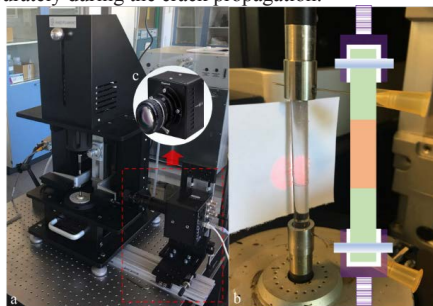

Figure 3. a. The filament stretching rheometer VADER 1000; **b**. Laser width measurement device; **c.** The Photron Mini UX100

Results and Discussion

The fracture process was too fast to be recorded by a conventional camera. We used the high-speed camera for recording the images of the fracture process. As shown in **Figure 4**, the crack was generated in the soft segment surface, not in the interface between the hard and soft materials.
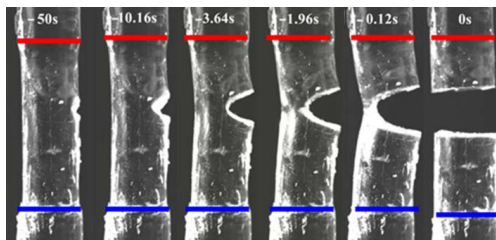

Figure 4. The image of 10mm soft segment alternate materials fracture process (blue line shows the lower interface, red for upper)

The growth of crack was predominantly contributed by normal stress ($F_n > F_t$). The Ft was increasing fast after the angle of crack rose to $90°$ ($F_n = F_t$) at the-10.16s, The Ft dominated the fracture process during from -10.16s to finish, the shape of crack was changed from isosceles triangles to parabola.

Conclusions

In summary, a new step-by-step pre-crosslinking method was designed to prepare new hard-soft alternate thiol-ene materials, which were constituted by two different mechanical properties ultraviolet-cured thiol-ene materials. It was very important that the reaction time of the polymerization process in the first two steps were strictly controlled. If the time was too long, it would cause the hard segment surface completely crosslinked and generate a weak interface, leading to the interface cracks or separation during demolding. Opposite, short exposure time would lead to the hard and soft liquids resulting in mixing of an undesired sample.

Acknowledgements

References

[1] C. D. Mueller, S. Nazarenko, T. Ebeling, T. L. Schuman, A. Hiltner, & E. Baer, Polym. Eng. Sci. 37(2) (1997) 355-362.

[2] J. Duvall, C. Sellitti, V. Topolkaraev, C. Myers, A. Hiltner, E. Baer, Polymer 35(18) (1994) 3948-3957.

[3] J. Duvall, C. Sellitti, C. Myers, A. Hiltner, E. Baer, J. Appl. Polym. Sci. 52(2) (1994) 52 195-206.

[4] J. W. Chan, B. Yu, C. E. Hoyle, A. B. Lowe, Polymer 50(14) (2009) 3158-3168.

[5] C. E. Hoyle, A. B. Lowe, C. N. Bowman, Chem. Soc. Rev. 39(4) (2010) 1355-1387.

Meng Shi

Phone:	+45 5269 9366
E-mail:	mshi@kt.dtu.dk

Supervisors: Nicolas von Solms
John M. Woodley

PhD Study
Started: January 2018
To be completed: December 2020

Migration of Gas and Water for the Replacement of CH₄ with CO₂-enriched Air in Hydrate Production

Abstract
Natural gas hydrate production via injecting CO_2 together with other gases could improve methane recovery ratio and ability of CO_2 storage simultaneously. The migration of gas and water occurrence in both formation and replacement process, which governs the seismic exploration, stability of seabed and distribution of natural gas hydrate. The movement of gas and water were identified through X-ray computed tomography (CT) imaging during the hydrate formation and replacement period. A series of experiments are carried out to optimize the injected CO_2/enriched air compositions and injection rates. The results of the investigation could provide more reliable data for gas production and capture, along with a reference for future natural gas hydrate exploitation.

Introduction
Clathrate hydrate crystals consist of cages composed of water molecules, stabilized by other, small, molecules trapped inside the cages as guest molecules. Natural gas hydrates belong to the group of clathrate hydrate, are known to be distributed in permafrost and continental shelves of the world's oceans with total carbon content twice that in other fossil fuels[1]. There are several methods such as thermal stimulation, depressurization, inhibitor injection and gas exchanging have been put forward for production of methane. In the above methods, depressurization technique has been applied successfully to produce gas in commercial quantities through advantages that economically viable production, no extra heat introduced and friendly-environment compared to thermal stimulation and inhibitor injection. The gas exchange method, in which gases such as CO_2 or CO_2 mixed with other gases are injected into hydrate reservoir to extract methane from hydrate[2][3]. This replacement method simultaneously achieves the sequestration of CO_2 for climate change mitigation and the enhanced recovery of CH_4 for energy production.

We know the atmosphere and the air that we breathe has never had as much carbon dioxide in it as it does today. For the first time in recorded history, the average monthly level of CO_2 in the atmosphere exceeded 410 parts per million (ppm) in the month of April, 2018. A CO_2 replacement method has been proven to be a mutually beneficial strategy for both methane exploitation and carbon dioxide storage. It is based on the

fact that the chemical potential of methane hydrate is higher than that of CO_2 hydrate, meaning the CO_2 hydrates are more stable. Recent studies showed that this process could be improved by injecting other gases together with CO_2, which improved methane recovery ratio and ability of CO_2 storage simultaneously[4][5]. Direct injection of flue gas from coal-fired power plant into hydrate reservoirs was extensively performed in lab-scale experiments[6]. Air is abundant and easily get regardless of time and place, which makes it the much more attractive for practical production of natural gas hydrate. Accordingly, a continuous supply of CO_2-enriched fresh air into the natural gas hydrate was proposed in this investigation.

Natural gas hydrate production options also face a potential hazard that fluid migration can result in porkmarks in subsea and gas release to seafloor contribute to instability or seep environment[7]. However, there are actually relatively few studies that focus on the effect of gas and water migration behavior on hydrate recovery rates, efficiency and even mechanism. In this study, X-ray computed tomography (CT) imaging was conducted to track movement of water and gas during the hydrate formation period. A series of experiments are carried out to optimize the injected CO_2-enriched air composition and injection rates.

Specific Objectives
The aim of this study is to track the influence of gas injection rate, production pressure and gas hydrate

saturation for water and gas migration behaviors under conditions close to the deep ocean sediment environment. Through this investigation, the results could provide more reliable data for gas production and capture, along with a reference for future natural gas hydrate exploitation.

Results and Discussion
In this study, methane hydrate is synthesized on a sandstone at condition of 7.5 MPa and 4°C. From CT number of different slices of sample shown in Figure 1, water saturated homogenously in sandstone. After methane injected into sample, only 0-30mm of sandstone from inlet detected that water permeated with methane. CT number increased in the same trend with that of after injection more methane gas after hydrate formation.
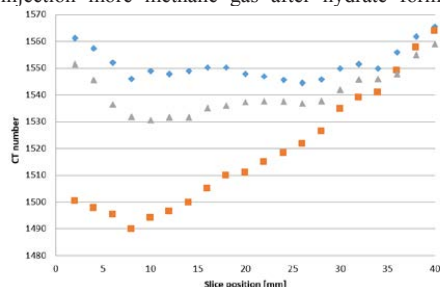

Figure 1: CT numbers of different positions at different stages.

Visually analysis are shown in Figure 2 in different stages, in which methane hydrate grows from inlet into direction of outlet. It is concluded that hydrate formation associated with gas migration. More experiments are under performing.
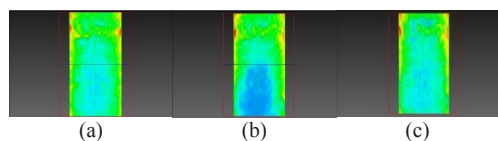

Figure 2: Image of gas and water distribution of different stages (a) wet sample, (b) after gas injection, (c) methane hydrate formation.

Conclusions
The migration of gas and water were identified through X-ray computed tomography imaging during the hydrate formation period. A concept was put forward that migration of gas and water effect process of gas hydrate production. migrated behavior of gas and water occurred in hydrate reservoir while production, sandstones with holes for gas going through were analyzed by X-ray computed tomography (CT) imagining. Preliminary results show that there is relationship with concentration of gas hydrate and migrated gas and water.

References
[1]   Sloan Jr ED. Fundamental principles and applications of natural gas hydrates. Nature 2003;426:353.

[2]   Chong ZR, Yang SHB, Babu P, Linga P, Li X-S. Review of natural gas hydrates as an energy resource: Prospects and challenges. Appl Energy 2016;162:1633–52. doi:10.1016/J.APENERGY.2014.12.061.

[3]   Komatsu H, Ota M, Smith RL, Inomata H. Review of CO2–CH4 clathrate hydrate replacement reaction laboratory studies – Properties and kinetics. J Taiwan Inst Chem Eng 2013;44:517–37. doi:10.1016/J.JTICE.2013.03.010.

[4]   Goel N. In situ methane hydrate dissociation with carbon dioxide sequestration: Current knowledge and issues. J Pet Sci Eng 2006;51:169–84. doi:10.1016/J.PETROL.2006.01.005.

[5]   Zhang L, Kuang Y, Zhang X, Song Y, Liu Y, Zhao J. Analyzing the Process of Gas Production from Methane Hydrate via Nitrogen Injection. Ind Eng Chem Res 2017;56:7585–92. doi:10.1021/acs.iecr.7b01011.

[6]   Mu L, von Solms N. Methane Production and Carbon Capture by Hydrate Swapping. Energy & Fuels 2017;31:3338–47. doi:10.1021/acs.energyfuels.6b01638.

[7]   Riboulot V, Sultan N, Imbert P, Ker S. Initiation of gas-hydrate pockmark in deep-water Nigeria: Geo-mechanical analysis and modelling. Earth Planet Sci Lett 2016;434:252–63. doi:10.1016/J.EPSL.2015.11.047.

Sigyn Björk Sigurðardóttir

Phone: +45 4525 6184
E-mail: sigsig@kt.dtu.dk

Supervisors: Manuel Pinelo
              Andreas Kaiser

PhD Study
  Started: June 2017
  To be completed: May 2020

Enzyme immobilization on inorganic powders for membrane bioreactor applications

Abstract
Enzyme immobilization is the predominant technique for stabilization of enzymes for their viable and economical use in industrial biocatalysis. Inorganic materials are inherently stable – their high thermal, mechanical, chemical and microbial stability ensures prolonged service life and high ability of regeneration of the native material properties. Thereby, inorganic materials provide a good support for enzyme immobilization for the preparation of highly stable and robust biocatalytic systems. For this purpose, four inorganic powders that are commonly used as membrane materials were tested as immobilization supports. Alcohol dehydrogenase was immobilized on the powders by physical adsorption and covalent bonding. The success of immobilization, i.e. enzyme activity and stability, was investigated with respect to the properties of the support.

Introduction
The use of enzymatic catalysis in industrial processes has become increasingly important in recent years, following the shift of focus towards more environmentally friendly processing and production methods along with advances in enzyme engineering [1]. One of the main complications involved in industrial applications of enzymatic catalysis is the decay in enzyme activity. In this regard, enzyme immobilization can offer increased enzyme stability as well as reusability, thus prolonging the useful life of the biocatalyst and benefitting the process economy. Membranes can be used as carriers for enzyme immobilization, where the advantages of both enzymes and membranes are exploited, i.e. the high efficiency and selectivity of the biocatalyst and the process intensification brought about by the membrane [2], [3]. Inorganic membranes offer several advantages over polymeric membranes, such as high chemical and mechanical stability, microbial resistance and longer service life [4], [5]. As a first step in the development of highly active and stable biocatalytic, inorganic membranes, the interactions between immobilized enzymes and different inorganic support materials were studied based on the fundamental properties of the support materials. For this purpose, four inorganic raw powders of materials that are commonly used for membrane fabrication and enzyme immobilization, including alumina, silicon carbide, titania and zirconia were selected as immobilization supports. ADH was immobilized on the powders by two different immobilization methods; physical adsorption and covalent bonding. Characterization of the powder properties included zeta potential, surface area and particle size distribution measurements, and these properties were used for the evaluation of enzyme activity and stability upon immobilization.
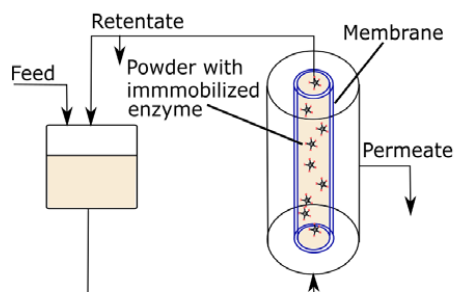

Fig. 1: Enzymes immobilized on inorganic powder for application in membrane bioreactors.

Results and Discussion
High enzyme activity retention was generally achieved upon immobilization on the inorganic powders. Nanoparticles are indeed advantageous for immobilization, as they provide high surface area and

high particle concentration in a suspension, as well as reduced mass transfer limitations [6].

The enzyme activity retention varied from low to high between the powders tested. These observations were mainly explained by the different zeta potentials of the powders and the isoelectric point of the enzyme. The activity retention was generally high when the powders and the enzyme had opposite surface charge, while the activity retention was considerably lower when the powder and the enzyme had similar surface charge. The charge repulsion between the similarly charged powder and enzyme thus impeded an efficient immobilization. This was especially important when the enzyme was immobilized by physical adsorption, where the enzyme was immobilized directly on the untreated surface of the powders. With covalent bonding on the other hand, the support was functionalized by (3-aminopropyl)triethoxysilane and glutaraldehyde prior to immobilization. The introduction of such agents onto a surface has been found to alter the chemistry and thereby the zeta potential of the surface [7], which in this case seemed to allow higher immobilization in the case of similarly charged powder and enzyme.

With nanoparticles as an immobilization support, an important factor for the stability of the system is the colloidal stability of the suspension, in addition to the stability of the enzyme. The storage stability of the immobilized enzyme on powder was found to be hampered by particle agglomeration, caused by low colloidal stability of the particles in the buffer used. The particular buffer was however chosen since the enzyme activity was found to be higher than in other buffers tested and commonly used for enzyme reactions. The balance between enzyme activity and colloidal stability is an important factor, which must be considered for the selection of the process conditions.

Conclusions

The results from the study of enzyme immobilization on raw inorganic powders have confirmed some fundamental aspects of enzyme immobilization on solid surfaces, notably regarding the effects of electrostatic forces on immobilization efficiency and colloidal stability on storage stability of nanoparticles. The results show the advantages and limitations of using nanoparticles as immobilization supports, and highlight which properties of nanoparticles need to be considered to ensure an efficient immobilization.

References

[1]   U. T. Bornscheuer, G. W. Huisman, R. J. Kazlauskas, S. Lutz, J. C. Moore, and K. Robins, "Engineering the third wave of biocatalysis," *Nature*, vol. 485, no. 7397, pp. 185–194, 2012.

[2]   X. Dong, W. Jin, N. Xu, and K. Li, "Dense ceramic catalytic membranes and membrane reactors for emergy and envorinmental applicaitons." pp. 10886–10902, 2011.

[3]   S. B. Sigurdardóttir *et al.*, "Enzyme Immobilization on Inorganic Surfaces for Membrane Reactor Applications : Mass Transfer Challenges , Enzyme Leakage and Reuse of Materials," 2018.

[4]   G. Ranieri, R. Mazzei, Z. Wu, K. Li, and L. Giorno, "Use of a ceramic membrane to improve the performance of two-separate-phase biocatalytic membrane reactor," *Molecules*, vol. 21, no. 3, 2016.

[5]   D. Menne *et al.*, "Regenerable polymer/ceramic hybrid nanofiltration membrane based on polyelectrolyte assembly by layer-by-layer technique," *J. Memb. Sci.*, vol. 520, pp. 924–932, 2016.

[6]   S. A. Ansari and Q. Husain, "Potential applications of enzymes immobilized on/in nano materials: A review," *Biotechnol. Adv.*, vol. 30, no. 3, pp. 512–523, 2012.

[7]   A. de Vasconcellos, A. H. Miller, D. A. G. Aranda, and J. G. Nery, "Biocatalysts based on nanozeolite-enzyme complexes: Effects of alkoxysilane surface functionalization and biofuel production using microalgae lipids feedstock," *Colloids Surfaces B Biointerfaces*, vol. 165, pp. 150–157, 2018.

Ting Song

Phone: +45 50251205
E-mail: tison@kt.dtu.dk

Supervisors: Peter Szabo
Anders Egede Daugaard
Suojiang Zhang, IPE, CAS
Xiangping Zhang, IPE, CAS

PhD Study
Started: November 2015
To be completed: January 2019

Poly(Vinylimidazole-co-butyl acrylate) Membranes for CO₂ Separation

Abstract

The PhD project focuses on the separation of CO_2 from CH_4 or N_2 with ionic liquid-based membranes. Poly(ionic liquid) (poly(IL)) membranes were prepared in this project. Vinylimidazole (Vim) and butyl acrylate (BuA) were copolymerized into poly(Vim-co-BuA) with different ratios through free radical polymerization. The copolymer with Vim and BuA ratio of 24:76 was chosen as a precursor of poly(IL) membranes. The copolymer was quarternized and crosslinked in a one-pot reaction into thin film membranes employing a mixture of mono and difunctional alkyl halides. Membranes were prepared using a mixture of 1:8, 1:2 and 1:0 of 1, 6-dibromohexane and 1-bromobutane, resulting in different degrees of crosslinking. The gas separation performance of membranes with different crosslinking degree were investigated. In order to improve the gas separation performance furthermore, free ionic liquid BMIM Tf_2N was introduced in the poly(IL) membrane.

Introduction

Carbon capture and utilization are regarded as one of the major challenges in the 21st century. Carbon dioxide (CO_2) can be commonly found in natural gas streams, biogas, flue gas and product of coal gasification.[1] The presence of CO_2 and other acid gases reduce the thermal efficiency and make the gas streams become acidic and corrosive, which in turn reduces the possibilities of gas compression and the transport within transportation systems.[2] Therefore, it is urgently necessary to develop new technologies for CO_2 separation with high efficiency, low energy consumption. Membrane separation is a promising technology for CO_2 capture due to its energy efficiency, simple process design, low cost and environmentally friendliness.[3] Recently, ionic liquids (ILs) have attracted great attention for their potential as alternative media for CO_2 separation due to their unique properties. However, it is difficult to realize industrialization using ILs to capture CO_2 due to their high viscosity, price and liquid morphology. In order to overcome these drawbacks of ILs, researchers combined ILs with membranes technology. At the beginning, ILs were embedded in porous polymer membranes, which were named supported ionic liquid membranes (SILMs), with weak capillary forces.[4] SILMs possess excellent CO_2 separation performance, where the CO_2 permeability can reach up to 2000 barrer with CO_2/N_2 and CO_2/CH_4 selectivity of more than 20.[5] While ILs in SILMs can be easily pushed out under high pressure. In

a later study, Noble et al.[6] polymerized ILs monomers to form stable poly(IL) membranes for gas separation. However, CO_2 permeability of such poly(IL) membranes are much lower than that of SILMs. According to previous investigations, combinations of poly(IL) and ILs in composite membranes improved CO_2 permeability by 400 % relative to neat poly(IL) membrane due to the introduction of free ILs.

Specific objective

Imidazole-based poly(ILs) are generally too brittle to form free-standing membranes and need porous polymer membranes as support. We therefore in this project synthesized the copolymer of VIm and BuA, to facilitate preparation of soft copolymers that could act as precursors for poly(ILs) membranes. By use of a simple one-pot quarternization and crosslinking reaction, these copolymers are used for preparation of flexible and free-standing poly(ILs) membranes, which were used for gas separation.

Methodology and results

The polymers synthesized in this project are homopolymers poly(Vim) and poly(BuA), and copolymers poly(Vim-co-BuA) with Vim and BuA feed molar ratio of 30:70, 50:50 and 70:30 as shown in Fig. 1. The molar composition of the copolymer was calculated from ^{1}H NMR, where the molar fraction of VIm was determined from the integration of the imidazole protons

at δ_H 7.4-6.4 ppm relative to the methylene protons (δ_H 4.1-3.5 ppm) in BuA. The content of VI and BuA in the copolymers synthesized were determined as 24:76, 48:52 and 63:37, respectively. Furthermore, the reactivity ratios of Vim and BuA were determined based on a series of low conversion copolymerizations of BuA and VIm with BuA feed composition of 10, 30, 50, 70 and 90 mol%, which by NLLSQ fit gave reactivity ratios of r_{BuA}=1.91 and r_{VIm}=0.094, while the method of Kelen and Tüdos gave r_{BuA}=2.02 and r_{VIm}=0.10.
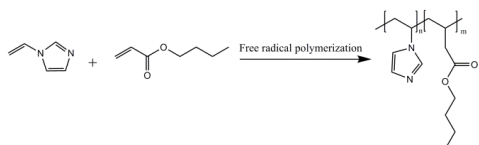

Fig. 1 Copolymerization of Vim and BuA.

Due to the low glass transition temperature and acceptable amount of Vim, the copolymer poly(VIm-co-BuA) with ratio of 24:76 was chosen as the precursor of free standing poly(IL) membrane. Poly(IL) membranes were formed in a one-pot solvent casting and crosslinking reaction using poly(VIm-co-BuA) (24:76), crosslinker (1, 6-dibromohexane) and blocking agent (1-bromobutane) at ambient conditions (as shown in Fig. 2). Membranes with different crosslinking degree, 20 %, 50

% and 100 %, were prepared by varying the ratio between crosslinker and blocking agent.
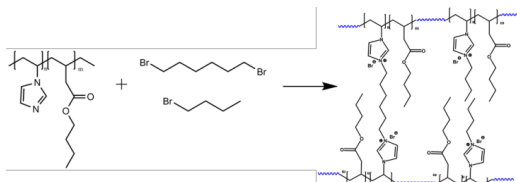

Fig. 2 Copolymerization of Vim and BuA.

The gas separation performances of all the membranes were evaluated with a single gas apparatus. The permeability of CO_2, N_2 and CH_4 and permselectivities of CO_2/N_2 and CO_2/CH_4 are listed in Table 1. The CO_2 permeability was increased from 33.7 to 54.4 barrer by decreasing crosslinking degree of the membrane from 100 % to 20 %. At the same time, N_2 permeability of the more flexible 20 % crosslinked membrane was also increased. For the membrane with 16 wt% free IL BMIM Tf_2N, CO_2 permeability increased from 33.71 to 38.77 barrer and permselectivity of CO_2/N_2 increased from 20.81 to 27.82. After all, 50% crosslinked membrane, which showed both a higher CO_2 permeability of 44.4 barrer and a good permselectivity of CO_2 over N_2 of 21.6, showed an optimal balance.

Table 1 The permeability of CO_2, N_2 and CH_4 and permselectivities of CO_2/N_2 and CO_2/CH_4.

Membrane	Permeability (Barrer)			Permselectivity	
	CO_2	N_2	CH_4	α_{CO_2/N_2}	α_{CO_2/CH_4}
20 %	54.38	11.79	6.16	4.61	8.83
50 %	44.35	2.05	5.16	21.63	8.59
100 %	33.71	1.62	3.64	20.81	9.19
100 % + 16 wt% IL	38.77	1.39	4.18	27.82	9.28

Conclusion

A series of homopolymers and copolymers of VIm and BuA were synthesized in the work. Poly(VIm-co-BuA) (24:76) was found to be the best compromise between content of VIm and thermal properties (T_g=-6.6 ºC), and it was therefore used for preparation of free-standing poly(RTILs) membranes. Membranes were prepared by crosslinking poly(VIm-co-BuA) with a combination of 1, 6-dibromohexane and 1-bromo-butane. The gas separation performances of membranes prepared in this work were investigated.

References

1   Y. Zhang, J. Sunarso, S. Liu and R. Wang, *Int. J. Greenh. Gas Control*, 2013, **12**, 84–107.

2   J. Deng, L. Bai, S. Zeng, X. Zhang, Y. Nie, L. Deng and S. Zhang, *RSC Adv.*, 2016, **6**, 45184–45192.

3   S. Rafiq, L. Deng and M.-B. Hägg, *ChemBioEng Rev.*, 2016, **3**, 68–85.

4   P. Scovazzo, J. Kieft, D. A. Finan, C. Koval, D. DuBois and R. Noble, *J. Memb. Sci.*, 2004, **238**, 57–63.

5   B. Sasikumar, G. Arthanareeswaran and A. F. Ismail, *J. Mol. Liq.*, 2018, 266, 330–341.

6   J. E. Bara, S. Lessmann, C. J. Gabriel, E. S. Hatakeyama, R. D. Noble and D. L. Gin, *Ind. Eng. Chem. Res.*, 2007, **46**, 5397–5404.

Magnus Zingler Stummann

Phone: +45 4525 2957

E-mail: mazi@kt.dtu.dk

Supervisors: Anker Degn Jensen

Martin Høj

Peter Arendt Jensen

Jostein Gabrielsen, Haldor Topsøe A/S

PhD Study

Started: October 2015

To be completed: November 2018

Hydrogen Assisted Catalytic Biomass Pyrolysis for Green Fuels

Abstract

Catalytic hydropyrolysis of biomass is a promising technology for production of sustainable liquid fuels. In this project we have shown that it is possible to decrease the oxygen content in produced oil by increasing the active metal loading of the catalyst and by increasing the support acidity, which also increases alkylation activity.

Introduction

Recent research has shown that catalytic hydropyrolysis of biomass is an efficient process for the production of renewable liquid fuels [1,2]. In this process fast pyrolysis and hydrodeoxygenation (HDO) is combined, ensuring that the reactive oxygenates formed during the pyrolysis, which may participate in polymerization reactions [3], are hydrogenated immediately, thus leading to a stable product with a low oxygen content compared to pyrolysis oil [4]. However, despite being a very promising process, there is very limited information in the open literature regarding the effect of the catalyst in the fluid bed reactor.

In this work we have investigated the effect of the CoMo loading and the support acidity on the product distribution and composition. The catalysts were tested in their sulfide form and the fresh catalysts were characterized with BET, ICP-OES, NH_3-TPD, and Raman spectroscopy, and the spent catalysts were

studied with SEM and STEM. The organic phase was analyzed with GC×GC-MS/FID, GC-AED, and the S, H, and O concentrations were measured.

Specific Objectives

- Commissioning and running a bench scale setup for catalytic hydropyrolysis in a fluid bed reactor with a downstream fixed bed HDO reactor.
- Synthesis and characterization of hydropyrolysis catalysts suitable for fluid bed operation.
- Performing an experimental investigation of hydropyrolysis of different biomass sources with systematic variation of process parameters.
- Performing detailed physical and chemical analysis of bio-oil products using e.g. elemental analyzer and GC-MS.
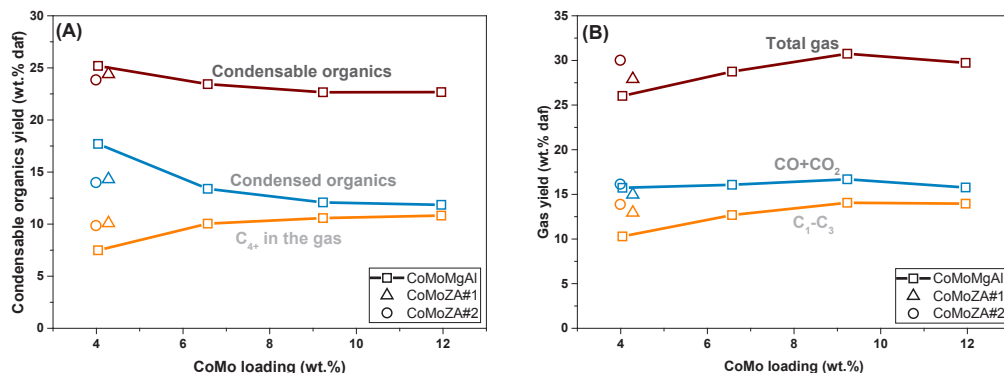

Figure 1 Effect of the CoMo loading and support acidity on the condensable organic yield (A), and gas yield (B).

Results and Discussion

Catalytic hydropyrolysis of beech wood was conducted in a fluid bed reactor at 450 °C and 26 bar pressure. Using $MgAl_2O_4$ (MgAl) as support the CoMo loading was varied between 4 and 12 wt.% with a Co/Mo ratio of 0.3 mol/mol. The effect of the support acidity was tested by maintaining a CoMo loading of 4 wt.% and testing two supports consisting of zeolite (H-ZSM-5) mixed with alumina, denoted at CoMoZA#1 and CoMoZA#2. CoMoZA#2 contained 44 % more zeolite than CoMoZA#1.

Increasing the CoMo loading from 4 to 12 wt.% decreased the condensable organic yield from 25.2 to
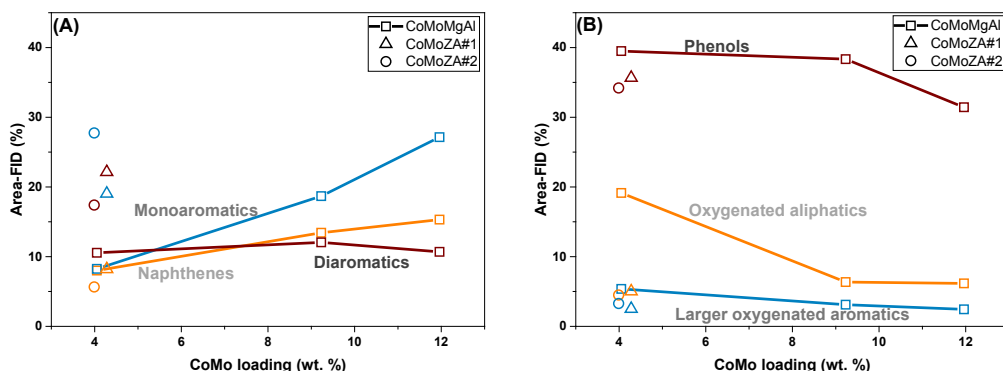
to alumina ratio. The results thus show that the oxygen content in the organic phase can be decreased both by using a higher metal loading and by increasing the support acidity.

Conclusion

This study confirms that catalytic hydropyrolysis is an attractive route for biomass to liquid transportation fuels. Most of the hydrogenation takes place during the catalytic hydropyrolysis, but a second reactor is needed in order to obtain an oxygen free oil. Furthermore, using a more acid support material leads to a decreased oxygen content in the organic phase and increases the alkylation activity, and thus can increase the

Figure 2 Effect of the CoMo loading and support acidity on the concentration of napthenes, mono and diaromatics (A), and oxygenates (B).

22.7 wt.% dry ash free (daf) while increasing the C_1-C_3 yield from 10.3 to 14.0 wt.% daf, as shown in Figure 1. Using CoMoZA#1 and CoMoZA#2 decreased the condensable organic yield to 24.4 and 23.9 wt.% daf, respectively. The C_1-C_3 gas yield also increased to 13.0 wt.% daf for CoMoZA#1 and 13.9 wt.% daf for CoMoZA#2 mainly due to an increase in the C_2-C_3 yield.

Analysis of the condensed organic phase showed that the concentration of monoaromatics and napthenes increased with increasing CoMo loading, while the concentration of oxygenates decreased, see Figure 2. Using CoMoZA#1 and CoMoZA#2 efficiently removed the oxygenated aliphatics, and increased the concentration of aromatics. The increased yield of aromatics was ascribed to higher alkylation activity for the zeolite based catalysts, which lead to an incorporation of the short oxygenates into the condensable organics. Furthermore, increasing the CoMo loading from 4 to 12 wt.% decreased the total oxygen content in the condensed organics from 9.0 to 4.7 wt.% dry basis (db) (see Table 2), while increasing the support acidity decreased the oxygen content to between 5.2 and 6.1 wt.% db, depending on the zeolite

condensable organic yield.

References

[1] Stummann, M.Z., Høj, M., Schandel, C.B, Hansen, A.B., Wiwel, P., Jensen, P.A., and Jensen, A.D. *Biomass Bioenergy* 115, 97 (2018)

[2] Marker, T.L, Felix, L.G., Linck, M.B., and Roberts, M.J. *Environ. Prog. Sustain. Energy.* 31, 31 (2011)

[3] Hurt, M.R., Degenstein, J.C., Gawecki, P., Borton II, D.J., Vinueza, N.R., Yang, L., Agrawal, R., Delgass, W.N., Ribeiro, F.H., and Kenttämaa, H.I. *Anal. Chem.* 85, 10927 (2013)

[4] Dayton, D.C., Carpenter, J., Farmer, J., Turk, B., and Gupta, R. *Energy Fuels* 27, 3778 (2014)

Table 1. Metal loading and oxygen content in the produced organic phase

	CoMoMgAl#1	CoMoMgAl#2	CoMoMgAl#3	CoMoZA#1	CoMoZA#2
CoMo (wt.%)	4.0	9.2	12.0	4.3	4.0
O (wt.% dry basis)	9.0	6.2	4.7	5.2	6.1

Li Sun

Phone:	+45 4525 2876
E-mail:	lsun@kt.dtu.dk

Supervisors:	Georgios M. Kontogeorgis
	Xiaodong Liang
	Nicolas von Solms

PhD Study

Started:	October	2016
To be completed:	September	2019

Modeling of Gas Solubility in Tetra-n-butyl Ammonium Bromine Aqueous Solution with the Electrolyte CPA Equation of State

Abstract

Study of gas solubility in aqueous solution is important for modeling of semi-clathrate hydrates systems. This work presents the thermodynamic study of the gas (carbon dioxide, nitrogen, methane) in Tetra-n-butyl ammonium bromide aqueous solution with the electrolyte Cubic-Plus-Association Equation of State. The adjustable interaction parameters between ions and gas are obtained by fitting the experimental data of gas solubility in aqueous solutions. The results show that this model can satisfactorily correlate gas solubility, with the relative average deviations being 7.2% and 6.9% for carbon dioxide system and methane system, respectively.

Introduction

Carbon dioxide (CO_2) and Methane (CH_4) are the main gases which cause greenhouse effect, and Nitrogen (N_2) is one of the major components of flue gas emitted from power-plants. The separation of these three gases is important for environmental protection. The difference in affinity between gases in the hydrate formation cause the difference between hydrate formation pressures of different gases, and the hydrate-based gas separation (HBGS) process is based on this theory. Compared to usual hydrates, semi-clathrate hydrates (SCH) are more stable, and SCH can be formed at room temperature and low pressure, with better thermal and low-pressure stability. Tetra-n-butyl ammonium bromide (TBAB) is the most studied additive for semi-clathrate hydrate. Study of gas solubility in TBAB aqueous solution is important for modeling semi-clathrate hydrates systems, and then for potential industrial application.

Gas Solubility in TBAB Aqueous Solution

For CO_2 solubility in TBAB aqueous solution, on the one hand, Kamata et al. [1] reported that when TBAB mass fraction is 10%, the CO_2 solubility was almost equal to that in pure water at atmospheric pressure. On the other hand, some researchers [2, 3] found that the presence of TBAB has subtle effects on gas solubility of CO_2 in water, and gave the complicated salting-in and salting-out regions. Muromachi et al. [4] measured N_2 solubility in TBAB aqueous solution at different temperature and salt concentration. The measurement errors of N_2 solubility is larger due to the small solubility values [4].

Muromachi et al. gave the salting-in and salting-out regions. For CH_4 solubility in TBAB aqueous solution, Wen and Hung's results [5] showed a decrease in salting-in, but Feillolay and Lucas' results [6] showed an increase in salting-in as the electrolyte molality increases.

Thermodynamic Model

In this work, the electrolyte Cubic-Plus-Association (e-CPA) equation of state proposed by Maribo-Mogensen et al. [7] is used. e-CPA includes the electrostatic contributions from the Debye–Hückel theory (which accounts for the long-range interaction of the ions), and the Born equation (which accounts for ion solvation). The classical van der Waals one-fluid mixing rule is used for mixtures of solvents, while the Huron-Vidal/NRTL (HV-NRTL) infinite pressure mixing rule is used for ion solvent interactions. The model of relative static permittivity in e-CPA eliminates the effect of kinetic depolarization, and the values of relative static permittivity calculated by e-CPA can be directly used for thermodynamic modeling of electrolytes.

Modeling Results and Discussion

This modeling work is based on the fluid phase modeling work for TBAB aqueous solutions [8], the properties of pure components and e-CPA parameters of TBAB aqueous solution binary system are from the former work in CERE. In this work, the salt-specific approach (cation-gas interaction parameter and anion-gas interaction parameter are same) is used, the temperature dependence of interaction energy parameters is neglected. There is

only one adjustable parameter for one TBAB + H_2O + gas ternary system: interaction parameter between ions and gas at 298.15 K, the adjustable parameter is obtained by fitting gas solubility data at different temperatures. the modeling results of gas solubility in TBAB aqueous solution are in Table 1. Figure 1 and Figure 2 show performance of CO_2 solubility in TBAB aqueous solution.

Table 1: Modeling results of gas solubility in TBAB aqueous solution with e-CPA*.

Gas	Data Points	$U_{ion-gas}/R$ [K]	RAD
CO_2	60 [2] 85 [3]	535	7.2%
N_2	36 [4]	1045	17.0%
CH_4	13 [6]	90	6.9%

*$U_{ion-gas}$ is the interaction parameter between ion and gas at 298.15 K, RAD is relative average deviations.
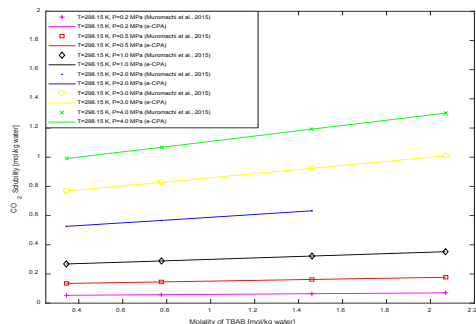

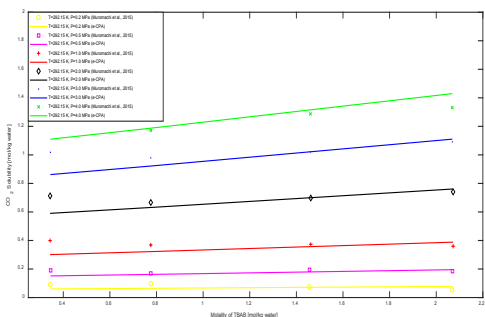**Figure 1:** Predicted CO_2 solubility in TBAB aqueous solution at T=298.15 K.

Figure 2: Predicted CO_2 solubility in TBAB aqueous solution at T=292.15 K.

It can be seen from Figure 1 and Figure 2, the CO_2 solubility increase continuously with salt concentration at high pressure. For CO_2 and CH_4 systems, e-CPA can

predict the gas solubility in TBAB aqueous solution well. The deviation of N_2 system is large, probably mainly because the measurement error is relatively large.

For all the three systems, the solubility deviations mainly happen in low salt concentrations, especially for CO_2 and CH_4 systems. The order of regression interaction parameter is: $N_2 > CO_2 > CH_4$, it is corresponding to the reverse order of gas dissolving capacity.

Conclusion

The salt effect of TBAB + gas + H_2O system is complex, which comes from temperature, pressure, salt concentration and these factors affect hydrophobic interactions, interstice and solvation. e-CPA can reasonably describe the salt effect. To clarify the salt effects clearly and accuracy, accurate solubility data are required.

Reference
[1] Y. Kamata, Y. Yamakoshi, T. Ebinuma, H. Oyama, W. Shimada, H. Narita, Hydrogen sulfide separation using tetra-n-butyl ammonium bromide semi-clathrate (TBAB) hydrate, Energy & Fuels, 19 (2005) 1717-1722.
[2] S. Muromachi, A. Shijima, H. Miyamoto, R. Ohmura, Experimental measurements of carbon dioxide solubility in aqueous tetra-n-butylammonium bromide solutions, The Journal of Chemical Thermodynamics, 85 (2015) 94-100.
[3] W. Lin, D. Dalmazzone, W. Fürst, A. Delahaye, L. Fournaison, P. Clain, Thermodynamic studies of CO2+ TBAB+ water system: experimental measurements and correlations, Journal of Chemical & Engineering Data, 58 (2013) 2233-2239.
[4] S. Muromachi, H. Miyamoto, R. Ohmura, Solubility of Nitrogen Gas in Aqueous Solution of Tetra-n-Butylammonium Bromide, International Journal of Thermophysics, 38 (2017) 173.
[5] W.-Y. Wen, J.H. Hung, Thermodynamics of hydrocarbon gases in aqueous tetraalkylammonium salt solutions, The Journal of Physical Chemistry, 74 (1970) 170-180.
[6] A. Feillolay, M. Lucas, Solubility of helium and methane in aqueous tetrabutylammonium bromide solutions at 25 and 35. deg, The Journal of Physical Chemistry, 76 (1972) 3068-3072.
[7] B. Maribo-Mogensen, G. Kontogeorgis, K. Thomsen, Development of an Electrolyte CPA Equation of state for Applications in the Petroleum and Chemical Industries, Technical University of Denmark, Department of Chemical and Biochemical Engineering 2014.
[8] L. Sun, X. Liang, N.v. Solms, G.M. Kontogeorgis, Modeling Tetra-n-butyl Ammonium Halides Aqueous Solutions with the Electrolyte CPA Equation of State, Fluid phase equilibria, submitted for publication.

Casper Stryhn Svith

Phone: +45 2077 2056
E-mail: cassvi@kt.dtu.dk

Supervisors: Kim Dam-Johansen
Hao Wu
Weigang Lin

PhD Study
 Started: September 2016
 To be completed: September 2019

Cyclone reactors: experimental and modeling study

Abstract
The main objective of this study is to obtain fundamental knowledge needed for utilization of cyclone reactors for industrial applications. This is achieved through experimental work in a pilot-scale cyclone reactor, as well as through modeling work based on chemical engineering models and computational fluid dynamic (CFD) models.

Introduction
Cyclone reactors are used in various industries for different applications, such as ore refining in the metals industry, raw meal preconditioning and emission reduction in the cement industry, and flue gas cleaning in the power industry.

A cyclone itself is a continuous and versatile separation device. The simple design makes it popular for application in harsh environments with extreme temperature, abrasion and corrosion.

The use of cyclones as reactors provides an opportunity for process intensification. Furthermore, the highly turbulent swirling flow of the gas phase provides intense mixing as well as separation of the solid phase from the gas phase. A cyclone reactor can be used for both homogenous and heterogeneous reactions in and/or between the gas and solid phase. The main principle of a cyclone reactor for a gas-solid system is sketched in Figure 1. Typically cyclones reactors have short gas residence times and long particle residence times. An increase in gas flowrate would reduce the gas mean residence time but increase the solid residence time [1]. This makes a cyclone reactor especially interesting for application involving gas-solid reactions where secondary reactions of the gaseous products should be minimized, for example in flash pyrolysis.

Extensive research has been carried out for cyclones as separators. However, despite the various application of cyclone reactors in industry, the literature on the subject is scarce and only few authors have developed generalized reactor models for cyclone reactors, which generally have not been validated for different cyclone geometries.
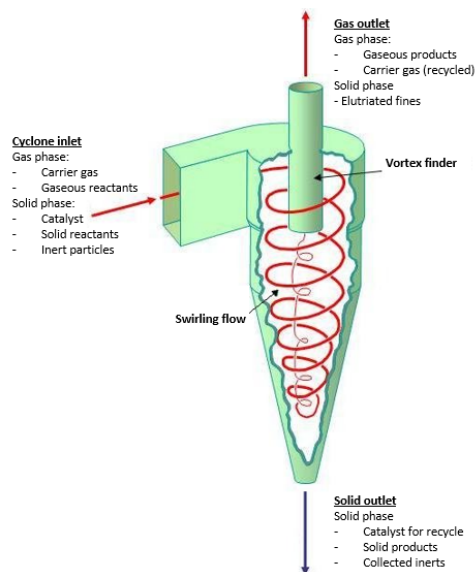

**Figure 1:** Cyclone reactor principle for gas solid systems

Specific objectives
The main objective of the PhD project is to study the important phenomena, such as gas phase mass transfer, mixing and gas-solid interactions in cyclones through pilot-scale experimental work, and modeling of both pilot and industrial scale applications.

Based on the data collected and knowledge obtained through the experimental and modeling work, reactor models for cyclone reactors will be developed and validated, and will be used for designing and optimizing cyclone reactors.

Methods

The gas phase mixing in cyclone reactors, are being investigated using a model reaction with a known kinetic model. The selective non-catalytic reduction (SNCR) process, with the global reaction mechanism shown below [2], has been chosen as the model reaction system.

$$4\,NO + 4\,NH + O_2 \rightarrow 4\,N_2 + 6\,H_2O$$
$$4\,NH_3 + 5\,O_2 \rightarrow 4\,NO + \; 6\,H_2O$$
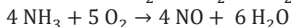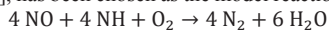
This is an existing application in industrial combustion plants such as circulating fluidized bed boilers etc. giving results a direct industrial relevance and comparison.

Pilot-scale experiments measuring the overall SNCR performance, as well as the internal concentration profiles of NO and ammonia, have been conducted using the setup illustrated in Figure 2. The setup was built here at DTU and have modified as part of the PhD project, in order to ensure operational stability and the quality of the measurements. A range of different operational conditions, have been investigated, including, inlet temperature, gas velocity, reactant concentrations and particle feeding rates.
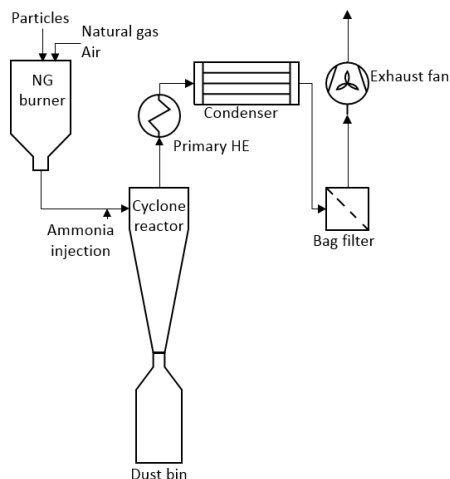
Figure 2: Overview of Cyclone reactor pilot setup

Ideal reactor models (CSTR and PFR) and simple residence time based reactor network models [3] are used to simulate the experimental data using both simple and detailed reaction kinetics.

Results and Discussion

Interpretation of both modeling results and measurement data and the differences between them, can give insight into the cyclone mixing patterns and their effect on the reactors conversion efficiency. This is used to develop more complex but realistic models and give answers on how to more effectively utilize cyclone reactors.

Figure 3 shows an example of simple outlet measurements compared with the results from the simple models for cyclone reactors available today. This clearly shows that non of the existing models can reproduce both the conversion of NO and NH_3 with sufficient accuracy.
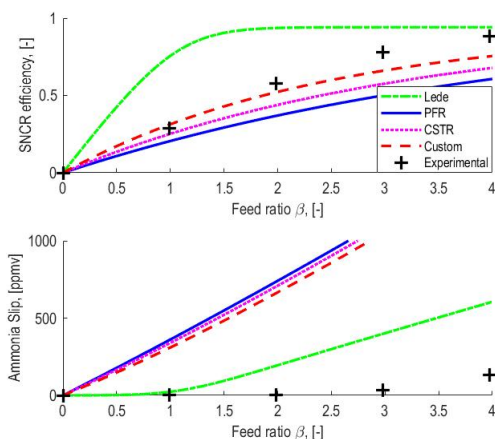
Figure 3: Experimental results and simple kinetic and reactor modeling results. With inlet temperature of 950 °C and NO concentration of 450 ppm

A new reactor network model is currently being developed using the gathered experimental data as well as literature data, while additional experimental work with a wide range of operational conditions continues in parallel.

Conclusions

There is a gap in the knowledge available about cyclones behavior as a reactor and what is needed for meaningful modeling of cyclone reactors for design and optimization purposes.

A pilot scale cyclone reactor setup for studying SNCR reactions and cyclone reactor properties, has modified and used to measure the effect of various operation conditions on the reactor performance. The data collected can be used to develop better models and improve the efficiency and design of cyclone reactors.

Future work

The steps to follow in the future are:

- Develop and test improved reactor network models
- Extend and generalize the developed model based on CFD results
- Study the influence of cyclone design on the reactor efficiency of cyclone reactors

References

1. J. Lede, H.Z. Li, F. Soulignac, J. Villermaux, Chem. Eng. Process 22 (1987) 215-222.
2. W. Duo, K. Dam-Johansen, K. Østergaard, Can. J. Chem. Eng. 70 (1992) 1014-1020
3. J. Lede, H.Z. Li, J. Villermaux, Chem. Eng. J. 42 (1989) 37-55

Joachim Thrane

Phone: +45 4525 2848

E-mail: joathr@kt.dtu.dk

Supervisors: Anker Degn Jensen

Martin Høj

Max Thorhauge, Haldor Topsøe A/S

PhD Study

Started: November 2017

To be completed: October 2020

Novel Catalysts for the Selective Oxidation of Methanol to Formaldehyde

Abstract

Various catalysts for the selective oxidation of methanol to formaldehyde have been synthesized, and their performance as catalysts have been investigated in a lab scale plug flow reactor setup. Molybdenum containing catalysts have the highest selectivity, but also vanadium containing catalysts have good selectivity. The 4.7 wt% MoO_3/HAP was shown to be more stable in a 40 h test, compared to the more initially more selective 25.8 wt% MoO_3/HAP.

Introduction

Formaldehyde is the most significant aldehyde commercially available as it is an irreplaceable C1 building block for higher-valued products due to its high reactivity [1]. The annual global production of formaldehyde are expected to increase with a CAGR of 4.8-5.8% and reach a market of 36.6 million tons by 2026 [2, 3]. Formaldehyde is mainly produced through either the silver process or the Formox process [1].

In the Formox process, the formaldehyde is formed over an iron molybdate catalyst (MoO_3/$Fe_2(MoO_4)_3$), which achieve high selectivities (92-95%) at high conversions (>99%) [1]. The catalyst, however, is not stable during reactions conditions due to formation of volatile molybdenum compounds [4]. It is thus of interest to develop novel, more stable catalysts for the oxidation of methanol to formaldehyde.

Specific Objectives

The objective of the overall PhD project is to investigate and develop new catalysts for the selective oxidation of methanol to formaldehyde. For the first part the goal was to investigate and establish the performance of state of the art catalysts found in the literature.

Experimental

Various catalyst systems have been prepared by methods such as impregnation, co-precipitation, citric acid-based sol-gel method and a reflux procedure. The samples were characterized by XRD and BET. The catalysts were tested in a fixed bed reactor with catalyst loadings of 10-50 mg. The feed flow consists of 15 NmL/min of O_2, 127.5 NmL/min of N_2 and methanol added through a bubble flask at 6 °C leading to a methanol feed concentration of 3.5-5%. Measurements were performed at app. 250 °C, 300 °C, 350 °C and 400 °C. Experiments with longer time on stream were done for some samples to investigate their stability. The effluent gas was analyzed using a gas chromatograph.

Results and Discussion

Figure 1 shows the DME corrected selectivity (DME is considered as two methanol when calculating selectivity) against the conversion of methanol for the catalysts containing molybdenum together with results for an industrial iron-molybdate catalyst.
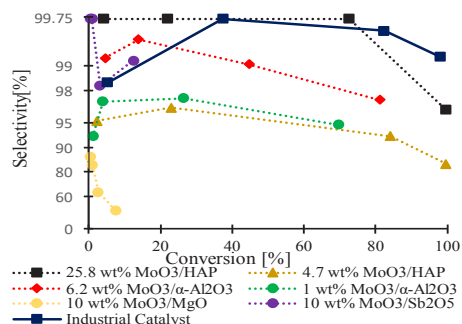

Figure 1. DME corrected selectivity to formaldehyde for molybdenum containing catalysts as function of conversion obtained at temperatures 250 °C, 300 °C, 350 °C and 400 °C.

Figure 2, shows similar results vanadium containing catalysts. It can be seen from Figure 1 and Figure 2 that catalysts with high selectivities at low conversions have been found. When looking at catalysts not containing Mo or V the results are as shown in Figure 3.
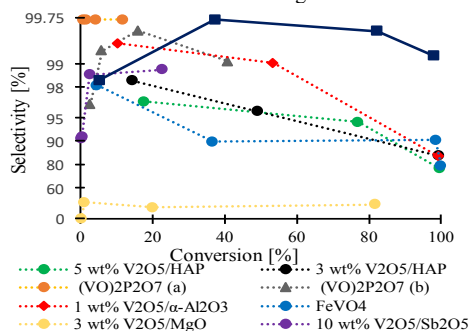

Figure 2. DME corrected selectivity to formaldehyde of vanadium containing catalysts as function of conversion obtained at temperatures 250 °C, 300 °C, 350 °C and 400 °C.
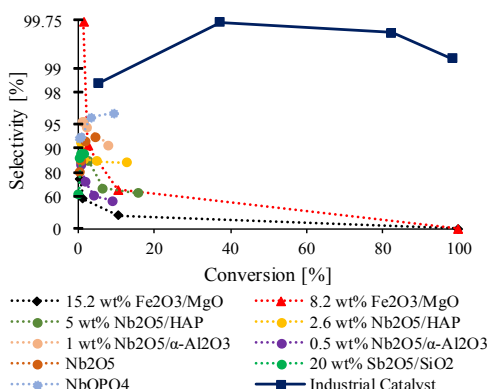

Figure 3. DME corrected selectivity to formaldehyde of catalysts not containing molybdenum or vanadium as function of conversion obtained at temperatures 250 °C, 300 °C, 350 °C and 400 °C.

It can be seen that none of the investigated systems in Figure 3 show promising selectivity. From Figure 1 and Figure 2, especially the 25.8 wt% MoO_3 supported on hydroxyapatite (HAP) is interesting, since it performs better than the industrial catalyst at conversions below 80% (temperatures below 350 °C). It can also be seen, that some of the vanadium containing catalysts have better DME corrected selectivity than the industrial catalyst at low conversion (low temperature). However, the selectivities at higher conversions for the vanadium based catalyst are generally not as high as for the molybdenum based catalysts. In most cases the vanadium catalysts have higher activity than the molybdenum based catalysts. This is also the case for the vanadium oxide (3 or 5 wt%) on hydroxyapatite catalysts.

The main problem for the ferric molybdate catalyst however, is not selectivity and activity, but stability. This was further investigated for the catalyst with activity and selectivity similar to the industrial catalyst, and are shown in Figure 4. It can be seen that the 4.7 wt% MoO_3/HAP seems to be more stable, though the initial selectivity is lower.
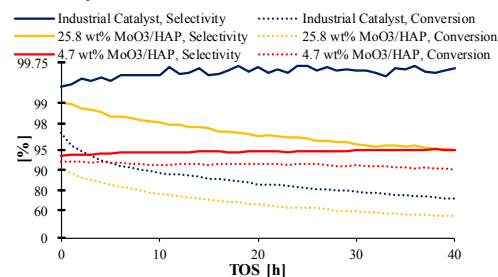

Figure 4. DME corrected selectivity to formaldehyde and methanol conversion, of MoO3/HAP systems compared with industrial catalyst over 40 h on stream.

Conclusions

A range of different catalysts have been synthesized and tested for selective oxidation of methanol to formaldehyde. In general, the Mo-based catalysts are more selective than the V-based catalysts, which are more selective than the catalysts not containing Mo or V. The screening indicated that a catalyst with 25.8 wt% MoO_3 on HAP has promising activity and selectivity, similar to an industrial iron molybdate catalyst, but a long term test showed that a low loading MoO_3/HAP was more stable.

References

1. A. W. Franz et al., Formaldehyde, Ullmann's encyclopedia of industrial chemistry, 2016, p. 1-34.
2. https://www.prnewswire.com/news-releases/global-formaldehyde-market-2018-2022-300633054.html, Accessed: 10.11.2018
3. https://www.transparencymarketresearch.com/form aldehyde-market.html, Accessed: 10.11.2018
4. B. I. Popov, V. N. Bibin, B. K. Boreskov, Study of an Iron-Molybdenum oxide catalyst for the oxidation of methanol to formaldehyde. IV. Entrainment of Molybdenum from the catalyst, the main reason for the decrease in its activity during use, Kinetika i Kataliz 17 (2) (1976) 371-377

Jiahuan Tong

Phone: +45 5273 1884
E-mail: jito@kt.dtu.dk

Supervisors: Nicolas von Solms
Suojiang Zhang
Xiaodong Liang

PhD Study
Started: March 2018
To be completed: March 2021

Theory, Simulation and Models for Electrolyte Systems with Focus on Ionic Liquids

Introduction

Electrolytes are an indispensable element in energy storage since the positive and negative electrodes are interconnected by an electrolyte that determines the charge transport during the charge/discharge process. Ideal electrolytes should fulfill the following requirements: wide voltage window, excellent electrochemical stability, high conductivity, high ionic concentration, small solvated ionic radius, low viscosity, environmental friendliness, low cost, and easy availability with high purity.[1,2]

The development of new electrolytes plays essential roles in the capacity, life expectancy, and safety of the batteries, e.g. in energy storage field, which support the development of green energies for a sustainable society. Ionic liquids are among the best candidates as additives or co-solvents used in batteries because of their unique physico-chemical properties such as wide potential window, high thermal stability, negligible vapour pressure (i.e., neither flammable nor volatile), relatively high ionic conductivity and electrochemical stability. In recent years, many researchers focus on developing new types of ionic liquids to improve the performances of new lithium batteries.

In this project, in order to deeply understand the molecular mechanism of the ionic liquids electrolytes. Screen and design suitable ionic liquids for electrolytes and develop a series of models of ionic liquid electrolytes with high electrochemical properties to help guide the experiment and application.

Project contents

This project will include the following contents (Fig.1):
1. Select several kinds of ionic liquids which have excellent conductivity and electrochemical window for ionic liquids electrolytes via COSMO-RS simulations.

2. Design the structure of cations and anions for potential ionic liquids and optimize structures using the software of Gaussian.
3. Establish models of ionic liquid electrolytes that consist of different type of ionic liquids as solvents and different lithium salts.
4. Investigate the relationship between the type of ionic liquids and the performance of electrolytes by molecular dynamics simulation, and determine the optimal type of ionic liquids for ionic liquid electrolytes.
5. Develop complex systems in ionic liquids electrolytes, containing different type of ionic liquids, organic solvents (ethylene carbonate, dimethyl carbonate, diethyl carbonate, ethyl methyl carbonate, etc.) and lithium salts at over wide ranges of temperature and concentration.
6. Compare properties of electrolyte (conductivity, electrochemical window, transport property, etc.) in different kinds and content of ionic liquids by molecular dynamics simulation to determine the optimal content of ionic liquids for ionic liquid electrolyte.
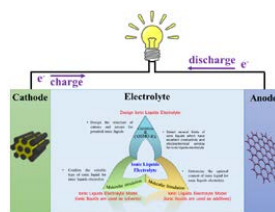

Figure 1. Project overview

In this work, molecular dynamic simulations of LiTFSI-organic electrolyte systems are carried out.

Parameters of simulation model

The simulation system is constructed with 2 mol/L LiTFSI and five kinds of solvents (Fig. 2). The system is

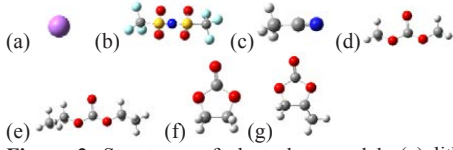in a cubic box with a dimension of 34 Å in length, width and height.

Figure 2. Structures of electrolyte model: (a) lithium (Li$^+$) (b) [bis(trifluoromethanesulfonyl)imide anion] (TFSI$^-$) (c) acetonitrile (ACN) (d) dimethyl carbonate (DMC) (e) diethyl carbonate (DEC) (f) ethylene carbonate (EC) (g) propylene carbonate (PC)

Simulation details

All molecular dynamic simulations were performed with the Gromacs package. The OPLA force field was used in all simulations. The initial configuration of the simulated mixture was constructed using Packmol. Then system was equilibrated in NVT ensemble for 5ns at 298K and 313K. After a further equilibration of 5ns in NPT ensemble at 1 atm pressure, the production run was carried out for 30ns in NPT ensemble and 10 ns in NVE ensemble with the final configuration. The periodic boundary condition was employed in all the three directions and the equation of motion was integrated with a time step of 1.0 fs using the velocity Verlet algorithm. The trajectories were saved every 0.1ps for further analysis. The short range van der Waals interaction was treated with Lennard-Jones potential and the long range electrostatic potential was dealt with Particle Mesh Ewald (PME) technique.

Results and discussion
Diffusion Property

In this project, mean-square displacement is obtained via the Einstein-Smoluchowski equation

$$\lim_{\Delta t \to \infty} \frac{\langle MSD(\Delta t) \rangle}{6 \Delta t} \qquad (1)$$

Where $MSD(\Delta t)$ is the mean-square displacement, $<>$ denotes the ensemble average, Δt is the time interval.

Therefore, we calculate the MSD for five different systems by MD simulations. In Fig. 3, we compare the MSD of Li$^+$, TFSI$^-$ at 298K and 313K for the LiTFSI-PC system. The results show that the MSD for both cation and anion increases as the temperature increases.
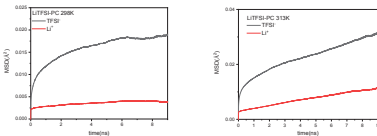

Figure 3. Mean square displacements of LiTFSI-PC

Conductivity

In this research, the conductivity of electrolyte is calculated according to the following formula

$$\sigma_{tot} = \lim_{t \to \infty} \frac{1}{6tVK_bT} \sum_{i,j}^{N} \langle (q_i[R_i(t) - R_i(0)]) \cdot (q_j[R_j(t) - R_j(0)]) \rangle \quad (2)$$

where the sum runs over all cations and anions i, j. N is the number of ions in the system, V is the volume of the simulation box, K_b is the Boltzmann's constant, T is the temperature, q_i is the charges of ion i, $R_i(t)$ is the position of the ith ion at time t, the brackets $<>$ denote the ensemble average.

The total conductivity into self and distinct terms by separating the sum in eq (2) into diagonal and off-diagonal contributions so that

$$\sigma_{tot} = \sigma_{cat}^s + \sigma_{an}^s + \sigma_{cat}^d + \sigma_{an}^d + \sigma_{cat,an}^d \qquad (3)$$

Therefore, the program of conductivity was written by Python language. The results of conductivity for three different systems are presented in Table 1.

Table 1. Results of conductivity (S/m) for all systems

conductivity	ACN	EC	PC	DEC	DMC
	298K	313K	298K	298K	298K
σ_{cat}^s	9.426	1.595	5.239	0.025	7.694
σ_{an}^s	2.466	0.911	1.522	1.069	2.042
σ_{cat}^d	-4.292	1.416	6.189	2.941	-3.441
σ_{an}^d	-2.271	-0.763	-1.286	-0.486	-1.661
$\sigma_{cat,an}^d$	0.0001	0.002	-0.018	-0.006	-0.013
σ_{tol}	5.329	3.161	11.645	3.543	4.621

All the conductivities for the five systems at 298K were shown in table 1. We could find that the LiTFSI-PC have the largest value at 298K. More important, the conductivity decreases as the number of methyl group increases at the same temperature for both the chain and ring structure electrolyte.
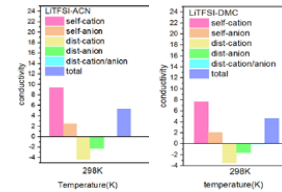

Figure 4. Contribution of self and distinct conductivity

In order to explore which items in eq (2) have a greater impact on the results. We calculated five types (cation(self), anion(self), cation(dist), anion(dist), cation/anion (dist)) contribution to the total value for LiTFSI-ACN and LiTFSI-DMC system and shown in Figure 4. The results show that the cation(self) and anion(self) have a greatest contribution.

Conclusion

It can be seen from the presented results that for LiTFSI-organic solvent electrolyte systems diffusion property increases as temperature increases. At the same temperature, the conductivity decreases as the number of methyl group increases.

References
1. I. Nezbeda, F. Moucka, W.R. Smith, Mol. Phys. 114 (2016) 1665-1690. J. Yu, S. M. Chen, W. J. Hao, S. J. Zhang, ACS Nano 10 (2016) 2500-2508.
2. C.G. Hanke, S.L. Price, R.M. Lynden-Bell, Mol. Phys 99 (10) (2001) 801–809.

Mauro Torli

Phone: +45 50 15 59 12
E-mail: mtor@kt.dtu.dk

Supervisors: Philip L. Fosbøl
Georgios M. Kontogeorgis

PhD Study
Started: June 2016
To be completed: May 2019

Thermodynamics, Design, Simulation and Benchmarking of Biofuel Processes

Abstract
Currently sugarcane and corn represent the two sources from which the largest share of ethanol is produced worldwide. However, the availability of those agricultural feedstocks is limited, because of competition with food production, arable land usage, and water availability. Forest residues, trees from plantations, straws, grasses and other agricultural residues may become a viable feedstocks for bio fuel production, but the very heterogeneous nature of these materials makes them inconvenient for bioconversion. An alternative bioconversion method which can solve the issues related to the heterogeneity of the raw materials is biomass gasification to syngas, followed by fermentation to biofuel. This relative new technology is extremely flexible and it has been applied, not only to the conversion of a large variety of biomasses, but also to the conversion of municipal solid waste and steel mill off-gas to biofuel.

Introduction
This PhD project is part of a large innovation action, SYNFERON, whose technology focuses are: fermentation of syngas to liquid and gaseous (methane) biofuels, design of novel bioreactors, pressure control and use of suitable surfactants for increasing the gas/liquid mass transfer efficiency, use of biomimetic membranes and development of diabatic distillation for gentle and cost-efficient purification of liquid biofuels and development of an optimized process design and comparison with existing technologies.

This PhD project is encompassed in the fourth work package of SYNFERON; and the objectives are: investigation of the current technologies in syngas fermentation for fuel production, develop and validate a thermodynamic model parameter base optimized for the biofuel processes, collecting data and models from literature and from the other team members and implement them in the process simulations.

Syngas fermentation process involves the gasification of biomass to syngas (mainly CO and H_2), which is then fermented by acetogenic bacteria to produce ethanol, acetic acid or other chemical commodities. The rate-limiting step of syngas fermentation is the gas-to-liquid mass transfer, and mass transfer limitations are expected to be even more severe than in the ordinary aerobic fermentation based on glucose. In fact, CO and H_2 solubilities are only 60% and 4% of O_2, and, in comparison to traditional sugar-to-ethanol fermentation,

more moles of gas must be transferred per carbon equivalent consumed. One way to increase the dissolution rate of the syngas in the fermenter medium is to increase the driving force for the mass transfer and this may be accomplished by raising the partial pressure of the syngas. For these conditions the Henry's law may not be sufficient for estimating the vapor-liquid equilibrium at high solute concentration, especially above 5-10 bar and for molar fractions larger than 0.03.

Specific Objectives
This work is focused on the thermodynamic modeling of 15 gas-solvent systems which are of relevance for process simulation studies in connection with the biological synthesis of biofuels from syngas. A model is presented which describes the solubility of CO, H_2, CO_2, CH_4 and N_2, i.e. the main component of biomass derived syngas, in combination with the three polar hydrogen bonding solvents: water, ethanol and acetic acid involved in the fermentation, both as solvents and reaction products. The selected method is γ-φ approach: UNIQUAC-Peng-Robinson (PR) for system containing water and ethanol, and UNIQUAC-Hayden-O'Connell Virial EoS for systems containing acetic acid.

The data regression is performed with additional constraints on the supercritical component standard state fugacities and, on the same thermodynamic basis; a new approach for gas solubility in mixed solvents is derived.

Results and Discussion

In the γ-φ approach the vapor liquid-equilibrium of supercritical components are commonly treated according to the un-symmetric convention, Eq. (1). The symmetric framework, Eq. (2), is generally more versatile, as for all components the reference state does not depend on the system composition. A fundamental problem in the application of the un-symmetric approach to gas solubility calculations is the difficulty in estimating the pure liquid reference fugacity $f_g^{hyL}(T,P)$ [1]; as, unlike subcritical substances, for a gas this property cannot be obtained from pure component data alone. Indeed, the symmetric convention has been applied to gas solubility equilibrium as well, although only in few studies. One approach involves the estimation of the hypothetical liquid fugacities from the generalized plots provided by Prausnitz and Shair [2].

In the present study the UNIQUAC model is applied, according the un-symmetric convention, to describe the vapor liquid equilibria of 14 gas-solvent systems of interest for the syngas fermentation process. An additional constraint on the standard fugacity of the supercritical components is implemented in the data regression in order to provide a thermodynamically consistent model, and possibly avoid obtaining ill-defined parameters. The constraint involved in the model parameter estimation is reported in Eq. (4). This relation can be easily derived equating Eq. (1) and Eq. (2) at the limit of infinite dilution, $x_g \to 0$.

$$(1)\ \hat{f}_g^{V}(T,P,\mathbf{n}) = H_g(T,P,\mathbf{n}_k)_{k \neq g}\, x_g\, \gamma_g^*(T,\mathbf{n})$$

$$(2)\ \hat{f}_g^{V}(T,P,\mathbf{n}) = f_g^{hyL}(T,P)\, x_g\, \gamma_g(T,\mathbf{n})$$

$$(3)\ H_g(T,P,\mathbf{n}_k)_{k \neq g} \lim_{x_g \to 0} x_g\, \gamma_g^*(T,\mathbf{n}) = f_g^{hyL}(T,P) \lim_{x_g \to 0} x_g\, \gamma_g(T,\mathbf{n})$$

$$(4) \Rightarrow H_g(T,P,\mathbf{n}_k)_{k \neq g} / \gamma_g^{\infty}(T,\mathbf{n}_k)_{k \neq g} = f_g^{hyL}(T,P)$$

$H_g(T,P,\mathbf{n}_k)_{k \neq g}$ is the Henry's law constant and $\gamma_g^{\infty}(T,\mathbf{n}_k)_{k \neq g}$ is the symmetric activity coefficient at infinite dilution. The hypothetical reference fugacity, $f_g^{hyL}(T,P)$, was estimated from the correlation provided by Prausnitz and Shair [2]. Eq. (4) implies the invariability of the ratio $H_g(T,P,\mathbf{n}_k)_{k \neq g}/\gamma_g^{\infty}(T,\mathbf{n}_k)_{k \neq g}$ across different systems of the same supercritical component; and consequently can be extended to the prediction of gas solubility in mixed solvents, Eq. (5), as proposed in [1].

$$(5)\ \left(\frac{H_g(T,P,\mathbf{n}_k)_{k \neq g}}{\gamma_g^{\infty}(T,\mathbf{n}_k)_{k \neq g}} \right)_{k=i,j} = \left(\frac{H_g(T,P)}{\gamma_g^{\infty}(T)} \right)_{solvent-i} = \left(\frac{H_g(T,P)}{\gamma_g^{\infty}(T)} \right)_{solvent-j}$$

Figure 1 shows CO_2 solubilities in water for pressure up to 220 bar and temperature up to 333 K. The two isotherms at 293 K and 298 K are plotted only for pressures below the liquid-liquid split.

In Figure 2 the solubility of CO_2 in C_2H_5OH-CH_3COOH mixture at 313 K are predicted for different pressures applying Eq. (5) and the UNIQUAC model with the parameters obtained from the regression of binary data alone (CO_2-C_2H_5OH and CO_2-CH_3COOH systems).
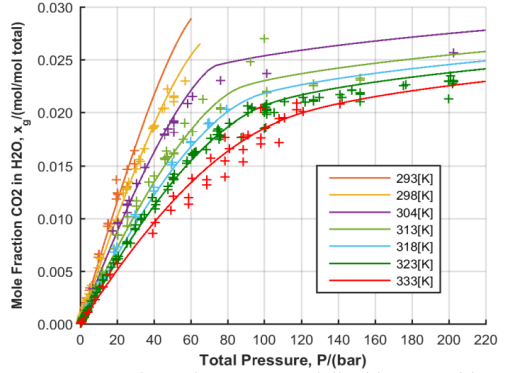

Figure 1: Isothermal pressure and liquid composition data for CO_2-H_2O system up to 220 bar: (+) experimental data and (—) model prediction
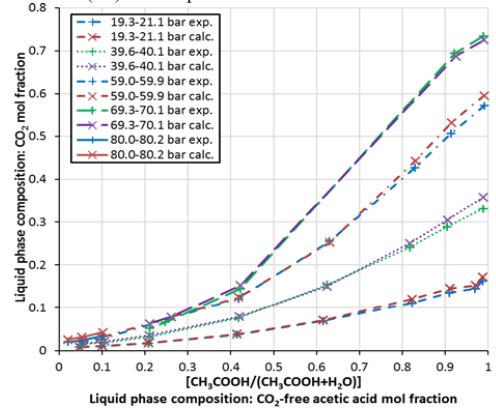

Figure 2: CO_2 mole fraction in the liquid as function of gas-free solvent composition. Experimental (exp.) [3] and calculated (calc.) values for 5 pressure ranges.

Conclusion

The UNIQUAC model was used in the γ-φ approach for correlating vapor-liquid equilibrium for the 14 gas-solvent systems of interest. The results show that the model performs well even at higher temperatures and pressures. The accurate predictions of the VLE behavior for the ternary system CO_2-C_2H_5OH-CH_3COOH prove that the proposed method for the estimation of gas solubilities in mixed solvents is repayable.

References

1. M. Torli, L. Geer, G. M. Kontogeorgis, Philip L. Fosbøl, submitted for publication, (2018).
2. J.M. Prausnitz, F.H. Shair, AIChE J. 7 (1961) 682-687.
3. A.Z. Panagiotopoulos, R.C. Willson, R.C. Reid, J. Chem. Eng. Data. 33 (1988) 321-327.

Burak Ulusoy

Phone: +45 4525 2800
E-mail: bulu@kt.dtu.dk

Supervisors: Kim Dam-Johansen
                Weigang Lin
                Hao Wu

PhD Study
  Started: September 2016
  To be completed: August 2019

NOx formation and reduction in fluidized bed combustion of biomass

Abstract
The focal point of this PhD project is to understand the NOx formation and reduction mechanisms in fluidized bed combustion of biomass. Comprehensive experimental and modelling work will be conducted on laboratory-scale reactors with the goal of minimizing NOx emissions during combustion. The initial part of the project will mainly deal with the NOx formation and reduction during char combustion, which is lesser understood compared to the gaseous NOx chemistry. Following this, lab-scale fluidized bed combustion experiments and modelling will be performed to facilitate the minimization of NOx emissions.

Introduction
Fluidized bed combustion is a promising technology for heat and power production from biomass. Due to the advantages of high fuel flexibility, high combustion efficiency, and low pollutant emission, the application of fluidized bed technology in biomass combustion industry has increased at a fast pace [1]. However, incentives for further reducing the NOx emission from fluidized bed combustion are driven by the harmful environmental impact and strict emissions regulations. It has been well established that upon release to the atmosphere, NOx compounds contribute to global warming, photochemical smog production, and acid rain formation.

In a fluidized bed combustor, the final NO emission is determined by the competing NO formation and reduction reactions. The NO primarily stems from the fuel bound nitrogen either through volatile or char nitrogen oxidation. Analogous to the formation reactions, NO is reduced through homogeneous thermal DeNOx reactions or heterogeneous reduction over char [2]. Controlling the NO emissions requires a thorough understanding of the underlying mechanisms, which is the primary goal of this work.

Objectives
This project aims to achieve a fundamental understanding of the underlying mechanisms of NOx formation and reduction in fluidized bed combustion of biomass. This will be acquired through experimental studies in laboratory-scale reactors, as well as mathematical and computational modelling work to describe the experimental data, which could then serve as

predictive tools or as sub-models in large-scale simulations.

Experimental Work
Continuous combustion experiments of pine wood, beech wood, straw, sunflower husk and seed, and sewage sludge were conducted in a pilot-scale fluidized bed reactor. The impact of fuel properties and co-combustion of selected fuels were examined at air staged and one-stage conditions. In addition, the interaction between ash forming elements and NO_X emission was investigated by combustion of washed and K-doped (KCl, K_2CO_3, and KOH) biomass.

The fluidized bed reactor is illustrated in Figure 1. Heated gas was introduced from the bottom as primary gas, while secondary gas was fed through the feeding tube to facilitate the continuous solid fuel feeding. The reactor temperature was monitored through four temperature sensors located throughout the reactor, while the bed pressure was followed by pressure sensors. The temperature was maintained constant during experimentation by four external heating elements. During experiments the temperature, pressure and outlet concentrations of NO, O_2, CO, and CO_2 were continuously monitored.

At standard conditions, 11.5 NL/min air was introduced as primary gas, while 15.5 NL/min N_2 was fed through the particle feeding tube. In air staged experiments, the amount of air was divided between the primary and secondary inlets, while keeping the total flow constant. The temperature in the bed was kept at 850ºC.
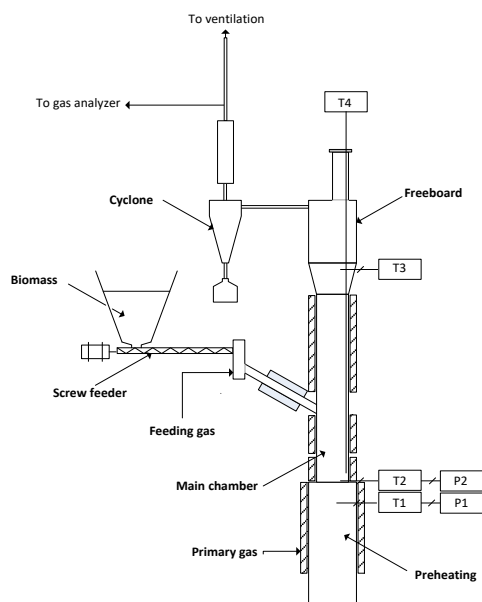
Figure 1: Schematic illustration of the fluid bed reactor.

Results and Discussion

Figure 2 illustrates the conversion of fuel N to NO during fluidized bed combustion of raw, washed, and K-doped biomass under non-staged conditions. The results indicate that the conversion to NO decreased with an increase in fuel nitrogen content. This has previously been reported [3] and attributed to the facilitation of thermal DeNO$_X$ reactions. The results moreover show that the conversion of fuel N to NO increased when washing the straw, and decreased slightly upon K-doping of the washed straw and raw pine wood. The largest influence of K-species was observed in the case of KCl-doped washed straw, showing a significantly lower conversion to NO, while for the pine wood, K-doping did not change the conversion to NO significantly. The effect of KCl was presumed to be indirect through the change in the radical pool and thereby CO concentration.
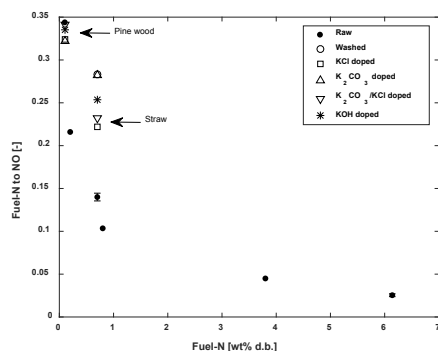

Figure 2: Conversion of fuel nitrogen to NO during fluidized bed combustion at standard conditions.

Figure 3 shows the average NO concentration during co-combustion of fuels in one-stage conditions. The results suggest that the NO emissions from straw-sunflower seed and straw-sunflower husk co-combustion were additive, while a synergy effect was observed in the case of sewage sludge-straw co-combustion. This may be attributed to the catalytic effect of sewage sludge ash on the nitrogen chemistry.
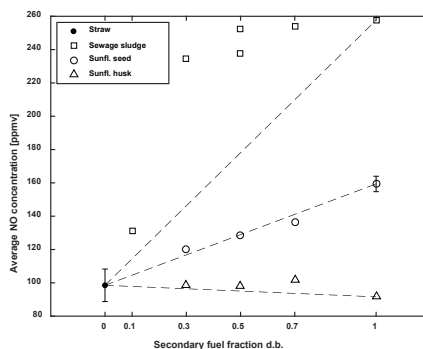

Figure 3: Average NO concentration during co-combustion of straw and other biomass (sunflower and husk, and sewage sludge) at standard conditions.

In air staged ($\lambda_1/ \lambda=0.5$) combustion, a similar synergy effect was observed, although the tendency was less clear than in one-stage combustion.

Conclusion

It was noted that the conversion of fuel N to NO decreased with an increase in fuel nitrogen content. Washing of straw increased the conversion to NO, while KCl doping decreased the conversion.

The ash forming elements in sewage sludge led to a synergy effect during co-combustion with straw, while no interaction was observed during straw-sunflower seed and straw-sunflower husk co-combustion.

Future work

Experiments will be carried out in the lab-scale fluidized bed reactor in which a water-cooled probe will be employed to measure gas phase composition throughout the reactor. Moreover, different additives will be employed for the simultaneous reduction of NO$_X$ emission and bed agglomeration.

CFD simulations will be performed in combination with skeletal NOx models to describe the chemistry in the lab-scale fluidized bed reactor, thereby providing a simplified gas phase model, useful in industrial applications.

References

1. R.I. Singh, A. Brink, M. Hupa, Appl. Therm. Eng., 52 (2) (2013) 585-614.
2. P. Glarborg, A.D. Jensen, J.E. Johnsson, Prog. Energy Combus. Sci. 29 (2003) 89-113.
3. J. Konttinen, S. Kallio, M. Hupa, F. Winter, Fuel 108 (2013) 238-246.

Edgar L. Camacho Vergara

Phone: +45 5017 8559

E-mail: elcver@kt.dtu.dk

Supervisors: Xiaodong Liang
Georgios M. Kontogeorgis

PhD Study
Started: November 2016
To be completed: November 2019

Phase Behavior of Inhomogeneous Fluids with Classical Density Functional Theory

Abstract

Classical Density Functional Theory (cDFT) [1] has been implemented to study the phase behavior of inhomogeneous fluids, which refers to systems where the microscopic density is not uniform. The study of these systems includes the calculation of interfacial tension and fluid adsorption in fluid-fluid and fluid-solid interfaces. The results obtained with this new classical DFT implementation can be compared with others models currently used by our research group CERE, such as Density Gradient Theory (DGT) [2] and Multicomponent Potential Theory of Adsorption (MPTA) [3] for interfacial tension and adsorption. However, in comparison to DGT and MPTA classical DFT has a broader scope and can be used to study both interfacial tension and adsorption. Moreover, it can be easily extended to study interfacial systems of more complex nature, such as wetting transitions, solvation force, micelle formation, capillary condensation and evaporation, colloidal stability, surfaces with grafted polymers, bio-adhesion, asphaltene adsorption, among others. Classical DFT offers a compromise as it offers the versatility of retaining the accuracy obtained in molecular simulations, but requiring only a fraction of the time. The latter is achieved with the use of modern equations of state for bulk fluids. In the current state of the PhD we are able of calculating interfacial tension and adsorption of pure compounds and mixtures of non-associating fluids successfully. The coming objectives are to study interfacial tension, adsorption in nanopores and asphaltene adsorption with the inclusion of interactions due to association of molecules.

Introduction

Surface thermodynamics, which involves the study of fluid-fluid, and solid-fluid interfaces is of great interest for the chemical, biochemical and petroleum industries as it is related to a great number of engineering applications. These applications range from the formation of emulsions and dispersions for food, medicine, detergents, paints and coatings, to improving oil recovery by the addition of surfactants to an oil reservoir, adsorption, wettability, capillarity, confining geometries, etc. [1]. Surface thermodynamics can also be understood as the study of inhomogeneous systems. To define that, it is important to note that bulk or uniform systems are those in which the particle density is constant and equal to the average density of the whole system, also known as bulk density. However, the homogeneity of bulk fluids is broken in the presence of interfaces or surfaces, as in a liquid in equilibrium with is vapor, or a gas adsorbed in a pore of a petroleum reservoir. On these kinds of systems, the microscopic particle density of the system varies in the proximities of the interface or surface, producing '*inhomogeneities*'.

Classical DFT has proven to be a versatile, reliable and accurate tool for the study of inhomogeneous systems as it forms a '*bridge*' between the microscopic detail and accuracy of molecular simulations and the efficient performance of bulk equations of state, such as SAFT like EoS (Figure 1). This allows to create simple but powerful implementations capable of describing the macroscopic thermodynamics properties of inhomogeneous systems in a unified framework.
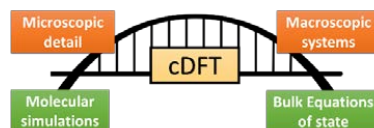

Figure 1: Connection between classical DFT and bulk equations of state.

The key of classical DFT is the definition of the Helmholtz free energy of the inhomogeneous fluid as a functional of the microscopic density. The functionals

must take into account the nature of the particle interactions of the system under study. These interactions are defined following the bulk equations of states, which for this work it is based on the Perturbed Chain Statistical Associating Fluid Theory (PC-SAFT) [4]. Therefore, the fluids are considered as a system of hard spheres that cannot overlap (volume exclusion), adding chain formation, dispersion and interactions due to association of molecules.

Interfacial Tension
Our classical DFT implementation based on the PC-SAFT equation of state inherits the molecular parameters fitted to vapor-liquid equilibrium data, and the binary parameters (k_{ij}) used to model the interaction of molecules of different components in a mixture. However, in the approximation of the free energy functionals, a global and unique adjustable parameter for all compounds is introduced to calculate interfacial tension. In Figure 2 are shown the results for the interfacial tension of several pure compounds and in Figure 3 the full prediction of interfacial tension of mixtures.
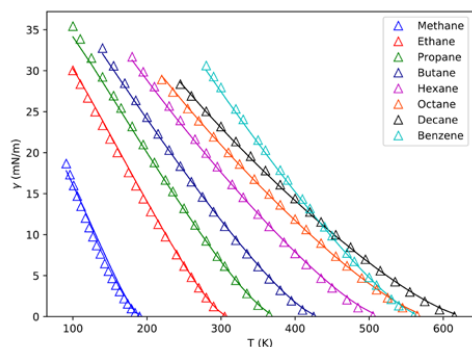

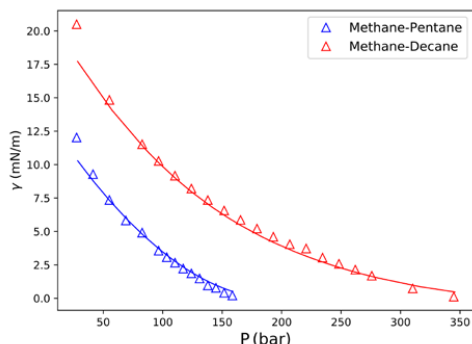**Figure 2:** Interfacial tension of pure compounds with cDFT.

Figure 3: Interfacial tension of mixtures of methane with n-pentane and n-decane, respectively with cDFT.

Adsorption on activated carbon
The calculation of adsorption is extended from interfacial tension with the introduction of an external potential used

to describe the solid-fluid interactions, with three adjustable parameters: interaction energy, size of the wall and specific area of the wall. In Figure 4 it is shown the adsorption of pure methane, nitrogen and carbon dioxide in the same activated carbon. Finally, in Figure 5 are shown the results of the full prediction of adsorption of nitrogen in the mixture methane-nitrogen.
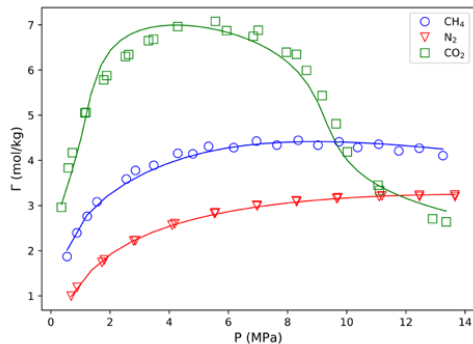

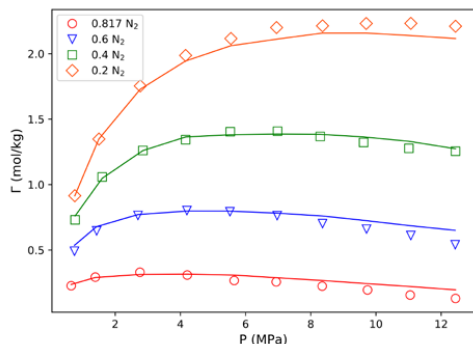**Figure 4:** Adsorption of pure CH_4, N_2 and CO_2

Figure 5: Adsorption of nitrogen in the mixture CH_4/N_2

Future Work
Future work includes the implementation of the association contribution to the Helmholtz free energy functional, which will allow the study of more complex systems of great relevance to the chemical, biochemical and petroleum industries.

References
1. J. Wu, AIChE J. 52 (3) (2006) 1169–1193.
2. X. Liang, M.L. Michelsen, G.M. Kontogeorgis, Fluid Phase Equilibria, (2016), vol. 428, 153-163.
3. A.A. Shapiro, E.H. Stenby, Journal of Colloid and Interface Science, (1998), vol. 201, no. 2, 146-157.
4. J. Gross, G. Sadowski, Ind. & Eng. Chem. Res. (2001) Vol. 40, No. 4, 1244-1260
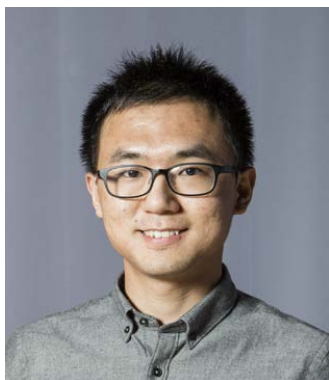
Ting Wang

Phone: +45 4525 2994
E-mail: tinwan@kt.dtu.dk

Supervisors: Søren Kiil
Claus E. Weinell
Kim Dam-Johansen
Erik Graversen, Hempel A/S
Juan José Segura, Hempel A/S

PhD Study
Started: September 2017
To be completed: August 2020

Coating interlayer adhesion loss

Abstract

Weak interlayer adhesion between an epoxy primer and polyurethane topcoat can result from improper curing of polyurethane topcoat under poor ventilation conditions. The hardening process of polyurethane under different ventilation conditions were studied. The degree of ventilation has limited effect on the curing between isocyanates and polyols. However, the solvent evaporation process was significantly influenced and impeded in poor ventilation conditions. The higher presence of solvent causes the softening of the polyurethane coating and reduces its hardness.

Introduction

Corrosion protection of steel structures, such as ships, wind turbines, bridges and oil rig, is almost exclusively done by the use of anticorrosive coating systems. [1] This multilayer coating system typically consists of a primer such as an epoxy primer, directly on the steel substrate, followed by an intermediate epoxy coating to build up a substantial protective coating thickness. Finally, a top coat of polyurethane (PU) is applied for protection against Sun light and to provide an aesthetically pleasing surface. Such a coating system can, in many cases, provide corrosion protection for more than 20 years. However, coating systems can fail due to weak interlayer adhesion that causes e.g. the top coat detach from the remaining coating system, which significantly minimizes the service life of coating films.

The weak adhesion of the PU topcoat to the underlying epoxy coating can occur under poor ventilation conditions. The adhesion between PU topcoat and epoxy primer is reduced and the topcoat might easily be removed. Poor ventilation conditions can slow the evaporation of solvents and trap solvents inside of coating system. In addition, due to short overcoating interval and poor ventilation conditions, some small molecules in the epoxy primer may not be completely evaporated before applying the PU topcoat. This might induce improper curing of PU topcoat.

Specific objectives

The focus of the project will be to investigate the mechanisms of interlayer adhesion loss. One main goal is to study the curing process of PU coating and investigate the parameters influencing the hardening process. The other goal is to find out a way to help the hardness development of the PU topcoat and offer satisfied adhesion even if epoxy-PU coating system is dried in poor ventilation conditions.

Results and Discussion

The hardness development of PU under different drying conditions was investigated with focus on the solvents present in the coating system.

Quantification of PU hardening process

The hardening process of PU coating was studied from the physical solvent evaporation process and chemical reaction between the isocyanate groups (NCO) of curing agents and the hydroxyl groups (OH) of polyols. The solvent evaporation process was monitored by regularly measuring the weight loss of coated panels on an analytical balance. The infrared (IR) technique was used to monitor the curing reaction. As shown in Figure 1(a), the curing reaction is followed by the NCO peak at around 2270 cm^{-1}, which is due to C=O stretching of NCO [2]. As the isocyanate reacts, the area of NCO peak decreases (Figure 1(b)). After 14 days, the PU coating is fully cured. The IR peak at around the 875 cm^{-1} was chosen as the reference peak. As shown in Figure 1(c), the peak area at 875 cm^{-1} remains almost constant during the curing process. This sharp absorbance peak is due to stearic acid calcium carbonate [3], a pigment in the PU formulation. The area ratio between the NCO peak and the reference peak was used to estimate the curing reaction between NCO groups and OH groups. IR spectra enables quantification of the PU curing reaction.
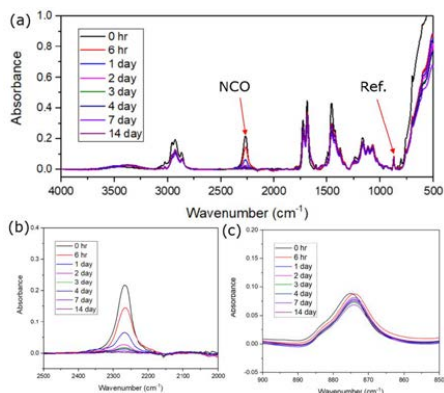
Figure 1: ATR-FTIR spectra of PU films with wet film thickness (WFT) 100 μm drying at the lab condition (a) Full spectra; (b) NCO peak; (c) Reference peak.
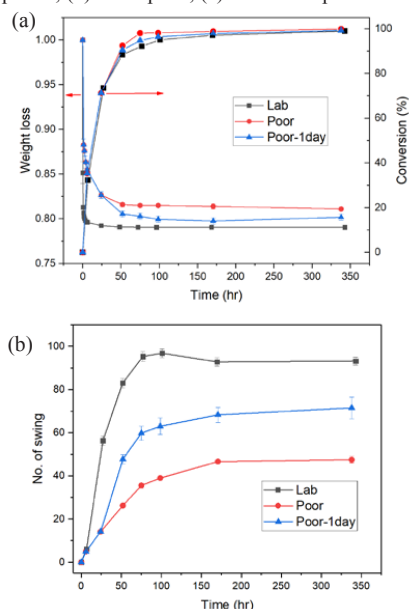

Figure 2: Curing process of PU films with WFT 100 μm dried at different conditions where Lab is in the normal lab conditions, Poor is in the poor ventilation conditions and Poor-1day is first day in poor ventilation conditions and then in the normal lab conditions: (a) Weight loss and surface conversion; (b) Hardness development using Pendulum hardness test.

Hardening of PU at different drying conditions

In Lab conditions, see Figure 2(a), the weight of PU films reduces very fast during the first 6 hours and becomes quite stable after 1 day. However, the curing reaction takes about 7 days to complete. Under Lab condition, the evaporation of solvent from the PU is nearly over after 6 hours, from there on the hardness development mainly is a consequence of the curing process (Figure 2(b)). However, in the Poor and Poor-

1day conditions, the solvent evaporation process takes a more important role in the hardness development of PU coating than in the Lab conditions. Compared to the Lab conditions, there is about 2% more solvent trapped inside the coating dried in the Poor condition. However, the curing reaction rates of PU coating at Lab, Poor, and Poor 1-day conditions are almost the same as shown in Figure 2(a). In Figure 2(b), it is clear to see that better ventilation contributes to higher hardness of PU films. This suggests that the solvent evaporation process is the key factor influencing the hardness development of PU films at different drying conditions as the curing reaction of isocyanates and polyols can complete in the end no matter what drying conditions.

Influence of solvent on the hardness

The solvent evaporation process of PU films was controlled to study the influence of trapped solvent on the hardness of coating films and the results are shown in Figure 3. The hardness of PU films and conversion of NCO groups were plotted along with trapped solvent content inside PU films after drying for 7 days. The conversion of PU films is very close and solvent evaporation process seems to have very little impact on the curing reaction. Initially, the hardness drops very fast when more solvent is trapped in the PU films, indicating that hardness is greatly reduced even though a very small amount solvent is trapped in PU coatings.
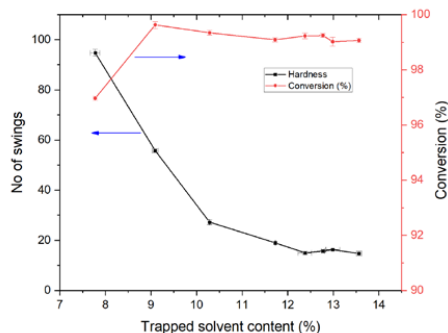
Figure 3: Hardness and surface conversion of PU films of WFT 100 μm with different amount of trapped solvent.

Conclusions

For only one layer PU coating, solvent evaporation process is a key factor influencing the hardness of PU film. Strategies help solvent evaporation, like reducing the catalyst content or using fast-evaporation solvents, might contribute to the hardness development of PU.

References
1. P.A. Sørensen, S. Kiil, K. Dam-Johansen, and C.E. Weinell, Journal of Coatings Technology and Research, 6(2) (2009) 135-176.
2. A.M. Kaminski, M.W. Urban, Journal of Coatings Technology, 69(872) (1997) 55-66.
3. Z. Cao, et al., Applied Surface Science, 378 (2016) 320-329.

Wendi Wang

Phone: +45 5017 8870
E-mail: wendiw@kt.dtu.dk

Supervisors: Anne Ladegaard Skov
Qian Huang
Ole Hassager

PhD Study
Started: June 2018
To be completed: May 2021

Rheological and Mechanical Properties of Polystyrene with Hydrogen Bonding

Abstract
Recent research work [1] shows that at room temperature, brittle polystyrene can become flexible by stretching polystyrene melts at a rate faster than the inverse rouse time, followed by rapid quenching below T_g. The long-lasting flexibility and good humidity resistance make polystyrene suitable for optical fibers. However, improvements are required to prevent potential cracks while bending. This project investigates if such improvement can be achieved by introducing hydrogen bonding. The rheological and mechanical properties of polystyrene with hydrogen bonding are studied and compared to pure polystyrene sample.

Introduction
Polystyrene is a hard and brittle material at room temperature, with glass transition temperature (T_g) around 100°C. It may become flexible when compressed at room temperature in a two-roll milling process (known as "mechanical rejuvenation"). However, this flexibility is temporary. Recently Huang et al. [1] has found that flexible polystyrenes can be obtained by stretching polystyrene melts at a rate faster than the inverse rouse time, followed by rapid quenching below T_g. The resulting samples remain flexible after half a year. This characteristic makes polystyrene a good candidate for optical fibers. However, cracks have been observed while trying to recover the bended sample as shown in Figure 1. The idea of this project is to add some hydrogen bonding between polystyrene molecules so that the cracks at large deformation can be prevented. The resulting system is actually a double network formed by entanglements and hydrogen bonding.
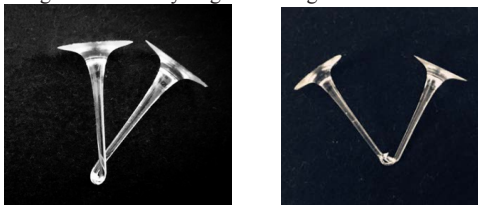
Experiments
Two different samples have been selected for this project: a pure polystyrene with T_g around 100°C and a polystyrene containing 5% acid group on the polymer chains with T_g around 114°C. These acid groups tend to form hydrogen bonding at room temperature.

The linear viscoelastic (LVE) properties of these two samples were obtained from small amplitude oscillatory shear measurements. An 8 mm plate-plate geometry was used on an ARES-G2 rheometer from TA Instruments. The non-linear extensional behaviors have been studied above T_g in controlled uniaxial extension using a filament stretching rheometer (VADER; Figure 2), where both normal force and diameter evolution were measured. Furthermore, tensile tests and 3-point bending tests were carried out on VADER and RSA3 Dynamic Mechanical Analyzer from TA Instruments, respectively.
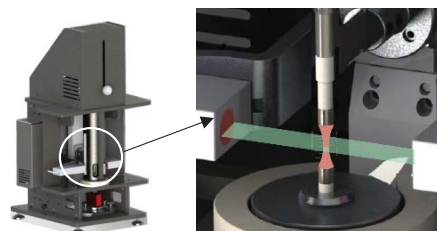

Figure 1: flexible polystyrene (left) and cracks when trying to recover the sample (right)

Figure 2: Filament Stretching Rheometer (VADER)

Results and Discussions

The LVE properties of these two samples have been tested at three different temperatures above T_g to build up the master curve at the reference temperature 130°C, as shown in Figure 3 (top). To compare these two samples, the frequency on the x-axis is normalized by the second crossover frequency ($1/\tau_c$) for each sample, as displayed in Figure 3 (bottom). The two curves overlap each other quite well, indicating a similar number of entanglements per chain for the two samples. It also suggests that the acid groups do not form hydrogen bonding at 130°C.
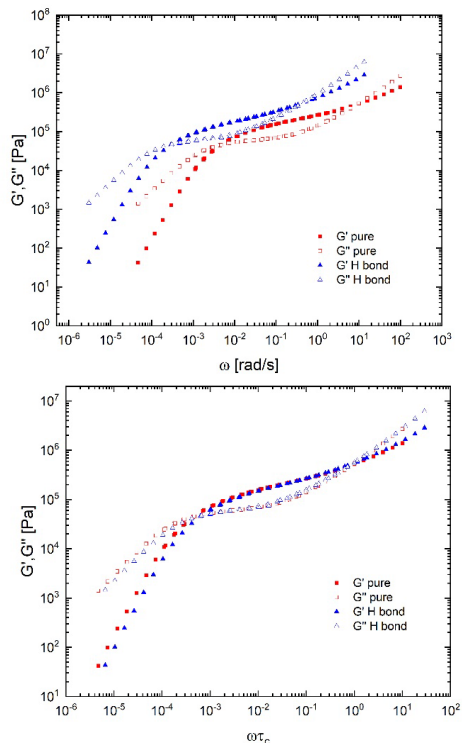

Figure 3: (top) LVE data (storage modulus G' and loss modulus G'' vs. angular frequency ω) at 130°C, (bottom) LVE data with normalized frequency at

The non-linear extensional behaviors have been tested at different stretching rate for both samples and compared in Figure 4 after normalization. These two samples show similar extensional behavior at high temperature above T_g.

Now we wonder if these two samples still have similar mechanical behaviors at room temperature. Both samples have been stretched faster than inverse Rouse time above T_g and quenched fast until room temperature. Then tensile tests have been performed with a constant rate 0.001 s^{-1} at room temperature (blue and red curves in Figure 5). At meantime, full-relaxed samples have also been quenched and tested (black and grey curves). Both two full-relaxed samples are brittle while the other two are flexible.

However, the strain softening, which is observed in the red curve (the slight overshoot) for the pure polystyrene sample, seems to be totally removed in the blue curve for the sample with hydrogen bonding. This phenomenon could be explained by enhanced network contribution according to Haward and Thackray model.[2]
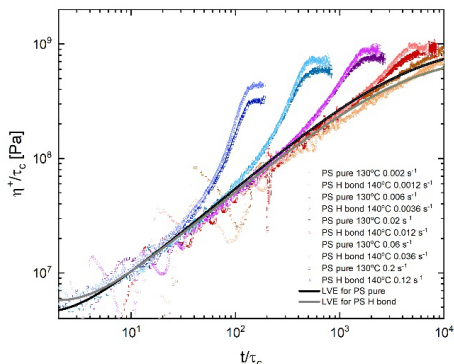
Figure 4: Comparison of normalized extensional stress growth coefficient for two polystyrene sample
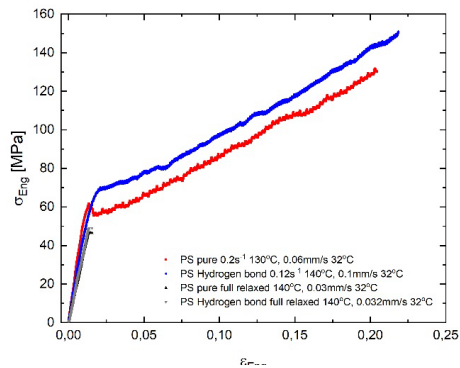
Figure 5: Engineering stress as a function of strain in tensile tests

Future work

The repeatability of experiments should be examined. Furthermore, it is interesting to test the effect of hydrogen bonding in bending tests; and depending on the results, a polystyrene containing higher acid group proportion will be studied.

References
1. Q. Huang et al., ACS Macro Lett. 7, (2018), 1126−1130
2. H. E. H. Meijer, Prog. Polym. Sci. 30, (2005), 915−938

Jifeng Yang

Phone: +45 4525 2817
E-mail: jifyan@kt.dtu.dk

Supervisors: Ulrich Krühne
                    Krist V. Gernaey
                    Mikkel Nordkvist, Alfa Laval

PhD Study
  Started: December 2015
  To be completed: November 2018

Simulating Pipe Cleaning Using Computational Fluid Dynamics

Abstract
Cleaning-in-place (CIP) is a time and resource consuming process in food and pharmaceutical industries. Computational Fluid Dynamics (CFD) has been used to simulate the displacement of cleaning agent by water in different pipe elements during CIP cycles. CFD can identify the cleaning of dead zones, compute the pressure drop in pipes and the displacement time. The results are helpful to improve the hygienic design of pipe systems and to optimize cleaning operations.

Introduction
In a mapping study of the cleaning-in-place (CIP) processes in a world-leading brewery, nearly 60% of the cleaning costs attribute to pipe cleaning operations. Most of the cleaning time and costs are spent on the alkaline/acid treatment, disinfection and three rinsing steps (two intermediate rinses and one final rinse). The recovery of the cleaning detergents can be up to 95% of the supply. In some industries, the final rinsing water can be partly recycled for the pre-rinse of the next CIP. The intermediate rinsing water is rarely recycled. Therefore, the overall recovery efficiency of rinsing water is very low, even less than 10%. Most of the rinsing water is directly disposed to the drain.

Computational fluid dynamics (CFD) is a state-of-the-art numerical technique for solving mass and heat transfer as well as reaction engineering problems in the chemical and food industries. In the field of CIP, CFD has been used to predict the local properties of various pipe geometries, such as the wall shear stress and its fluctuating rate, detergent mixing, and heat distribution, etc. The main advantages of CFD are that: (1) it is possible to test different designs without building prototypes; (2) it is possible to obtain the local properties where measurement cannot reach. Therefore, CFD has been carried out by other researchers to improve the hygienic design of pipes by showing the effects of wall shear stress and fluctuating on cleaning behavior.

In our previous work, CFD has been used for a new purpose, that is, to simulate the displacement of cleaning detergent by water in straight pipes [1]. CFD is able to compute the rinsing time, the minimum water consumption and the minimum wastewater generation. In this report, CFD is applied to simulate more complex pipe geometries, like bends, expansions, contractions and T-joints, in order to generate comparable results of various geometries. This study has been implemented with an education training purpose. All simulations were conducted by the attendees in the intensive CFD course (28831, Computational Fluid Dynamics in Chemical Engineering) at Technical University of Denmark in January 2018. Such a pedagogical approach to ask students to solve relevant questions through individual exploration or collaboration in groups is called problem-based learning (PBL). However, this report will focus mainly on the scientific outputs from the students rather than the evaluation of students' performance.

Methods
The straightforward steps to implement typical CFD simulations comprise geometry construction, mesh creation, model set-up, model computation and result analysis. The simulation included two parts:

- *Steady-state simulation*: comparing results with different mesh density and quality, and selecting the appropriate mesh size for final models; indicating dead zones where local wall shear stress was less than the critical value of 3 Pa, less than which should be avoided in hygienic design [2].

- *Transient simulation*: calculating the displacement time to remove 99% of tracer from the dead zone volume ($t_{99,volume}$) or from a monitoring point ($t_{99point}$) which was located in the dead zone determined from the steady-state analysis.

The investigated geometries and the corresponding indexes included: A – squared corner; B – round corner;

C – U bend; D – orifice; E – sharp concentric contraction; F – gradual concentric contraction; G – sharp eccentric contraction; H – gradual eccentric contraction; I – sharp concentric expansion; J – gradual concentric expansion; K – sharp eccentric expansion; L – gradual eccentric expansion; M – T joint with direct entrance and exit; N – T joint with exit perpendicular to entrance and dead zone; O – T joint with entrance perpendicular to exit and dead zone; P – combined geometries B, E, I and N.

Results and Discussions

Figure 1 shows an example of the dead zones where the local wall shear stress is below a critical value of 3 Pa. The dead areas identified from simple geometries can also be denoted in the complex case. In the given example, dead zones include the exterior surface of bend, large pipe corner of contraction, large pipe and connection of expansion, and the dead leg of T joint
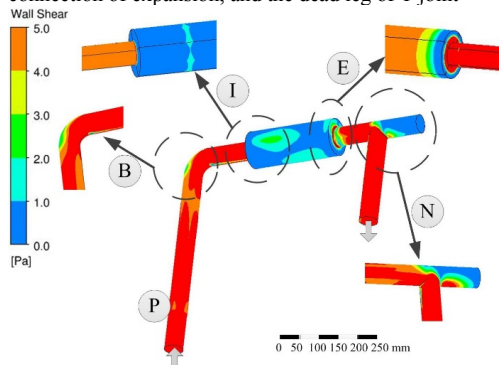

Figure 1: Predicted wall shear stress on the surfaces of five geometries.

The equivalent lengths of different pipe elements are displayed in Figure 2. The determination of equivalent length is critical for calculating the pressure drop within a pipe system with various pipe connections. According to the results in Figure 2, the existence of orifice (D) and sharp contractions (E and G) reduces pressure extremely. The use of gradual contractions (F and H) can also cause significant pressure drop to the system.
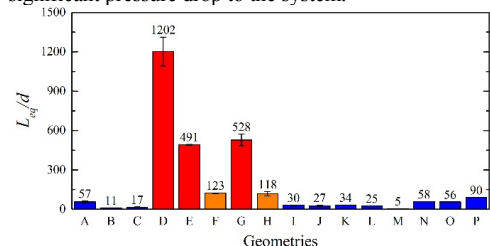

Figure 2: Equivalent length of different pipe elements simulated by CFD. The letters denote geometry indexes.

Figure 3 displays the predicted values of $t_{99,volume}$ and $t_{99,point}$ for different pipe elements. According to the results, bends and contractions are easy to be rinsed, except the sharp eccentric contraction geometry (G). Pipe

expansions, orifices and T joint N are comparably harder to be flushed. T joints M and O as well as the gradual eccentric expansion (L) are the most difficult to clean. For most geometries, the point-based displacement times are larger than the volume-based values, meaning that determining the displacement time by a local sensor is a safe way to validate the removal of a soluble tracer but causes slightly excessive waste. For the geometries B, G and H, a measurement-based displacement time is inadequate to reduce the overall tracer concentration to a safe level. Moreover, a higher flow velocity shortens the displacement time significantly.
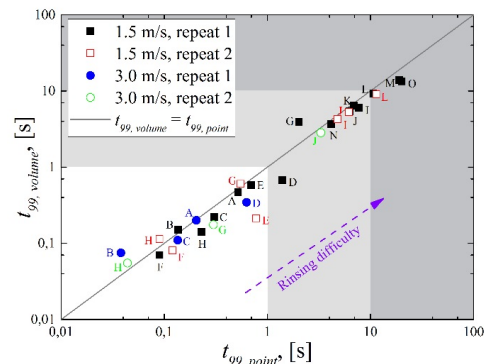
Figure 3: Predicted displacement times to remove 99% of agent components from the dead zone volume or from the monitoring point in the stagnant zone.

Conclusions

CFD has been used to simulate the displacement of cleaning agent by water in different pipe elements during CIP. The dead zones can be indicated by displaying local wall shear stress on the surfaces. Large pressure drops occur after orifice, sharp contractions and gradual contractions. Applying a local sensor to determine the rinsing time is a safe way to validate the removal of a soluble tracer but causes slightly excessive waste of water.

Acknowledgements

References

1. J. Yang, B.B.B. Jensen, M. Nordkvist, P. Rasmussen, K.V. Gernaey, U. Krühne. CFD modelling of axial mixing in the intermediate and final rinses of cleaning-in-place procedures of straight pipes. Journal of Food Engineering 221 (2018) 95-105.
2. B.B.B. Jensen, A. Friis. Critical wall shear stress for the EHEDG test method. Chemical Engineering and Processing: Process Intensification 43.7 (2004) 831-840

Ying Zeng

Phone:	+45 4525 2952
E-mail:	yzen@kt.dtu.dk

Supervisors:	Søren Kiil
	Claus Erik Weinell
	Kim Dam-Johansen
	Louise Ring, Hempel

PhD Study

Started:	October 2016
To be completed:	October 2019

Novel testing methods for intumescent coatings

Abstract

The thermal shield of intumescent coatings is an effective way to protect the structural steel in the event of a fire. This project involves design and validation of a lab-scale setup for fast and reliable fire tests and evaluation of the effect (or synergistic effect) of different concentrations of the ingredients on the performance of intumescent coatings based on a basic hydrocarbon formulation. The evaluation is for understanding the roles of ingredients thoroughly by linking their responses in the fire tests with the char characterizations and mapping the intumescent mechanism.

Introduction

The protection of structural steel on exposure to a fire has become paramount to prevent the loss of lives and assets with increasing use of structural steel as a material to create the shape of construction projects. Structural steel only retains 60% of its original strength when its temperature reaches a critical value and loses it bearing ability under full design load [1]. For regular loaded structural components, such as onshore platforms, 550ºC has been selected as a standard critical temperature for steel. While for heavily loaded structural components, such as offshore platforms, 400°C has been selected as a standard. This critical temperature is also known as ''failure temperature'', and the time for reaching it in the event of a fire is called the "failure time" [2].

An efficient way to protect the building structure and prolong the time before the failure temperature is reached is by intumescent coatings. At elevated temperature, intumescent coatings swell to a multicellular char layer, which acts as a physical barrier to slow heat and mass transfer between gas and condensed phase and thereby protects the underlying substrate. The most effective intumescent coatings are the ones that have best fire-resistance performance and therefore can provide the longest failure time for the substrate in the fire tests.

Instead of natural fire that has varied relationships between temperature and time, fire tests usually refer to the tests under standard fires for which the fixed temperature-time responses are imposed in order to roughly simulate the evolution of natural fires and meanwhile facilitate the normalization of fire test procedure. Depending on the source of fuel, most of the standard fires are classified into two types: cellulosic fire (ISO 834) and hydrocarbon fire (e.g. UL 1709). Their corresponding intumescent coatings are called cellulosic intumescent coatings and hydrocarbon intumescent coatings. The latter is the focus of the present project, as it is the most challenging type used for high-risk environments such as petrochemical complexes and offshore platforms.

Generally, intumescent coatings consist of three essential ingredients: acid source (e.g. ammonium polyphosphate), carbon source (e.g. dipentaerythritol), and blowing agent (e.g. melamine). Other ingredients are incorporated into the formulation as well to improve its function (e.g. composite fibers). All the ingredients are bound together by a polymeric binder. The physical and chemical interactions among these compounds are complex and have not been fully quantified in the literature, especially for the case of the hydrocarbon intumescent coatings [3]. To optimize the formulation of hydrocarbon intumescent coatings, it is fundamental to understand the effect (or synergic effect) of ingredients on the physical (expansion and strength) and chemical (thermal conductivity and thermal stability) properties of char.

Specific Objectives

This Ph.D. project aims at:

- Design and validate a lab-scale setup for standard hydrocarbon fire tests of intumescent coatings
- Study the effect of functional fillers (e.g. zinc borate, ammonium polyphosphate) on the performance of intumescent coatings and on the morphological structure of intumescent chars.

Results and Discussion

Five hydrocarbon intumescent coatings (ZB0, ZB5, ZB10, ZB15, and ZB20) with 0, 5, 10, 15, and 20 wt.% zinc borate, respectively, were manufactured to evaluate the effect of zinc borate on the fire-resistance performance of the coatings in a hydrocarbon fire scenario (standard UL 1709). The formulations of the intumescent coatings are not given here for the sake of confidentiality. The fire-resistance experiments were carried out with a laboratory oven that can simulate the temperature-time curve defined by the standard hydrocarbon fire test UL1709.

About 6 mm of the coating was applied to the surface of a grit-blasted steel plate (area of 60 x 60 mm^2 and 3 mm thickness). The coated steel plate held in place with a tailor-made insulating cap was put inside the oven chamber during the fire-resistance experiment. A thermocouple (type K, -50°C - 1200°C) was attached to the backside of the steel plate to record its temperature versus time response. By 3-fold repetition of the fire-resistance experiments with an intumescent coating, the repeatability of the experiment was assessed and the results show that the standard deviations of the time to reach the critical temperatures (400°C and 550°C) are less than 1%.
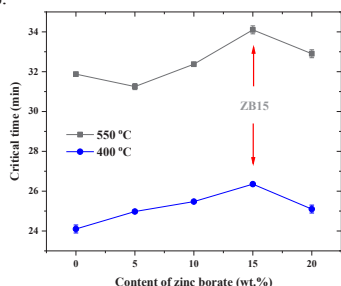

Figure 1: Average exposure time to reach the critical temperature of the steel substrate based on repeated fire-resistance experiments.

Figure 1 shows the exposure times of the five intumescent coatings to reach the critical temperatures (400°C and 550°C) during fire-resistance experiments. The best performing formulation is ZB15, which has the longest critical time for both 400 and 550°C, while the worst performance changed from ZB0 to ZB5 when the critical temperature increased from 400 to 550°C. Even though the absolute difference between the critical times of the formulations is only a few minutes, the trends in Figure 1 clearly demonstrate that zinc borate can improve the fire-resistance performance of hydrocarbon intumescent coatings.

To understand the different performance of the coatings, the expansion of the intumescent chars is determined by averaging the height measurements of the chars produced from the repetitive fire-resistance experiments. The results are plotted in Figure 2, which clearly show that the expansion of the chars is dramatically constrained with zinc borate in the formulation. From a comparison of Figure 1 and Figure 2, it can be seen that the higher expansion of the char did not bring a better fire-resistance protection of the substrate. It is usually the case that the char has a high expansion but an inferior structure.
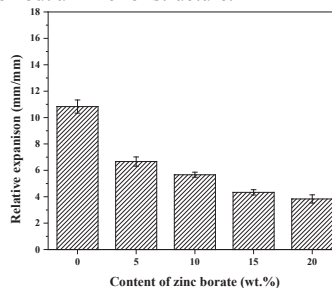

Figure 2: Relative char expansions estimated from measurements of the sample thickness before and after the fire-resistance experiments.

Figure 3 shows the cross-sections of the intumescent char ZB0 and ZB20. The fluffy and friable char formed from formulation ZB0 cannot provide sufficient protection regardless of the highest expansion. This undesirable structure is improved with zinc borate by making uniform the char structure with fewer and smaller voids (cells). However, a high level of zinc borate might introduce delamination and cracks to the char structure as found in the case of ZB20. The pluses and minuses of increasing zinc borate content in the hydrocarbon intumescent coatings might be responsible for the threshold (15 wt.% zinc borate) of the fire-resistance performance presented in Figure 1.

Figure 3: The cross-section of the char ZB0 and ZB20 with the big voids (width >5 mm) highlighted in red.

Conclusions

The fire-resistance performance of the hydrocarbon intumescent coatings is improved by formulating more zinc borate into the coatings. The formulation with 15 wt.% zinc borate (ZB15) is the most efficient coating with the longest critical time for both 400 and 550°C. The chars produced from the fire-resistance experiments show that zinc borate can lower the cell (void) size and make uniform in the char structure with the sacrifice of the high expansion.

References

1. M. Jimenez, S. Duquesne, S. Bourbigot, Ind. Eng. Chem. Res. 45 (2006) 7475-7481.
2. M. Jimenez, S. Duquesne, S. Bourbigot, Ind. Eng. Chem. Res. 45 (2006) 4500-4508.
3. J. Alongi, Z. Han, S. Bourbigot, Prog. Polym. Sci. 51 (2015) 28-73.
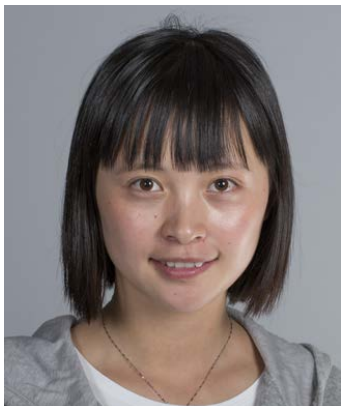
Yu Zhang

Phone: +45 9186 8186
E-mail: yuzha@kt.dtu.dk

Supervisors: Peter Glarborg
                    Anker D. Jensen
                    Jakob M. Christensen

PhD Study
  Started: September 2016
  To be completed: August 2019

Catalytic Oxidation of Methane

Abstract

Natural gas is an interesting engine fuel for ships in coastal zones, where high sulfur marine fuels cannot be used. However, unburnt methane poses another severe emission problem. The current study seeks to develop a catalyst for methane emission abatement from natural gas engines. Motivated by the good performance of the commercial Rh-Cr-Al catalyst, zeolite supported Rh and Pd catalysts were prepared and tested for methane oxidation in the temperature range of 250-550 °C, in a simulated exhaust gas (2500 ppm CH_4, 10 vol.% O_2, 5 vol.% H_2O, and 1-20 ppm SO_2 when present). Compared with Pd catalysts, Rh supported on ZSM-5 catalysts shows comparable activity at the same loading (1 wt.%), but higher SO_2 tolerance. For 2 wt.% Rh/ZSM-5 catalyst, by elevating the operation temperature (450-500 °C) and decreasing the SO_2 concentration (20 ppm to 1 ppm) in the reaction gas, it is possible to improve the CH_4 removal efficiency (13 % to 79 %).

Introduction

Natural gas provides high fuel efficiency compared with diesel and gasoline. Dual-Fuel engine can switch between diesel mode and natural gas mode flexibly to lower NOx and PM emissions and meet the strict regulations [1]. However, the unburnt CH_4, which has a greenhouse impact of 25 times larger than that of CO_2, becomes another environmental issue for this Dual-Fuel engine. In order to solve this problem, a CH_4 catalytic oxidation unit, which could fully convert the unburnt CH_4 to CO_2 and H_2O, is necessary in the exhaust gas pipe.

The catalysts studied in the literature for CH_4 oxidation can be divided into two groups, namely noble metal based catalysts (Pd, Pt, Rh, Au) and non-noble metal based catalysts. Among the catalysts, Pd based catalyst is most active for CH_4 oxidation with a mixed metal and oxidized phase as active site [2].

Zeolites are reported to have pore structure and acidic sites which could incorporate with the active metals to enhance the activity and avoid sintering at high temperatures [3]. 1 wt.% Pd/H-ZSM-5 could fully convert CH_4 to final products at 320 °C and the activity was stable in the subsequent 3 runs even to a temperature as high as 800 °C.

Rh based catalysts also showed great potential towards total oxidation of CH_4. The performance of Rh based catalysts is influenced by the supports indicated by decreasing activity towards partial oxidation of CH_4 in the order: Rh/TiO_2>>Rh/Al_2O_3>>Rh/MgO [4].

Specific objectives

The objectives of this PhD project focus on developing a catalyst which can be used under practical engine exhaust condition: low temperature (< 550 °C), 2000-2500 ppm CH_4, presence of a large amount of H_2O (~ 10 vol. %), and low concentrations of SO_2 (~ 1 ppm). The scope of the PhD work includes:

- Literature study on catalytic oxidation of CH_4 focused on SO_2 resistance.
- Activity, stability and SO_2 resistance tests of the commercial Rh-Cr-Al catalyst.
- Catalyst preparation: Rh and Pd supported on zeolites, SiO_2, Al_2O_3.
- Thermal, water and SO_2 deactivation of the Rh catalysts at different temperatures (400-550 °C), SO_2 concentrations (1-20 ppm).
- Catalyst characterization: fresh and spent.
- Identification of the optimum operation conditions.

Results and discussion

The conversion of CH_4 over the commercial Rh-Al-Cr catalyst could stabilize at 22 % after running in the presence 5 vol.% H_2O and 20 ppm SO_2 for 10 days.

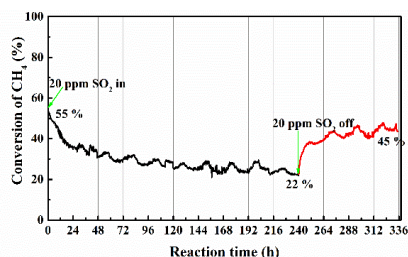After removal of SO_2 for 12 h, without any heating, the activity can be self-regenerated to 46 %. (Figure 1)

Figure 1: SO_2 resistance of commercial catalyst (450 °C, 5 vol.% H_2O, 20 ppm SO_2)

The activity of 1 wt.% Pd/ZSM-5 and 1 wt.% Rh/ZSM-5 catalysts (prepared in house) in the presence of 5 vol.% H_2O are compared in Figure 2. It indicates that Rh has similar activity as Pd when distributed on the same support in the absence of SO_2.
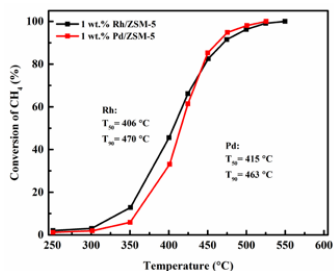

Figure 2: Conversion of CH_4 over 1 wt.% Rh/ZSM-5 and 1 wt.% Pd/ZSM-5 in the absence of SO_2. 2500 ppm CH_4, 10 vol. % O_2, 5 vol.% H_2O, in N_2, GHSV= 150, 000 ml/(g_{cat}·h).
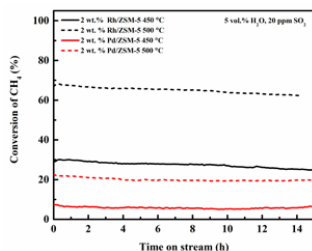

Figure 3: Conversion of CH_4 over 2 wt.% Rh/ZSM-5 and 2 wt.% Pd/ZSM-5 in the presence of 20 ppm SO_2. 2500 ppm CH_4, 10 vol. % O_2, 5 vol.% H_2O, 20 ppm SO_2, in N_2, GHSV= 150, 000 ml/(g_{cat}·h).

With addition of 20 ppm SO_2 into the reaction stream, the activity decreased for both Rh and Pd catalyst with a higher and more stable conversion of CH_4 for Rh (Figure 3.) The conversion of CH_4 over 2 wt. % Rh/ZSM-5 were 25 % and 65 % at 450 and 500 °C respectively, while that over 2 wt. % Pd/ZSM-5 were 7 % and 20 %.

The influence of operation temperature and SO_2 concentration on 2 wt.% Rh/ZSM-5 catalyst was further studied and the results are shown in Figure 4. The conversion of CH_4 can be improved by operating at a higher temperature and lower SO_2 concentration. At 450 °C, the conversion of CH_4 decreased from 27 % to 13 % as the SO_2 concentration increased from 1 ppm to 20 ppm. The conversion of CH_4 in 1 ppm SO_2 could be improved from 27 % to 79 % as the operation temperature was elevated from 450 to 500 °C.
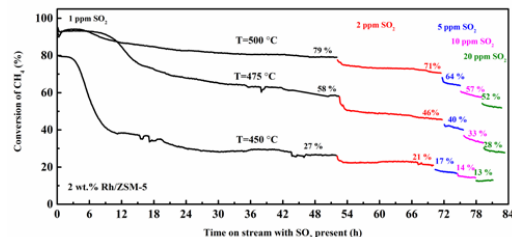

Figure 4: Conversion of CH4 over 2 wt.% Rh/ZSM-5 catalyst in the presence of 1-20 ppm SO_2 at 450, 475, and 500 °C. 2500 ppm CH_4, 10 vol. % O_2, 5 vol.% H_2O, 1-20 ppm SO_2, in N_2, GHSV= 150, 000 ml/(g_{cat}·h).

Conclusions and Future work
Rh/ZSM-5 and Pd/ZSM-5 have comparable activity in the presence of 5 vol.% H_2O, while the SO_2 resistance of Rh catalyst is greatly superior much stronger thanPd catalyst. The CH_4 removal efficiency of 2 wt.% Rh/ZSM-5 can be improved by elevating operation temperature and decreasing SO_2 concentration. The SO_2 concentration in the real engine exhaust condition is always below 1 ppm, thus it is possible to get high CH_4 removal efficiency and longer lifetime with Rh catalyst.

Future work will mainly focus on mechanistic studies of deactivation caused by H_2O and SO_2. Detailed characterizations of fresh and spent catalysts will be carried out to identify the active sites and the structural changes of the catalyst after deactivation.

References
1. A. Gremminger, P. Lott, M. Merts, Applied Catalysis B: Environmental 218 (2017) 833-843.
2. J.H. Chen, H. Arandiyan, X. Gao, Catal Surv Aisa 19 (2015) 140-171.
3. Y. Lou, J. Ma, W.D. Hu, ACS Catal 6 (2016) 8127-8139.
4. M.P. Cecilia, B. Bernard, A.S. Miguel, Catalysis Today 213 (2013) 155-162.

Zhibo Zhang

Phone: +45 52695821
E-mail: zhiz@kt.dtu.dk

Supervisors: Manuel Pinelo
Suojiang Zhang
Nicolas von Solms

PhD Study
Started: December 2015
To be completed: February 2019

Ionic Liquids as Bifunctional Cosolvents enhanced CO₂ Conversion Catalysed by NADH-dependent Formate Dehydrogenase

Cascade Biocatalysis in Membranes with Ionic liquids for the Production of Methanol from CO₂

Abstract

The PhD Project focuses on improving conversion of CO_2 catalyzed by formate dehydrogenase. The main bottleneck of enzymatic reaction is the low solubility of the substrate (CO_2) in the liquid media and the low stability of NADH in the presence of CO_2 (acid gas). In order to overcome these problems, a new novel solvent (Ionic liquids) is evaluated. Enzymatic conversion of CO_2 was improved – as compared to the reaction conducted in buffer- after evaluating different kinds of ionic liquids as co-solvents and the reaction mechanism was studied and proposed.

Introduction

To minimize environmental problems and produce clean energy, efficient utilization of CO_2 and carbon regeneration has been the focus of a tremendous amount of research.[1] Enzymatic conversion of CO_2 to formate, formaldehyde, and methanol has inspired many researchers in the past several years.[2] However, enzymatic hydrogenation of CO_2 to formic acid (CH_2O_2), formaldehyde (CH_2O) and methanol (CH_3OH) is hampered by the low concentration of CO_2 that is available for the enzyme (formic acid dehydrogenase) in the reaction mixture. Increasing CO_2 concentration could result in an increased conversion, as reported by Liu.[3] CO_2 is highly soluble in ionic liquids (ILs), and such high solubility is explained via electrostatic forces, van der Waals forces, hydrogen bonds and other physical effects.[4] One serious limitation of conducting the reaction in carbon dioxide is to maintain the stability of NADH, as it is easily affected by the solution's pH. The investigations on the interaction between ILs and coenzyme (NADH) could then play a key role in the conversion of CO_2. NADH is used not only as hydrogen donor to catalyse reduction of CO_2 but is also employed to follow the progression of the reaction and thus it can be used to quantify the produced formate. The objective of present work was to investigate the activity of NADH in ILs to improve the efficiency of enzymatic reaction and to increase enzymatic conversion by capturing CO_2 with ionic liquids.

Specific Objective

The objective of this work is to improve the enzymatic conversion of CO_2 in the contained-IL buffer. In order to achieve such a goal, three requirements have to be met: First, ionic liquids must have great ability to absorb CO_2. Second, the coenzyme (NADH) must keep its activity in the presence of the ionic liquids. Last, formate dehydrogenase should be able to keep its activity in the ionic liquid.

Results and Discussion

Table 1. Stability of NADH in aqueous ILs.

Entry	IL	Residue$_{(NADH)}$ (%) (SD)	pH (SD)
1	IL1	100.0 (± 0.1)	7.8 (± 0.20)
2	IL2	12.8 (± 3.1)	5.3 (± 0.12)
3	IL3	3.1 (± 0.5)	2.8 (± 0.18)
4	IL4	4.7 (± 0.6)	2.6 (± 0.18)
5	IL5	11.1 (± 2.6)	2.3 (± 0.16)
6	IL6	99.7 (± 0.6)	9.3 (± 0.14)

Screen ionic liquids for absorb CO_2.

Six different ILs were selected for enzymatic reaction. These ILs were selected based on the great ability to absorb CO_2 with similar structure in cation and expect to find structure-performance relationship. Besides, these

ILs' pH are range from acid to alkali. Therefore, NADH stability will firstly be evaluated in these ILs.

Stability of NADH in ILs

To verify if NADH stability in all kinds of ILs, five ILs were subsequently screened under identical conditions in terms of their respective reactivity with NADH (Table 2, entries 1~5). The results showed that the stability of NADH was found to be highly dependent on the pH value of the system. Under neutral-basic conditions, almost no degradation of NADH was detected (entry 1). In contrast, the concentration of NADH diminished markedly under acidic conditions (entry 2). Notably, under strongly acidic conditions, the absorption at 340 nm assigned to NADH disappeared coincidently with the appearance of a blue-shifted peak at 332 nm. Finally, when IL6 at known to be a strong basic IL was employed rather than imidazolium-based ILs (entry 6), only traces of degradation of NADH were observed. In the following degradation mechanism investigation, the analysis tools UV, NMR were used for identifying degradation procedure. According to experimental results, there are two possible degradation pathways, which were further confirmed by molecular simulation (DFT calculation).

Activity of Formate dehydrogenase (FDH) in ionic liquids.

Table 2. Enzymatic Conversion of CO_2 to Formate

Entry	Solvent(v/v)	Yield of formate (%) (SD)
1	Phosphate buffer	1.1 (± 0.5)
2	10% IL4	0.2 (± 0.3)
3	20% IL4	2.9 (± 0.4)
4	40% IL4	2.3 (± 0.4)

After evaluating these ILs for NADH stability above, IL4 was used for running enzymatic reaction. In the case of IL4, CO_2 conversion reached the maximum at 20% IL4 (2.9%), which is more than two folds as compared with conversion in phosphate buffer (1.1%). As is known, water with small amounts of salts was considered to be the best media for proteins. Normally, high concentration of ILs (salts) will cause conformational changes of peptide chains and cause enzyme denaturation, due to electrostatic unbalance between peptide chains. Crystallization and aggregation of proteins dramatically occurred upon increasing the concentration of ILs. Furthermore, in pure ILs, enzymes can hardly be dissolved in homogenous phase without causing denaturation.

Conclusion

We demonstrated that degradation of NADH occurs during carbon dioxide hydrogenation at low pH The mechanism of NADH degradation was investigated by UV, NMR, and DFT. By selecting neutral-basic ionic liquids and adjusting concentration of the ionic liquids in the buffer, 20% IL4 was the one found to be optimal for conducting the reaction. Finally, CO_2 conversion was more than twice as compared with the enzymatic reaction in the phosphate buffer (traditional buffer). This study is a significant contribution to improve yields formate dehydrogenase catalysed reactions in a novel medium (ionic liquid) and paves the way for improving biocatalysts using ionic liquids.

References

1. Xu, B. H.; Wang, J. Q.; Sun, J.; Huang, Y.; Zhang, J. P.; Zhang, X. P.; Zhang, S. J., Fixation of CO2 into cyclic carbonates catalyzed by ionic liquids: a multi-scale approach. *Green Chem* **2015,** *17* (1), 108-122.

2. (a) Obert, R.; Dave, B. C., Enzymatic conversion of carbon dioxide to methanol: Enhanced methanol production in silica sol-gel matrices. *J Am Chem Soc* **1999,** *121* (51), 12192-12193; (b) Shi, J. F.; Jiang, Y. J.; Jiang, Z. Y.; Wang, X. Y.; Wang, X. L.; Zhang, S. H.; Han, P. P.; Yang, C., Enzymatic conversion of carbon dioxide. *Chem Soc Rev* **2015,** *44* (17), 5981-6000.

3. Wang, Y. Z.; Li, M. F.; Zhao, Z. P.; Liu, W. F., Effect of carbonic anhydrase on enzymatic conversion of CO_2 to formic acid and optimization of reaction conditions. *J Mol Catal B-Enzym* **2015,** *116*, 89-94.

4. D'Alessandro, D. M.; Smit, B.; Long, J. R., Carbon Dioxide Capture: Prospects for New Materials. *Angew Chem Int Edit* **2010,** *49* (35), 6058-6082.

Liyan Zhao

Phone: +45 50271099

E-mail: liyzh@kt.dtu.dk

Supervisors: Kim Dam-Johansen

                Weigang Lin

                Hao Wu

PhD Study

Started: May 2018

To be completed: May 2021

Mechanisms of High Temperature Agglomeration in Fluidized Beds

Abstract

This PhD project focuses on understanding the mechanisms of high temperature agglomeration in fluidized bed combustion and gasification of biomass. The effect of gas atmosphere, bed temperature, biomass properties and bed materials on agglomeration will be studied in a laboratory scale fluidized bed reactor under combustion and gasification conditions. Based on the experimental results, a model will be developed to evaluate the agglomeration tendency and countermeasures will be tested and optimized.

Introduction

Fluidized beds are widely applied in combustion and gasification of biomass due to the advantages of high fuel flexibility, uniform temperature profile and high efficiency [1,2]. However, bed agglomeration induced by biomass ash may strongly influence the performance of fluidized bed combustors and gasifiers. In severe cases, it may lead to defluidization and unscheduled plant shutdown[3].

Agglomeration in combustion and gasification of biomass is primarily attributed to the presence of molten phase, i.e. the low melting point alkali containing compounds originated from biomass. During combustion and gasification, potassium in biomass may be transformed into gaseous phase, such as KCl and KOH vapor, and condensed phase, such as K_2SO_4 aerosols and K-silicates in ash particles[4]. The interactions of the potassium species with bed materials (mainly SiO_2) may result in the formation of a molten phase on the surface of bed materials, causing agglomeration [5].

Agglomeration in fluidized bed is influenced by biomass properties (such as ash content and composition), bed material properties (such as size and material type), and operation conditions (such as temperature, gas atmosphere and superficial gas velocity)[3,6]. Biomass with high ash content and high content of K and Si shows a high agglomeration tendency. It is attribute to the rapidly interaction between potassium species and silicon compounds in the ash and the easily formation of K-silicates with low melting point during combustion or gasification[7]. The other potassium species may also be present, such as

KCl, K_2CO_3 and K_2SO_4, depending on the biomass type and reaction conditions[8]. The different mechanisms for biomass with different compositions may be attributed to the different interaction mechanisms between various potassium species and bed materials[6]. Under different gas atmospheres, the presentence of steam or H_2 may accelerate the reaction between potassium species with silica sand[6].

However, comprehensive mechanisms for full spectrum of different types of agglomeration are still missing. Therefore, an improved understanding of agglomeration mechanism in fluidized bed, including the differences in combustion and gasification, is important for developing effective countermeasures.

Specific Objectives

The specific objectives of the project are to:
- Investigate the influence of gas atmosphere, bed temperature, and biomass properties, on the agglomeration mechanisms
- Investigate the different agglomeration mechanisms under combustion and gasification conditions
- Develop a model to evaluate the agglomeration tendency in fluidized bed combustion and gasification
- Test and optimize countermeasures for the agglomeration in fluidized bed combustion and gasification

Approaches

Bed agglomeration during biomass combustion and gasification will be studied in a laboratory-scale fluidized bed reactor at DTU Chemical Engineering, as illustrated in Figure 1. The setup consists of five parts: a gas supplying system, a fuel feeding system, a fluidized bed reactor, a gas analysis system and a data acquisition system. During experiment, the temperature and pressure drop over the bed are continuously monitored for detection of the occurrence of agglomeration and defluidization.
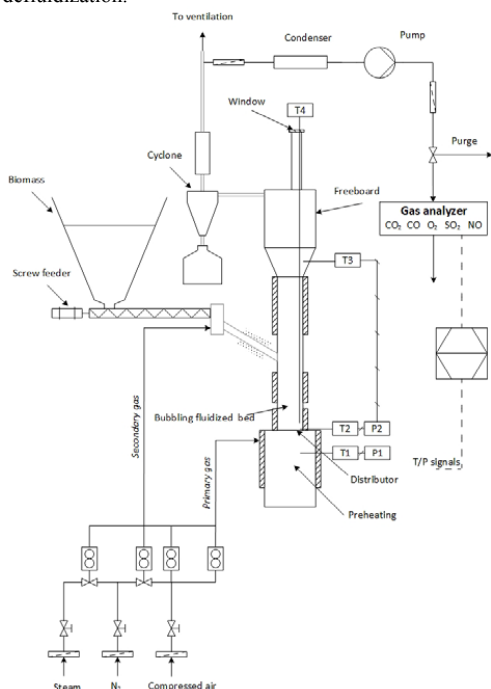

Figure 1: A schematic drawing of the lab scale fluidized bed reactor

The influences of biomass properties, operational parameters (including gas atmospheres, temperatures, excess air ratio, superficial velocity etc.), as well as different additives and bed materials on agglomeration will be investigated.

Ex-situ characterization tools, including scanning electron microscopy coupled with energy-dispersive x-ray spectroscopy (SEM/EDS), X-ray diffraction (XRD), Simultaneous Thermal Analysis (STA) will be used to support the proposed agglomeration mechanisms. Thermodynamics calculations will be performed by Factsage software.

Acknowledgements

References

[1] G. A. J. Wiltsee, C. R. McGowin, and E. E. Hughes, National Renewable Energy Lab., Golden, CO, Burlington, Vermont, United States, 1993.

[2] R. Warnecke, Biomass and Bioenergy, 18 (6) (2000) 489–497.

[3] W. Lin, K. Dam-Johansen, and F. Frandsen, Chem. Eng. J., 96 (1–3) (2003) 171–185.

[4] D. C. Dayton, R. J. French, and T. A. Milne, Energy and Fuels, 9 (5) (1995) 855–865.

[5] B. Gatternig and J. Karl, Energy and Fuels, 29 (2015) 931–941.

[6] T. Ma, C. Fan, L. Hao, S. Li, W. Song, and W. Lin, Energy and Fuels, 30 (8) (2016) 6395–6404.

[7] F. Scala and R. Chirone, Biomass and Bioenergy, 32 (2008) 252–266.

[8] M. Öhman, L. Pommer, and A. Nordin, Energy and Fuels, 19 (4) (2005) 1742–1748.

Libor Zverina

Phone: +45 4588 0199
E-mail: libzve@kt.dtu.dk

Supervisors: Anders Daugaard
John Woodley
Manuel Pinelo

PhD Study
Started: March 2018
To be completed: February 2021

Tubular Membrane Reactors for Immobilization of Enzymes

Abstract
Enzyme immobilization is a promising tool to improve stability and productivity of enzymes that could otherwise not be exploited in large-scale biocatalytic processes. This project aims to immobilize enzymes on functionalized tubular membranes and to utilize these membranes in gas/liquid biocatalytic reactors. Here, a versatile method of controlled surface modification is presented. This method is applicable to commercially available hollow-fiber membranes and leads to functionalized membranes suitable for gas/liquid biocatalytic reactors.

Introduction
A new class of enzymes, cytochrome P450 monooxygenases, has emerged as highly attractive enzymes for special synthesis and production of active pharmaceutical ingredients. These enzymes have an unmatched selectivity and could potentially be used across a broad range of fields. However, their stability and productivity is currently too low for industrial exploitation. Therefore, there is a need for development of new biocatalytic reactors that can accommodate such unstable classes of enzymes in gas/liquid reactions [1,2].

Immobilization of enzymes serves as a key enabling technology for practical and commercial viability of green and sustainable manufacturing of chemicals. The main role of enzyme immobilization is to improve stability, recyclability, overall operational performance and hence, cost-effectiveness of enzymes in biocatalytic processes [3].

To develop a sustainable biocatalytic process with high productivity on scale, biocatalyzed reactions with different classes of enzymes can be integrated with a flow reactor technology. The continuous process offers several advantages over custom batch setups, such as limitation of substrate/product inhibition effects, in-line purification, easy recovery of the product and no mechanical mixing [4]. In particular for biocatalytic oxidations, membrane reactors can not only provide sufficient oxygen supply, but also enable collection of kinetic data crucial for the system evaluation [5].

In tubular membrane bioreactors, the membrane should be hydrophobic and available in low diameters to provide high interface area between the reaction liquid phase and the gas phase. Moreover, it should be susceptible to chemical modifications that serve as an immobilization matrix and provide beneficial chemical environment for the immobilized enzyme. Hollow-fiber polyethersulfone (PES) membranes meet all the above mentioned criteria [6].

Specific Objectives
The objective of the project is preparation of surface functional tubular membrane reactors with full control over surface properties. Ultimately, these systems will be used for immobilization of enzymes and applied as biocatalytic tubular membrane reactors (Figure 1).
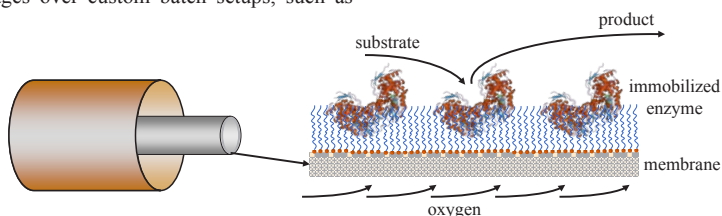

Figure 1: Tubular membrane reactor with an immobilized enzyme.

Figure 2: Activation reaction and subsequent graft polymerization of PES membrane.

Results and Discussion

The original hollow-fiber PES membrane was first activated by heterogeneous ortholithiation with n-butyllithium (n-BuLi) and subsequent acylation with 4-chloromethylbenzoylchloride (CMBC) to introduce benzyl chloride groups serving as initiators in the next step. Thereafter, surface-initiated atom transfer radical polymerization (SI-ATRP) with 2-hydroxyethyl methacrylate (HEMA) was performed to obtain a polymer-grafted membrane, as shown in Figure 2.

Concentration of reagents was varied in the activation step and reaction time was varied in the subsequent polymerization. Chemical changes to the membrane were observed by Fourier-transform infrared (FT-IR) spectroscopy (Figure 3).
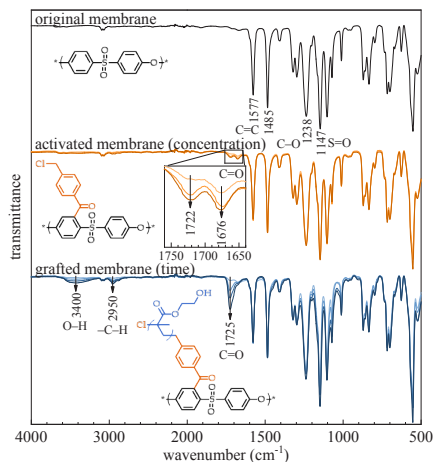

Figure 3: Normalized FT-IR spectra of the original, activated, and grafted membranes.

With increasing concentration of reagents in the activation step, the amount of benzyl chloride initiators on the membrane surface increases, ultimately resulting in a specific graft density. Chain length of the grafted polymer can be controlled by polymerization time.

In gas/liquid biocatalytic reactions, the membrane provides contact between the two phases. For this application, water flux through the membrane should be suppressed. Effects of chain length and graft density on water flux were therefore studied (Figure 4). It is clearly seen how water flux across the membrane can be reduced by increasing chain length of the grafted polymer. High graft density membranes exhibit extremely low to zero water flux.

Figure 4: Water flux at 4 bar of the original membrane (reference), membranes grafted for 5, 15 and 30 min (low graft density), and membranes with low and high graft density (polymerization time 30 min).

Conclusions

Heterogeneous activation can be applied to commercial hollow-fiber PES membranes and provides control over graft density. Subsequently, SI-ATRP of various monomers can be performed from the activated membrane surface with control over the chain length through polymerization time. This modification suppresses water flux through the membrane leading to tubular membranes suitable for gas/liquid biocatalytic reactors. The versatility of SI-ATRP enables tailoring of the chemical environment on the membrane surface that will be efficient in enzyme immobilization and beneficial for the enzyme activity, stability and overall productivity.

References

[1] M. Sono, M.P. Roach, E.D. Coulter, J.H. Dawson, Chem. Rev. 96 (1996) 2841–2888.
[2] R. Bernhardt, V.B. Urlacher, Appl. Microbiol. Biotechnol. 98 (2014) 6185–6203.
[3] R.A. Sheldon, S. van Pelt, Chem. Soc. Rev. 42 (2013) 6223–6235.
[4] L. Tamborini, P. Fernandes, F. Paradisi, F. Molinari, Trends Biotechnol. 36 (2018) 73–88.
[5] R.H. Ringborg, A. Toftgaard Pedersen, J.M. Woodley, ChemCatChem 9 (2017) 3285–3288.
[6] C. Hoffmann, H. Silau, M. Pinelo, J.M. Woodley, A.E. Daugaard, Mater. Today Commun. 14 (2018) 160–168.